

RECEIVED: August 12, 2023

REVISED: October 20, 2023

ACCEPTED: October 22, 2023

PUBLISHED: January 2, 2024

Forward production of a Drell-Yan pair and a jet at small x at next-to-leading order

Pieter Taels

*Universiteit Antwerpen, Departement fysica,
Groenenborgerlaan 171, 2020 Antwerpen, Belgium*

E-mail: pieter.taels@uantwerpen.be

ABSTRACT: We perform the analytical next-to-leading order calculation of the process $p + A \rightarrow \gamma^* + \text{jet} + X$, at forward rapidities and low x . These kinematics justify a hybrid approach, where a quark from the ‘projectile’ proton scatters off the gluon distribution of the ‘target’, which can be a nucleus or a highly boosted proton. By using the Color Glass Condensate effective theory approach, this gluon distribution is allowed to be so dense that the quark undergoes multiple scattering. Moreover, large high-energy logarithms in the ratio of the hard scale and the center-of-mass energy are resummed by the Balitsky, Kovchegov, Jalilian-Marian, Iancu, McLerran, Weigert, Leonidov, Kovner or BK-JIMWLK evolution equations. We demonstrate that all ultraviolet divergences encountered in the calculation cancel, while the high-energy divergences are absorbed into BK-JIMWLK. The remaining singularities are collinear in nature and can be either absorbed into the Dokshitzer-Gribov-Lipatov-Altarelli-Parisi evolution of the incoming quark, when they stem from initial-state radiation, or else can be treated by a jet function in case they are caused by final-state emissions. The resulting cross section is completely finite and expressed in function of only a small set of color operators.

KEYWORDS: Deep Inelastic Scattering or Small- x Physics, Higher-Order Perturbative Calculations

ARXIV EPRINT: [2308.02449](https://arxiv.org/abs/2308.02449)

Contents

1	Introduction	1
2	Leading-order cross section	3
3	Virtual next-to-leading order corrections	11
3.1	Self-energy corrections	11
3.2	Vertex corrections	17
3.3	Antiquark vertex corrections	23
3.4	Instantaneous four-fermion interaction	29
3.5	Instantaneous $gq\gamma q$ interaction	31
3.6	Quark field-strength renormalization	34
4	Ultraviolet divergences	35
4.1	Longitudinal polarization	36
4.2	Transverse polarization	38
4.3	Contribution to the cross section due to ultraviolet counterterms	43
5	Real next-to-leading order corrections	43
5.1	Initial-state radiation	43
5.2	Final-state radiation	45
6	Infrared safety in the initial state	48
6.1	Collinear divergences from initial-state radiation	49
6.2	From parton to hadron level	50
7	Infrared safety in the final state	53
7.1	Jet algorithm	53
7.2	Gluon inside the jet	54
7.3	Gluon outside the jet	57
8	High-energy resummation	58
8.1	Leftovers from ultraviolet- and collinear subtractions	59
8.2	Virtual contributions	60
8.3	Real contributions	62
8.4	JIMWLK	63
9	Next-to-leading order cross section	65
9.1	Virtual contributions	68
9.1.1	Longitudinal polarization	68
9.1.2	Transverse polarization	76
9.2	Real NLO corrections	82
9.2.1	Longitudinal polarization	82
9.2.2	Transverse polarization	88
10	Conclusions	93

A	Transverse integral identities	95
B	Dirac algebra	99
C	Example calculation	100
D	Ultraviolet behavior of amplitude \mathcal{M}_{V2}	105
E	Quark field-strength renormalization	106

1 Introduction

In order to apply Quantum Chromodynamics (QCD) to the analysis of collider experiments with hadrons, the standard approach is to rely on collinear factorization. A hard scale μ justifies a perturbative treatment of the underlying partonic hard scattering process, while the hadron structure is parameterized by parton distribution functions (PDFs) or fragmentation functions (FFs). Using the Dokshitzer-Gribov-Lipatov-Altarelli-Parisi (DGLAP) equations [1–3], the scale dependence of the PDFs and FFs can be perturbatively calculated, resumming large collinear logarithms in the ratio μ^2/μ_0^2 of the hard scale and the hadronic one.

However, collinear factorization is known to break down whenever there is an additional large ratio of scales in the process under consideration. For example, it is implicitly assumed that the center-of-mass energy \sqrt{s} is of the same order as the hard scale μ . At high energies or low $x \sim \mu^2/s$, this condition can be violated, and it becomes necessary to perform an additional resummation of large high-energy- or rapidity logarithms $\alpha_s \ln s/\mu^2 \sim \alpha_s \ln 1/x \gg 1$. A commonly used framework to do so is High-Energy Factorization (HEF) [4–6], in which the Balitsky-Fadin-Kuraev-Lipatov (BFKL) equations [7, 8] are used to resum the high-energy logarithms on top of the collinear ones already resummed by DGLAP.

In this paper, we work within another framework applicable at small x , known as the Color Glass Condensate (CGC) [9–19]. The CGC is an effective theory based upon the separation of fast and slow gluon fields in a highly boosted proton or nucleus (a shockwave). Only the former are regarded as quantum fields, while the latter are integrated out and treated as a semiclassical background field with a characteristic scale Q_s . This scale is known as the saturation scale, because it marks the onset of a regime in which nonlinear gluon recombinations counteract the exponential growth of the gluon density predicted by BFKL [20]. The renormalization group evolution associated with the CGC effective theory leads to the nonlinear Balitsky, Kovchegov, Jalilian-Marian, Iancu, McLerran, Weigert, Leonidov, Kovner or BK-JIMWLK evolution equations [12–19, 21–24]. In a sense, JIMWLK can be regarded as the generalization to the nonlinear saturation regime of the linear BFKL evolution, to which it corresponds in the hard scattering limit $k_T^2 \gg Q_s^2$, with k_T the typical transverse momentum of the small- x gluons. Moreover, in contrast to BFKL approaches such as HEF, the CGC in general does not factorize in terms of a single unintegrated gluon distribution. Instead, it incorporates *all* operators of ‘genuine-twist’ Q_s^2/μ^2 [25, 26].

Although there have been many hints, conclusive experimental proof of saturation is still lacking, see for instance [27] and references therein. After all, it is an effect hidden in a corner of phase space. Precise theoretical predictions are, therefore, essential, and since the last decade a lot of progress has been made to compute several relevant processes in the saturation regime at next-to-leading order (NLO) accuracy. Nowadays, the impact factors are known for single inclusive hadron production in proton-nucleus collisions [28, 29], inclusive deep-inelastic scattering (DIS) [30–35], DIS with massive quarks [36–38], exclusive vector meson production in DIS [39–42], photon plus dijet production in DIS [43], diffractive dijet or dihadron production in DIS [44, 45], inclusive dijet [46] or dihadron [47, 48] production in DIS, semi-inclusive DIS [49], and inclusive dijet photoproduction [50]. The next-to-leading logarithmic extension of the JIMWLK equations has been studied in refs. [51–54]. Finally, results for multiparticle production at tree level were obtained in [55–60]. We will not attempt to list all NLO calculations in other approaches to low- x physics; a recent example in BFKL can be found in ref. [61].

Here, we are interested in the production of a Drell-Yan [62] pair and a jet, i.e., $p + A \rightarrow \gamma^*/Z + X \rightarrow \ell^+ + \ell^- + \text{jet} + X$. At leading order (LO) in the CGC, the calculation was first performed in ref. [63] and the process further studied in, e.g., refs. [64, 65]. This reaction has also been extensively analyzed within the HEF framework (at LO). In [66], it was used to study different prescriptions for the low- x evolution, expanding the BFKL resummation to take additional physical mechanisms into account. In [67], the HEF calculation was compared with the collinear results at LO and NLO, incorporating initial- and final-state parton showers. In both works, the theoretical predictions were compared with $Z + \text{jet}$ data from the LHCb collaboration [68].

In this work, we contribute to the above-mentioned theory effort by presenting the next-to-leading order calculation for the $p + A \rightarrow \gamma^* + \text{jet} + X$ process at forward rapidities and at high energies. The result equally applies to the production of a Z-boson when replacing the electromagnetic coupling constant. The resulting cross section is easily promoted to the inclusive production of a Drell-Yan pair plus a jet by multiplying with the $\gamma^* \rightarrow \ell^- + \ell^+$ decay rate, provided the angular distribution of the leptons in their rest frame is integrated out [70]. Note that the virtual photon and the jet are required to be sufficiently close in rapidity such that BFKL ladders à la Mueller-Navelet [69] can be disregarded, or parametrically: $\Delta\eta_{\gamma^*-\text{jet}} \ll 1/\alpha_s$.

In the kinematics under consideration, a quark or gluon carrying a longitudinal momentum fraction x_p from the ‘projectile’ proton, probes the low- x_A gluon distribution of the ‘target’ proton or nucleus. This motivates us to work in an approximation known as the hybrid or dilute-dense factorization scheme [71, 72], in which the partonic structure of the projectile proton can be parameterized with collinear PDFs, while the CGC is applied to the gluon structure of the target.¹ In spirit, this hybrid scheme is in fact very similar to the dipole picture [74, 75] used in deep-inelastic scattering. In particular, it allows one to formulate the $p + A \rightarrow \gamma^* + \text{jet} + X$ cross section as a convolution of the projectile

¹In the recently appeared work [73], the hybrid approach has been generalized to include transverse-momentum dependence also on the projectile side.

quark PDF with the perturbative $q \rightarrow \gamma^* + q(+g)$ splitting inside the semiclassical color background field of the target, described by the CGC. In this work, we limit ourselves to the quark channel, and perform the calculation using light-cone perturbation theory (LCPT) [76–78]. We refer to [33] for a very clear presentation of LCPT in the context of the dipole picture and the CGC.

As in most higher-order calculations, we will encounter different classes of divergences. We will use the standard approach of dimensional regularization [79] to treat ultraviolet (UV) and infrared (IR) singularities. At the present perturbative order, the former only appear in the loop diagrams, and will be shown to cancel in the total virtual NLO contribution. Infrared or, in this case, collinear divergences, appear both in virtual diagrams (more specifically in the asymptotic quark self-energy corrections), and on the cross section level after integrating over the momentum of the radiated gluon. The poles stemming from collinear gluon radiation in the initial state will be shown to cancel with the DGLAP evolution of the incoming quark, while those in the final state will be regulated by a jet definition. Finally, we will regularize high-energy or rapidity divergences with a cutoff method, as is customary in CGC calculations, and demonstrate how they are absorbed in the JIMWLK evolution of the target.

The paper is organized as follows: we start with the derivation of the cross section at leading order in section 2, which allows us to introduce the conventions of our light-cone perturbation theory approach to the CGC. In section 3, we list all the one-loop virtual diagrams and their corresponding amplitudes. The cancellation of the ultraviolet divergences which they contain is then treated in section 4. In the next section, 5, we present the results of all the real radiative corrections to the cross section. The treatment of the corresponding collinear singularities in the initial and final state is discussed in sections 6 and 7, respectively. In section 8, we show how the remaining rapidity singularities can be absorbed into the JIMWLK evolution of the leading-order cross section, after which we present the completely finite total cross section in section 9. We conclude with a discussion of the applications of our calculation and further research directions. Readers interested in the technicalities of deriving the one-loop amplitudes in our framework are referred to the appendix, section C, where the calculation of one virtual diagram is presented in full detail.

2 Leading-order cross section

In this first section, we briefly review the leading-order (LO) calculation of inclusive forward virtual photon plus jet production ($p + A \rightarrow \gamma^* + \text{jet} + X$). Along the way, we will specify the notations and conventions that we use throughout this work. First and foremost, let us introduce our convention for light-cone (LC) momenta, namely:

$$k^+ = \frac{k_0 + k_3}{\sqrt{2}} \quad \text{and} \quad k^- = \frac{k_0 - k_3}{\sqrt{2}}, \tag{2.1}$$

where 3 is the direction along the beam line. Transverse momenta or coordinates are always written in boldface, and directly evaluated in Euclidean space. The metric is, therefore, defined by the scalar product:

$$k \cdot p = k^+ p^- + k^- p^+ - \mathbf{k} \cdot \mathbf{p}. \tag{2.2}$$

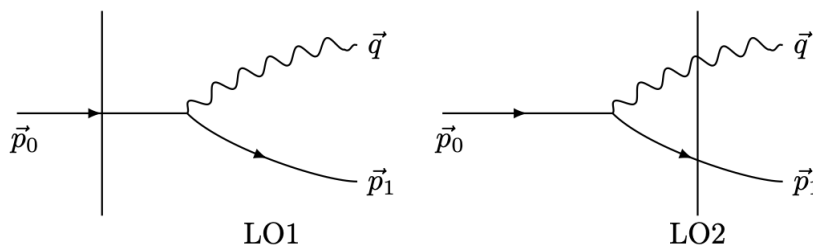


Figure 1. The two Feynman graphs for the LO partonic $q + A \rightarrow \gamma^* + q$ process. The highly boosted target A , a shockwave, is represented by the full vertical line.

In light-cone perturbation theory, all particle momenta obey the mass-shell condition: $k^- = (\mathbf{k}^2 + m^2)/2k^+$. For this reason, we can use the compact notation $\vec{k} = (k^+, \mathbf{k})$ for a generic momentum vector.

Figure 1 depicts the two Feynman diagrams corresponding to the partonic $q + A \rightarrow \gamma^* + q$ process. All fermions are taken to be massless, and we choose a frame in which the momentum of the incoming quark is oriented along the positive light-cone direction:

$$\vec{p}_0 = (p_0^+, \mathbf{p}_0 = 0). \tag{2.3}$$

As is conventional, the gluon fields are described using the light-cone gauge $A^+ = 0$. Such a gauge condition cannot, however, be set for the virtual photon field, which has a virtual mass M and is described by the Proca equation. Taking $\vec{q} = (q^+, \mathbf{q})$ to be the momentum of the virtual photon, we make the following choice for its transverse ($\lambda = 1, 2$) and longitudinal polarization vectors ϵ_λ^μ resp. ϵ_0^μ :

$$\epsilon_\lambda^\mu = \left(0, \frac{\mathbf{q} \cdot \epsilon_\lambda}{q^+}, \epsilon_\lambda\right) \quad \text{and} \quad \epsilon_0^\mu = \left(\frac{q^+}{M}, \frac{\mathbf{q}^2 - M^2}{2q^+M}, \frac{\mathbf{q}}{M}\right). \tag{2.4}$$

Furthermore, in what follows we work with linear transverse polarization vectors $\epsilon_\lambda^i = \delta^{i\lambda}$.

In D dimensions, the leading-order partonic cross section is given by:

$$d\hat{\sigma}_{\text{LO}} = \frac{\mu^{2(4-D)}}{2p_0^+} \frac{dp_1^+ d^{D-2}\mathbf{p}_1 \theta(p_1^+)}{(2\pi)^{D-1} 2p_1^+} \frac{dq^+ d^{D-2}\mathbf{q} \theta(q^+)}{(2\pi)^{D-1} 2q^+} 2\pi \delta(p_0^+ - p_1^+ - q^+) \frac{1}{D-2} |\mathcal{M}_{\text{LO}}|^2, \tag{2.5}$$

where $\vec{p}_1 = (p_1^+, \mathbf{p}_1)$ is the momentum of the outgoing quark, and where $\mathcal{M}_{\text{LO}} = \mathcal{M}_{\text{LO1}} + \mathcal{M}_{\text{LO2}}$ is the sum of the two amplitudes associated with the diagrams in figure 1. From eq. (2.5), the pp - or pA cross section is obtained after convolving with the quark PDF and averaging over the semiclassical gluon fields in the target (an operation we denote with $\langle \dots \rangle$):

$$\begin{aligned} d\sigma_{\text{LO}} &= \int \frac{dp_0^+}{p_0^+} \frac{p_0^+}{p_p^+} f_q\left(\frac{p_0^+}{p_p^+}, \mu^2\right) \langle d\hat{\sigma}_{\text{LO}} \rangle, \\ &= x_p f_q(x_p, \mu^2) \frac{2\pi \mu^{2(4-D)}}{2(p_0^+)^2} \frac{dp_1^+ d^{D-2}\mathbf{p}_1 \theta(p_1^+)}{(2\pi)^{D-1} 2p_1^+} \frac{dq^+ d^{D-2}\mathbf{q} \theta(q^+)}{(2\pi)^{D-1} 2q^+} \\ &\quad \times \frac{1}{D-2} \langle |\mathcal{M}_{\text{LO1}} + \mathcal{M}_{\text{LO2}}|^2 \rangle \Big|_{p_0^+ = p_1^+ + q^+}. \end{aligned} \tag{2.6}$$

In the above equation, $x_p = p_0^+/p_p^+$ is the plus-momentum fraction of the quark with respect to its parent (projectile) proton.

As already mentioned, we work in the dipole picture, formulated in LCPT. In this approach, the projectile dynamics take place on a much shorter timescale than those of the target. Therefore, on the partonic level the projectile can be described by a Fock state with perturbatively calculable dynamics, interacting with a static external potential provided by the target. The amplitudes \mathcal{M} are defined as follows:

$${}_f\langle \mathbf{q}(\vec{p}_1)\gamma^*(\vec{q})|\hat{F} - 1|\mathbf{q}(\vec{p}_0)\rangle_i = 2\pi\delta(p_0^+ - p_1^+ - q^+)\mathcal{M}, \quad (2.7)$$

where the external potential \hat{F} (-1 for reasons of unitarity) is evaluated between the Fock states of the incoming (i) quark, and the outgoing (f) quark together with the virtual photon. The first step is to calculate the perturbative evolution of the asymptotic Fock states to and from the position of the shockwave at $x^+ = 0$. Indeed, the two interacting or ‘dressed’ Fock states $|\dots\rangle_{i,f}$ are related to eigenstates $|\dots\rangle$ of the free Hamiltonian through the time evolution:

$$\begin{aligned} |\mathbf{q}(\vec{p}_0)\rangle_i &= \hat{\mathcal{U}}(0, -\infty)|\mathbf{q}(\vec{p}_0)\rangle, \\ {}_f\langle \mathbf{q}(\vec{p}_1)\gamma^*(\vec{q})| &= \langle \mathbf{q}(\vec{p}_1)\gamma^*(\vec{q})|\hat{\mathcal{U}}(+\infty, 0), \end{aligned} \quad (2.8)$$

where $\hat{\mathcal{U}}$ is the LC-time evolution operator defined as:

$$\hat{\mathcal{U}}(b, a) \equiv \hat{T} \exp\left(-i \int_a^b dx^+ \hat{\mathcal{H}}(x^+)\right), \quad (2.9)$$

with \hat{T} the (LC)-time ordering operator and $\hat{\mathcal{H}}(x^+)$ the LC Hamiltonian. In the interaction picture, the time evolution of the latter is given by:

$$\hat{\mathcal{H}}(x^+) = e^{i\hat{H}_0 x^+} \hat{V} e^{-i\hat{H}_0 x^+}, \quad (2.10)$$

with \hat{H}_0 the free Hamiltonian, and \hat{V} the collection of interaction terms. Acting with (2.9) on the Fock state $|\mathbf{q}(\vec{p}_0)\rangle$, which is per definition an eigenstate of the free Hamiltonian with $\hat{H}_0|\mathbf{q}(\vec{p}_0)\rangle = p_0^-|\mathbf{q}(\vec{p}_0)\rangle$, we obtain:

$$\begin{aligned} |\mathbf{q}(\vec{p}_0)\rangle_i &= \hat{\mathcal{U}}(0, -\infty)|\mathbf{q}(\vec{p}_0)\rangle \\ &= |\mathbf{q}(\vec{p}_0)\rangle - i \int_{-\infty}^0 dx^+ \text{PS}(\vec{\ell}, \vec{k}) |\mathbf{q}(\vec{\ell})\gamma^*(\vec{k})\rangle \\ &\quad \times \langle \mathbf{q}(\vec{\ell})\gamma^*(\vec{k})|e^{i(\ell^- + k^-)x^+} \hat{V} e^{-ip_0^- x^+} |\mathbf{q}(\vec{p}_0)\rangle \\ &= |\mathbf{q}(\vec{p}_0)\rangle + \int \text{PS}(\vec{\ell}, \vec{k}) \frac{\langle \mathbf{q}(\vec{\ell})\gamma^*(\vec{k})|\hat{V}|\mathbf{q}(\vec{p}_0)\rangle}{p_0^- - \ell^- - k^- + i0^+} |\mathbf{q}(\vec{\ell})\gamma^*(\vec{k})\rangle, \end{aligned} \quad (2.11)$$

up to the perturbative order we are interested in, and where we have introduced the following notation for the phase-space integration measure:

$$\int \text{PS}(\vec{\ell}) = \mu^{4-D} \int \frac{d^{D-1}\vec{\ell}\theta(\ell^+)}{(2\pi)^{D-1}2\ell^+}. \quad (2.12)$$

Likewise, at leading order:

$$\begin{aligned}
 \langle \mathbf{q}(\vec{p}_1)\gamma^*(\vec{q})|\hat{\mathcal{U}}(+\infty, 0) &= \langle \mathbf{q}(\vec{p}_1)\gamma^*(\vec{q})| \\
 &+ \int \text{PS}(\vec{\ell})\langle \mathbf{q}(\vec{p}_1)\gamma^*(\vec{q})|\exp\left(-i\int_0^{+\infty} dx^+\hat{\mathcal{H}}(x^+)\right)|\mathbf{q}(\vec{\ell})\rangle\langle \mathbf{q}(\vec{\ell})|, \\
 &= \langle \mathbf{q}(\vec{p}_1)\gamma^*(\vec{q})| + \int \text{PS}(\vec{\ell})\frac{\langle \mathbf{q}(\vec{p}_1)\gamma^*(\vec{q})|\hat{V}|\mathbf{q}(\vec{\ell})\rangle}{p_1^+ + q^- - \ell^- + i0^+}\langle \mathbf{q}(\vec{\ell})|.
 \end{aligned} \tag{2.13}$$

Combining (2.7), (2.11), and (2.13), we obtain:

$$\begin{aligned}
 \int \langle \mathbf{q}(\vec{p}_1)\gamma^*(\vec{q})|\hat{F}-1|\mathbf{q}(\vec{p}_0)\rangle_i &= \langle \mathbf{q}(\vec{p}_1)\gamma^*(\vec{q})|\hat{F}-1|\mathbf{q}(\vec{p}_0)\rangle \\
 &+ \int \text{PS}(\vec{\ell})\frac{\langle \mathbf{q}(\vec{p}_1)\gamma^*(\vec{q})|\hat{V}|\mathbf{q}(\vec{\ell})\rangle}{p_1^- + q^- - \ell^- + i0^+}\langle \mathbf{q}(\vec{\ell})|\hat{F}-1|\mathbf{q}(\vec{p}_0)\rangle \\
 &+ \int \text{PS}(\vec{\ell}, \vec{k})\frac{\langle \mathbf{q}(\vec{\ell})\gamma^*(\vec{k})|\hat{V}|\mathbf{q}(\vec{p}_0)\rangle}{p_0^- - \ell^- - k^- + i0^+}\langle \mathbf{q}(\vec{p}_1)\gamma^*(\vec{q})|\hat{F}-1|\mathbf{q}(\vec{\ell})\gamma^*(\vec{k})\rangle.
 \end{aligned} \tag{2.14}$$

In the eikonal approximation we are using, the potential \hat{F} can never change the particle content of the Fock states, which are orthogonal. The first term in the above equation, therefore, disappears. The second and third lines correspond to the first and second diagram in figure 1, respectively. In the former, the incoming quark scatters off the external potential after which it emits a virtual photon. In the latter, the photon is emitted before the interaction with the potential. We will now evaluate eq. (2.14) further, starting with the perturbative interaction terms in the numerators. The relevant piece of the interaction part of the QED LC Hamiltonian is, with the short-hand notations $\int d^{D-3}\vec{x} = \int dx^- d^{D-2}\mathbf{x}$ and $\vec{x} = (x^-, \mathbf{x})$:

$$\hat{V} = \mu^{D-4} \int d^{D-3}\vec{x} : g_{\text{em}}\bar{\psi}(\vec{x})\mathcal{A}(\vec{x})\psi(\vec{x}) :, \tag{2.15}$$

where $::$ denotes normal ordering. Using the definitions of the fermion- and boson fields in terms of the creation- and annihilation operators:

$$\begin{aligned}
 \psi(\vec{x}) &= \int \text{PS}(\vec{k})(e^{-i\vec{k}\cdot\vec{x}}u(\vec{k})b_{\vec{k}} + e^{i\vec{k}\cdot\vec{x}}v(\vec{k})d_{\vec{k}}^\dagger), \\
 \mathcal{A}(\vec{x}) &= \int \text{PS}(\vec{k})(e^{-i\vec{k}\cdot\vec{x}}\not{\epsilon}(\vec{k})a_{\vec{k}} + e^{i\vec{k}\cdot\vec{x}}\not{\epsilon}^*(\vec{k})a_{\vec{k}}^\dagger),
 \end{aligned} \tag{2.16}$$

it is then a straightforward exercise to show that:

$$\begin{aligned}
 \langle \mathbf{q}(\vec{\ell})\gamma^*(\vec{k})|\hat{V}|\mathbf{q}(\vec{p}_0)\rangle &= \langle 0|b_{\vec{\ell}}a_{\vec{k}}\hat{V}b_{\vec{p}_0}^\dagger|0\rangle, \\
 &= (2\pi)^{D-1}\delta^{(D-1)}(\vec{p}_0 - \vec{\ell} - \vec{k})g_{\text{em}}\bar{u}(\vec{\ell})\not{\epsilon}^*(\vec{k})u(\vec{p}_0).
 \end{aligned} \tag{2.17}$$

We note that the Fock states are normalized the usual way with the help of the (anti)-commutation relations:

$$\begin{aligned}
 \{b_{\vec{k}}, b_{\vec{p}}^\dagger\} &= \{d_{\vec{k}}, d_{\vec{p}}^\dagger\} = (2k^+)(2\pi)^{D-1}\delta^{(D-1)}(\vec{k} - \vec{p}), \\
 [a_{\vec{k}}, a_{\vec{p}}^\dagger] &= (2k^+)(2\pi)^{D-1}\delta^{(D-1)}(\vec{k} - \vec{p}),
 \end{aligned} \tag{2.18}$$

such that, demanding that for empty states $\langle 0|0\rangle = 1$, it follows that, e.g.,

$$\langle \mathbf{q}(\vec{\ell}_2)\gamma^*(\vec{k}_2)|\mathbf{q}(\vec{\ell}_1)\gamma^*(\vec{k}_1)\rangle = 2k_1^+(2\pi)^{D-1}\delta^{(D-1)}(\vec{k}_1 - \vec{k}_2)2\ell_1^+(2\pi)^{D-1}\delta^{(D-1)}(\vec{\ell}_1 - \vec{\ell}_2). \tag{2.19}$$

In order not to clutter the formulas, we will always suppress spinor indices, fundamental color indices, and fermion helicity indices.

We now proceed by simplifying the Dirac algebra in (2.14). Keeping the anticommutation relation $\{\gamma^\mu, \gamma^\nu\} = 2g^{\mu\nu}$ in mind, we introduce the projectors $\mathcal{P}_G = \gamma^- \gamma^+ / 2$ and $\mathcal{P}_B = \gamma^+ \gamma^- / 2$ which allow us to define ‘good’ and ‘bad’ spinor components:

$$\begin{aligned} u(\vec{k}) &= (\mathcal{P}_G + \mathcal{P}_B)u(\vec{k}) \equiv u_G(\vec{k}) + u_B(\vec{k}), \\ \bar{u}(\vec{k}) &= \bar{u}(\vec{k})(\mathcal{P}_G + \mathcal{P}_B) \equiv \bar{u}_B(\vec{k}) + \bar{u}_G(\vec{k}). \end{aligned} \quad (2.20)$$

The same definitions hold for the antifermion spinors $v(\vec{k})$. The Dirac equation $\not{k}u(\vec{k}) = 0$ then introduces a dependence between both components:

$$u_B(\vec{k}) = \frac{\gamma^+}{2k^+} \mathbf{k} \cdot \boldsymbol{\gamma} u_G(k^+), \quad (2.21)$$

with exactly the same equation holding for the antifermion spinors, at least in the massless case. Note that the good spinors only depend on the plus-momentum component.

Relation (2.21) allows us to rewrite a generic spinor product $\bar{u}(\vec{k}_1)\not{\epsilon}(\vec{k}_3)u(\vec{k}_2)$ as:

$$\begin{aligned} &\bar{u}(\vec{k}_1)\not{\epsilon}(\vec{k}_3)u(\vec{k}_2) \\ &= \bar{u}_G(k_1^+) \left(1 + \frac{\mathbf{k}_1 \cdot \boldsymbol{\gamma} \gamma^+}{2k_1^+}\right) \left(\gamma^+ \epsilon^-(\vec{k}_3) + \gamma^- \epsilon^+(\vec{k}_3) - \boldsymbol{\gamma} \cdot \boldsymbol{\epsilon}(\vec{k}_3)\right) \left(\frac{\gamma^+ \mathbf{k}_2 \cdot \boldsymbol{\gamma}}{2k_2^+} + 1\right) u_G(k_2^+). \end{aligned} \quad (2.22)$$

Applying the above identity to the spinor product in (2.17), using the polarization vectors (2.4), we find in the case of a transversely polarized photon:

$$\begin{aligned} \langle \mathbf{q}(\vec{\ell}) \boldsymbol{\gamma}_\lambda^*(\vec{k}) | \hat{V} | \mathbf{q}(\vec{p}_0) \rangle &= g_{\text{em}} (2\pi)^{D-1} \delta^{(D-1)}(\vec{p}_0 - \vec{\ell} - \vec{k}) \\ &\times \bar{u}_G(\ell^+) \gamma^+ \left(\frac{\mathbf{k}^\lambda}{k^+} + \frac{\ell^\lambda}{2\ell^+} \boldsymbol{\gamma}^\lambda \boldsymbol{\gamma}^\lambda + \frac{\mathbf{p}^\lambda}{2p_0^+} \boldsymbol{\gamma}^\lambda \boldsymbol{\gamma}^\lambda \right) u_G(p_0^+), \end{aligned} \quad (2.23)$$

since from $\{\gamma^\mu, \gamma^\nu\} = 2g^{\mu\nu}$ it follows that $\gamma^+ \gamma^+ = 0$ and $\{\gamma^\pm, \gamma^i\} = 0$. For this same reason, it is easy to see that $\bar{u}_G \boldsymbol{\gamma}^i u_G = 0$. Finally, for the momentum configurations in (2.14), we end up with:

$$\begin{aligned} \langle \mathbf{q}(\vec{p}_1) \boldsymbol{\gamma}_\lambda^*(\vec{q}) | \hat{V} | \mathbf{q}(\vec{\ell}) \rangle &= g_{\text{em}} (2\pi)^{D-1} \delta^{(D-1)}(\vec{p}_1 + \vec{q} - \vec{\ell}) \\ &\times \frac{p_1^+ \mathbf{q}^\lambda - q^+ \mathbf{p}_1^\lambda}{2p_1^+(p_1^+ + q^+)} \bar{u}_G(p_1^+) \gamma^+ \left[\left(1 + \frac{2p_1^+}{q^+}\right) \delta^{\lambda\bar{\lambda}} - i\sigma^{\lambda\bar{\lambda}} \right] u_G(\ell^+), \end{aligned} \quad (2.24)$$

and:

$$\begin{aligned} \langle \mathbf{q}(\vec{\ell}) \boldsymbol{\gamma}_\lambda^*(\vec{k}) | \hat{V} | \mathbf{q}(\vec{p}_0) \rangle &= g_{\text{em}} (2\pi)^{D-1} \delta^{(D-1)}(\vec{p}_0 - \vec{\ell} - \vec{k}) \\ &\times \frac{-\ell^\lambda}{2\ell^+} \bar{u}_G(\ell^+) \gamma^+ \left[\left(1 + \frac{2\ell^+}{k^+}\right) \delta^{\lambda\bar{\lambda}} - i\sigma^{\lambda\bar{\lambda}} \right] u_G(p_0^+), \end{aligned} \quad (2.25)$$

In the above formulas, we replaced the product of two transverse gamma matrices with:

$$\boldsymbol{\gamma}^i \boldsymbol{\gamma}^j = -\delta^{ij} - i\sigma^{ij}, \quad (2.26)$$

where the Dirac sigma is defined as $\sigma^{ij} = (i/2)[\gamma^i, \gamma^j]$.

Let us now turn to the interaction of the projectile with the target, which is, as explained above, described by an external potential. Moreover, the Color Glass Condensate approach asserts that, in the eikonal approximation, this potential is built from Wilson lines along the projectile direction x^+ :

$$\begin{aligned} U_{\mathbf{x}} &\equiv \mathcal{P} \exp \left(-ig_s \int_{-\infty}^{+\infty} dx^+ A_a^-(x^+, \mathbf{x}) t^a \right), \\ W_{\mathbf{x}} &\equiv \mathcal{P} \exp \left(-ig_s \int_{-\infty}^{+\infty} dx^+ A_a^-(x^+, \mathbf{x}) T^a \right), \end{aligned} \quad (2.27)$$

where \mathcal{P} is the path-ordering operator, g_s is the strong coupling, A_a^- the minus-component of the gluon field, and where t^a and T^a are the generators of $SU(N_c)$ in the fundamental and adjoint representation, respectively. The precise form of the potential depends on the Fock state. In transverse coordinate space, each (anti)quark and gluon in the projectile adds a Wilson line to the potential that inherits the quark or gluon transverse coordinate and color representation. In the present case, the projectile-target interactions in (2.14) are given by:

$$\begin{aligned} \langle \mathbf{q}(\vec{\ell}) | \hat{F} - 1 | \mathbf{q}(\vec{p}_0) \rangle &= 2p_0^+ 2\pi\delta(p_0^+ - \ell^+) \int_{\mathbf{x}} e^{-i\mathbf{x}\cdot\vec{\ell}} (U_{\mathbf{x}} - 1), \\ \langle \mathbf{q}(\vec{p}_1) \gamma^*(\vec{q}) | \hat{F} - 1 | \mathbf{q}(\vec{\ell}) \gamma^*(\vec{k}) \rangle &= 2p_1^+ 2\pi\delta(p_1^+ - \ell^+) 2q^+ 2\pi\delta(q^+ - k^+) \\ &\quad \times \int_{\mathbf{x}} e^{-i\mathbf{x}\cdot(\mathbf{p}_1 - \vec{\ell})} (U_{\mathbf{x}} - 1), \end{aligned} \quad (2.28)$$

where we introduced the short-hand notation $\int_{\mathbf{x}} = \mu^{D-4} \int d^{D-2}\mathbf{x}$ for the integration over $D-2$ transverse coordinate space. Moreover, in the present eikonal approximation, the interaction preserves plus-momentum and the helicity. Combining (2.7), (2.14), (2.24), (2.25), and (2.28), we can finally write down the expressions for the leading-order amplitudes:

$$\begin{aligned} \mathcal{M}_{\text{LO1}}^\lambda &= \frac{-g_{\text{em}} q^+ \mathbf{P}_\perp^\lambda}{p_0^+ \mathbf{P}_\perp^2 + p_1^+ M^2} \bar{u}_G(p_1^+) \gamma^+ \mathcal{S}^{\lambda\bar{\lambda}} \left(1 + \frac{2p_1^+}{q^+} \right) u_G(p_0^+) \int_{\mathbf{x}} e^{-i\mathbf{k}_\perp \cdot \mathbf{x}} (U_{\mathbf{x}} - 1), \\ \mathcal{M}_{\text{LO2}}^\lambda &= \frac{-g_{\text{em}} q^+ \mathbf{q}^\lambda}{p_0^+ \mathbf{q}^2 + p_1^+ M^2} \bar{u}_G(p_1^+) \gamma^+ \mathcal{S}^{\lambda\bar{\lambda}} \left(1 + \frac{2p_1^+}{q^+} \right) u_G(p_0^+) \int_{\mathbf{x}} e^{-i\mathbf{k}_\perp \cdot \mathbf{x}} (U_{\mathbf{x}} - 1), \end{aligned} \quad (2.29)$$

where we have introduced the following momentum combinations, which will be used throughout this work:

$$\mathbf{P}_\perp \equiv \frac{q^+ \mathbf{p}_1 - p_1^+ \mathbf{q}}{p_0^+} \quad \text{and} \quad \mathbf{k}_\perp \equiv \mathbf{p}_1 + \mathbf{q}, \quad (2.30)$$

as well as the definition:

$$\mathcal{S}^{\lambda\bar{\lambda}}(\xi) \equiv \xi \delta^{\lambda\bar{\lambda}} \mathbb{1}_4 - i\sigma^{\lambda\bar{\lambda}}. \quad (2.31)$$

A similar calculation for the longitudinally polarized virtual photon gives:

$$\begin{aligned} \mathcal{M}_{\text{LO1}}^0 &= \frac{g_{\text{em}} p_0^+ \mathbf{P}_\perp^2 - p_1^+ M^2}{M p_0^+ \mathbf{P}_\perp^2 + p_1^+ M^2} \bar{u}_G(p_1^+) \gamma^+ u_G(p_0^+) \int_{\mathbf{x}} e^{-i\mathbf{k}_\perp \cdot \mathbf{x}} (U_{\mathbf{x}} - 1), \\ \mathcal{M}_{\text{LO2}}^0 &= -\frac{g_{\text{em}} p_0^+ \mathbf{q}^2 - p_1^+ M^2}{M p_0^+ \mathbf{q}^2 + p_1^+ M^2} \bar{u}_G(p_1^+) \gamma^+ u_G(p_0^+) \int_{\mathbf{x}} e^{-i\mathbf{k}_\perp \cdot \mathbf{x}} (U_{\mathbf{x}} - 1). \end{aligned} \quad (2.32)$$

Multiplying the amplitudes (2.29) and (2.32) with their complex conjugate, and summing over the polarization indices λ of the transversely polarized virtual photon or vector boson, we arrive at:

$$\sum_{\lambda} |\mathcal{M}_{\text{LO1}}^{\lambda} + \mathcal{M}_{\text{LO2}}^{\lambda}|^2 = g_{\text{em}}^2 N_c \left(\frac{q^+ \mathbf{q}}{p_0^+ \mathbf{q}^2 + p_1^+ M^2} + \frac{q^+ \mathbf{P}_{\perp}}{p_0^+ \mathbf{P}_{\perp}^2 + p_1^+ M^2} \right)^2 |\mathcal{S}_{\text{LO}}^{\text{T}, \lambda' \bar{\lambda}}|^2 \times \int_{\mathbf{x}, \mathbf{x}'} e^{-i \mathbf{k}_{\perp} \cdot (\mathbf{x} - \mathbf{x}')} (s_{\mathbf{x} \mathbf{x}'} + 1), \quad (2.33)$$

and:

$$|\mathcal{M}_{\text{LO1}}^0 + \mathcal{M}_{\text{LO2}}^0|^2 = g_{\text{em}}^2 \frac{N_c}{M^2} \left(\frac{p_0^+ \mathbf{P}_{\perp}^2 - p_1^+ M^2}{p_0^+ \mathbf{P}_{\perp}^2 + p_1^+ M^2} - \frac{p_0^+ \mathbf{q}^2 - p_1^+ M^2}{p_0^+ \mathbf{q}^2 + p_1^+ M^2} \right)^2 |\mathcal{S}_{\text{LO}}^0|^2 \times \int_{\mathbf{x}, \mathbf{x}'} e^{-i \mathbf{k}_{\perp} \cdot (\mathbf{x} - \mathbf{x}')} (s_{\mathbf{x} \mathbf{x}'} + 1). \quad (2.34)$$

In the above results, we used $s_{\mathbf{x} \mathbf{x}'}$ to denote the dipole color operator:

$$s_{\mathbf{x} \mathbf{x}'} = \frac{1}{N_c} \text{Tr}(U_{\mathbf{x}} U_{\mathbf{x}'}^{\dagger}), \quad (2.35)$$

where we take the trace over the fundamental $\text{SU}(N_c)$ color indices (which we do not write explicitly). The traces over spinor indices are given by:

$$|\mathcal{S}_{\text{LO}}^{\text{T}, \lambda' \bar{\lambda}}|^2 \equiv \text{Tr} \left[\bar{u}_G(p_0^+) \gamma^+ \mathcal{S}^{\lambda \lambda'} \left(1 + \frac{2p_1^+}{q^+} \right)^{\dagger} u_G(p_1^+) \bar{u}_G(p_1^+) \gamma^+ \mathcal{S}^{\lambda \bar{\lambda}} \left(1 + \frac{2p_1^+}{q^+} \right) u_G(p_0^+) \right], \quad (2.36)$$

$$|\mathcal{S}_{\text{LO}}^0|^2 \equiv \text{Tr} \left[\bar{u}_G(p_0^+) \gamma^+ u_G(p_1^+) \bar{u}_G(p_1^+) \gamma^+ u_G(p_0^+) \right].$$

Applying the cyclic permutation property of the trace as well as the completeness relation (a summation over fermion spin is understood):

$$u_G(q^+) \bar{u}_G(q^+) \gamma^+ = 2q^+ \mathcal{P}_G, \quad (2.37)$$

we obtain:

$$|\mathcal{S}_{\text{LO}}^{\text{T}, \lambda' \bar{\lambda}}|^2 = \text{Tr} \left[2p_0^+ \mathcal{P}_G \mathcal{S}^{\lambda \lambda'} \left(1 + \frac{2p_1^+}{q^+} \right)^{\dagger} 2p_1^+ \mathcal{P}_G \mathcal{S}^{\lambda \bar{\lambda}} \left(1 + \frac{2p_1^+}{q^+} \right) \right]. \quad (2.38)$$

Since the projector \mathcal{P}_G commutes with transverse gamma matrices, from which the structures $\mathcal{S}^{\lambda \lambda'}$ are built, the above expression further simplifies to:

$$|\mathcal{S}_{\text{LO}}^{\text{T}, \lambda' \bar{\lambda}}|^2 = 4p_0^+ p_1^+ \text{Tr} \left[\mathcal{P}_G \left(\left(1 + \frac{2p_1^+}{q^+} \right) \delta^{\lambda \lambda'} \mathbf{1}_4 + i \sigma^{\lambda \lambda'} \right) \left(\left(1 + \frac{2p_1^+}{q^+} \right) \delta^{\lambda \bar{\lambda}} \mathbf{1}_4 - i \sigma^{\lambda \bar{\lambda}} \right) \right], \quad (2.39)$$

$$= 4p_0^+ p_1^+ \text{Tr} \left[\mathcal{P}_G \left(\left(1 + \frac{2p_1^+}{q^+} \right)^2 \delta^{\lambda' \bar{\lambda}} \mathbf{1}_4 + \sigma^{\lambda \lambda'} \sigma^{\lambda \bar{\lambda}} + 2i \sigma^{\lambda \lambda'} \left(1 + \frac{2p_1^+}{q^+} \right) \right) \right].$$

Finally, with the help of the identities:

$$\sigma^{\lambda \lambda'} \sigma^{\lambda \bar{\lambda}} = (D - 3) \delta^{\lambda' \bar{\lambda}} \mathbf{1}_4 + i(D - 4) \sigma^{\lambda' \bar{\lambda}}, \quad (2.40)$$

as well as:

$$\text{Tr}(\mathcal{P}_G) = 2, \quad \text{Tr}(\mathcal{P}_G \sigma^{ij}) = 0, \quad (2.41)$$

we end up with:

$$|\mathcal{S}_{\text{LO}}^{\text{T},\lambda'\bar{\lambda}}|^2 = 8p_0^+ p_1^+ \delta^{\lambda'\bar{\lambda}} \left(\left(1 + \frac{2p_1^+}{q^+}\right)^2 + D - 3 \right), \quad (2.42)$$

and similarly

$$|\mathcal{S}_{\text{LO}}^0|^2 = 8p_1^+ p_0^+. \quad (2.43)$$

In appendix B, the most important gamma-matrix identities used in this work are collected.

Combining (2.5), (2.33), (2.34), (2.42), and (2.43), we eventually arrive at the following result for the partonic cross sections:

$$\begin{aligned} \frac{d\hat{\sigma}_{\text{LO}}^{\text{T}}}{dzd\bar{z}d^2\mathbf{P}_\perp d^2\mathbf{k}_\perp} &= \frac{g_{\text{em}}^2 N_c}{(2\pi)^5} \delta(1-z-\bar{z}) \frac{1+(1-z)^2}{z} \left(\frac{\mathbf{P}_\perp}{\mathbf{P}_\perp^2 + \bar{z}M^2} + \frac{\mathbf{q}}{\mathbf{q}^2 + \bar{z}M^2} \right)^2 \\ &\times \int_{\mathbf{x}, \mathbf{x}'} e^{-i\mathbf{k}_\perp \cdot (\mathbf{x} - \mathbf{x}')} (s_{\mathbf{x}\mathbf{x}'} + 1), \end{aligned} \quad (2.44)$$

$$\begin{aligned} \frac{d\hat{\sigma}_{\text{LO}}^{\text{L}}}{dzd\bar{z}d^2\mathbf{P}_\perp d^2\mathbf{k}_\perp} &= \frac{g_{\text{em}}^2 N_c}{(2\pi)^5} \delta(1-z-\bar{z}) \frac{1}{2z\bar{z}M^2} \left(\frac{\mathbf{P}_\perp^2 - \bar{z}M^2}{\mathbf{P}_\perp^2 + \bar{z}M^2} - \frac{\mathbf{q}^2 - \bar{z}M^2}{\mathbf{q}^2 + \bar{z}M^2} \right)^2 \\ &\times \int_{\mathbf{x}, \mathbf{x}'} e^{-i\mathbf{k}_\perp \cdot (\mathbf{x} - \mathbf{x}')} (s_{\mathbf{x}\mathbf{x}'} + 1), \end{aligned} \quad (2.45)$$

defining the momentum fractions $z \equiv q^+/p_0^+$ and $\bar{z} = 1 - z$. In principle, the ‘1’ in the last lines of the above two expressions can be dropped, since performing the integral over \mathbf{x} would yield a delta function forcing $\mathbf{k}_\perp = 0$. But then, remembering definitions (2.30), it is easy to see that the hard parts in the first lines of (2.44) and (2.45) evaluate to zero. Moreover, the dipole $s_{\mathbf{x}\mathbf{x}'}$ quantifies the potential provided by the target and experienced by the projectile. It is built from Wilson lines that depend on the semi-classical gauge fields A^- of the highly boosted target shockwave. These fields carry the information on the target gluon structure, which is at least partially nonperturbative. To indicate that, on the hadronic level, the fields still need to be related to the target properties, for instance using a model or by linking them to gluon transverse momentum dependent PDFs, we write the above mentioned ‘target average’ $\langle \dots \rangle$. Likewise, the incoming quark can be related to its parent proton by convolving the cross section with the quark PDF, and a factor $\frac{\alpha_{\text{em}}}{3\pi} d \ln M^2$ takes the $\gamma^* \rightarrow \ell^+ \ell^-$ splitting into account in the simple scenario where only the total three-momentum and the invariant mass of the lepton pair is measured [70]. We finally obtain:

$$\begin{aligned} &\frac{d\sigma_{\text{LO}}}{dzd\bar{z}d^2\mathbf{P}_\perp d^2\mathbf{k}_\perp d \ln M^2} \\ &= \frac{2\alpha_{\text{em}}^2 N_c}{3\pi} \frac{1}{(2\pi)^4} x_p f_q(x_p, \mu^2) \left[\frac{1+(1-z)^2}{z} \left(\frac{\mathbf{P}_\perp}{\mathbf{P}_\perp^2 + \bar{z}M^2} + \frac{\mathbf{q}}{\mathbf{q}^2 + \bar{z}M^2} \right)^2 \right. \\ &\quad \left. + \frac{1}{2z\bar{z}M^2} \left(\frac{\mathbf{P}_\perp^2 - \bar{z}M^2}{\mathbf{P}_\perp^2 + \bar{z}M^2} - \frac{\mathbf{q}^2 - \bar{z}M^2}{\mathbf{q}^2 + \bar{z}M^2} \right)^2 \right] \int_{\mathbf{x}, \mathbf{x}'} e^{-i\mathbf{k}_\perp \cdot (\mathbf{x} - \mathbf{x}')} \langle s_{\mathbf{x}\mathbf{x}'} + 1 \rangle, \end{aligned} \quad (2.46)$$

in agreement with earlier results in the literature [63, 64].

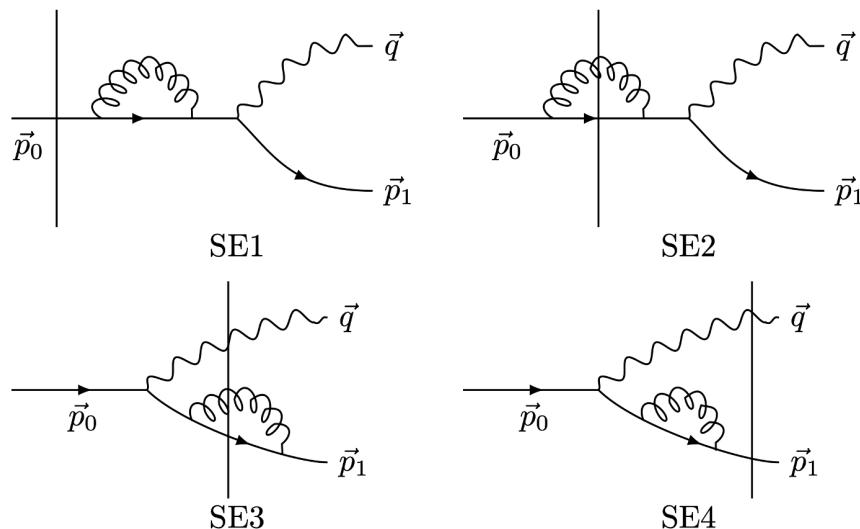


Figure 2. The four virtual contributions with a gluon loop on the quark, which in two cases (SE2 and SE3) scatters off the shockwave. Similar one-loop corrections on the asymptotic incoming or outgoing quark are treated separately in subsection 3.6.

Before turning to the next-to-leading order calculation, we remark that, apart from the universal coupling constant g_{em} , the four amplitudes in (2.29) and (2.32) all contain a spinor structure $\bar{u}_G(p_1^+) \gamma^+ (\dots) u_G(p_0^+)$. In fact, this will also be true for all the NLO amplitudes. For ease of notation, we therefore define the ‘reduced amplitudes’ $\tilde{\mathcal{M}}$:

$$\mathcal{M} = g_{em} \bar{u}_G(p_1^+) \gamma^+ \tilde{\mathcal{M}} u_G(p_0^+), \quad (2.47)$$

with which we will work in what follows. We also define, for later convenience:

$$\mathcal{S}_{LO}^{\lambda\bar{\lambda}} \equiv \mathcal{S}^{\lambda\bar{\lambda}} \left(1 + \frac{2p_1^+}{q^+} \right). \quad (2.48)$$

3 Virtual next-to-leading order corrections

In this section, we review all the one-loop Feynman graphs for the channel $q + A \rightarrow \gamma^* + q$. The corresponding amplitudes are presented in general D dimensions, as many of them contain ultraviolet divergences which will be regulated using dimensional regularization. The resulting UV poles are subtracted from the amplitudes with the help of counterterms that will, in turn, be shown to cancel in the next section. Readers who are interested how the amplitudes themselves are obtained within our LCPT approach to the CGC are referred to appendix C, where a representative amplitude is calculated from start to finish.

3.1 Self-energy corrections

Diagram SE1. The reduced amplitude corresponding to a quark self-energy correction after having hit the shockwave, but before the emission of the photon (see figure 2), reads:

$$\begin{aligned} \tilde{\mathcal{M}}_{SE1}^0 &= \frac{\alpha_s C_F}{D-2} \frac{1}{M} \frac{p_0^+ \mathbf{P}_\perp^2 - p_1^+ M^2}{p_0^+ \mathbf{P}_\perp^2 + p_1^+ M^2} \int_{k_{\min}^+}^{p_0^+} \frac{dk^+}{k^+} \left(\frac{k^+}{p_0^+} \right)^2 \mathcal{S}_{SE}^{jj}(p_0^+) \\ &\times \mathcal{A}_0(\Delta_P) \int_{\mathbf{x}} e^{-i\mathbf{k}_\perp \cdot \mathbf{x}} (U_{\mathbf{x}} - 1), \end{aligned} \quad (3.1)$$

for a longitudinally polarized virtual photon, and

$$\begin{aligned} \tilde{\mathcal{M}}_{\text{SE1}}^\lambda = & -\frac{\alpha_s C_F}{D-2} \frac{q^+ \mathbf{P}_\perp^\lambda}{p_0^+ \mathbf{P}_\perp^2 + p_1^+ M^2} \int_{k_{\min}^+}^{p_0^+} \frac{dk^+}{k^+} \left(\frac{k^+}{p_0^+}\right)^2 \mathcal{S}_{\text{LO}}^{\lambda\bar{\lambda}} \mathcal{S}_{\text{SE}}^{jj}(p_0^+) \\ & \times \mathcal{A}_0(\Delta_{\text{P}}) \int_{\mathbf{x}} e^{-i\mathbf{k}_\perp \cdot \mathbf{x}} (U_{\mathbf{x}} - 1), \end{aligned} \quad (3.2)$$

when the photon is transversely polarized. In the above formulas, $C_F = (N_c^2 - 1)/2N_c$, and we defined the Dirac structures:

$$\mathcal{S}_{\text{SE}}^{\eta\eta'}(p_0^+) \equiv \left[\left(1 - \frac{2p_0^+}{k^+}\right) \delta^{\eta\bar{\eta}} \mathbf{1}_4 - i\sigma^{\eta\bar{\eta}} \right] \left[\left(\frac{2p_0^+}{k^+} - 1\right) \delta^{\eta\eta'} \mathbf{1}_4 - i\sigma^{\eta\eta'} \right], \quad (3.3)$$

as well as:

$$\Delta_{\text{P}} \equiv -\frac{k^+(p_0^+ - k^+)}{p_0^+ p_1^+ q^+} (p_0^+ \mathbf{P}_\perp^2 + p_1^+ M^2) - i0^+. \quad (3.4)$$

At a later stage we will evaluate the k^+ -integral and encounter logarithmic branch cuts. Therefore, we keep track of the infinitesimal imaginary part $i0^+$ in the above expression, stemming from the energy denominator from which this term stems.

The quantity $\mathcal{A}_0(\Delta_{\text{P}})$ in eqs. (3.1) and (3.2) results from the integration over the gluon transverse loop momentum, which we have evaluated using integral identity eq. (A.8). As could be expected, the result is divergent in the ultraviolet, and we use dimensional regularization with $D = 4 - 2\epsilon_{\text{UV}}$ to regulate it. Finally, $\tilde{\mathcal{M}}_{\text{SE1}}^\lambda$ and $\tilde{\mathcal{M}}_{\text{SE1}}^0$ diverge in the limit of vanishing gluon plus-momentum $k^+ \rightarrow 0$. This rapidity divergence is regulated using a cutoff k_{\min}^+ .

We now introduce a counterterm to cancel the UV-pole in expression (3.1):

$$\begin{aligned} \tilde{\mathcal{M}}_{\text{SE1,UV}}^0 = & \frac{\alpha_s C_F}{D-2} \frac{1}{M} \frac{p_0^+ \mathbf{P}_\perp^2 - p_1^+ M^2}{p_0^+ \mathbf{P}_\perp^2 + p_1^+ M^2} \int_{k_{\min}^+}^{p_0^+} \frac{dk^+}{k^+} \left(\frac{k^+}{p_0^+}\right)^2 \mathcal{S}_{\text{SE}}^{jj}(p_0^+) \\ & \times \mathcal{A}_0(\Delta_{\text{UV}}) \int_{\mathbf{x}} e^{-i\mathbf{k}_\perp \cdot \mathbf{x}} (U_{\mathbf{x}} - 1). \end{aligned} \quad (3.5)$$

The UV-subtracted amplitude can then be evaluated in $D = 4$ dimensions:

$$\begin{aligned} \tilde{\mathcal{M}}_{\text{SE1,sub}}^0 = & \tilde{\mathcal{M}}_{\text{LO1}}^0 \frac{\alpha_s C_F}{\pi} \int_{k_{\min}^+}^{p_0^+} \frac{dk^+}{8k^+} \left(\frac{k^+}{p_0^+}\right)^2 \mathcal{S}_{\text{SE}}^{jj}(p_0^+) \ln \frac{\Delta_{\text{UV}}}{\Delta_{\text{P}}} \\ = & \tilde{\mathcal{M}}_{\text{LO1}}^0 \frac{\alpha_s C_F}{\pi} \int_{k_{\min}^+}^{p_0^+} \frac{dk^+}{4k^+} \left(\frac{k^+}{p_0^+}\right)^2 \left(\left(1 - \frac{2p_0^+}{k^+}\right)^2 + 1 \right) \ln \frac{\Delta_{\text{P}}}{\Delta_{\text{UV}}}. \end{aligned} \quad (3.6)$$

The exact same steps we just took can be followed in the transversely polarized case, defining a counterterm:

$$\begin{aligned} \tilde{\mathcal{M}}_{\text{SE1,UV}}^\lambda = & -\frac{\alpha_s C_F}{D-2} \frac{q^+ \mathbf{P}_\perp^\lambda}{p_0^+ \mathbf{P}_\perp^2 + p_1^+ M^2} \int_{k_{\min}^+}^{p_0^+} \frac{dk^+}{k^+} \left(\frac{k^+}{p_0^+}\right)^2 \mathcal{S}_{\text{LO}}^{\lambda\bar{\lambda}} \mathcal{S}_{\text{SE}}^{jj}(p_0^+) \\ & \times \mathcal{A}_0(\Delta_{\text{UV}}) \int_{\mathbf{x}} e^{-i\mathbf{k}_\perp \cdot \mathbf{x}} (U_{\mathbf{x}} - 1), \end{aligned} \quad (3.7)$$

such that the UV-subtracted amplitude can be evaluated in $D = 4$ dimensions, yielding:

$$\tilde{\mathcal{M}}_{\text{SE1,sub}}^\lambda = \tilde{\mathcal{M}}_{\text{LO1}}^\lambda \frac{\alpha_s C_F}{\pi} \int_{k_{\min}^+}^{p_0^+} \frac{dk^+}{4k^+} \left(\frac{k^+}{p_0^+}\right)^2 \left(\left(1 - \frac{2p_0^+}{k^+}\right)^2 + 1 \right) \ln \frac{\Delta_{\text{P}}}{\Delta_{\text{UV}}}. \quad (3.8)$$

Comparing the above result with (3.6), it is clear that the loop correction calculated here is independent of the polarization of the virtual photon.

Diagram SE2. Using the expressions (A.2) and (A.3) for the so-called Weizsäcker-Williams fields $A^i(\mathbf{x})$ and $A^i(\mathbf{x}, \Delta)$, as well as the property (A.4), one obtains for the diagrams where the quark self-energy loop scatters off the shockwave before emitting a virtual photon (see figure 2):

$$\begin{aligned} \tilde{\mathcal{M}}_{\text{SE2}}^0 &= -\frac{\alpha_s}{D-2} \frac{1}{M} \frac{p_0^+ \mathbf{P}_\perp^2 - p_1^+ M^2}{p_0^+ \mathbf{P}_\perp^2 + p_1^+ M^2} \int_{k_{\min}^+}^{p_0^+} \frac{dk^+}{k^+} \left(\frac{k^+}{p_0^+} \right)^2 \mathcal{S}_{\text{SE}}^{jj}(p_0^+) \\ &\quad \times \int_{\mathbf{x}, \mathbf{z}} A^i(\mathbf{x} - \mathbf{z}) A^i(\mathbf{x} - \mathbf{z}, \Delta_{\text{P}}) \\ &\quad \times e^{-i\mathbf{k}_\perp \cdot \left(\frac{p_0^+ - k^+}{p_0^+} \mathbf{x} + \frac{k^+}{p_0^+} \mathbf{z} \right)} (t^c U_{\mathbf{x}} U_{\mathbf{z}}^\dagger t^c U_{\mathbf{z}} - C_F), \end{aligned} \quad (3.9)$$

and:

$$\begin{aligned} \tilde{\mathcal{M}}_{\text{SE2}}^\lambda &= \frac{\alpha_s}{D-2} \frac{q^+ \mathbf{P}_\perp^\lambda}{p_0^+ \mathbf{P}_\perp^2 + p_1^+ M^2} \int_{k_{\min}^+}^{p_0^+} \frac{dk^+}{k^+} \left(\frac{k^+}{p_0^+} \right)^2 \mathcal{S}_{\text{LO}}^{\lambda\bar{\lambda}} \mathcal{S}_{\text{SE}}^{jj}(p_0^+) \\ &\quad \times \int_{\mathbf{x}, \mathbf{z}} A^i(\mathbf{x} - \mathbf{z}) A^i(\mathbf{x} - \mathbf{z}, \Delta_{\text{P}}) \\ &\quad \times e^{-i\mathbf{k}_\perp \cdot \left(\frac{p_0^+ - k^+}{p_0^+} \mathbf{x} + \frac{k^+}{p_0^+} \mathbf{z} \right)} (t^c U_{\mathbf{x}} U_{\mathbf{z}}^\dagger t^c U_{\mathbf{z}} - C_F). \end{aligned} \quad (3.10)$$

Note that we have used the Fierz identity $t^a W^{ab} = U^\dagger t^b U$ to transform Wilson lines W in the adjoint representation, which parameterize the virtual gluon interacting with the shockwave, into the usual Wilson lines U in the fundamental representation (2.27).

In the limit $\mathbf{z} \rightarrow \mathbf{x}$, or equivalently when the virtual gluon obtains an infinitely large transverse momentum, the amplitudes (3.10) and (3.9) exhibit an UV divergence. Indeed, introducing the notation $\int_{\mathbf{p}} = \mu^{4-D} \int d^{D-2} \mathbf{p} / (2\pi)^{D-2}$ that we will use throughout this work, we have from definitions (A.2) and (A.3):

$$\begin{aligned} &A^i(\mathbf{x} - \mathbf{z}) A^i(\mathbf{x} - \mathbf{z}, \Delta) \\ &= - \int_{\mathbf{k}, \ell} e^{-i(\mathbf{k} + \ell) \cdot (\mathbf{x} - \mathbf{z})} \frac{\mathbf{k}^i}{k^2} \frac{\ell^i}{\ell^2 + \Delta}, \\ &= - \frac{\mu^{2(4-D)}}{2(2\pi^2)^{\frac{D-2}{2}}} \frac{1}{|\mathbf{x} - \mathbf{z}|^{\frac{3D-10}{4}}} \Gamma\left(\frac{D-2}{2}\right) (\sqrt{\Delta})^{\frac{D-2}{2}} K_{\frac{D-2}{2}}(|\mathbf{x} - \mathbf{z}| \sqrt{\Delta}), \end{aligned} \quad (3.11)$$

which is singular for $\mathbf{x} - \mathbf{z} \rightarrow 0$ but tends to zero for $\mathbf{x} - \mathbf{z} \rightarrow \infty$. Moreover, since $\lim_{\Delta \rightarrow 0} \sqrt{\Delta} K_1(\sqrt{\Delta}) = 1$, there are no extra divergences generated when integrating over k^+ (since $\Delta_{\text{P}}(k^+ \rightarrow p_0^+) \rightarrow 0$).

A counterterm for this UV divergence can be constructed from (3.10) and (3.9) by setting $\mathbf{z} = \mathbf{x}$ everywhere except in the singular part, after which the integral over \mathbf{z} can be

evaluated by reverting to momentum space and using the standard result (A.8):

$$\begin{aligned} \tilde{\mathcal{M}}_{\text{SE2,UV}}^0 &= -\frac{\alpha_s C_F}{D-2} \frac{1}{M} \frac{p_0^+ \mathbf{P}_\perp^2 - p_1^+ M^2}{p_0^+ \mathbf{P}_\perp^2 + p_1^+ M^2} \int_{k_{\min}^+}^{p_0^+} \frac{dk^+}{k^+} \left(\frac{k^+}{p_0^+} \right)^2 \mathcal{S}_{\text{SE}}^{jj}(p_0^+) \\ &\quad \times \mathcal{A}_0(\Delta_{\text{UV}}) \int_{\mathbf{x}} e^{-i\mathbf{k}_\perp \cdot \mathbf{x}} (U_{\mathbf{x}} - 1) = -\tilde{\mathcal{M}}_{\text{SE1,UV}}^0, \end{aligned} \quad (3.12)$$

and similarly for the transverse case:

$$\tilde{\mathcal{M}}_{\text{SE2,UV}}^\lambda = -\tilde{\mathcal{M}}_{\text{SE1,UV}}^\lambda. \quad (3.13)$$

Therefore, the UV counterterms of the amplitudes $\tilde{\mathcal{M}}_{\text{SE2}}^{\lambda,0}$ happen to be the exact opposite of those for $\tilde{\mathcal{M}}_{\text{SE1}}^{\lambda,0}$.

The UV-subtracted amplitudes read, in $D = 4$ dimensions:

$$\begin{aligned} \tilde{\mathcal{M}}_{\text{SE2,sub}}^0 &= \alpha_s \frac{1}{M} \frac{p_0^+ \mathbf{P}_\perp^2 - p_1^+ M^2}{p_0^+ \mathbf{P}_\perp^2 + p_1^+ M^2} \int_{k_{\min}^+}^{p_0^+} \frac{dk^+}{k^+} \left(\frac{k^+}{p_0^+} \right)^2 \left(\left(1 - \frac{2p_0^+}{k^+} \right)^2 + 1 \right) \\ &\quad \times \left[\int_{\mathbf{x}, \mathbf{z}} A^i(\mathbf{x} - \mathbf{z}) A^i(\mathbf{x} - \mathbf{z}, \Delta_{\text{P}}) e^{-i\mathbf{k}_\perp \cdot \left(\frac{p_0^+ - k^+}{p_0^+} \mathbf{x} + \frac{k^+}{p_0^+} \mathbf{z} \right)} (t^c U_{\mathbf{x}} U_{\mathbf{z}}^\dagger t^c U_{\mathbf{z}} - C_F) \right. \\ &\quad \left. - \mathcal{A}_0(\Delta_{\text{UV}}) \int_{\mathbf{x}} e^{-i\mathbf{k}_\perp \cdot \mathbf{x}} C_F (U_{\mathbf{x}} - 1) \right], \end{aligned} \quad (3.14)$$

and:

$$\begin{aligned} \tilde{\mathcal{M}}_{\text{SE2,sub}}^\lambda &= -\alpha_s \frac{q^+ \mathbf{P}_\perp^{\bar{\lambda}}}{p_0^+ \mathbf{P}_\perp^2 + p_1^+ M^2} \mathcal{S}^{\lambda \bar{\lambda}} \left(1 + 2 \frac{p_1^+}{q^+} \right) \int_{k_{\min}^+}^{p_0^+} \frac{dk^+}{k^+} \left(\frac{k^+}{p_0^+} \right)^2 \left(\left(1 - \frac{2p_0^+}{k^+} \right)^2 + 1 \right) \\ &\quad \times \left[\int_{\mathbf{x}, \mathbf{z}} A^i(\mathbf{x} - \mathbf{z}) A^i(\mathbf{x} - \mathbf{z}, \Delta_{\text{P}}) e^{-i\mathbf{k}_\perp \cdot \left(\frac{p_0^+ - k^+}{p_0^+} \mathbf{x} + \frac{k^+}{p_0^+} \mathbf{z} \right)} (t^c U_{\mathbf{x}} U_{\mathbf{z}}^\dagger t^c U_{\mathbf{z}} - C_F) \right. \\ &\quad \left. - \mathcal{A}_0(\Delta_{\text{UV}}) \int_{\mathbf{x}} e^{-i\mathbf{k}_\perp \cdot \mathbf{x}} C_F (U_{\mathbf{x}} - 1) \right]. \end{aligned} \quad (3.15)$$

Diagram SE3. This diagram is the counterpart of graph SE2, when the emission of the virtual photon takes place before the quark self-energy loop (see figure 2). The corresponding amplitudes read:

$$\begin{aligned} \tilde{\mathcal{M}}_{\text{SE3}}^0 &= \frac{\alpha_s (-1)^{4-D}}{D-2} \frac{p_0^+ \mathbf{q}^2 - p_1^+ M^2}{p_0^+ \mathbf{q}^2 + p_1^+ M^2} \frac{1}{M} \int_{k_{\min}^+}^{p_1^+} \frac{dk^+}{k^+} \left(\frac{k^+}{p_1^+} \right)^2 \mathcal{S}_{\text{SE}}^{jj}(p_1^+) \\ &\quad \times \int_{\mathbf{x}, \mathbf{z}} A^i(\mathbf{z} - \mathbf{x}) A^i(\mathbf{z} - \mathbf{x}, \Delta_{\text{q}}) \\ &\quad \times e^{-i\mathbf{k}_\perp \cdot \left(\frac{p_1^+ - k^+}{p_1^+} \mathbf{x} + \frac{k^+}{p_1^+} \mathbf{z} \right)} (t^c U_{\mathbf{x}} U_{\mathbf{z}}^\dagger t^c U_{\mathbf{z}} - C_F), \end{aligned} \quad (3.16)$$

and:

$$\begin{aligned}
 \tilde{\mathcal{M}}_{\text{SE3}}^\lambda &= \frac{\alpha_s (-1)^{4-D}}{D-2} \frac{q^+ \mathbf{q}^\lambda}{p_0^+ \mathbf{q}^2 + p_1^+ M^2} \int_{k_{\min}^+}^{p_1^+} \frac{dk^+}{k^+} \left(\frac{k^+}{p_1^+} \right)^2 \mathcal{S}_{\text{SE}}^{jj}(p_1^+) \mathcal{S}_{\text{LO}}^{\lambda\bar{\lambda}} \\
 &\quad \times \int_{\mathbf{x}, \mathbf{z}} A^i(\mathbf{z} - \mathbf{x}) A^i(\mathbf{z} - \mathbf{x}, \Delta_{\mathbf{q}}) \\
 &\quad \times e^{-i\mathbf{k}_\perp \cdot \left(\frac{p_1^+ - k^+}{p_1^+} \mathbf{x} + \frac{k^+}{p_1^+} \mathbf{z} \right)} (t^c U_{\mathbf{x}} U_{\mathbf{z}}^\dagger t^c U_{\mathbf{z}} - C_F).
 \end{aligned} \tag{3.17}$$

In the above, we defined:

$$\Delta_{\mathbf{q}} \equiv \frac{k^+(p_1^+ - k^+)}{(p_1^+)^2 q^+} (p_0^+ \mathbf{q}^2 + p_1^+ M^2) - i0^+. \tag{3.18}$$

Just like the amplitudes $\tilde{\mathcal{M}}_{\text{SE2}}^{\lambda,0}$, also (3.17) and (3.16) are UV-divergent in the limit $\mathbf{z} \rightarrow \mathbf{x}$. Again, this divergence can be extracted by setting $\mathbf{z} = \mathbf{x}$ everywhere except in the singular part, defining the counterterms:

$$\begin{aligned}
 \tilde{\mathcal{M}}_{\text{SE3,UV}}^0 &= -\alpha_s C_F \frac{p_0^+ \mathbf{q}^2 - p_1^+ M^2}{p_0^+ \mathbf{q}^2 + p_1^+ M^2} \frac{1}{M} \int_{k_{\min}^+}^{p_1^+} \frac{dk^+}{k^+} \left(\frac{k^+}{p_1^+} \right)^2 \left(\left(1 - \frac{2p_1^+}{k^+} \right)^2 + D - 3 \right) \\
 &\quad \times \mathcal{A}_0(\Delta_{\text{UV}}) \int_{\mathbf{x}} e^{-i\mathbf{k}_\perp \cdot \mathbf{x}} (U_{\mathbf{x}} - 1), \\
 \tilde{\mathcal{M}}_{\text{SE3,UV}}^\lambda &= -\alpha_s C_F \frac{q^+ \mathbf{q}^\lambda}{p_0^+ \mathbf{q}^2 + p_1^+ M^2} \mathcal{S}_{\text{LO}}^{\lambda\bar{\lambda}} \int_{k_{\min}^+}^{p_1^+} \frac{dk^+}{k^+} \left(\frac{k^+}{p_1^+} \right)^2 \left(\left(1 - \frac{2p_1^+}{k^+} \right)^2 + D - 3 \right) \\
 &\quad \times \mathcal{A}_0(\Delta_{\text{UV}}) \int_{\mathbf{x}} e^{-i\mathbf{k}_\perp \cdot \mathbf{x}} (U_{\mathbf{x}} - 1).
 \end{aligned} \tag{3.19}$$

The subtracted amplitudes then become:

$$\begin{aligned}
 \tilde{\mathcal{M}}_{\text{SE3,sub}}^0 &= -\alpha_s \frac{p_0^+ \mathbf{q}^2 - p_1^+ M^2}{p_0^+ \mathbf{q}^2 + p_1^+ M^2} \frac{1}{M} \int_{k_{\min}^+}^{p_1^+} \frac{dk^+}{k^+} \left(\frac{k^+}{p_1^+} \right)^2 \left(\left(1 - \frac{2p_1^+}{k^+} \right)^2 + 1 \right) \\
 &\quad \times \left[\int_{\mathbf{x}, \mathbf{z}} A^i(\mathbf{z} - \mathbf{x}) A^i(\mathbf{z} - \mathbf{x}, \Delta_{\mathbf{q}}) e^{-i\mathbf{k}_\perp \cdot \left(\frac{p_1^+ - k^+}{p_1^+} \mathbf{x} + \frac{k^+}{p_1^+} \mathbf{z} \right)} (t^c U_{\mathbf{x}} U_{\mathbf{z}}^\dagger t^c U_{\mathbf{z}} - C_F) \right. \\
 &\quad \left. - \mathcal{A}_0(\Delta_{\text{UV}}) \int_{\mathbf{x}} e^{-i\mathbf{k}_\perp \cdot \mathbf{x}} C_F (U_{\mathbf{x}} - 1) \right],
 \end{aligned} \tag{3.20}$$

and:

$$\begin{aligned}
 \tilde{\mathcal{M}}_{\text{SE3,sub}}^\lambda &= -\alpha_s \frac{q^+ \mathbf{q}^\lambda}{p_0^+ \mathbf{q}^2 + p_1^+ M^2} \mathcal{S}_{\text{LO}}^{\lambda\bar{\lambda}} \int_{k_{\min}^+}^{p_1^+} \frac{dk^+}{k^+} \left(\frac{k^+}{p_1^+} \right)^2 \left(\left(1 - \frac{2p_1^+}{k^+} \right)^2 + 1 \right) \\
 &\quad \times \left[\int_{\mathbf{x}, \mathbf{z}} A^i(\mathbf{z} - \mathbf{x}) A^i(\mathbf{z} - \mathbf{x}, \Delta_{\mathbf{q}}) e^{-i\mathbf{k}_\perp \cdot \left(\frac{p_1^+ - k^+}{p_1^+} \mathbf{x} + \frac{k^+}{p_1^+} \mathbf{z} \right)} (t^c U_{\mathbf{x}} U_{\mathbf{z}}^\dagger t^c U_{\mathbf{z}} - C_F) \right. \\
 &\quad \left. - \mathcal{A}_0(\Delta_{\text{UV}}) \int_{\mathbf{x}} e^{-i\mathbf{k}_\perp \cdot \mathbf{x}} C_F (U_{\mathbf{x}} - 1) \right].
 \end{aligned} \tag{3.21}$$

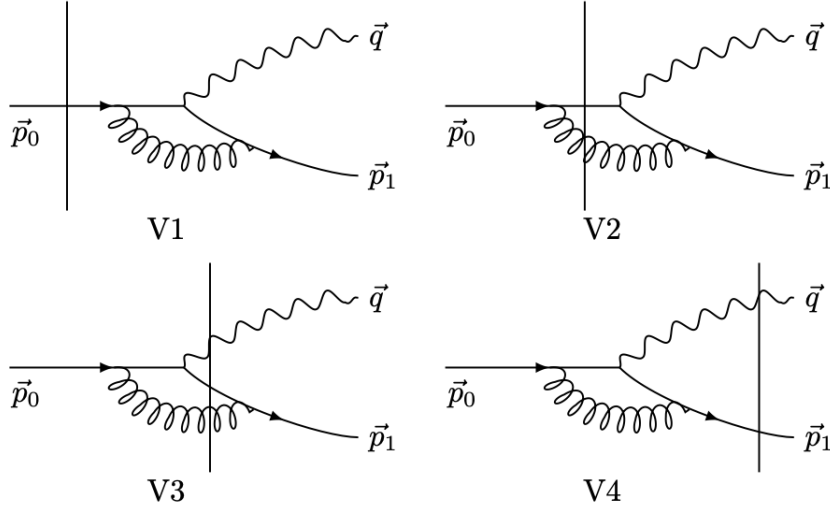


Figure 3. The four virtual contributions with a vertex correction, which in two cases (V2 and V3) scatters off the shockwave.

Diagram SE4. Evaluating the Feynman diagrams corresponding to a quark self-energy correction after the photon emission, but before the scattering off the shockwave (see figure 2), we find:

$$\begin{aligned}
 \tilde{\mathcal{M}}_{\text{SE4}}^0 &= \alpha_s C_F \frac{p_0^+ \mathbf{q}^2 - p_1^+ M^2}{p_0^+ \mathbf{q}^2 + p_1^+ M^2} \frac{1}{M} \int_{k_{\min}^+}^{p_1^+} \frac{dk^+}{k^+} \left(\frac{k^+}{p_1^+} \right)^2 \left(\left(1 - \frac{2p_1^+}{k^+} \right)^2 + D - 3 \right) \\
 &\quad \times \mathcal{A}_0(\Delta_q) \int_{\mathbf{x}} e^{-i\mathbf{k}_\perp \cdot \mathbf{x}} (U_{\mathbf{x}} - 1), \\
 \tilde{\mathcal{M}}_{\text{SE4}}^\lambda &= \alpha_s C_F \frac{q^+ \mathbf{q}^\lambda}{p_0^+ \mathbf{q}^2 + p_1^+ M^2} \mathcal{S}^{\lambda\bar{\lambda}} \left(1 + 2 \frac{p_1^+}{q^+} \right) \int_{k_{\min}^+}^{p_1^+} \frac{dk^+}{k^+} \left(\frac{k^+}{p_1^+} \right)^2 \left(\left(1 - \frac{2p_1^+}{k^+} \right)^2 + D - 3 \right) \\
 &\quad \times \mathcal{A}_0(\Delta_q) \int_{\mathbf{x}} e^{-i\mathbf{k}_\perp \cdot \mathbf{x}} (U_{\mathbf{x}} - 1).
 \end{aligned} \tag{3.22}$$

The counterterms are simply defined by setting $\mathcal{A}_0(\Delta_q) \rightarrow \mathcal{A}_0(\Delta_{\text{UV}})$, and are once again opposite to those of $\tilde{\mathcal{M}}_{\text{SE3}}^{0,\lambda}$:

$$\tilde{\mathcal{M}}_{\text{SE4,UV}}^{0,\lambda} = -\tilde{\mathcal{M}}_{\text{SE3,UV}}^{0,\lambda}. \tag{3.23}$$

In $D = 4$ dimensions, the subtracted amplitudes are then given by:

$$\tilde{\mathcal{M}}_{\text{SE4,sub}}^{0,\lambda} = \tilde{\mathcal{M}}_{\text{LO2}}^{0,\lambda} \frac{\alpha_s C_F}{4\pi} \int_{k_{\min}^+}^{p_1^+} \frac{dk^+}{k^+} \left(\frac{k^+}{p_1^+} \right)^2 \left(\left(1 - \frac{2p_1^+}{k^+} \right)^2 + 1 \right) \ln \frac{\Delta_q}{\Delta_{\text{UV}}}. \tag{3.24}$$

3.2 Vertex corrections

Diagram V1. The amplitude for Feynman diagram V1 (see figure 3) reads, when the produced virtual photon is longitudinally polarized:

$$\begin{aligned}
 \tilde{\mathcal{M}}_{V1}^0 &= -\frac{\alpha_s C_F}{p_0^+ \mathbf{P}_\perp^2 + p_1^+ M^2} \frac{1}{M} \frac{1}{D-2} \int_{k_{\min}^+}^{p_1^+} \frac{dk^+}{k^+} \frac{(k^+ q^+)^2}{p_0^+ (p_1^+ - k^+) (p_0^+ - k^+)} \mathcal{S}_V^{j0j} \\
 &\times \left\{ \left[-\Delta_P + \frac{(p_0^+ - k^+) (p_1^+ - k^+)}{p_1^+ (q^+)^2} (p_0^+ \mathbf{P}_\perp^2 - p_1^+ M^2) \right] \mathcal{A}_0(\Delta_P) \right. \\
 &\quad \left. - 2\hat{M}^2 \left(\frac{k^+}{p_1^+} \right)^2 \mathbf{P}_\perp^2 \mathcal{B}_1(0, \Delta_P, \frac{k^+}{p_1^+} \mathbf{P}_\perp) \right\} \int_{\mathbf{x}} e^{-i\mathbf{k}_\perp \cdot \mathbf{x}} (U_{\mathbf{x}} - 1), \tag{3.25}
 \end{aligned}$$

with the Dirac structure (simplified using the spinor relations in section B):

$$\begin{aligned}
 \mathcal{S}_V^{\bar{\eta}0\eta'} &\equiv \left[\left(1 - 2\frac{p_1^+}{k^+} \right) \delta^{\eta\bar{\eta}} \mathbf{1}_4 - i\sigma^{\eta\bar{\eta}} \right] \left[\left(2\frac{p_0^+}{k^+} - 1 \right) \delta^{\eta'\eta} \mathbf{1}_4 - i\sigma^{\eta'\eta'} \right], \\
 \mathcal{S}_V^{j0j} &= -(D-2) \left(\left(2\frac{p_1^+}{k^+} - 1 \right) \left(2\frac{p_0^+}{k^+} - 1 \right) + D - 3 \right), \tag{3.26}
 \end{aligned}$$

and the definition:

$$\hat{M}^2 \equiv \frac{(p_1^+ - k^+) (p_0^+ - k^+)}{(q^+)^2} M^2 + i0^+. \tag{3.27}$$

Expression (3.25) features the familiar UV-divergent integral $\mathcal{A}_0(\Delta_P)$, as well as the integral \mathcal{B}_1 whose expression is a finite albeit complicated sum of hypergeometric functions, see eqs. (A.10) and (A.14) in the appendix.

When the virtual photon is transversely polarized, the amplitude reads:

$$\begin{aligned}
 \tilde{\mathcal{M}}_{V1}^\lambda &= -\frac{\alpha_s C_F}{p_0^+ \mathbf{P}_\perp^2 + p_1^+ M^2} \mathbf{P}_\perp^{\eta'} \frac{1}{D-2} \int_{k_{\min}^+}^{p_1^+} \frac{dk^+}{k^+} \frac{(k^+ q^+)^2}{p_0^+ (p_1^+ - k^+) (p_0^+ - k^+)} \frac{k^+}{p_1^+} \\
 &\times \left\{ \left[\left(\frac{1}{2} - p_1^+ \frac{p_0^+ - k^+}{q^+ k^+} \right) \delta^{\bar{\lambda}\eta'} \mathcal{S}_V^{j\bar{\lambda}j} + \epsilon^{ij} \mathcal{S}_V^{i\bar{\lambda}j} \frac{\epsilon^{\bar{\lambda}\eta'}}{D-3} \frac{1}{2} \right] \mathcal{A}_0(\Delta_P) \right. \\
 &\quad \left. + \left[-\left(\frac{p_0^+ (p_1^+ - k^+)}{k^+ q^+} \left(\frac{k^+}{p_1^+} \right)^2 \mathbf{P}_\perp^2 + \frac{1}{2} \left(\Delta_P + \left(\frac{k^+}{p_1^+} \right)^2 \mathbf{P}_\perp^2 \right) \right) \delta^{\bar{\lambda}\eta'} \mathcal{S}_V^{j\bar{\lambda}j} \right. \right. \\
 &\quad \left. \left. + \epsilon^{ij} \mathcal{S}_V^{i\bar{\lambda}j} \frac{\epsilon^{\bar{\lambda}\eta'}}{D-3} \frac{1}{2} \left(\Delta_P + \left(\frac{k^+}{p_1^+} \right)^2 \mathbf{P}_\perp^2 \right) \right] \mathcal{B}_1(0, \Delta_P, \frac{k^+}{p_1^+} \mathbf{P}_\perp) \right\} \\
 &\times \int_{\mathbf{x}} e^{-i\mathbf{k}_\perp \cdot \mathbf{x}} (U_{\mathbf{x}} - 1), \tag{3.28}
 \end{aligned}$$

with:

$$\begin{aligned}
 \mathcal{S}_V^{\bar{\eta}\bar{\lambda}\eta'} &= \left[\left(1 - 2\frac{p_1^+}{k^+} \right) \delta^{\eta\bar{\eta}} \mathbf{1}_4 - i\sigma^{\eta\bar{\eta}} \right] \left[\left(1 - 2\frac{k^+ - p_1^+}{q^+} \right) \delta^{\lambda\bar{\lambda}} \mathbf{1}_4 - i\sigma^{\lambda\bar{\lambda}} \right] \\
 &\times \left[\left(2\frac{p_0^+}{k^+} - 1 \right) \delta^{\eta'\eta} \mathbf{1}_4 - i\sigma^{\eta'\eta'} \right], \\
 \mathcal{S}_V^{j\bar{\lambda}j} &= (D-2) \left(1 - 2\frac{k^+ - p_1^+}{q^+} \right) \left(\left(1 - 2\frac{p_1^+}{k^+} \right) \left(2\frac{p_0^+}{k^+} - 1 \right) - (D-3) \right) \delta^{\lambda\bar{\lambda}} \mathbf{1}_4 \\
 &\quad - i \left[(D-2) \left(\left(1 - 2\frac{p_1^+}{k^+} \right) \left(2\frac{p_0^+}{k^+} - 1 \right) - (D-3) \right) + 8(D-4) \right] \sigma^{\lambda\bar{\lambda}}. \tag{3.29}
 \end{aligned}$$

We introduce the following counterterms to absorb the UV divergences:

$$\begin{aligned} \tilde{\mathcal{M}}_{V1,UV}^0 = & -\frac{\alpha_s C_F}{p_0^+ \mathbf{P}_\perp^2 + p_1^+ M^2} \frac{1}{M} \frac{1}{D-2} \int_{k_{\min}^+}^{p_1^+} \frac{dk^+}{k^+} \frac{(k^+ q^+)^2}{p_0^+ (p_1^+ - k^+) (p_0^+ - k^+)} \mathcal{S}_V^{j0j} \\ & \times \left[-\Delta_P + \frac{(p_0^+ - k^+) (p_1^+ - k^+)}{p_1^+ (q^+)^2} (p_0^+ \mathbf{P}_\perp^2 - p_1^+ M^2) \right] \mathcal{A}_0(\Delta_{UV}) \int_{\mathbf{x}} e^{-i\mathbf{k}_\perp \cdot \mathbf{x}} (U_{\mathbf{x}} - 1), \end{aligned} \quad (3.30)$$

and

$$\begin{aligned} \tilde{\mathcal{M}}_{V1,UV}^\lambda = & -\frac{\alpha_s C_F}{p_0^+ \mathbf{P}_\perp^2 + p_1^+ M^2} \mathbf{P}_\perp^{\eta'} \frac{1}{D-2} \int_{k_{\min}^+}^{p_1^+} \frac{dk^+}{k^+} \frac{(k^+ q^+)^2}{p_0^+ (p_1^+ - k^+) (p_0^+ - k^+)} \frac{k^+}{p_1^+} \\ & \times \left[\left(\frac{1}{2} - p_1^+ \frac{p_0^+ - k^+}{q^+ k^+} \right) \delta^{\bar{\lambda}\eta'} \mathcal{S}_V^{j\bar{\lambda}j} + \epsilon^{ij} \mathcal{S}_V^{i\bar{\lambda}j} \frac{\epsilon^{\bar{\lambda}\eta'}}{D-3} \frac{1}{2} \right] \mathcal{A}_0(\Delta_{UV}) \\ & \times \int_{\mathbf{x}} e^{-i\mathbf{k}_\perp \cdot \mathbf{x}} (U_{\mathbf{x}} - 1). \end{aligned} \quad (3.31)$$

The subtracted amplitudes, therefore, become:

$$\begin{aligned} \tilde{\mathcal{M}}_{V1,sub}^0 = & \frac{\alpha_s C_F}{p_0^+ \mathbf{P}_\perp^2 + p_1^+ M^2} \frac{1}{M} \int_{k_{\min}^+}^{p_1^+} \frac{dk^+}{k^+} \frac{(k^+ q^+)^2}{p_0^+ (p_1^+ - k^+) (p_0^+ - k^+)} \left(\left(2 \frac{p_1^+}{k^+} - 1 \right) \left(2 \frac{p_0^+}{k^+} - 1 \right) + 1 \right) \\ & \times \left\{ \left[-\Delta_P + \frac{(p_0^+ - k^+) (p_1^+ - k^+)}{p_1^+ (q^+)^2} (p_0^+ \mathbf{P}_\perp^2 - p_1^+ M^2) \right] \frac{1}{4\pi} \ln \frac{\Delta_{UV}}{\Delta_P} \right. \\ & \left. - 2 \hat{M}^2 \left(\frac{k^+}{p_1^+} \right)^2 \mathbf{P}_\perp^2 \mathcal{B}_1(0, \Delta_P, \frac{k^+}{p_1^+} \mathbf{P}_\perp) \right\} \int_{\mathbf{x}} e^{-i\mathbf{k}_\perp \cdot \mathbf{x}} (U_{\mathbf{x}} - 1), \end{aligned} \quad (3.32)$$

and:

$$\begin{aligned} \tilde{\mathcal{M}}_{V1,sub}^\lambda = & -\frac{\alpha_s C_F}{p_0^+ \mathbf{P}_\perp^2 + p_1^+ M^2} \mathbf{P}_\perp^{\eta'} \frac{1}{D-2} \int_{k_{\min}^+}^{p_1^+} \frac{dk^+}{k^+} \frac{(k^+ q^+)^2}{p_0^+ (p_1^+ - k^+) (p_0^+ - k^+)} \frac{k^+}{p_1^+} \\ & \times \left\{ \left[\left(\frac{1}{2} - p_1^+ \frac{p_0^+ - k^+}{q^+ k^+} \right) \delta^{\bar{\lambda}\eta'} \mathcal{S}_V^{j\bar{\lambda}j} + \epsilon^{ij} \mathcal{S}_V^{i\bar{\lambda}j} \frac{\epsilon^{\bar{\lambda}\eta'}}{D-3} \frac{1}{2} \right] \frac{1}{4\pi} \ln \frac{\Delta_{UV}}{\Delta_P} \right. \\ & + \left[-\left(\frac{p_0^+ (p_1^+ - k^+)}{k^+ q^+} \right) \left(\frac{k^+}{p_1^+} \right)^2 \mathbf{P}_\perp^2 + \frac{1}{2} \left(\Delta_P + \left(\frac{k^+}{p_1^+} \right)^2 \mathbf{P}_\perp^2 \right) \right] \delta^{\bar{\lambda}\eta'} \mathcal{S}_V^{j\bar{\lambda}j} \\ & \left. + \epsilon^{ij} \mathcal{S}_V^{i\bar{\lambda}j} \frac{\epsilon^{\bar{\lambda}\eta'}}{D-3} \frac{1}{2} \left(\Delta_P + \left(\frac{k^+}{p_1^+} \right)^2 \mathbf{P}_\perp^2 \right) \right] \mathcal{B}_1(0, \Delta_P, \frac{k^+}{p_1^+} \mathbf{P}_\perp) \left. \right\} \\ & \times \int_{\mathbf{x}} e^{-i\mathbf{k}_\perp \cdot \mathbf{x}} (U_{\mathbf{x}} - 1). \end{aligned} \quad (3.33)$$

Diagram V2. The amplitude for Feynman diagram V2 (see figure 3) reads, in case of a longitudinally polarized virtual photon:

$$\tilde{\mathcal{M}}_{V2}^0 = \frac{\alpha_s}{M} \int_{k_{\min}^+}^{p_1^+} \frac{dk^+}{k^+} \frac{(k^+)^3 q^+}{(p_0^+)^2 p_1^+ (p_1^+ - k^+)} \mathcal{S}_V^{\bar{\eta}0\eta'} \quad (3.34)$$

$$\times \int_{\mathbf{x}, \mathbf{z}} \int_{\mathbf{k}_1} e^{-i\mathbf{k}_1 \cdot (\mathbf{x} - \mathbf{z})} \frac{\mathbf{k}_1^{\eta'}}{\mathbf{k}_1^2} \int_{\ell} \frac{\ell^{\bar{\eta}}}{\ell^2} \frac{e^{i \left(\ell + \frac{k^+}{p_1^+} \mathbf{P}_\perp \right) \cdot (\mathbf{x} - \mathbf{z})}}{\left(\ell + \frac{k^+}{p_1^+} \mathbf{P}_\perp \right)^2 + \Delta_P} \quad (3.35)$$

$$\times \left[\left(\boldsymbol{\ell} - \frac{p_0^+(p_1^+ - k^+)}{q^+ p_1^+} \mathbf{P}_\perp \right)^2 - \frac{(p_1^+ - k^+)(p_0^+ - k^+)}{(q^+)^2} M^2 \right] \quad (3.36)$$

$$\times e^{-i\mathbf{k}_\perp \cdot \left(\frac{p_0^+ - k^+}{p_0^+} \mathbf{x} + \frac{k^+}{p_0^+} \mathbf{z} \right)} [U_{\mathbf{z}} t^c U_{\mathbf{z}}^\dagger U_{\mathbf{x}} t^c - C_F]. \quad (3.37)$$

To the best of our knowledge, the transverse integral over $\boldsymbol{\ell}$ does not allow a general analytic solution.² However, we expect amplitude $\tilde{\mathcal{M}}_{V2}^0$ to contain a UV divergence in the limit $\mathbf{z} \rightarrow \mathbf{x}$. With the same procedure as for the counterterms in section 3.1, namely setting $\mathbf{z} = \mathbf{x}$ in the phase and the Wilson-line structures, but not within the divergent integrations, the integral over \mathbf{z} can be carried out, after which one obtains:

$$\begin{aligned} \lim_{\mathbf{z} \rightarrow \mathbf{x}} \tilde{\mathcal{M}}_{V2}^0 &= \frac{\alpha_s C_F}{M} \frac{1}{D-2} \int_{k_{\min}^+}^{p_1^+} \frac{dk^+}{k^+} \frac{(k^+)^3 q^+}{(p_0^+)^2 p_1^+ (p_1^+ - k^+)} \mathcal{S}_V^{j0j} \\ &\times \int \boldsymbol{\ell} \frac{\boldsymbol{\ell} \cdot \left(\boldsymbol{\ell} + \frac{k^+}{p_1^+} \mathbf{P}_\perp \right)}{\ell^2 \left(\boldsymbol{\ell} + \frac{k^+}{p_1^+} \mathbf{P}_\perp \right)^2 \left(\boldsymbol{\ell} + \frac{k^+}{p_1^+} \mathbf{P}_\perp \right)^2 + \Delta_P} \frac{1}{\left(\boldsymbol{\ell} + \frac{k^+}{p_1^+} \mathbf{P}_\perp \right)^2 + \Delta_P} \\ &\times \left[\left(\boldsymbol{\ell} - \frac{p_0^+(p_1^+ - k^+)}{q^+ p_1^+} \mathbf{P}_\perp \right)^2 - \frac{(p_1^+ - k^+)(p_0^+ - k^+)}{(q^+)^2} M^2 \right] \\ &\times \int_{\mathbf{x}} e^{-i\mathbf{k}_\perp \cdot \mathbf{x}} (U_{\mathbf{x}} - 1). \end{aligned} \quad (3.38)$$

The loop integral can now be evaluated with the help of the identities (A.15):

$$\begin{aligned} \mathcal{I}_{V2}^0 &= \int \boldsymbol{\ell} \frac{\boldsymbol{\ell} \cdot \left(\boldsymbol{\ell} + \frac{k^+}{p_1^+} \mathbf{P}_\perp \right)}{\ell^2 \left(\boldsymbol{\ell} + \frac{k^+}{p_1^+} \mathbf{P}_\perp \right)^2 \left(\boldsymbol{\ell} + \frac{k^+}{p_1^+} \mathbf{P}_\perp \right)^2 + \Delta_P} \frac{1}{\left(\boldsymbol{\ell} + \frac{k^+}{p_1^+} \mathbf{P}_\perp \right)^2 + \Delta_P} \\ &\times \left[\left(\boldsymbol{\ell} - \frac{p_0^+(p_1^+ - k^+)}{q^+ p_1^+} \mathbf{P}_\perp \right)^2 - \frac{(p_1^+ - k^+)(p_0^+ - k^+)}{(q^+)^2} M^2 \right] \\ &= \mathcal{A}_0(\Delta_P) - p_0^+ \frac{p_1^+ - k^+}{k^+ q^+} \left(\frac{k^+}{p_1^+} \right)^2 \mathbf{P}_\perp^2 \mathcal{B}_1(0, \Delta_P, -\frac{k^+}{p_1^+} \mathbf{P}_\perp) \\ &\quad + \frac{1}{2} \frac{(p_1^+ - k^+)(p_0^+ - k^+)}{(q^+)^2 p_1^+} \left(p_0^+ \mathbf{P}_\perp^2 - p_1^+ M^2 \right) \\ &\times \left[\mathcal{B}_0(\Delta_P) + \mathcal{B}_0(\Delta_P, -\frac{k^+}{p_1^+} \mathbf{P}_\perp) - \left(\frac{k^+}{p_1^+} \right)^2 \mathbf{P}_\perp^2 \mathcal{C}_0(\Delta_P, -\frac{k^+}{p_1^+} \mathbf{P}_\perp) \right]. \end{aligned} \quad (3.39)$$

The infrared poles contained in the structures $\mathcal{B}_0(\Delta_P)$, $\mathcal{B}_0(0, \Delta_P, -\frac{k^+}{p_1^+} \mathbf{P}_\perp)$, and $\mathcal{C}_0(\Delta_P, -\frac{k^+}{p_1^+} \mathbf{P}_\perp)$ all cancel (see eqs. (A.13) and (A.17)). Since $\mathcal{B}_1(0, \Delta_P, -\frac{k^+}{p_1^+} \mathbf{P}_\perp)$ is finite, the only remaining singularity is the ultraviolet one contained in $\mathcal{A}_0(\Delta_P)$. We can, therefore, define the counterterm

$$\begin{aligned} \tilde{\mathcal{M}}_{V2,UV}^0 &= \frac{\alpha_s C_F}{M} \frac{1}{D-2} \int_{k_{\min}^+}^{p_1^+} \frac{dk^+}{k^+} \frac{(k^+)^3 q^+}{(p_0^+)^2 p_1^+ (p_1^+ - k^+)} \mathcal{S}_V^{j0j} \\ &\times \mathcal{A}_0(\Delta_{UV}) \int_{\mathbf{x}} e^{-i\mathbf{k}_\perp \cdot \mathbf{x}} (U_{\mathbf{x}} - 1). \end{aligned} \quad (3.40)$$

²See [46, 50] for very similar integrals in NLO $\gamma^{(*)} + A \rightarrow \text{dijet} + X$ calculations.

Finally, the subtracted longitudinal amplitude reads

$$\begin{aligned}
 \tilde{\mathcal{M}}_{V2,\text{sub}}^0 &= \frac{\alpha_s}{M} \int_{k_{\min}^+}^{p_1^+} \frac{dk^+}{k^+} \frac{(k^+)^3 q^+}{(p_0^+)^2 p_1^+ (p_1^+ - k^+)} \mathcal{S}_V^{\bar{\eta}0\eta'} \\
 &\times \left[\int_{\mathbf{x}, \mathbf{z}} iA^{\eta'}(\mathbf{x} - \mathbf{z}) \int_{\ell} \frac{\ell^{\bar{\eta}}}{\ell^2} \frac{e^{i\left(\ell + \frac{k^+}{p_1^+} \mathbf{P}_{\perp}\right) \cdot (\mathbf{x} - \mathbf{z})}}{\left(\ell + \frac{k^+}{p_1^+} \mathbf{P}_{\perp}\right)^2 + \Delta_P} \right. \\
 &\times \left(\left(\ell - \frac{p_0^+ (p_1^+ - k^+)}{q^+ p_1^+} \mathbf{P}_{\perp} \right)^2 - \frac{(p_1^+ - k^+)(p_0^+ - k^+)}{(q^+)^2} M^2 \right) \\
 &\times e^{-i\mathbf{k}_{\perp} \cdot \left(\frac{p_0^+ - k^+}{p_0^+} \mathbf{x} + \frac{k^+}{p_0^+} \mathbf{z} \right)} [U_{\mathbf{z}} t^c U_{\mathbf{z}}^{\dagger} U_{\mathbf{x}} t^c - C_F] \\
 &\left. - \frac{\delta^{\bar{\eta}\eta'}}{2} \mathcal{A}_0(\Delta_{UV}) \int_{\mathbf{x}} e^{-i\mathbf{k}_{\perp} \cdot \mathbf{x}} C_F (U_{\mathbf{x}} - 1) \right]. \tag{3.41}
 \end{aligned}$$

The amplitude for the emission of a transversely polarized virtual photon is equal to:

$$\begin{aligned}
 \tilde{\mathcal{M}}_{V2}^{\lambda} &= \alpha_s \int_0^{p_1^+} \frac{dk^+}{k^+} \frac{(k^+)^3 q^+}{p_1^+ (p_0^+)^2 (p_1^+ - k^+)} \mathcal{S}_V^{\bar{\eta}\lambda\eta'} \\
 &\times \int_{\mathbf{x}, \mathbf{z}} iA^{\eta'}(\mathbf{x} - \mathbf{z}) \int_{\ell} e^{i\ell \cdot (\mathbf{x} - \mathbf{z})} \frac{\ell^{\bar{\eta}} - \frac{k^+}{p_1^+} \mathbf{P}_{\perp}^{\bar{\eta}}}{\left(\ell - \frac{k^+}{p_1^+} \mathbf{P}_{\perp}\right)^2} \frac{\ell^{\lambda} - \frac{p_0^+ - k^+}{q^+} \mathbf{P}_{\perp}^{\lambda}}{\ell^2 + \Delta_P} \\
 &\times e^{-i\mathbf{k}_{\perp} \cdot \left(\frac{p_0^+ - k^+}{p_0^+} \mathbf{x} + \frac{k^+}{p_0^+} \mathbf{z} \right)} [U_{\mathbf{z}} t^c U_{\mathbf{z}}^{\dagger} U_{\mathbf{x}} t^c - C_F]. \tag{3.42}
 \end{aligned}$$

Like in the longitudinal case (3.37), we are not aware of an analytic solution for the integral over ℓ . The integral, however, can be shown to be free from UV (and rapidity-) divergences (see appendix D).

Diagram V3. We obtain for diagram V3 (see figure 3):

$$\begin{aligned}
 \tilde{\mathcal{M}}_{V3}^0 &= -\frac{\alpha_s}{M} \int_{k_{\min}^+}^{p_1^+} \frac{dk^+}{k^+} \frac{(k^+)^3 q^+}{(p_1^+)^2 p_0^+ (p_0^+ - k^+)} \mathcal{S}_V^{\bar{\eta}0\eta'} \\
 &\times \int_{\mathbf{x}, \mathbf{z}} iA^{\bar{\eta}}(\mathbf{x} - \mathbf{z}) \int_{\ell} \frac{\ell^{\eta'}}{\ell^2} \frac{e^{i\left(\ell + \frac{k^+}{p_1^+} \mathbf{q}\right) \cdot (\mathbf{z} - \mathbf{x})}}{\left(\ell + \frac{k^+}{p_1^+} \mathbf{q}\right)^2 + \Delta_q} \\
 &\times \left[\left(\ell + \frac{p_0^+ - k^+}{q^+} \mathbf{q} \right)^2 - \frac{(p_1^+ - k^+)(p_0^+ - k^+)}{(q^+)^2} M^2 \right] \\
 &\times e^{-i\mathbf{k}_{\perp} \cdot \left(\frac{p_1^+ - k^+}{p_1^+} \mathbf{x} + \frac{k^+}{p_1^+} \mathbf{z} \right)} [U_{\mathbf{z}} t^c U_{\mathbf{z}}^{\dagger} U_{\mathbf{x}} t^c - C_F]. \tag{3.43}
 \end{aligned}$$

Similarly to the amplitude $\tilde{\mathcal{M}}_{V2}^0$, eq. (3.43) contains a UV divergence in the limit $\mathbf{z} \rightarrow \mathbf{x}$:

$$\begin{aligned}
 \lim_{\mathbf{z} \rightarrow \mathbf{x}} \tilde{\mathcal{M}}_{V3}^0 &= \frac{\alpha_s C_F}{M} \frac{1}{D-2} \int_{k_{\min}^+}^{p_1^+} \frac{dk^+}{k^+} \frac{(k^+)^3 q^+}{(p_1^+)^2 p_0^+ (p_0^+ - k^+)} \mathcal{S}_V^{j0j} \\
 &\times \int_{\ell} \frac{\ell \cdot \left(\ell + \frac{k^+}{p_1^+} \mathbf{q} \right)}{\ell^2 \left(\ell + \frac{k^+}{p_1^+} \mathbf{q} \right)^2} \frac{1}{\left(\ell + \frac{k^+}{p_1^+} \mathbf{q} \right)^2 + \Delta_q}
 \end{aligned}$$

$$\begin{aligned}
& \times \left[\left(\boldsymbol{\ell} + \frac{p_0^+ - k^+}{q^+} \mathbf{q} \right)^2 - \frac{(p_1^+ - k^+)(p_0^+ - k^+)}{(q^+)^2} M^2 \right] \\
& \times \int_{\mathbf{x}} e^{-i\mathbf{k}_\perp \cdot \mathbf{x}} (U_{\mathbf{x}} - 1).
\end{aligned} \tag{3.44}$$

The integral over $\boldsymbol{\ell}$ can be calculated with the help of the identities (A.10) and (A.15) in the appendix:

$$\begin{aligned}
\mathcal{I}_{V3}^0 &= \int_{\boldsymbol{\ell}} \frac{\boldsymbol{\ell} \cdot \left(\boldsymbol{\ell} + \frac{k^+}{p_1^+} \mathbf{q} \right)}{\ell^2 \left(\boldsymbol{\ell} + \frac{k^+}{p_1^+} \mathbf{q} \right)^2} \frac{1}{\left(\boldsymbol{\ell} + \frac{k^+}{p_1^+} \mathbf{q} \right)^2 + \Delta_{\mathbf{q}}} \\
& \times \left[\left(\boldsymbol{\ell} + \frac{p_0^+ - k^+}{q^+} \mathbf{q} \right)^2 - \frac{(p_1^+ - k^+)(p_0^+ - k^+)}{(q^+)^2} M^2 \right] \\
&= \mathcal{A}_0(\Delta_{\mathbf{q}}) + p_1^+ \frac{p_0^+ - k^+}{q^+ k^+} \left(\frac{k^+}{p_1^+} \right)^2 \mathbf{q}^2 \mathcal{B}_1(0, \Delta_{\mathbf{q}}, \frac{k^+}{p_1^+} \mathbf{q}) \\
& + \frac{1}{2} \frac{(p_1^+ - k^+)(p_0^+ - k^+)}{(q^+)^2 p_1^+} \left(p_0^+ \mathbf{q}^2 - p_1^+ M^2 \right) \\
& \times \left[\mathcal{B}_0(\Delta_{\mathbf{q}}) + \mathcal{B}_0(\Delta_{\mathbf{q}}, \frac{k^+}{p_1^+} \mathbf{q}) - \left(\frac{k^+}{p_1^+} \right)^2 \mathbf{q}^2 \mathcal{C}_0(\Delta_{\mathbf{q}}, \frac{k^+}{p_1^+} \mathbf{q}) \right].
\end{aligned} \tag{3.45}$$

Due to the cancellation of IR divergences in the last line of (3.45), the only remaining divergence is the ultraviolet one in $\mathcal{A}_0(\Delta_{\mathbf{q}})$. We can, therefore, define the counterterm:

$$\begin{aligned}
\tilde{\mathcal{M}}_{V3,UV}^0 &= \frac{\alpha_s C_F}{M} \frac{1}{D-2} \int_{k_{\min}^+}^{p_1^+} \frac{dk^+}{k^+} \frac{(k^+)^3 q^+}{(p_1^+)^2 p_0^+ (p_0^+ - k^+)} \mathcal{S}_V^{j0j} \\
& \times \mathcal{A}_0(\Delta_{UV}) \int_{\mathbf{x}} e^{-i\mathbf{k}_\perp \cdot \mathbf{x}} (U_{\mathbf{x}} - 1),
\end{aligned} \tag{3.46}$$

which leads to the following UV-subtracted amplitude:

$$\begin{aligned}
\tilde{\mathcal{M}}_{V3,sub}^0 &= -\frac{\alpha_s}{M} \int_0^{p_1^+} \frac{dk^+}{k^+} \frac{(k^+)^3 q^+}{(p_1^+)^2 p_0^+ (p_0^+ - k^+)} \mathcal{S}_V^{\bar{\eta}0\eta'} \\
& \times \left[\int_{\mathbf{x}, \mathbf{z}} iA^{\bar{\eta}}(\mathbf{x} - \mathbf{z}) \int_{\boldsymbol{\ell}} \frac{\boldsymbol{\ell}^{\eta'}}{\ell^2} \frac{e^{i \left(\boldsymbol{\ell} + \frac{k^+}{p_1^+} \mathbf{q} \right) \cdot (\mathbf{z} - \mathbf{x})}}{\left(\boldsymbol{\ell} + \frac{k^+}{p_1^+} \mathbf{q} \right)^2 + \Delta_{\mathbf{q}}} \right. \\
& \times \left(\left(\boldsymbol{\ell} + \frac{p_0^+ - k^+}{q^+} \mathbf{q} \right)^2 - \frac{(p_1^+ - k^+)(p_0^+ - k^+)}{(q^+)^2} M^2 \right) \\
& \times e^{-i\mathbf{k}_\perp \cdot \left(\frac{p_1^+ - k^+}{p_1^+} \mathbf{x} + \frac{k^+}{p_1^+} \mathbf{z} \right)} [U_{\mathbf{z}} t^c U_{\mathbf{z}}^\dagger U_{\mathbf{x}} t^c - C_F] \\
& \left. + \frac{\delta^{\bar{\eta}\eta'}}{2} \mathcal{A}_0(\Delta_{UV}) \int_{\mathbf{x}} e^{-i\mathbf{k}_\perp \cdot \mathbf{x}} C_F (U_{\mathbf{x}} - 1) \right].
\end{aligned} \tag{3.47}$$

In the transversely polarized case, the amplitude is given by:

$$\begin{aligned}
 \tilde{\mathcal{M}}_{V3}^\lambda &= \alpha_s \int_0^{p_1^+} \frac{dk^+}{k^+} \frac{q^+(k^+)^3}{p_0^+(p_1^+)^2(p_0^+ - k^+)} \mathcal{S}_V^{\bar{\eta}\lambda\eta'} \\
 &\times \int_{\mathbf{x}, \mathbf{z}} iA^{\bar{\eta}}(\mathbf{z} - \mathbf{x}) \int_\ell e^{-i\left(\ell + \frac{k^+}{p_1^+} \mathbf{q}\right) \cdot (\mathbf{x} - \mathbf{z})} \frac{\ell^{\eta'}}{\ell^2} \frac{\ell^{\bar{\lambda}} + \frac{p_0^+ - k^+}{q^+} \mathbf{q}^{\bar{\lambda}}}{\left(\ell + \frac{k^+}{p_1^+} \mathbf{q}\right)^2 + \Delta_q} \\
 &\times e^{-i\mathbf{k}_\perp \cdot \left(\frac{p_1^+ - k^+}{p_1^+} \mathbf{x} + \frac{k^+}{p_1^+} \mathbf{z}\right)} [U_{\mathbf{z}} t^c U_{\mathbf{z}}^\dagger U_{\mathbf{x}} t^c - C_F].
 \end{aligned} \tag{3.48}$$

It can be shown that, similarly to the case of \mathcal{M}_{V2}^λ (section D), although we cannot analytically evaluate the transverse integration, \mathcal{M}_{V3}^λ is free from UV (and rapidity-) divergences.

Diagram V4. One obtains for the vertex correction where the outgoing quark scatters off the shockwave (see figure 3):

$$\begin{aligned}
 \tilde{\mathcal{M}}_{V4}^0 &= \frac{1}{p_0^+ \mathbf{q}^2 + p_1^+ M^2} \frac{\alpha_s C_F}{M} \frac{1}{D-2} \int_{k_{\min}^+}^{p_1^+} \frac{dk^+}{k^+} \frac{(q^+)^2 (k^+)^2}{p_0^+(p_1^+ - k^+)(p_0^+ - k^+)} \mathcal{S}_V^{j0j} \\
 &\times \left\{ \left[-\Delta_q + \frac{(p_1^+ - k^+)(p_0^+ - k^+)}{p_1^+(q^+)^2} (p_0^+ \mathbf{q}^2 - p_1^+ M^2) \right] \mathcal{A}_0(\Delta_q) \right. \\
 &\left. - 2 \left(\frac{k^+}{p_1^+} \right)^2 \mathbf{q}^2 \hat{M}^2 \mathcal{B}_1(0, \Delta_q, \frac{k^+}{p_1^+} \mathbf{q}) \right\} \int_{\mathbf{x}} e^{-i\mathbf{k}_\perp \cdot \mathbf{x}} (U_{\mathbf{x}} - 1),
 \end{aligned} \tag{3.49}$$

and

$$\begin{aligned}
 \tilde{\mathcal{M}}_{V4}^\lambda &= \frac{\mathbf{q}^\rho}{p_0^+ \mathbf{q}^2 + p_1^+ M^2} \frac{\alpha_s C_F}{D-2} \int_{k_{\min}^+}^{p_1^+} \frac{dk^+}{k^+} \frac{k^+}{p_1^+} \frac{(k^+ q^+)^2}{p_0^+(p_1^+ - k^+)(p_0^+ - k^+)} \\
 &\times \left\{ \left[\left(\frac{1}{2} + p_0^+ \frac{p_1^+ - k^+}{k^+ q^+} \right) \mathcal{S}_V^{j\rho j} + \epsilon^{\rho\bar{\lambda}} \frac{1}{2} \frac{1}{D-3} \epsilon^{ij} \mathcal{S}_V^{i\bar{\lambda}j} \right] \mathcal{A}_0(\Delta_q) \right. \\
 &+ \left[\left(\frac{1}{2} \left(\Delta_q + \left(\frac{k^+}{p_1^+} \right)^2 \mathbf{q}^2 \right) - \frac{k^+(p_1^+ - k^+)M^2}{p_1^+ q^+} \right) \mathcal{S}_V^{j\rho j} \right. \\
 &\left. \left. + \epsilon^{\rho\bar{\lambda}} \frac{1}{D-3} \frac{1}{2} \left(\Delta_q + \left(\frac{k^+}{p_1^+} \right)^2 \mathbf{q}^2 \right) \epsilon^{ij} \mathcal{S}_V^{i\bar{\lambda}j} \right] \mathcal{B}_1(0, \Delta_q, \frac{k^+}{p_1^+} \mathbf{q}) \right\} \\
 &\times \int_{\mathbf{x}} e^{-i\mathbf{k}_\perp \cdot \mathbf{x}} (U_{\mathbf{x}} - 1).
 \end{aligned} \tag{3.50}$$

The corresponding UV counterterms read:

$$\begin{aligned}
 \tilde{\mathcal{M}}_{V4,UV}^0 &= \frac{1}{p_0^+ \mathbf{q}^2 + p_1^+ M^2} \frac{\alpha_s C_F}{M} \frac{1}{D-2} \int_{k_{\min}^+}^{p_1^+} \frac{dk^+}{k^+} \frac{(q^+)^2 (k^+)^2}{p_0^+(p_1^+ - k^+)(p_0^+ - k^+)} \mathcal{S}_V^{j0j} \\
 &\times \left[-\Delta_q + \frac{(p_1^+ - k^+)(p_0^+ - k^+)}{p_1^+(q^+)^2} (p_0^+ \mathbf{q}^2 - p_1^+ M^2) \right] \mathcal{A}_0(\Delta_{UV}) \\
 &\times \int_{\mathbf{x}} e^{-i\mathbf{k}_\perp \cdot \mathbf{x}} (U_{\mathbf{x}} - 1),
 \end{aligned} \tag{3.51}$$

and

$$\begin{aligned}
 \tilde{\mathcal{M}}_{V4,UV}^\lambda &= \frac{\mathbf{q}^\rho}{p_0^+ \mathbf{q}^2 + p_1^+ M^2} \frac{\alpha_s C_F}{D-2} \int_{k_{\min}^+}^{p_1^+} \frac{dk^+}{k^+} \frac{k^+}{p_1^+} \frac{(k^+ q^+)^2}{p_0^+ (p_1^+ - k^+) (p_0^+ - k^+)} \\
 &\times \left[\left(\frac{1}{2} + p_0^+ \frac{p_1^+ - k^+}{k^+ q^+} \right) \mathcal{S}_V^{j\rho j} + \epsilon^{\rho\bar{\lambda}} \frac{1}{2} \frac{1}{D-3} \epsilon^{ij} \mathcal{S}_V^{i\bar{\lambda}j} \right] \mathcal{A}_0(\Delta_{UV}) \\
 &\times \int_{\mathbf{x}} e^{-i\mathbf{k}_\perp \cdot \mathbf{x}} (U_{\mathbf{x}} - 1).
 \end{aligned} \tag{3.52}$$

Therefore, the subtracted amplitudes become:

$$\begin{aligned}
 \tilde{\mathcal{M}}_{V4,\text{sub}}^0 &= \frac{1}{p_0^+ \mathbf{q}^2 + p_1^+ M^2} \frac{\alpha_s C_F}{M} \frac{1}{2} \int_{k_{\min}^+}^{p_1^+} \frac{dk^+}{k^+} \frac{(q^+)^2 (k^+)^2}{p_0^+ (p_1^+ - k^+) (p_0^+ - k^+)} \mathcal{S}_V^{j0j} \\
 &\times \left\{ \left[-\Delta_{\mathbf{q}} + \frac{(p_1^+ - k^+) (p_0^+ - k^+)}{p_1^+ (q^+)^2} (p_0^+ \mathbf{q}^2 - p_1^+ M^2) \right] \frac{1}{4\pi} \ln \frac{\Delta_{UV}}{\Delta_{\mathbf{q}}} \right. \\
 &\left. - 2 \left(\frac{k^+}{p_1^+} \right)^2 \mathbf{q}^2 \hat{M}^2 \mathcal{B}_1(0, \Delta_{\mathbf{q}}, \frac{k^+}{p_1^+} \mathbf{q}) \right\} \int_{\mathbf{x}} e^{-i\mathbf{k}_\perp \cdot \mathbf{x}} (U_{\mathbf{x}} - 1),
 \end{aligned} \tag{3.53}$$

and:

$$\begin{aligned}
 \tilde{\mathcal{M}}_{V4,\text{sub}}^\lambda &= \frac{\mathbf{q}^\rho}{p_0^+ \mathbf{q}^2 + p_1^+ M^2} \frac{\alpha_s C_F}{2} \int_{k_{\min}^+}^{p_1^+} \frac{dk^+}{k^+} \frac{k^+}{p_1^+} \frac{(k^+ q^+)^2}{p_0^+ (p_1^+ - k^+) (p_0^+ - k^+)} \\
 &\times \left\{ \left[\left(\frac{1}{2} + p_0^+ \frac{p_1^+ - k^+}{k^+ q^+} \right) \mathcal{S}_V^{j\rho j} + \epsilon^{\rho\bar{\lambda}} \frac{1}{2} \epsilon^{ij} \mathcal{S}_V^{i\bar{\lambda}j} \right] \frac{1}{4\pi} \ln \frac{\Delta_{UV}}{\Delta_{\mathbf{q}}} \right. \\
 &+ \left[\left(-\frac{1}{2} \left(\Delta_{\mathbf{q}} + \left(\frac{k^+}{p_1^+} \right)^2 \mathbf{q}^2 \right) + \frac{k^+ (p_0^+ - k^+) \mathbf{q}^2}{p_1^+ q^+} \right) \mathcal{S}_V^{j\rho j} \right. \\
 &\left. \left. + \epsilon^{\rho\bar{\lambda}} \frac{1}{D-3} \frac{1}{2} \left(\Delta_{\mathbf{q}} + \left(\frac{k^+}{p_1^+} \right)^2 \mathbf{q}^2 \right) \epsilon^{ij} \mathcal{S}_V^{i\bar{\lambda}j} \right] \mathcal{B}_1(0, \Delta_{\mathbf{q}}, \frac{k^+}{p_1^+} \mathbf{q}) \right\} \\
 &\times \int_{\mathbf{x}} e^{-i\mathbf{k}_\perp \cdot \mathbf{x}} (U_{\mathbf{x}} - 1).
 \end{aligned} \tag{3.54}$$

3.3 Antiquark vertex corrections

Diagram A1. We obtain for the amplitude corresponding to diagram A1 in figure 4, which we dub an ‘antiquark vertex’ correction:

$$\begin{aligned}
 \tilde{\mathcal{M}}_{A1}^0 &= \frac{1}{p_0^+ \mathbf{P}_\perp^2 + p_1^+ M^2} \frac{\alpha_s C_F}{M} \frac{1}{D-2} \int_{p_1^+}^{p_0^+} \frac{dk^+}{k^+} \frac{k^+ p_1^+ (p_0^+ - k^+)}{p_0^+ q^+} \mathcal{S}_V^{j0j} \\
 &\times \left[2M^2 \mathcal{A}_0(\hat{M}^2) + \frac{(q^+)^2 \Delta_{\mathbf{P}}}{(p_1^+ - k^+) (p_0^+ - k^+)} \mathcal{A}_0(\Delta_{\mathbf{P}}) \right. \\
 &- 2M^2 \Delta_{\mathbf{P}} \mathcal{B}_0(\Delta_{\mathbf{P}}, \hat{M}^2, \frac{p_0^+ - k^+}{q^+} \mathbf{P}_\perp) \\
 &\left. + 2 \frac{k^+}{p_1^+} \frac{p_0^+ - k^+}{q^+} M^2 \mathbf{P}_\perp^2 \mathcal{B}_1(\Delta_{\mathbf{P}}, \hat{M}^2, \frac{p_0^+ - k^+}{q^+} \mathbf{P}_\perp) \right] \int_{\mathbf{x}} e^{-i\mathbf{k}_\perp \cdot \mathbf{x}} (U_{\mathbf{x}} - 1),
 \end{aligned} \tag{3.55}$$

and:

$$\begin{aligned} \tilde{\mathcal{M}}_{A1,UV}^\lambda &= \frac{\mathbf{P}_\perp^\rho}{p_0^+ \mathbf{P}_\perp^2 + p_1^+ M^2} \frac{\alpha_s C_F}{D-2} \int_{p_1^+}^{p_0^+} \frac{dk^+}{k^+} \frac{(k^+)^2 q^+}{2p_0^+(p_1^+ - k^+)} \\ &\times \left(\mathcal{S}_V^{j\rho j} + \frac{1}{D-3} \epsilon^{\rho\bar{\lambda}} \epsilon^{ij} \mathcal{S}_V^{i\bar{\lambda}j} \right) \mathcal{A}_0(\Delta_{UV}) \int_{\mathbf{x}} e^{-i\mathbf{k}_\perp \cdot \mathbf{x}} (U_{\mathbf{x}} - 1). \end{aligned} \quad (3.58)$$

The subtracted amplitudes then become:

$$\begin{aligned} \tilde{\mathcal{M}}_{A1,\text{sub}}^0 &= \frac{-1}{p_0^+ \mathbf{P}_\perp^2 + p_1^+ M^2} \frac{\alpha_s C_F}{M} \int_{p_1^+}^{p_0^+} \frac{dk^+}{k^+} \frac{k^+ p_1^+ (p_0^+ - k^+)}{p_0^+ q^+} \left(\left(2 \frac{p_1^+}{k^+} - 1 \right) \left(2 \frac{p_0^+}{k^+} - 1 \right) + 1 \right) \\ &\times \left[\left(2M^2 \frac{1}{4\pi} \ln \frac{\Delta_{UV}}{\hat{M}^2} + \frac{(q^+)^2 \Delta_P}{(p_1^+ - k^+)(p_0^+ - k^+)} \frac{1}{4\pi} \ln \frac{\Delta_{UV}}{\Delta_P} \right. \right. \\ &- 2M^2 \Delta_P \mathcal{B}_0(\Delta_P, \hat{M}^2, \frac{p_0^+ - k^+}{q^+} \mathbf{P}_\perp) \\ &\left. \left. + 2 \frac{k^+}{p_1^+} \frac{p_0^+ - k^+}{q^+} M^2 \mathbf{P}_\perp^2 \mathcal{B}_1(\Delta_P, \hat{M}^2, \frac{p_0^+ - k^+}{q^+} \mathbf{P}_\perp) \right] \int_{\mathbf{x}} e^{-i\mathbf{k}_\perp \cdot \mathbf{x}} (U_{\mathbf{x}} - 1), \end{aligned} \quad (3.59)$$

and:

$$\begin{aligned} \tilde{\mathcal{M}}_{A1,\text{sub}}^\lambda &= \frac{\mathbf{P}_\perp^\rho}{p_0^+ \mathbf{P}_\perp^2 + p_1^+ M^2} \frac{\alpha_s C_F}{D-2} \int_{p_1^+}^{p_0^+} \frac{dk^+}{k^+} \frac{k^+ p_1^+ q^+}{p_0^+(p_1^+ - k^+)} \\ &\times \left\{ \frac{k^+}{2p_1^+} \left(\mathcal{S}_V^{j\rho j} + \frac{1}{D-3} \epsilon^{\rho\bar{\lambda}} \epsilon^{ij} \mathcal{S}_V^{i\bar{\lambda}j} \right) \frac{1}{4\pi} \ln \frac{\Delta_{UV}}{\hat{M}^2} \right. \\ &- \left(\frac{p_0^+ - k^+}{q^+} \mathcal{S}_V^{j\rho j} + \frac{k^+}{p_1^+} \frac{1}{D-3} \epsilon^{\rho\bar{\lambda}} \epsilon^{ij} \mathcal{S}_V^{i\bar{\lambda}j} \right) \Delta_P \mathcal{B}_0(\Delta_P, \hat{M}^2, \frac{p_0^+ - k^+}{q^+} \mathbf{P}_\perp) \\ &+ \frac{k^+(p_0^+ - k^+)}{2p_1^+(q^+)^2} \left(\frac{2p_1^+(p_0^+ - k^+) - k^+ q^+}{p_0^+ p_1^+} (p_0^+ \mathbf{P}_\perp^2 + p_1^+ M^2) \right. \\ &+ \left. \left. \left((p_0^+ - k^+) \mathbf{P}_\perp^2 - (p_1^+ - k^+) M^2 \right) \mathcal{S}_V^{j\rho j} \mathcal{B}_1(\Delta_P, \hat{M}^2, \frac{p_0^+ - k^+}{q^+} \mathbf{P}_\perp) \right. \right. \\ &- \left. \left. \frac{k^+}{2p_1^+} \left(\Delta_P - \hat{M}^2 - \left(\frac{p_0^+ - k^+}{q^+} \mathbf{P}_\perp \right)^2 \right) \frac{1}{D-3} \epsilon^{\rho\bar{\lambda}} \epsilon^{ij} \mathcal{S}_V^{i\bar{\lambda}j} \mathcal{B}_1(\Delta_P, \hat{M}^2, \frac{p_0^+ - k^+}{q^+} \mathbf{P}_\perp) \right\} \\ &\times \int_{\mathbf{x}} e^{-i\mathbf{k}_\perp \cdot \mathbf{x}} (U_{\mathbf{x}} - 1). \end{aligned} \quad (3.60)$$

Diagram A2. For the production amplitudes of a longitudinally or transversely polarized virtual photon, we obtain, respectively:

$$\begin{aligned} \tilde{\mathcal{M}}_{A2}^0 &= - \frac{\alpha_s}{M} \int_{p_1^+}^{p_0^+} \frac{dk^+}{k^+} \frac{(k^+)^2 (p_0^+ - k^+)}{(p_0^+)^2 (p_1^+ - k^+)} \mathcal{S}_V^{\bar{\eta}0\eta'} \\ &\times \int_{\mathbf{x}, \mathbf{z}} iA^{\eta'}(\mathbf{x} - \mathbf{z}) \int_{\boldsymbol{\ell}} e^{-i\boldsymbol{\ell} \cdot (\mathbf{x} - \mathbf{z})} \frac{\boldsymbol{\ell}^{\bar{\eta}} + \frac{k^+}{p_1^+} \mathbf{P}_\perp^{\bar{\eta}} \left(\boldsymbol{\ell} + \frac{p_0^+ - k^+}{q^+} \mathbf{P}_\perp \right)^2 - \hat{M}^2}{\boldsymbol{\ell}^2 + \Delta_P \left(\boldsymbol{\ell} + \frac{p_0^+ - k^+}{q^+} \mathbf{P}_\perp \right)^2 + \hat{M}^2} \\ &\times e^{-i\mathbf{k}_\perp \cdot \left(\frac{p_0^+ - k^+}{p_0^+} \mathbf{x} + \frac{k^+}{p_0^+} \mathbf{z} \right)} (t^c U_{\mathbf{x}} U_{\mathbf{z}}^\dagger t^c U_{\mathbf{z}} - C_F), \end{aligned} \quad (3.61)$$

and:

$$\begin{aligned}
 \tilde{\mathcal{M}}_{A2}^\lambda &= \alpha_s \int_{p_1^+}^{p_0^+} \frac{dk^+ (k^+)^2 (p_0^+ - k^+)}{k^+ (p_0^+)^2 (p_1^+ - k^+)} \mathcal{S}_V^{\bar{\eta}\lambda\eta'} \\
 &\times \int_{\mathbf{x}, \mathbf{z}} iA^{\eta'}(\mathbf{x} - \mathbf{z}) \int_{\boldsymbol{\ell}} e^{-i\boldsymbol{\ell} \cdot (\mathbf{x} - \mathbf{z})} \frac{\ell^{\bar{\eta}} + \frac{k^+}{p_1^+} \mathbf{P}_\perp^{\bar{\eta}}}{\ell^2 + \Delta_P} \frac{\left(\ell^{\bar{\lambda}} + \frac{p_0^+ - k^+}{q^+} \mathbf{P}_\perp^{\bar{\lambda}} \right)}{\left(\ell + \frac{p_0^+ - k^+}{q^+} \mathbf{P}_\perp \right)^2 + \hat{M}^2} \\
 &\times e^{-i\mathbf{k}_\perp \cdot \left(\frac{p_0^+ - k^+}{p_0^+} \mathbf{x} + \frac{k^+}{p_0^+} \mathbf{z} \right)} (t^c U_{\mathbf{x}} U_{\mathbf{z}}^\dagger t^c U_{\mathbf{z}} - C_F).
 \end{aligned} \tag{3.62}$$

Similarly to the integrals encountered in amplitudes $\tilde{\mathcal{M}}_{V2,3}$, the transverse integrals over $\boldsymbol{\ell}$ do not admit an analytic solution, at least to the best of our knowledge. It is, however, possible to study their behavior in the limit $\lim_{\mathbf{z} \rightarrow \mathbf{x}}$ where they might exhibit a UV divergence, which turns out to be the case for the ‘longitudinal’ amplitude (3.61):

$$\begin{aligned}
 \lim_{\mathbf{z} \rightarrow \mathbf{x}} \tilde{\mathcal{M}}_{A2}^0 &= \frac{\alpha_s C_F}{M} \frac{1}{D-2} \int_{p_1^+}^{p_0^+} \frac{dk^+ (k^+)^2 (p_0^+ - k^+)}{k^+ (p_0^+)^2 (p_1^+ - k^+)} \mathcal{S}_V^{j0j} \\
 &\times \left[\mathcal{A}_0(\Delta_P) - 2\hat{M}^2 \mathcal{B}_0(\Delta_P, \hat{M}^2, \frac{p_0^+ - k^+}{q^+} \mathbf{P}_\perp) \right. \\
 &\left. - 2\hat{M}^2 \frac{p_0^+ - k^+}{q^+} \frac{k^+}{p_1^+} \mathbf{P}_\perp^2 \mathcal{C}_1(\Delta_P, \hat{M}^2, \frac{p_0^+ - k^+}{q^+} \mathbf{P}_\perp) \right] \int_{\mathbf{x}} e^{-i\mathbf{k}_\perp \cdot \mathbf{x}} (U_{\mathbf{x}} - 1).
 \end{aligned} \tag{3.63}$$

The counterterm, therefore, reads:

$$\begin{aligned}
 \tilde{\mathcal{M}}_{A2,UV}^0 &= \frac{\alpha_s C_F}{M} \frac{1}{D-2} \int_{p_1^+}^{p_0^+} \frac{dk^+ (k^+)^2 (p_0^+ - k^+)}{k^+ (p_0^+)^2 (p_1^+ - k^+)} \mathcal{S}_V^{j0j} \\
 &\times \mathcal{A}_0(\Delta_{UV}) \int_{\mathbf{x}} e^{-i\mathbf{k}_\perp \cdot \mathbf{x}} (U_{\mathbf{x}} - 1),
 \end{aligned} \tag{3.64}$$

such that the subtracted amplitude becomes:

$$\begin{aligned}
 \tilde{\mathcal{M}}_{A2,\text{sub}}^0 &= - \frac{\alpha_s}{M} \int_{p_1^+}^{p_0^+} \frac{dk^+ (k^+)^2 (p_0^+ - k^+)}{k^+ (p_0^+)^2 (p_1^+ - k^+)} \mathcal{S}_V^{\bar{\eta}0\eta'} \\
 &\times \left[\int_{\mathbf{x}, \mathbf{z}} iA^{\eta'}(\mathbf{x} - \mathbf{z}) \int_{\boldsymbol{\ell}} e^{-i\boldsymbol{\ell} \cdot (\mathbf{x} - \mathbf{z})} \frac{\ell^{\bar{\eta}} + \frac{k^+}{p_1^+} \mathbf{P}_\perp^{\bar{\eta}}}{\ell^2 + \Delta_P} \frac{\left(\ell + \frac{p_0^+ - k^+}{q^+} \mathbf{P}_\perp \right)^2 - \hat{M}^2}{\left(\ell + \frac{p_0^+ - k^+}{q^+} \mathbf{P}_\perp \right)^2 + \hat{M}^2} \right. \\
 &\times e^{-i\mathbf{k}_\perp \cdot \left(\frac{p_0^+ - k^+}{p_0^+} \mathbf{x} + \frac{k^+}{p_0^+} \mathbf{z} \right)} (t^c U_{\mathbf{x}} U_{\mathbf{z}}^\dagger t^c U_{\mathbf{z}} - C_F) \\
 &\left. + \frac{\delta^{\bar{\eta}\eta'}}{D-2} \mathcal{A}_0(\Delta_{UV}) \int_{\mathbf{x}} e^{-i\mathbf{k}_\perp \cdot \mathbf{x}} C_F (U_{\mathbf{x}} - 1) \right].
 \end{aligned} \tag{3.65}$$

Amplitude $\tilde{\mathcal{M}}_{A2}^\lambda$ turns out to be UV-finite.

Diagram A3. We obtain for the amplitudes where both the virtual quark and antiquark, as well as the outgoing quark scatter off the shockwave (figure 4):

$$\begin{aligned}
 \tilde{\mathcal{M}}_{A3}^0 &= \frac{\alpha_s}{M} \int_{p_1^+}^{p_0^+} \frac{dk^+}{k^+} \frac{2k^+(p_0^+ - k^+)}{q^+ p_0^+} \mathcal{S}_V^{\bar{\eta}0\eta'} \int_{\mathbf{x}_1, \mathbf{x}_2, \mathbf{x}_3} \hat{M}^2 \mathcal{K}(\mathbf{x}_1 - \mathbf{x}_2, \hat{M}^2) \\
 &\times \int_{\ell, \ell_2} e^{-i\ell \cdot \mathbf{x}_{12}} e^{-i\ell_2 \cdot \mathbf{x}_{23}} \frac{\ell^{\eta'}}{\ell^2} \frac{\ell^{\bar{\eta}} - \frac{k^+}{p_1^+} \ell_2^{\bar{\eta}}}{\left(\ell - \frac{p_0^+ - k^+}{q^+} \ell_2\right)^2 - \frac{p_0^+(p_0^+ - k^+)(p_1^+ - k^+)}{p_1^+(q^+)^2} \ell_2^2} \\
 &\times e^{-i\mathbf{p}_1 \cdot \mathbf{x}_3} e^{-i\mathbf{q} \cdot \left(\frac{p_0^+ - k^+}{q^+} \mathbf{x}_1 - \frac{p_1^+ - k^+}{q^+} \mathbf{x}_2\right)} [U_{\mathbf{x}_3} t^c U_{\mathbf{x}_2}^\dagger U_{\mathbf{x}_1} t^c - C_F],
 \end{aligned} \tag{3.66}$$

and

$$\begin{aligned}
 \tilde{\mathcal{M}}_{A3}^\lambda &= \alpha_s \int_{p_1^+}^{p_0^+} \frac{dk^+}{k^+} \frac{k^+(p_0^+ - k^+)}{q^+ p_0^+} \mathcal{S}_V^{\bar{\eta}\lambda\eta'} \int_{\mathbf{x}_1, \mathbf{x}_2, \mathbf{x}_3} iA^\lambda(\mathbf{x}_1 - \mathbf{x}_2, \hat{M}^2) \\
 &\times \int_{\ell, \ell_2} e^{-i\ell \cdot \mathbf{x}_{12}} e^{-i\ell_2 \cdot \mathbf{x}_{23}} \frac{\ell^{\eta'}}{\ell^2} \frac{\ell^{\bar{\eta}} - \frac{k^+}{p_1^+} \ell_2^{\bar{\eta}}}{\left(\ell - \frac{p_0^+ - k^+}{q^+} \ell_2\right)^2 - \frac{p_0^+(p_0^+ - k^+)(p_1^+ - k^+)}{p_1^+(q^+)^2} \ell_2^2} \\
 &\times e^{-i\mathbf{p}_1 \cdot \mathbf{x}_3} e^{-i\mathbf{q} \cdot \left(\frac{p_0^+ - k^+}{q^+} \mathbf{x}_1 - \frac{p_1^+ - k^+}{q^+} \mathbf{x}_2\right)} [U_{\mathbf{x}_3} t^c U_{\mathbf{x}_2}^\dagger U_{\mathbf{x}_1} t^c - C_F].
 \end{aligned} \tag{3.67}$$

In the above expressions, we used the short-hand notation $\mathbf{x}_{ij} = \mathbf{x}_i - \mathbf{x}_j$. The definition of \mathcal{K} can be found in the appendix, eq. (A.6). Investigating the limit $\mathbf{x}_1 \rightarrow \mathbf{x}_2 \rightarrow \mathbf{x}_3$ in search for ultraviolet divergences, it turns out that $\tilde{\mathcal{M}}_{A3}^\lambda$ is finite while $\tilde{\mathcal{M}}_{A3}^0$ contains an ultraviolet pole, which can be absorbed into the counterterm:

$$\begin{aligned}
 \tilde{\mathcal{M}}_{A3,UV}^0 &= -\frac{\alpha_s C_F}{M} \frac{1}{D-2} \int_{p_1^+}^{p_0^+} \frac{dk^+}{k^+} \frac{k^+(p_0^+ - k^+)}{q^+ p_0^+} \mathcal{S}_V^{j0j} \\
 &\times \mathcal{A}_0(\Delta_{UV}) \int_{\mathbf{x}} e^{-i\mathbf{k}_\perp \cdot \mathbf{x}} (U_{\mathbf{x}} - 1).
 \end{aligned} \tag{3.68}$$

The subtracted amplitude becomes:

$$\begin{aligned}
 \tilde{\mathcal{M}}_{A3,sub}^0 &= \frac{\alpha_s}{M} \mathcal{S}_V^{\bar{\eta}0\eta'} \int_{p_1^+}^{p_0^+} \frac{dk^+}{k^+} \frac{k^+(p_0^+ - k^+)}{q^+ p_0^+} \\
 &\times \left[\int_{\mathbf{x}_1, \mathbf{x}_2, \mathbf{x}_3} 2\hat{M}^2 \mathcal{K}(\mathbf{x}_1 - \mathbf{x}_2, \hat{M}^2) \right. \\
 &\times \int_{\ell, \ell_2} e^{-i\ell \cdot \mathbf{x}_{12}} e^{-i\ell_2 \cdot \mathbf{x}_{23}} \frac{\ell^{\eta'}}{\ell^2} \frac{\ell^{\bar{\eta}} - \frac{k^+}{p_1^+} \ell_2^{\bar{\eta}}}{\left(\ell - \frac{p_0^+ - k^+}{q^+} \ell_2\right)^2 - \frac{p_0^+(p_0^+ - k^+)(p_1^+ - k^+)}{p_1^+(q^+)^2} \ell_2^2} \\
 &\times e^{-i\mathbf{p}_1 \cdot \mathbf{x}_3} e^{-i\mathbf{q} \cdot \left(\frac{p_0^+ - k^+}{q^+} \mathbf{x}_1 - \frac{p_1^+ - k^+}{q^+} \mathbf{x}_2\right)} [U_{\mathbf{x}_3} t^c U_{\mathbf{x}_2}^\dagger U_{\mathbf{x}_1} t^c - C_F] \\
 &\left. + \frac{\delta^{\bar{\eta}\eta'}}{D-2} \mathcal{A}_0(\Delta_{UV}) \int_{\mathbf{x}} e^{-i\mathbf{k}_\perp \cdot \mathbf{x}} C_F (U_{\mathbf{x}} - 1) \right].
 \end{aligned} \tag{3.69}$$

Diagram A4. In the longitudinal case, the amplitude is given by:

$$\begin{aligned}
 \tilde{\mathcal{M}}_{A4}^0 &= \frac{p_0^+ \mathbf{q}^2 - p_1^+ M^2}{p_0^+ \mathbf{q}^2 + p_1^+ M^2} \frac{\alpha_s C_F}{M} \frac{1}{D-2} \int_{p_1^+}^{p_0^+} \frac{dk^+}{k^+} \frac{k^+(p_0^+ - k^+)}{p_0^+ q^+} \mathcal{S}_V^{j0j} \\
 &\times \left(\mathcal{A}_0(\hat{Q}^2) + \frac{k^+}{p_1^+} \frac{p_0^+ - k^+}{q^+} \mathbf{q}^2 \mathcal{B}_1(0, \hat{Q}^2, \frac{p_0^+ - k^+}{q^+} \mathbf{q}) \right) \\
 &\times \int_{\mathbf{x}} e^{-i\mathbf{k}_\perp \cdot \mathbf{x}} (U_{\mathbf{x}} - 1),
 \end{aligned} \tag{3.70}$$

where we have defined:

$$\hat{Q}^2 \equiv -\frac{p_0^+(p_0^+ - k^+)(p_1^+ - k^+)}{p_1^+(q^+)^2} \mathbf{q}^2 + i0^+. \tag{3.71}$$

Likewise, in the transverse case, we find:

$$\begin{aligned}
 \tilde{\mathcal{M}}_{A4}^\lambda &= \frac{\mathbf{q}^\rho}{p_0^+ \mathbf{q}^2 + p_1^+ M^2} \frac{\alpha_s C_F}{D-2} \int_{p_1^+}^{p_0^+} \frac{dk^+}{k^+} \frac{q^+(k^+)^2}{2p_0^+(p_1^+ - k^+)} \\
 &\times \left\{ \left[\mathcal{S}_V^{j\rho j} + \epsilon^{ij} \mathcal{S}_V^{i\bar{\lambda}j} e^{\rho\bar{\lambda}} \frac{1}{D-3} \right] \mathcal{A}_0(\hat{Q}^2) \right. \\
 &+ \left[-\left(\hat{Q}^2 - \left(\frac{p_0^+ - k^+}{q^+} \mathbf{q} \right)^2 \right) \mathcal{S}_V^{j\rho j} + \frac{k^+(p_0^+ - k^+)}{p_1^+ q^+} \mathbf{q}^2 \epsilon^{ij} \mathcal{S}_V^{i\bar{\lambda}j} e^{\rho\bar{\lambda}} \frac{1}{D-3} \right] \\
 &\times \left. \mathcal{B}_1(0, \hat{Q}^2, \frac{p_0^+ - k^+}{q^+} \mathbf{q}) \right\} \int_{\mathbf{x}} e^{-i\mathbf{k}_\perp \cdot \mathbf{x}} (U_{\mathbf{x}} - 1).
 \end{aligned} \tag{3.72}$$

Clearly, both $\tilde{\mathcal{M}}_{A4}^0$ and $\tilde{\mathcal{M}}_{A4}^\lambda$ are divergent in the ultraviolet. The poles are extracted by defining the counterterms:

$$\begin{aligned}
 \tilde{\mathcal{M}}_{A4,UV}^0 &= \frac{p_0^+ \mathbf{q}^2 - p_1^+ M^2}{p_0^+ \mathbf{q}^2 + p_1^+ M^2} \frac{\alpha_s C_F}{M} \frac{1}{D-2} \int_{p_1^+}^{p_0^+} \frac{dk^+}{k^+} \frac{k^+(p_0^+ - k^+)}{p_0^+ q^+} \mathcal{S}_V^{j0j} \\
 &\times \mathcal{A}_0(\Delta_{UV}) \int_{\mathbf{x}} e^{-i\mathbf{k}_\perp \cdot \mathbf{x}} (U_{\mathbf{x}} - 1),
 \end{aligned} \tag{3.73}$$

and:

$$\begin{aligned}
 \tilde{\mathcal{M}}_{A4,UV}^\lambda &= \frac{\mathbf{q}^\rho}{p_0^+ \mathbf{q}^2 + p_1^+ M^2} \frac{\alpha_s C_F}{D-2} \int_{p_1^+}^{p_0^+} \frac{dk^+}{k^+} \frac{q^+(k^+)^2}{2p_0^+(p_1^+ - k^+)} \\
 &\times \left[\mathcal{S}_V^{j\rho j} + \epsilon^{ij} \mathcal{S}_V^{i\bar{\lambda}j} e^{\rho\bar{\lambda}} \frac{1}{D-3} \right] \mathcal{A}_0(\Delta_{UV}) \int_{\mathbf{x}} e^{-i\mathbf{k}_\perp \cdot \mathbf{x}} (U_{\mathbf{x}} - 1).
 \end{aligned} \tag{3.74}$$

The subtracted amplitudes, therefore, become:

$$\begin{aligned}
 \tilde{\mathcal{M}}_{A4,sub}^0 &= \tilde{\mathcal{M}}_{LO2}^0 \times \frac{\alpha_s C_F}{\pi} \int_{p_1^+}^{p_0^+} \frac{dk^+}{4k^+} \frac{k^+(p_0^+ - k^+)}{p_0^+ q^+} \left(\left(2\frac{p_1^+}{k^+} - 1 \right) \left(2\frac{p_0^+}{k^+} - 1 \right) + 1 \right) \\
 &\times \left(\ln \frac{\Delta_{UV}}{\hat{Q}^2} + 4\pi \frac{k^+}{p_1^+} \frac{p_0^+ - k^+}{q^+} \mathbf{q}^2 \mathcal{B}_1(0, \hat{Q}^2, \frac{p_0^+ - k^+}{q^+} \mathbf{q}) \right),
 \end{aligned} \tag{3.75}$$

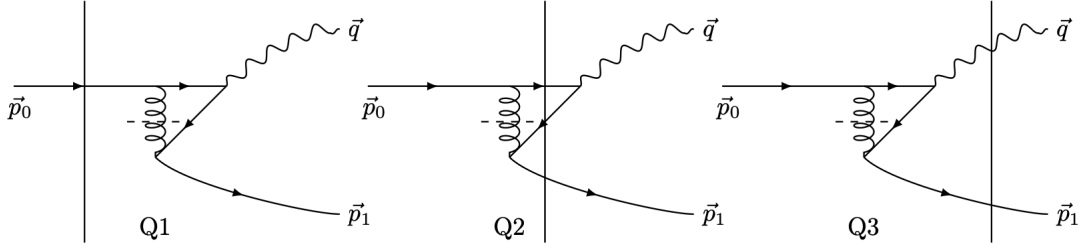


Figure 5. The three virtual contributions with an instantaneous $qq\bar{q}q$ vertex or, equivalently, a fictitious instantaneous gluon in the t -channel.

in the longitudinally polarized case, and:

$$\begin{aligned}
 \tilde{\mathcal{M}}_{A4,\text{sub}}^\lambda &= \frac{\mathbf{q}^\rho}{p_0^+ \mathbf{q}^2 + p_1^+ M^2} \frac{\alpha_s C_F}{D-2} \int_{p_1^+}^{p_0^+} \frac{dk^+}{k^+} \frac{q^+(k^+)^2}{2p_0^+(p_1^+ - k^+)} \\
 &\times \left\{ \left[\mathcal{S}_V^{j\rho j} + \epsilon^{ij} \mathcal{S}_V^{i\bar{\lambda}j} \epsilon^{\rho\bar{\lambda}} \frac{1}{D-3} \right] \frac{1}{4\pi} \ln \frac{\Delta_{UV}}{\hat{Q}^2} \right. \\
 &+ \left. \left[- \left(\hat{Q}^2 - \left(\frac{p_0^+ - k^+}{q^+} \mathbf{q} \right)^2 \right) \mathcal{S}_V^{j\rho j} + \frac{k^+(p_0^+ - k^+)}{p_1^+ q^+} \mathbf{q}^2 \epsilon^{ij} \mathcal{S}_V^{i\bar{\lambda}j} \epsilon^{\rho\bar{\lambda}} \frac{1}{D-3} \right] \right. \\
 &\left. \times \mathcal{B}_1 \left(0, \hat{Q}^2, \frac{p_0^+ - k^+}{q^+} \mathbf{q} \right) \right\} \int_{\mathbf{x}} e^{-i\mathbf{k}_\perp \cdot \mathbf{x}} (U_{\mathbf{x}} - 1), \tag{3.76}
 \end{aligned}$$

when the photon is transversely polarized.

3.4 Instantaneous four-fermion interaction

Diagram Q1. We obtain the following amplitudes for the first diagram in figure 5:

$$\tilde{\mathcal{M}}_{Q1}^0 = \frac{-\alpha_s C_F M}{p_0^+ \mathbf{P}_\perp^2 + p_1^+ M^2} \int_0^{q^+} d\ell_1^+ \frac{8p_1^+ \ell_1^+ (q^+ - \ell_1^+)}{q^+ (p_0^+ - \ell_1^+)^2} \mathcal{A}_0(\tilde{M}^2) \int_{\mathbf{x}} e^{-i\mathbf{k}_\perp \cdot \mathbf{x}} (U_{\mathbf{x}} - 1), \tag{3.77}$$

with:

$$\tilde{M}^2 \equiv -\frac{\ell_1^+ (q^+ - \ell_1^+)}{(q^+)^2} M^2 - i0^+. \tag{3.78}$$

In the transverse case, the amplitude simply disappears (it is proportional to an integral of the form $\int_{\ell} \ell^i / (\ell^2 + \Delta)$):

$$\tilde{\mathcal{M}}_{Q1}^\lambda = 0. \tag{3.79}$$

The UV counterterm for $\tilde{\mathcal{M}}_{Q1}^0$ is given by:

$$\tilde{\mathcal{M}}_{Q1,\text{UV}}^0 = -\frac{\alpha_s C_F M}{p_0^+ \mathbf{P}_\perp^2 + p_1^+ M^2} \int_0^{q^+} d\ell_1^+ \frac{8p_1^+ \ell_1^+ (q^+ - \ell_1^+)}{q^+ (p_0^+ - \ell_1^+)^2} \mathcal{A}_0(\Delta_{UV}) \int_{\mathbf{x}} e^{-i\mathbf{k}_\perp \cdot \mathbf{x}} (U_{\mathbf{x}} - 1) \tag{3.80}$$

such that the subtracted amplitude is equal to:

$$\tilde{\mathcal{M}}_{Q1,\text{sub}}^0 = -\frac{\alpha_s C_F M}{p_0^+ \mathbf{P}_\perp^2 + p_1^+ M^2} \int_0^{q^+} d\ell_1^+ \frac{8p_1^+ \ell_1^+ (q^+ - \ell_1^+)}{q^+ (p_0^+ - \ell_1^+)^2} \frac{1}{4\pi} \ln \frac{\Delta_{UV}}{\tilde{M}^2} \int_{\mathbf{x}} e^{-i\mathbf{k}_\perp \cdot \mathbf{x}} (U_{\mathbf{x}} - 1). \tag{3.81}$$

Diagram Q2. We obtain for the amplitude in which the outgoing photon is longitudinally polarized:

$$\begin{aligned}
 \tilde{\mathcal{M}}_{Q2}^0 &= -\frac{8\alpha_s}{M} \int_0^{q^+} d\ell_1^+ \frac{1}{(p_0^+ - \ell_1^+)^2} \frac{p_1^+ \ell_1^+}{p_1^+ + \ell_1^+} \int_{\mathbf{x}_1, \mathbf{x}_2, \mathbf{x}_3} \tilde{M}^2 \mathcal{K}(\mathbf{x}_{12}, \tilde{M}^2) \\
 &\quad \times \int_{\ell, \ell_2} \frac{e^{i\ell \cdot \mathbf{x}_{13}} e^{i\ell_2 \cdot \mathbf{x}_{23}}}{\left(\ell + \frac{\ell_1^+}{\ell_1^+ + p_1^+} \ell_2\right)^2 + \frac{p_1^+ \ell_1^+ p_0^+ \ell_2^2}{(q^+ - \ell_1^+)(p_1^+ + \ell_1^+)^2}} \\
 &\quad \times e^{-i\mathbf{q} \cdot \left(\frac{q^+ - \ell_1^+}{q^+} \mathbf{x}_2 + \frac{\ell_1^+}{q^+} \mathbf{x}_1\right)} e^{-i\mathbf{p}_1 \cdot \mathbf{x}_3} [U_{\mathbf{x}_3} t^a U_{\mathbf{x}_2}^\dagger U_{\mathbf{x}_1} t^a - C_F],
 \end{aligned} \tag{3.82}$$

and for the transverse case:

$$\begin{aligned}
 \tilde{\mathcal{M}}_{Q2}^\lambda &= -4\alpha_s \int_0^{q^+} d\ell_1^+ \frac{1}{(p_0^+ - \ell_1^+)^2} \frac{p_1^+ \ell_1^+}{p_1^+ + \ell_1^+} \mathcal{S}^{\lambda\bar{\lambda}} \left(\frac{2\ell_1^+}{q^+} - 1\right) \\
 &\quad \times \int_{\mathbf{x}_1, \mathbf{x}_2, \mathbf{x}_3} iA^{\bar{\lambda}}(\mathbf{x}_{12}, \tilde{M}^2) \\
 &\quad \times \int_{\ell, \ell_2} \frac{e^{i\ell \cdot \mathbf{x}_{13}} e^{i\ell_2 \cdot \mathbf{x}_{23}}}{\left(\ell + \frac{\ell_1^+}{\ell_1^+ + p_1^+} \ell_2\right)^2 + \frac{p_1^+ \ell_1^+ p_0^+ \ell_2^2}{(q^+ - \ell_1^+)(p_1^+ + \ell_1^+)^2}} \\
 &\quad \times e^{-i\mathbf{q} \cdot \left(\frac{q^+ - \ell_1^+}{q^+} \mathbf{x}_2 + \frac{\ell_1^+}{q^+} \mathbf{x}_1\right)} e^{-i\mathbf{p}_1 \cdot \mathbf{x}_3} [U_{\mathbf{x}_3} t^a U_{\mathbf{x}_2}^\dagger U_{\mathbf{x}_1} t^a - C_F].
 \end{aligned} \tag{3.83}$$

To investigate whether these amplitudes contain any divergences, we will take the $\mathbf{x}_3 \rightarrow \mathbf{x}_2 \rightarrow \mathbf{x}_1 \rightarrow \mathbf{x}$ limit in the non-divergent piece, i.e. the last line, which allows us to evaluate the integrals over \mathbf{x}_2 and \mathbf{x}_3 inside the transverse momentum integrations. We easily obtain:

$$\begin{aligned}
 \lim_{\mathbf{x}_i \rightarrow \mathbf{x}} \tilde{\mathcal{M}}_{Q2}^0 &= \frac{4\alpha_s C_F}{M} \int_0^{q^+} d\ell_1^+ \frac{(q^+ - \ell_1^+)}{(p_0^+ - \ell_1^+)^2} \frac{\ell_1^+}{q^+} \mathcal{A}_0(\tilde{M}^2) \int_{\mathbf{x}} e^{-i\mathbf{k}_\perp \cdot \mathbf{x}} (U_{\mathbf{x}} - 1) \\
 &\quad + \text{finite terms},
 \end{aligned} \tag{3.84}$$

where we made us of identities (A.8) and (A.9). The counterterm for $\tilde{\mathcal{M}}_{Q2,UV}^0$, therefore, reads:

$$\begin{aligned}
 \tilde{\mathcal{M}}_{Q2,UV}^0 &= \frac{4\alpha_s C_F}{M} \int_0^{q^+} d\ell_1^+ \frac{(q^+ - \ell_1^+)}{(p_0^+ - \ell_1^+)^2} \frac{\ell_1^+}{q^+} \mathcal{A}_0(\Delta_{UV}) \int_{\mathbf{x}} e^{-i\mathbf{k}_\perp \cdot \mathbf{x}} (U_{\mathbf{x}} - 1), \\
 &= \frac{4\alpha_s C_F}{M} \left(-2 + \frac{(p_0^+ + p_1^+)}{q^+} \ln \frac{p_0^+}{p_1^+}\right) \mathcal{A}_0(\Delta_{UV}) \int_{\mathbf{x}} e^{-i\mathbf{k}_\perp \cdot \mathbf{x}} (U_{\mathbf{x}} - 1),
 \end{aligned} \tag{3.85}$$

and the subtracted amplitude is given by:

$$\begin{aligned}
 \tilde{\mathcal{M}}_{Q2,sub}^0 &= -\frac{8\alpha_s}{M} \left[\int_0^{q^+} d\ell_1^+ \frac{1}{(p_0^+ - \ell_1^+)^2} \frac{p_1^+ \ell_1^+}{p_1^+ + \ell_1^+} \int_{\mathbf{x}_1, \mathbf{x}_2, \mathbf{x}_3} \tilde{M}^2 \mathcal{K}(\mathbf{x}_{12}, \tilde{M}^2) \right. \\
 &\quad \times \int_{\ell, \ell_2} \frac{e^{i\ell \cdot \mathbf{x}_{13}} e^{i\ell_2 \cdot \mathbf{x}_{23}}}{\left(\ell + \frac{\ell_1^+}{\ell_1^+ + p_1^+} \ell_2\right)^2 + \frac{p_1^+ \ell_1^+ p_0^+ \ell_2^2}{(q^+ - \ell_1^+)(p_1^+ + \ell_1^+)^2}} \\
 &\quad \times e^{-i\mathbf{q} \cdot \left(\frac{q^+ - \ell_1^+}{q^+} \mathbf{x}_2 + \frac{\ell_1^+}{q^+} \mathbf{x}_1\right)} e^{-i\mathbf{p}_1 \cdot \mathbf{x}_3} [U_{\mathbf{x}_3} t^a U_{\mathbf{x}_2}^\dagger U_{\mathbf{x}_1} t^a - C_F] \\
 &\quad \left. - \left(1 - \frac{p_0^+ + p_1^+}{2q^+} \ln \frac{p_0^+}{p_1^+}\right) \mathcal{A}_0(\Delta_{UV}) \int_{\mathbf{x}} e^{-i\mathbf{k}_\perp \cdot \mathbf{x}} C_F (U_{\mathbf{x}} - 1) \right].
 \end{aligned} \tag{3.86}$$

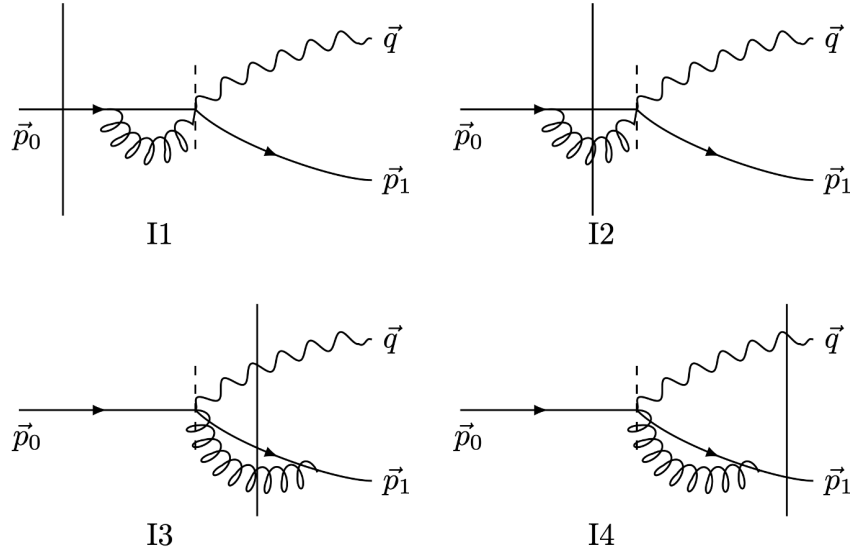


Figure 6. The four virtual diagrams with an instantaneous $q\bar{q}\gamma q$ -vertex. Two additional diagrams where the gluon is attached to the asymptotic incoming or outgoing quark disappear.

In the transversely polarized case, the amplitude turns out to be free from UV divergences:

$$\lim_{x_i \rightarrow x} \tilde{\mathcal{M}}_{Q2}^\lambda = 0. \quad (3.87)$$

Diagram Q3. We obtain the following expressions for the production amplitudes for a longitudinally resp. transversely polarized virtual photon:

$$\tilde{\mathcal{M}}_{Q3}^0 = -\frac{p_0^+ \mathbf{q}^2 - p_1^+ M^2}{p_0^+ \mathbf{q}^2 + p_1^+ M^2} \frac{\alpha_s C_F}{M} \int_0^{q^+} d\ell_1^+ \frac{4\ell_1^+(q^+ - \ell_1^+)}{q^+(p_0^+ - \ell_1^+)^2} \mathcal{A}_0(\tilde{Q}^2) \int_{\mathbf{x}} e^{-i\mathbf{k}_\perp \cdot \mathbf{x}} (U_{\mathbf{x}} - 1), \quad (3.88)$$

with

$$\tilde{Q}^2 \equiv \frac{\ell_1^+ p_0^+(q^+ - \ell_1^+)}{p_1^+(q^+)^2} \mathbf{q}^2 - i0^+, \quad (3.89)$$

and:

$$\tilde{\mathcal{M}}_{Q3}^\lambda = 0. \quad (3.90)$$

The counterterm for $\tilde{\mathcal{M}}_{Q3}^0$ is given by:

$$\tilde{\mathcal{M}}_{Q3,UV}^0 = -\frac{p_0^+ \mathbf{q}^2 - p_1^+ M^2}{p_0^+ \mathbf{q}^2 + p_1^+ M^2} \frac{\alpha_s C_F}{M} \int_0^{q^+} d\ell_1^+ \frac{4\ell_1^+(q^+ - \ell_1^+)}{q^+(p_0^+ - \ell_1^+)^2} \mathcal{A}_0(\Delta_{UV}) \int_{\mathbf{x}} e^{-i\mathbf{k}_\perp \cdot \mathbf{x}} (U_{\mathbf{x}} - 1), \quad (3.91)$$

such that the subtracted amplitude reads:

$$\tilde{\mathcal{M}}_{Q3,sub}^0 = -\frac{p_0^+ \mathbf{q}^2 - p_1^+ M^2}{p_0^+ \mathbf{q}^2 + p_1^+ M^2} \frac{\alpha_s C_F}{4\pi M} \int_0^{q^+} d\ell_1^+ \frac{4\ell_1^+(q^+ - \ell_1^+)}{q^+(p_0^+ - \ell_1^+)^2} \ln \frac{\Delta_{UV}}{\tilde{Q}^2} \int_{\mathbf{x}} e^{-i\mathbf{k}_\perp \cdot \mathbf{x}} (U_{\mathbf{x}} - 1). \quad (3.92)$$

3.5 Instantaneous $q\bar{q}\gamma q$ interaction

Diagram I1. We obtain the following result for the amplitude corresponding to graph I1 (see figure 6) in the longitudinal case:

$$\tilde{\mathcal{M}}_{I1}^0 = -\frac{\alpha_s C_F}{M} \int_0^{p_0^+} \frac{dk^+}{k^+} \left(\frac{k^+}{p_0^+} \right)^2 \frac{q^+}{(p_1^+ - k^+)} \left(\frac{2p_0^+}{k^+} + D - 4 \right) \mathcal{A}_0(\Delta_P) \int_{\mathbf{x}} e^{-i\mathbf{k}_\perp \cdot \mathbf{x}} (U_{\mathbf{x}} - 1). \quad (3.93)$$

The amplitude disappears when the outgoing virtual photon is transversely polarized:

$$\tilde{\mathcal{M}}_{\text{I1}}^\lambda = 0. \quad (3.94)$$

Clearly, $\tilde{\mathcal{M}}_{\text{I1}}^0$ has a ultraviolet divergence, contained inside \mathcal{A}_0 . We extract it by defining the counterterm:

$$\begin{aligned} \tilde{\mathcal{M}}_{\text{I1,UV}}^0 &= -\frac{\alpha_s C_F}{M} \int_0^{p_0^+} \frac{dk^+}{k^+} \left(\frac{k^+}{p_0^+}\right)^2 \frac{q^+}{(p_1^+ - k^+)} \left(\frac{2p_0^+}{k^+} + D - 4\right) \\ &\quad \times \mathcal{A}_0(\Delta_{\text{UV}}) \int_{\mathbf{x}} e^{-i\mathbf{k}_\perp \cdot \mathbf{x}} (U_{\mathbf{x}} - 1), \end{aligned} \quad (3.95)$$

such that the subtracted amplitude reads:

$$\tilde{\mathcal{M}}_{\text{I1,sub}}^0 = \frac{\alpha_s C_F}{4\pi M} \frac{q^+}{2p_0^+} \int_0^{p_0^+} \frac{dk^+}{k^+ - p_1^+} \ln \frac{\Delta_{\text{UV}}}{\Delta_{\text{P}}} \int_{\mathbf{x}} e^{-i\mathbf{k}_\perp \cdot \mathbf{x}} (U_{\mathbf{x}} - 1). \quad (3.96)$$

Diagram I2. We obtain for the amplitude when the virtual photon is longitudinally polarized:

$$\begin{aligned} \tilde{\mathcal{M}}_{\text{I2}}^0 &= \frac{\alpha_s}{M} \int_0^{p_0^+} \frac{dk^+}{k^+} \left(\frac{k^+}{p_0^+}\right)^2 \frac{p_0^+ - k^+}{p_1^+ - k^+} \int_{\mathbf{x}, \mathbf{z}} iA^{\eta'}(\mathbf{x} - \mathbf{z}) \mathcal{S}^{\eta'} \left(\frac{2p_0^+}{k^+} - 1\right) \\ &\quad \times \left[\frac{q^+ iA^i(\mathbf{x} - \mathbf{z}, \Delta_{\text{P}})}{p_0^+ - k^+} (\delta^{\eta i} + i\sigma^{\eta i}) \right. \\ &\quad \left. - \frac{2p_1^+ - k^+}{p_1^+} \mathbf{P}_\perp^i \mathcal{K}(\mathbf{x} - \mathbf{z}, \Delta_{\text{P}}) \left(\delta^{\eta i} + \frac{k^+}{2p_1^+ - k^+} i\sigma^{\eta i} \right) \right] \\ &\quad \times e^{-i\mathbf{k}_\perp \cdot \left(\frac{p_0^+ - k^+}{p_0^+} \mathbf{x} + \frac{k^+}{p_0^+} \mathbf{z}\right)} (t^a U_{\mathbf{x}} U_{\mathbf{z}}^\dagger t^a U_{\mathbf{z}} - C_F). \end{aligned} \quad (3.97)$$

Likewise, in the transverse case:

$$\begin{aligned} \tilde{\mathcal{M}}_{\text{I2}}^\lambda &= \alpha_s \int_0^{p_0^+} \frac{dk^+}{k^+} \left(\frac{k^+}{p_0^+}\right)^2 (p_0^+ - k^+) \int_{\mathbf{x}, \mathbf{z}} iA^{\bar{\eta}}(\mathbf{x} - \mathbf{z}) \mathcal{K}(\mathbf{x} - \mathbf{z}, \Delta_{\text{P}}) \\ &\quad \times \left[\left(\frac{1}{p_1^+ - k^+} + \frac{1}{p_0^+}\right) \delta^{\eta\lambda} + \left(\frac{1}{p_1^+ - k^+} - \frac{1}{p_0^+}\right) i\sigma^{\eta\lambda} \right] \mathcal{S}^{\eta\bar{\eta}} \left(\frac{2p_0^+}{k^+} - 1\right) \\ &\quad \times e^{-i\mathbf{k}_\perp \cdot \left(\frac{p_0^+ - k^+}{p_0^+} \mathbf{x} + \frac{k^+}{p_0^+} \mathbf{z}\right)} (t^a U_{\mathbf{x}} U_{\mathbf{z}}^\dagger t^a U_{\mathbf{z}} - C_F). \end{aligned} \quad (3.98)$$

Not surprisingly, the amplitude $\tilde{\mathcal{M}}_{\text{I2}}^0$ contains an ultraviolet divergence in the limit $\mathbf{z} \rightarrow \mathbf{x}$:

$$\begin{aligned} \lim_{\mathbf{z} \rightarrow \mathbf{x}} \tilde{\mathcal{M}}_{\text{I2}}^0 &= \frac{\alpha_s C_F}{M} \int_0^{p_0^+} \frac{dk^+}{k^+} \left(\frac{k^+}{p_0^+}\right)^2 \frac{q^+}{(p_1^+ - k^+)} \left(\frac{2p_0^+}{k^+} + D - 4\right) \\ &\quad \times \mathcal{A}_0(\Delta_{\text{P}}) \int_{\mathbf{x}} e^{-i\mathbf{k}_\perp \cdot \mathbf{x}} (U_{\mathbf{x}} - 1). \end{aligned} \quad (3.99)$$

Defining the counterterm:

$$\begin{aligned} \tilde{\mathcal{M}}_{\text{I2,UV}}^0 &= \frac{\alpha_s C_F}{M} \int_0^{p_0^+} \frac{dk^+}{k^+} \left(\frac{k^+}{p_0^+}\right)^2 \frac{q^+}{(p_1^+ - k^+)} \left(\frac{2p_0^+}{k^+} + D - 4\right) \\ &\quad \times \mathcal{A}_0(\Delta_{\text{UV}}) \int_{\mathbf{x}} e^{-i\mathbf{k}_\perp \cdot \mathbf{x}} (U_{\mathbf{x}} - 1) = -\tilde{\mathcal{M}}_{\text{I1,UV}}^0, \end{aligned} \quad (3.100)$$

we obtain the following result for the UV-subtracted amplitude:

$$\begin{aligned}
 \tilde{\mathcal{M}}_{I2,\text{sub}}^0 &= \frac{\alpha_s}{M} \int_0^{p_0^+} \frac{dk^+}{k^+} \frac{k^+}{p_0^+} \left[\frac{k^+}{p_0^+} \frac{p_0^+ - k^+}{p_1^+ - k^+} \int_{\mathbf{x}, \mathbf{z}} iA^{\eta'}(\mathbf{x} - \mathbf{z}) \mathcal{S}^{\eta\eta'} \left(\frac{2p_0^+}{k^+} - 1 \right) \right. \\
 &\quad \times \left(\frac{q^+ iA^i(\mathbf{x} - \mathbf{z}, \Delta_P)}{p_0^+ - k^+} (\delta^{\eta i} + i\sigma^{\eta i}) - \frac{2p_1^+ - k^+}{p_1^+} \mathbf{P}_\perp^i \mathcal{K}(\mathbf{x} - \mathbf{z}, \Delta_P) \left(\delta^{\eta i} + \frac{k^+}{2p_1^+ - k^+} i\sigma^{\eta i} \right) \right) \\
 &\quad \times e^{-i\mathbf{k}_\perp \cdot \left(\frac{p_0^+ - k^+}{p_0^+} \mathbf{x} + \frac{k^+}{p_0^+} \mathbf{z} \right)} (t^a U_{\mathbf{x}} U_{\mathbf{z}}^\dagger t^a U_{\mathbf{z}} - C_F) \\
 &\quad \left. - \frac{2q^+}{(p_1^+ - k^+)} \mathcal{A}_0(\Delta_{UV}) \int_{\mathbf{x}} e^{-i\mathbf{k}_\perp \cdot \mathbf{x}} C_F (U_{\mathbf{x}} - 1) \right].
 \end{aligned} \tag{3.101}$$

Diagram I3. The results for the amplitudes corresponding to the Feynman graph I3 read:

$$\begin{aligned}
 \tilde{\mathcal{M}}_{I3}^0 &= \frac{\alpha_s}{M} \int_0^{p_1^+} dk^+ \frac{k^+(p_1^+ - k^+)}{(p_1^+)^2} \mathcal{S}^{\eta\bar{\eta}} \left(1 - \frac{2p_1^+}{k^+} \right) \int_{\mathbf{x}, \mathbf{z}} iA^{\bar{\eta}}(\mathbf{x} - \mathbf{z}) \\
 &\quad \times \left[\left(\frac{2p_0^+ - k^+}{p_1^+(p_0^+ - k^+)} \mathbf{q}^i \mathcal{K}(\mathbf{x} - \mathbf{z}, \Delta_P) + \frac{q^+ iA^i(\mathbf{x} - \mathbf{z}, \Delta_q)}{(p_0^+ - k^+)(p_1^+ - k^+)} \right) \delta^{\eta i} \right. \\
 &\quad \left. - \left(\frac{k^+}{p_1^+(p_0^+ - k^+)} \mathbf{q}^i \mathcal{K}(\mathbf{x} - \mathbf{z}, \Delta_P) + \frac{q^+ iA^i(\mathbf{x} - \mathbf{z}, \Delta_q)}{(p_0^+ - k^+)(p_1^+ - k^+)} \right) i\sigma^{\eta i} \right] \\
 &\quad \times e^{-i\mathbf{k}_\perp \cdot \left(\frac{p_1^+ - k^+}{p_1^+} \mathbf{x} + \frac{k^+}{p_1^+} \mathbf{z} \right)} (t^a U_{\mathbf{x}} U_{\mathbf{z}}^\dagger t^a U_{\mathbf{z}} - C_F),
 \end{aligned} \tag{3.102}$$

and:

$$\begin{aligned}
 \tilde{\mathcal{M}}_{I3}^\lambda &= \alpha_s \int_0^{p_1^+} dk^+ \frac{k^+(p_1^+ - k^+)}{(p_1^+)^2} \mathcal{S}^{\eta\bar{\eta}} \left(1 - \frac{2p_1^+}{k^+} \right) \\
 &\quad \times \left[\left(\frac{1}{p_1^+} + \frac{1}{p_0^+ - k^+} \right) \delta^{\eta\lambda} + \left(\frac{1}{p_1^+} - \frac{1}{p_0^+ - k^+} \right) i\sigma^{\eta\lambda} \right] \\
 &\quad \times \int_{\mathbf{x}, \mathbf{z}} iA^{\bar{\eta}}(\mathbf{x} - \mathbf{z}) \mathcal{K}(\mathbf{x} - \mathbf{z}, \Delta_P) e^{-i\mathbf{k}_\perp \cdot \left(\frac{p_1^+ - k^+}{p_1^+} \mathbf{x} + \frac{k^+}{p_1^+} \mathbf{z} \right)} (t^c U_{\mathbf{x}} U_{\mathbf{z}}^\dagger t^c U_{\mathbf{z}} - C_F).
 \end{aligned} \tag{3.103}$$

Amplitude $\tilde{\mathcal{M}}_{I3}^0$ is UV divergent in the limit $\mathbf{z} \rightarrow \mathbf{x}$:

$$\begin{aligned}
 \lim_{\mathbf{z} \rightarrow \mathbf{x}} \tilde{\mathcal{M}}_{I3}^0 &= \frac{\alpha_s C_F}{M} \int_0^{p_1^+} dk^+ \frac{k^+}{(p_1^+)^2} \frac{q^+}{(p_0^+ - k^+)} \left(\frac{2p_1^+}{k^+} + D - 4 \right) \mathcal{A}_0(\Delta_q) \\
 &\quad \times e^{-i\mathbf{k}_\perp \cdot \mathbf{x}} (U_{\mathbf{x}} - 1).
 \end{aligned} \tag{3.104}$$

The counterterm reads:

$$\begin{aligned}
 \tilde{\mathcal{M}}_{I3,\text{UV}}^0 &= \frac{\alpha_s C_F}{M} \int_0^{p_1^+} dk^+ \frac{k^+}{(p_1^+)^2} \frac{q^+}{(p_0^+ - k^+)} \left(\frac{2p_1^+}{k^+} + D - 4 \right) \\
 &\quad \times \mathcal{A}_0(\Delta_{UV}) e^{-i\mathbf{k}_\perp \cdot \mathbf{x}} (U_{\mathbf{x}} - 1),
 \end{aligned} \tag{3.105}$$

such that the subtracted amplitude becomes:

$$\begin{aligned}
\tilde{\mathcal{M}}_{\text{I3,sub}}^0 &= \frac{\alpha_s}{M} \int_{\mathbf{x}} e^{-i\mathbf{k}_\perp \cdot \mathbf{x}} \int_0^{p_1^+} \frac{dk^+}{p_0^+ - k^+} \left[\int_{\mathbf{z}} \frac{k^+(p_1^+ - k^+)}{(p_1^+)^2} iA^i(\mathbf{x} - \mathbf{z}) \right. \\
&\quad \times \left(-\frac{2p_1^+}{k^+} \frac{q^+ iA^i(\mathbf{x} - \mathbf{z}, \Delta_q)}{p_1^+ - k^+} \right. \\
&\quad \left. \left. + \frac{k^+}{p_1^+} \mathbf{q}^i \mathcal{K}(\mathbf{x} - \mathbf{z}, \Delta_P) \left(\frac{2p_0^+ - k^+}{k^+} \left(1 - \frac{2p_1^+}{k^+} \right) - 1 \right) \right) \right. \\
&\quad \left. \times e^{\frac{k^+}{p_1^+} \mathbf{k}_\perp \cdot (\mathbf{x} - \mathbf{z})} (t^a U_{\mathbf{x}} U_{\mathbf{z}}^\dagger t^a U_{\mathbf{z}} - C_F) - \frac{2q^+}{p_1^+} \mathcal{A}_0(\Delta_{UV}) C_F (U_{\mathbf{x}} - 1) \right].
\end{aligned} \tag{3.106}$$

Diagram I4. We obtain for the last diagram in figure 6:

$$\begin{aligned}
\tilde{\mathcal{M}}_{\text{I4}}^0 &= -\frac{\alpha_s C_F}{M} \int_0^{p_1^+} dk^+ \frac{q^+ k^+}{(p_1^+)^2 (p_0^+ - k^+)} \left(\frac{2p_1^+}{k^+} + D - 4 \right) \\
&\quad \times \mathcal{A}_0(\Delta_q) \int_{\mathbf{x}} e^{-i\mathbf{k}_\perp \cdot \mathbf{x}} (U_{\mathbf{x}} - 1),
\end{aligned} \tag{3.107}$$

and:

$$\tilde{\mathcal{M}}_{\text{I4}}^\lambda = 0. \tag{3.108}$$

The counterterm reads:

$$\begin{aligned}
\tilde{\mathcal{M}}_{\text{I4,UV}}^0 &= -\frac{\alpha_s C_F}{M} \int_0^{p_1^+} dk^+ \frac{q^+ k^+}{(p_1^+)^2 (p_0^+ - k^+)} \left(\frac{2p_1^+}{k^+} + D - 4 \right) \\
&\quad \times \mathcal{A}_0(\Delta_{UV}) \int_{\mathbf{x}} e^{-i\mathbf{k}_\perp \cdot \mathbf{x}} (U_{\mathbf{x}} - 1) = -\tilde{\mathcal{M}}_{\text{I3,UV}}^0,
\end{aligned} \tag{3.109}$$

with the subtracted amplitude:

$$\tilde{\mathcal{M}}_{\text{I4,sub}}^0 = \frac{\alpha_s C_F}{2\pi M} \int_0^{p_1^+} dk^+ \frac{q^+}{p_1^+ (k^+ - p_0^+)} \ln \frac{\Delta_{UV}}{\Delta_q} \int_{\mathbf{x}} e^{-i\mathbf{k}_\perp \cdot \mathbf{x}} (U_{\mathbf{x}} - 1). \tag{3.110}$$

3.6 Quark field-strength renormalization

The last class of virtual diagrams that we consider are those corresponding to self-energy corrections on the asymptotic quarks. Although the corresponding amplitudes vanish in dimensional renormalization, we will compute them explicitly. Indeed, they consist of two identical parts with an opposite sign, one corresponding to an ultraviolet pole, the other to an infrared one. Since in dimensional renormalization $\epsilon_{UV} = \epsilon_{IR}$, the net result is zero, although in our analysis we will treat the ultraviolet and infrared parts separately.

The amplitudes corresponding to the diagrams in figure 7 each feature a vanishing energy denominator, e.g., $\propto (p_0^- - p_0^-)^{-1}$ for Z1 and Z2. One possible solution would be to add an artificial mass term, calculate them, and taking the massless limit in the end. Instead, we make use of the normalization properties of the Fock states (see e.g., [21, 32, 80]).

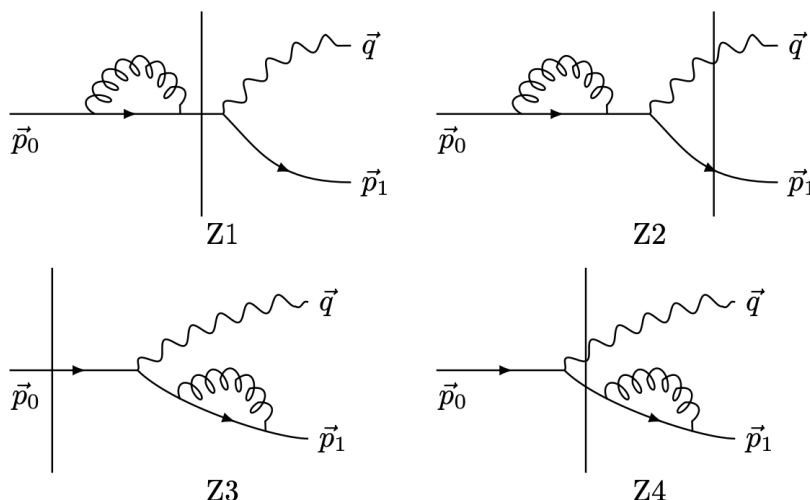


Figure 7. The four virtual contributions with a gluon loop on the asymptotic in- or outgoing quark.

Indeed, as demonstrated in appendix E, the total contribution of the diagrams in figure 7 can be summarized into the following renormalization constant of the quark field strength:

$$\mathcal{Z} = 1 - \frac{\alpha_s C_F}{\pi} \left(\frac{1}{\epsilon_{\text{UV}}} - \frac{1}{\epsilon_{\text{coll}}} \right) \left(-\frac{3}{2} + \ln \frac{p_0^+}{k_{\text{min}}^+} + \ln \frac{p_1^+}{k_{\text{min}}^+} \right), \quad (3.111)$$

which appears on the level of the squared amplitude as:

$$2\mathcal{M}_{\text{LO}}^\dagger (\mathcal{M}_{\text{Z1}} + \mathcal{M}_{\text{Z2}} + \mathcal{M}_{\text{Z3}} + \mathcal{M}_{\text{Z4}}) = (\mathcal{Z} - 1) |\mathcal{M}_{\text{LO}}|^2, \quad (3.112)$$

irrespective of the polarization of the emitted virtual photon.

In anticipation of what follows, we rewrite \mathcal{Z} as

$$\mathcal{Z} = 1 + \mathcal{Z}_{\text{UV}} + \mathcal{Z}_{\text{UV}}^\dagger + \mathcal{Z}_{\text{IS}} + \mathcal{Z}_{\text{IS}}^\dagger + \mathcal{Z}_{\text{FS}} + \mathcal{Z}_{\text{FS}}^\dagger, \quad (3.113)$$

with:

$$\begin{aligned} \mathcal{Z}_{\text{UV}} &= \frac{\alpha_s C_F}{\pi} \left(\frac{1}{\epsilon_{\text{UV}}} + \ln \frac{\mu^2}{\mu_R^2} \right) \left(\frac{3}{4} - \frac{1}{2} \ln \frac{p_0^+}{k_{\text{min}}^+} - \frac{1}{2} \ln \frac{p_1^+}{k_{\text{min}}^+} \right), \\ \mathcal{Z}_{\text{IS}} &= \frac{\alpha_s C_F}{\pi} \left(\frac{1}{\epsilon_{\text{coll}}} + \ln \frac{\mu^2}{\mu_R^2} \right) \left(-\frac{3}{8} + \frac{1}{2} \ln \frac{p_0^+}{k_{\text{min}}^+} \right), \\ \mathcal{Z}_{\text{FS}} &= \frac{\alpha_s C_F}{\pi} \left(\frac{1}{\epsilon_{\text{coll}}} + \ln \frac{\mu^2}{\mu_R^2} \right) \left(-\frac{3}{8} + \frac{1}{2} \ln \frac{p_1^+}{k_{\text{min}}^+} \right). \end{aligned} \quad (3.114)$$

Since the scale μ_R^2 cancels on the cross-section level, we are free to adjust it at will.

4 Ultraviolet divergences

At the perturbative order of our calculation, all short-distance or ultraviolet divergences are contained in the virtual corrections presented in the previous section. Because contributions to the running coupling take place at higher perturbative orders, and since we work in the massless limit, these singularities have to cancel on the level of the total virtual amplitude.

In this section, we will demonstrate that this is indeed the case, which is an important check of the calculation.

Two classes of virtual amplitudes, namely the self-energy corrections in section 3.1, and the ones with an instantaneous $gq\gamma q$ interaction (section 3.5), are somewhat particular. Indeed, we have seen that (see eqs. (3.12), (3.13), and (3.23)):

$$\tilde{\mathcal{M}}_{\text{SE}2,\text{UV}}^{0,\lambda} = -\tilde{\mathcal{M}}_{\text{SE}1,\text{UV}}^{0,\lambda} \quad \text{and} \quad \tilde{\mathcal{M}}_{\text{SE}4,\text{UV}}^{0,\lambda} = -\tilde{\mathcal{M}}_{\text{SE}3,\text{UV}}^{0,\lambda}, \quad (4.1)$$

and, therefore, all UV divergences already cancel in the sum of these four self-energy amplitudes. The same is true for the amplitudes with an instantaneous $gq\gamma q$ vertex and a longitudinally polarized photon (eqs. (3.100) and (3.109)):

$$\tilde{\mathcal{M}}_{\text{I}2,\text{UV}}^0 = -\tilde{\mathcal{M}}_{\text{I}1,\text{UV}}^0 \quad \text{and} \quad \tilde{\mathcal{M}}_{\text{I}4,\text{UV}}^0 = -\tilde{\mathcal{M}}_{\text{I}3,\text{UV}}^0, \quad (4.2)$$

while in the transverse case, the amplitudes never exhibit UV divergencies to begin with.

All the ultraviolet divergences we encountered are contained in integrals $\mathcal{A}_0(\Delta)$ (A.8) which, when evaluated in dimensional regularization, give:

$$\mathcal{A}_0(\Delta) \equiv \int_{\ell} \frac{1}{\ell^2 + \Delta} = \frac{1}{4\pi} \left(\frac{1}{\epsilon_{\text{UV}}} - \gamma_E + \ln 4\pi + \ln \frac{\mu^2}{\Delta} \right) + \mathcal{O}(\epsilon_{\text{UV}}). \quad (4.3)$$

Following the $\overline{\text{MS}}$ scheme, we will extract the poles together with the universal constants $-\gamma_E + \ln 4\pi$, writing:

$$\mathcal{A}_0(\Delta) = \frac{1}{4\pi} \left(\frac{1}{\bar{\epsilon}} + \ln \frac{\mu^2}{\Delta} \right) + \mathcal{O}(\epsilon_{\text{UV}}), \quad (4.4)$$

where we defined:

$$\frac{1}{\bar{\epsilon}} \equiv \frac{1}{\epsilon_{\text{UV}}} - \gamma_E + \ln 4\pi. \quad (4.5)$$

4.1 Longitudinal polarization

Vertex corrections. We start by collecting the UV-divergent parts of the vertex-correction amplitudes, which are absorbed in the counterterms. The counterterms (3.30) and (3.40) can be combined into:

$$\tilde{\mathcal{M}}_{\text{V}1,\text{UV}}^0 + \tilde{\mathcal{M}}_{\text{V}2,\text{UV}}^0 = \tilde{\mathcal{M}}_{\text{LO}1}^0 \times -\frac{\alpha_s C_F}{D-2} \int_{k_{\min}^+}^{p_1^+} \frac{dk^+ (k^+)^2}{k^+ p_0^+ p_1^+} \mathcal{S}_V^{j0j} \mathcal{A}_0(\Delta_{\text{UV}}), \quad (4.6)$$

while summing (3.46) and (3.51) gives:

$$\tilde{\mathcal{M}}_{\text{V}3,\text{UV}}^0 + \tilde{\mathcal{M}}_{\text{V}4,\text{UV}}^0 = \tilde{\mathcal{M}}_{\text{LO}2}^0 \times -\frac{\alpha_s C_F}{D-2} \int_{k_{\min}^+}^{p_1^+} \frac{dk^+ (k^+)^2}{k^+ p_0^+ p_1^+} \mathcal{S}_V^{j0j} \mathcal{A}_0(\Delta_{\text{UV}}). \quad (4.7)$$

In the above expressions, \mathcal{S}_V^{j0j} is the symmetric part of the Dirac structure (3.26). We then easily find:

$$\tilde{\mathcal{M}}_{\text{V}1,\text{UV}}^0 + \tilde{\mathcal{M}}_{\text{V}2,\text{UV}}^0 = \tilde{\mathcal{M}}_{\text{LO}1}^0 \frac{\alpha_s C_F}{\pi} \left[\left(\frac{1}{\bar{\epsilon}} + \ln \frac{\mu^2}{\Delta_{\text{UV}}} \right) \left(-\frac{3p_1^+ + 2q^+}{4p_0^+} + \ln \frac{p_1^+}{k_{\min}^+} \right) - \frac{1}{4} \frac{p_1^+}{p_0^+} \right], \quad (4.8)$$

and:

$$\tilde{\mathcal{M}}_{\text{V}3,\text{UV}}^0 + \tilde{\mathcal{M}}_{\text{V}4,\text{UV}}^0 = \tilde{\mathcal{M}}_{\text{LO}2}^0 \frac{\alpha_s C_F}{\pi} \left[\left(\frac{1}{\bar{\epsilon}} + \ln \frac{\mu^2}{\Delta_{\text{UV}}} \right) \left(-\frac{3p_1^+ + 2q^+}{4p_0^+} + \ln \frac{p_1^+}{k_{\min}^+} \right) - \frac{1}{4} \frac{p_1^+}{p_0^+} \right]. \quad (4.9)$$

Antiquark vertex corrections. Likewise, let us collect the UV counterterms for the four amplitudes with an antiquark vertex. We see that the first three of them: (3.57), (3.64), and (3.68), nicely combine into:

$$\begin{aligned} & \tilde{\mathcal{M}}_{A1,UV}^0 + \tilde{\mathcal{M}}_{A2,UV}^0 + \tilde{\mathcal{M}}_{A3,UV}^0 \\ &= \tilde{\mathcal{M}}_{LO1}^0 \times -\frac{\alpha_s C_F}{D-2} \int_{p_1^+}^{p_0^+} \frac{dk^+}{k^+} \frac{k^+(p_0^+ - k^+)}{p_0^+ q^+} \mathcal{S}_V^{j0j} \mathcal{A}_0(\Delta_{UV}). \end{aligned} \quad (4.10)$$

The UV counterterm (3.73) is equal to:

$$\tilde{\mathcal{M}}_{A4,UV}^0 = \tilde{\mathcal{M}}_{LO2}^0 \times -\frac{\alpha_s C_F}{D-2} \int_{p_1^+}^{p_0^+} \frac{dk^+}{k^+} \frac{k^+(p_0^+ - k^+)}{p_0^+ q^+} \mathcal{S}_V^{j0j} \mathcal{A}_0(\Delta_{UV}). \quad (4.11)$$

Using expression (3.26) for the symmetrized part of the Dirac structure, the plus-momentum integral in the above expressions can be easily evaluated, yielding:

$$\tilde{\mathcal{M}}_{A1+2+3,UV}^0 = \tilde{\mathcal{M}}_{LO1}^0 \frac{\alpha_s C_F}{\pi} \left[\left(\frac{1}{\tilde{\epsilon}} + \ln \frac{\mu^2}{\Delta_{UV}} \right) \left(\frac{7}{4} + \frac{p_1^+}{4p_0^+} - \frac{3p_1^+ + p_0^+}{2q^+} \ln \frac{p_0^+}{p_1^+} \right) - \frac{q^+}{4p_0^+} \right], \quad (4.12)$$

and:

$$\tilde{\mathcal{M}}_{A4,UV}^0 = \tilde{\mathcal{M}}_{LO2}^0 \frac{\alpha_s C_F}{\pi} \left[\left(\frac{1}{\tilde{\epsilon}} + \ln \frac{\mu^2}{\Delta_{UV}} \right) \left(\frac{7}{4} + \frac{p_1^+}{4p_0^+} - \frac{3p_1^+ + p_0^+}{2q^+} \ln \frac{p_0^+}{p_1^+} \right) - \frac{q^+}{4p_0^+} \right]. \quad (4.13)$$

Instantaneous four-fermion vertex. Another category of ultraviolet-singular virtual diagrams are those with an instantaneous four-fermion vertex. Summing the counterterms (3.80) and (3.85), we obtain an expression proportional to the leading-order amplitude \mathcal{M}_{LO1}^0 :

$$\tilde{\mathcal{M}}_{Q1,UV}^0 + \tilde{\mathcal{M}}_{Q2,UV}^0 = \tilde{\mathcal{M}}_{LO1}^0 4\alpha_s C_F \int_0^{q^+} d\ell_1^+ \frac{(q^+ - \ell_1^+) \ell_1^+}{(p_0^+ - \ell_1^+)^2 q^+} \mathcal{A}_0(\Delta_{UV}). \quad (4.14)$$

Likewise, the counterterm (3.91) for the amplitude $\tilde{\mathcal{M}}_{Q3}^0$ is:

$$\tilde{\mathcal{M}}_{Q3,UV}^0 = \tilde{\mathcal{M}}_{LO2}^0 4\alpha_s C_F \int_0^{q^+} d\ell_1^+ \frac{\ell_1^+(q^+ - \ell_1^+)}{q^+(p_0^+ - \ell_1^+)^2} \mathcal{A}_0(\Delta_{UV}). \quad (4.15)$$

Evaluating the plus-momentum integrals, we obtain:

$$\tilde{\mathcal{M}}_{Q1+2,UV}^0 = \tilde{\mathcal{M}}_{LO1}^0 \frac{\alpha_s C_F}{\pi} \left(\frac{1}{\tilde{\epsilon}} + \ln \frac{\mu^2}{\Delta_{UV}} \right) \left(-2 + \frac{p_0^+ + p_1^+}{q^+} \ln \frac{p_0^+}{p_1^+} \right), \quad (4.16)$$

and:

$$\tilde{\mathcal{M}}_{Q3,UV}^0 = \tilde{\mathcal{M}}_{LO2}^0 \frac{\alpha_s C_F}{\pi} \left(\frac{1}{\tilde{\epsilon}} + \ln \frac{\mu^2}{\Delta_{UV}} \right) \left(-2 + \frac{p_0^+ + p_1^+}{q^+} \ln \frac{p_0^+}{p_1^+} \right). \quad (4.17)$$

Total UV contribution. The last set of UV divergences are those stemming from the field-strength renormalization diagrams, see eqs. (3.112) and (3.114):

$$\mathcal{Z}_{\text{UV}} \tilde{\mathcal{M}}_{\text{LO1},2}^0 = \tilde{\mathcal{M}}_{\text{LO1},2}^0 \frac{\alpha_s C_F}{\pi} \left(\frac{1}{\bar{\epsilon}} - \ln 4\pi e^{-\gamma_E} + \ln \frac{\mu^2}{\mu_R^2} \right) \left(\frac{3}{4} - \frac{1}{2} \ln \frac{p_0^+}{k_{\text{min}}^+} - \frac{1}{2} \ln \frac{p_1^+}{k_{\text{min}}^+} \right). \quad (4.18)$$

Combining them with the results from the previous paragraphs, namely (4.8), (4.12), and (4.16), we obtain:

$$\begin{aligned} & \tilde{\mathcal{M}}_{\text{V1+2,UV}}^0 + \tilde{\mathcal{M}}_{\text{A1+2+3,UV}}^0 + \tilde{\mathcal{M}}_{\text{Q1+2,UV}}^0 + \mathcal{Z}_{\text{UV}} \tilde{\mathcal{M}}_{\text{LO1}}^0 \\ &= \tilde{\mathcal{M}}_{\text{LO1}}^0 \frac{\alpha_s C_F}{\pi} \left[\left(-\frac{3}{4} + \frac{1}{2} \ln \frac{p_1^+}{k_{\text{min}}^+} + \frac{1}{2} \ln \frac{p_0^+}{k_{\text{min}}^+} \right) \ln \frac{4\pi e^{-\gamma_E} \mu^2}{\Delta_{\text{UV}}} - \frac{1}{4} \right]. \end{aligned} \quad (4.19)$$

Likewise, combining (4.18) with eqs. (4.9), (4.13), and (4.17):

$$\begin{aligned} & \tilde{\mathcal{M}}_{\text{V3+4,UV}}^0 + \tilde{\mathcal{M}}_{\text{A4,UV}}^0 + \tilde{\mathcal{M}}_{\text{Q3,UV}}^0 + \mathcal{Z}_{\text{UV}} \tilde{\mathcal{M}}_{\text{LO2}}^0 \\ &= \tilde{\mathcal{M}}_{\text{LO2}}^0 \frac{\alpha_s C_F}{\pi} \left[\left(-\frac{3}{4} + \frac{1}{2} \ln \frac{p_1^+}{k_{\text{min}}^+} + \frac{1}{2} \ln \frac{p_0^+}{k_{\text{min}}^+} \right) \ln \frac{4\pi e^{-\gamma_E} \mu^2}{\Delta_{\text{UV}}} - \frac{1}{4} \right]. \end{aligned} \quad (4.20)$$

The above two results confirm our earlier claim, namely that in the longitudinal case all the UV divergences encountered in our calculation cancel between the different virtual diagrams. Note that there are still divergences left, in the form of single logarithms depending on the plus-momentum cutoff k_{min}^+ . In section 8, we will show how they can be absorbed into the high-energy evolution of the target gluon density.

4.2 Transverse polarization

When the outgoing virtual photon is transversely polarized, the structure of the ultraviolet cancellation is slightly different compared to the longitudinal case. In particular, there are no contributions from the diagrams with an instantaneous four-fermion vertex. Moreover, since the Dirac structure is now much more complicated than in the previous case, we are forced to replace the spinor structures with simpler ones, obviously in such a way that this procedure still yields the correct cross section. Hence, although the ultraviolet divergences should already cancel at the level of the amplitude, as was the case in the previous section, in practice we will demonstrate this cancellation in a way closer to the level of the squared amplitude.

The first step is to expand the ‘even’ and ‘odd’ parts of the Dirac structure $\mathcal{S}_V^{\bar{\eta}\lambda\eta'}$ (3.29) as follows:

$$\begin{aligned} \mathcal{S}_V^{j\bar{\lambda}j} &= (D-2) \left(1 - 2 \frac{k^+ - p_1^+}{q^+} \right) \left(\left(1 - 2 \frac{p_1^+}{k^+} \right) \left(2 \frac{p_0^+}{k^+} - 1 \right) - (D-3) \right) \delta^{\lambda\bar{\lambda}} \\ &\quad - (D-2) \left(\left(1 - 2 \frac{p_1^+}{k^+} \right) \left(2 \frac{p_0^+}{k^+} - 1 \right) - (D-3) + 8 \frac{D-4}{D-2} \right) i\sigma^{\lambda\bar{\lambda}}, \end{aligned} \quad (4.21)$$

and:

$$\begin{aligned} \epsilon^{\bar{\lambda}\rho} \epsilon^{\bar{\eta}\eta'} \mathcal{S}_V^{\bar{\eta}\rho\eta'} &= \epsilon^{\bar{\lambda}\rho} \epsilon^{\bar{\eta}\eta'} \left[\left(1 - 2 \frac{k^+ - p_1^+}{q^+} \right) \left(2 \frac{p_0^+ + p_1^+}{k^+} - 2 - (D-4) \right) \delta^{\lambda\rho} i\sigma^{\bar{\eta}\eta'} \right. \\ &\quad \left. - \left(1 - 2 \frac{p_1^+}{k^+} \right) \sigma^{\lambda\rho} \sigma^{\bar{\eta}\eta'} + \left(2 \frac{p_0^+}{k^+} - 1 \right) \sigma^{\bar{\eta}\eta'} \sigma^{\lambda\rho} + i\sigma^{\eta\bar{\eta}} \sigma^{\lambda\rho} \sigma^{\eta\eta'} \right]. \end{aligned} \quad (4.22)$$

All the amplitudes we consider here are virtual, hence they will contribute to the cross section being multiplied with the conjugate of the leading-order amplitude, which contains the Dirac structure:

$$\mathcal{S}^{\lambda\lambda'} \left(1 + \frac{2p_1^+}{q^+}\right)^\dagger = \left(1 + \frac{2p_1^+}{q^+}\right) \delta^{\lambda\lambda'} + i\sigma^{\lambda\lambda'}. \quad (4.23)$$

After multiplication with the above LO Dirac structure and evaluating the trace, the different spinor structures appearing in (4.21) and (4.22) all become proportional to $\delta^{\bar{\lambda}\lambda'}$:

$$\begin{aligned} \text{Tr}\left\{\mathcal{P}_G \mathcal{S}^{\lambda\lambda'\dagger} \left(1 + \frac{2p_1^+}{q^+}\right) \delta^{\lambda\bar{\lambda}}\right\} &= 2 \frac{p_0^+ + p_1^+}{q^+} \delta^{\bar{\lambda}\lambda'}, \\ \text{Tr}\left\{\mathcal{P}_G \mathcal{S}^{\lambda\lambda'\dagger} \left(1 + \frac{2p_1^+}{q^+}\right) i\sigma^{\lambda\bar{\lambda}}\right\} &= -2(D-3) \delta^{\bar{\lambda}\lambda'}, \\ \epsilon^{\bar{\lambda}\rho} \epsilon^{\bar{\eta}\eta'} \text{Tr}\left\{\mathcal{P}_G \mathcal{S}^{\lambda\lambda'\dagger} \left(1 + \frac{2p_1^+}{q^+}\right) \delta^{\lambda\rho} i\sigma^{\bar{\eta}\eta'}\right\} &= 4\delta^{\bar{\lambda}\lambda'}, \\ \epsilon^{\bar{\lambda}\rho} \epsilon^{\bar{\eta}\eta'} \text{Tr}\left\{\mathcal{P}_G \mathcal{S}^{\lambda\lambda'\dagger} \left(1 + \frac{2p_1^+}{q^+}\right) \sigma^{\lambda\rho} \sigma^{\bar{\eta}\eta'}\right\} &= 4\delta^{\bar{\lambda}\lambda'} \left(1 + \frac{2p_1^+}{q^+} - (D-4)\right), \\ \epsilon^{\bar{\lambda}\rho} \epsilon^{\bar{\eta}\eta'} \text{Tr}\left\{\mathcal{P}_G \mathcal{S}^{\lambda\lambda'\dagger} \left(1 + \frac{2p_1^+}{q^+}\right) \sigma^{\bar{\eta}\eta'} \sigma^{\lambda\rho}\right\} &= 4\delta^{\bar{\lambda}\lambda'} \left(1 + \frac{2p_1^+}{q^+} + D-4\right), \\ \epsilon^{\bar{\lambda}\rho} \epsilon^{\bar{\eta}\eta'} \text{Tr}\left\{\mathcal{P}_G \mathcal{S}^{\lambda\lambda'\dagger} \left(1 + \frac{2p_1^+}{q^+}\right) i\sigma^{\eta\bar{\eta}} \sigma^{\lambda\rho} \sigma^{\eta\eta'}\right\} &= 4\delta^{\bar{\lambda}\lambda'} (D-4) \left(1 + \frac{2p_1^+}{q^+}\right), \end{aligned} \quad (4.24)$$

where we made use of the identities in appendix B. Therefore, in anticipation of the fact that the virtual amplitudes we consider will be multiplied with the leading-order one, we can rescale the Dirac structures in (4.21) and (4.22) as follows:

$$\begin{aligned} i\sigma^{\lambda\bar{\lambda}} &\rightarrow -(D-3) \frac{q^+}{p_1^+ + p_0^+} \delta^{\bar{\lambda}\lambda}, \\ \epsilon^{\bar{\lambda}\rho} \epsilon^{\bar{\eta}\eta'} \delta^{\lambda\rho} i\sigma^{\bar{\eta}\eta'} &\rightarrow 2 \frac{q^+}{p_1^+ + p_0^+} \delta^{\bar{\lambda}\lambda}, \\ \epsilon^{\bar{\lambda}\rho} \epsilon^{\bar{\eta}\eta'} \sigma^{\lambda\rho} \sigma^{\bar{\eta}\eta'} &\rightarrow 2 \left(1 - (D-4) \frac{q^+}{p_1^+ + p_0^+}\right) \delta^{\bar{\lambda}\lambda}, \\ \epsilon^{\bar{\lambda}\rho} \epsilon^{\bar{\eta}\eta'} \sigma^{\bar{\eta}\eta'} \sigma^{\lambda\rho} &\rightarrow 2 \left(1 + (D-4) \frac{q^+}{p_1^+ + p_0^+}\right) \delta^{\bar{\lambda}\lambda}, \\ \epsilon^{\bar{\lambda}\rho} \epsilon^{\bar{\eta}\eta'} i\sigma^{\eta\bar{\eta}} \sigma^{\lambda\rho} \sigma^{\eta\eta'} &\rightarrow 2(D-4) \delta^{\bar{\lambda}\lambda}, \end{aligned} \quad (4.25)$$

such that the even and odd parts of \mathcal{S}_V can be replaced by:

$$\begin{aligned} \mathcal{S}_V^{j\bar{\lambda}j} &\rightarrow (D-2) \delta^{\bar{\lambda}\lambda} \frac{q^+}{p_1^+ + p_0^+} \left[\left(\left(1 - 2 \frac{k^+ - p_1^+}{q^+}\right) \left(1 + \frac{2p_1^+}{q^+}\right) + (D-3) \right) \right. \\ &\quad \left. \times \left(\left(1 - 2 \frac{p_1^+}{k^+}\right) \left(2 \frac{p_0^+}{k^+} - 1\right) - (D-3) \right) + 8 \frac{(D-4)(D-3)}{D-2} \right], \end{aligned} \quad (4.26)$$

and

$$\begin{aligned} \epsilon^{\bar{\lambda}\rho} \epsilon^{\bar{\eta}\eta'} \mathcal{S}_V^{\bar{\eta}\rho\eta'} &\rightarrow \frac{8q^+}{p_1^+ + p_0^+} \delta^{\bar{\lambda}\lambda} \left[\left(1 + \frac{2p_1^+ - k^+}{q^+}\right) \left(\frac{p_0^+ + p_1^+}{k^+} - 1\right) \right. \\ &\quad \left. + \frac{D-4}{2} \left(\frac{q^+}{k^+} + \frac{k^+}{q^+}\right) \right]. \end{aligned} \quad (4.27)$$

Likewise, the leading-order Dirac structure is to be replaced with:

$$\mathcal{S}^{\lambda\bar{\lambda}} \left(1 + \frac{2p_1^+}{q^+} \right) \rightarrow \left(\left(1 + \frac{2p_1^+}{q^+} \right) + (D-3) \frac{q^+}{p_1^+ + p_0^+} \right) \delta^{\lambda\bar{\lambda}}. \quad (4.28)$$

In the following paragraphs, we will use an underline to denote the (reduced) amplitudes in which the rescaling procedure (4.25) has been performed. For instance, the leading-order amplitudes (2.29) become:

$$\begin{aligned} \underline{\tilde{\mathcal{M}}}_{\text{LO1}}^{\lambda'} &= \frac{-q^+ \mathbf{P}_\perp^{\lambda'}}{p_0^+ \mathbf{P}_\perp^2 + p_1^+ M^2} \frac{q^+}{p_1^+ + p_0^+} \left(\left(\frac{p_1^+ + p_0^+}{q^+} \right)^2 + D - 3 \right) \int_{\mathbf{x}} e^{-i\mathbf{k}_\perp \cdot \mathbf{x}} (U_{\mathbf{x}} - 1), \\ \underline{\tilde{\mathcal{M}}}_{\text{LO2}}^{\lambda'} &= \frac{-q^+ \mathbf{q}^{\lambda'}}{p_0^+ \mathbf{q}^2 + p_1^+ M^2} \frac{q^+}{p_1^+ + p_0^+} \left(\left(\frac{p_1^+ + p_0^+}{q^+} \right)^2 + D - 3 \right) \int_{\mathbf{x}} e^{-i\mathbf{k}_\perp \cdot \mathbf{x}} (U_{\mathbf{x}} - 1). \end{aligned} \quad (4.29)$$

Vertex corrections. Let us first study the UV counterterm $\tilde{\mathcal{M}}_{\text{V1,UV}}^\lambda$ (3.31). Applying the rescaling procedure $\tilde{\mathcal{M}}_{\text{V1,UV}}^\lambda \rightarrow \underline{\tilde{\mathcal{M}}}_{\text{V1,UV}}^\lambda$ and expanding $\mathcal{A}_0(\Delta_P)$, we get:

$$\begin{aligned} \underline{\tilde{\mathcal{M}}}_{\text{V1,UV}}^\lambda &= \underline{\tilde{\mathcal{M}}}_{\text{LO1}}^\lambda \times \frac{\alpha_s C_F}{\pi} \frac{1}{\left(\frac{p_1^+ + p_0^+}{q^+} \right)^2 + D - 3} \int_{k_{\min}^+}^{p_1^+} dk^+ \frac{q^+ (k^+)^2}{4p_1^+ p_0^+ (p_1^+ - k^+) (p_0^+ - k^+)} \\ &\times \left\{ \left(\frac{1}{2} + p_0^+ \frac{p_1^+ - k^+}{k^+ q^+} \right) \left[\left(\left(1 - 2 \frac{k^+ - p_1^+}{q^+} \right) \left(1 + \frac{2p_1^+}{q^+} \right) + (D-3) \right) \right. \right. \\ &\times \left. \left(\left(1 - 2 \frac{p_1^+}{k^+} \right) \left(2 \frac{p_0^+}{k^+} - 1 \right) - (D-3) \right) + 8 \frac{(D-4)(D-3)}{D-2} \right] \\ &+ \frac{4}{(D-3)(D-2)} \left[\left(1 + \frac{2p_1^+ - k^+}{q^+} \right) \left(\frac{p_0^+ + p_1^+}{k^+} - 1 \right) + \frac{D-4}{2} \left(\frac{q^+}{k^+} + \frac{k^+}{q^+} \right) \right] \left. \right\} \\ &\times \left(\frac{1}{\bar{\epsilon}} + \ln \frac{\mu^2}{\Delta_{\text{UV}}} \right) \end{aligned} \quad (4.30)$$

Expanding around $\epsilon_{\text{UV}} = 0$, we obtain, introducing for convenience $x = k^+ / p_1^+$, $a = p_0^+ / p_1^+$, and $b = k_{\min}^+ / p_1^+$:

$$\begin{aligned} \underline{\tilde{\mathcal{M}}}_{\text{V1,UV}}^\lambda &= \underline{\tilde{\mathcal{M}}}_{\text{LO1}}^\lambda \frac{\alpha_s C_F}{\pi} \left\{ \frac{3}{4} \frac{a(a-1)}{a^2+1} \int_0^1 \frac{dx}{x-1} \right. \\ &+ \left(\frac{1}{\bar{\epsilon}} + \ln \frac{\mu^2}{\Delta_{\text{UV}}} \right) \left(-\frac{1+2a}{2(1+a^2)} - \ln b \right) \\ &+ \left. \frac{6a^5 - 17a^4 + 14a^3 - 6a^2 - 8a + 3}{8a(a^2+1)^2} - \frac{3}{4} \frac{a-1}{a^2+1} \ln \frac{a-1}{a} \right\}. \end{aligned} \quad (4.31)$$

Following the same procedure for $\tilde{\mathcal{M}}_{\text{V4,UV}}^\lambda$ in (3.52), we get:

$$\begin{aligned} \tilde{\mathcal{M}}_{\text{V4,UV}}^\lambda &= \underline{\tilde{\mathcal{M}}}_{\text{LO2}}^\lambda \frac{\alpha_s C_F}{\pi} \left\{ \frac{3}{4} \frac{a(a-1)}{a^2+1} \int_0^1 \frac{dx}{x-1} + \left(\frac{1}{\bar{\epsilon}} + \ln \frac{\mu^2}{\Delta_{\text{UV}}} \right) \left(-\frac{1+2a}{2(1+a^2)} - \ln b \right) \right. \\ &+ \left. \frac{6a^5 - 17a^4 + 14a^3 - 6a^2 - 8a + 3}{8a(a^2+1)^2} - \frac{3}{4} \frac{a-1}{a^2+1} \ln \frac{a-1}{a} \right\}. \end{aligned} \quad (4.32)$$

Antiquark vertex diagrams. The counterterm $\tilde{\mathcal{M}}_{A1,UV}^\lambda$ (3.58) reads, after rescaling according to eq. (4.25):

$$\begin{aligned}
 \underline{\tilde{\mathcal{M}}}_{A1,UV}^\lambda &= \tilde{\mathcal{M}}_{LO1}^\lambda \times -\frac{\alpha_s C_F}{\pi} \frac{1}{\left(\frac{p_1^+ + p_0^+}{q^+}\right)^2 + D - 3} \int_{p_1^+}^{p_0^+} \frac{dk^+}{k^+} \frac{k^+}{8p_1^+} \frac{k^+ p_1^+}{p_0^+ (p_1^+ - k^+)} \\
 &\times \left(\frac{1}{\tilde{\epsilon}} + \ln \frac{\mu^2}{\Delta_{UV}} \right) \left\{ \left[\left(\left(1 - 2 \frac{k^+ - p_1^+}{q^+} \right) \left(1 + \frac{2p_1^+}{q^+} \right) + (D - 3) \right) \right. \right. \\
 &\times \left. \left. \left(\left(1 - 2 \frac{p_1^+}{k^+} \right) \left(2 \frac{p_0^+}{k^+} - 1 \right) - (D - 3) \right) + 8 \frac{(D - 4)(D - 3)}{D - 2} \right] \right. \\
 &\left. \left. + \frac{8}{(D - 3)(D - 2)} \left[\left(1 + \frac{2p_1^+ - k^+}{q^+} \right) \left(\frac{p_0^+ + p_1^+}{k^+} - 1 \right) + \frac{D - 4}{2} \left(\frac{q^+}{k^+} + \frac{k^+}{q^+} \right) \right] \right\}. \tag{4.33}
 \end{aligned}$$

Expanding around $\epsilon_{UV} = 0$, and reintroducing $x = k^+/p_1^+$, $a = p_0^+/p_1^+$:

$$\begin{aligned}
 \underline{\tilde{\mathcal{M}}}_{A1,UV}^\lambda &= \tilde{\mathcal{M}}_{LO1}^\lambda \frac{\alpha_s C_F}{\pi} \left\{ \left(\frac{1}{\tilde{\epsilon}} + \ln \frac{\mu^2}{\Delta_{UV}} \right) \left(-\frac{3}{4} + \frac{1 + 2a}{2(1 + a^2)} + \frac{1}{2} \ln a \right) \right. \\
 &\left. + \frac{3}{4} \frac{a(a - 1)}{a^2 + 1} \int_1^a \frac{dx}{x - 1} + (a - 1) \frac{3 + 6a - 18a^2 + 18a^3 - 17a^4}{8a(a^2 + 1)^2} \right\}. \tag{4.34}
 \end{aligned}$$

Likewise, the UV counterterm (3.74) becomes:

$$\begin{aligned}
 \tilde{\mathcal{M}}_{A4,UV}^\lambda &= \tilde{\mathcal{M}}_{LO2}^\lambda \times -\alpha_s C_F \frac{1}{\left(\frac{p_1^+ + p_0^+}{q^+}\right)^2 + D - 3} \int_{p_1^+}^{p_0^+} \frac{dk^+}{k^+} \frac{(k^+)^2}{2p_0^+ (p_1^+ - k^+)} \\
 &\times \left(\frac{1}{\tilde{\epsilon}} + \ln \frac{\mu^2}{\Delta_{UV}} \right) \left\{ \left[\left(\left(1 - 2 \frac{k^+ - p_1^+}{q^+} \right) \left(1 + \frac{2p_1^+}{q^+} \right) + D - 3 \right) \right. \right. \\
 &\times \left. \left. \left(\left(1 - 2 \frac{p_1^+}{k^+} \right) \left(2 \frac{p_0^+}{k^+} - 1 \right) - (D - 3) \right) + 8 \frac{(D - 4)(D - 3)}{D - 2} \right] \right. \\
 &\left. \left. + \frac{8}{(D - 2)(D - 3)} \left[\left(1 + \frac{2p_1^+ - k^+}{q^+} \right) \left(\frac{p_0^+ + p_1^+}{k^+} - 1 \right) + \frac{D - 4}{2} \left(\frac{q^+}{k^+} + \frac{k^+}{q^+} \right) \right] \right\}. \tag{4.35}
 \end{aligned}$$

After performing the integrations over the gluon plus-momentum:

$$\begin{aligned}
 \tilde{\mathcal{M}}_{A4,UV}^\lambda &= \tilde{\mathcal{M}}_{LO2}^\lambda \frac{\alpha_s C_F}{\pi} \left\{ \left(\frac{1}{\tilde{\epsilon}} + \ln \frac{\mu^2}{\Delta_{UV}} \right) \left(-\frac{3}{4} + \frac{1 + 2a}{2(1 + a^2)} + \frac{1}{2} \ln a \right) \right. \\
 &\left. + \frac{3}{4} \frac{a(a - 1)}{a^2 + 1} \int_1^a \frac{dx}{x - 1} + (a - 1) \frac{3 + 6a - 18a^2 + 18a^3 - 17a^4}{8a(a^2 + 1)^2} \right\}. \tag{4.36}
 \end{aligned}$$

Total UV contributions. In order to add the results (4.31) and (4.34) for $\underline{\tilde{\mathcal{M}}}_{V1,UV}^\lambda$ and $\underline{\tilde{\mathcal{M}}}_{A1,UV}^\lambda$, some closer attention is needed to the two plus-momentum integrals we left unevaluated. Indeed, there is a singularity for $x \rightarrow 1$ at the end- resp. starting point of the

leftover integration in $\tilde{\mathcal{M}}_{V1,UV}^\lambda$ and $\tilde{\mathcal{M}}_{A1,UV}^\lambda$. Introducing an infinitesimal regulator $i0^+$,³ these integrals can be added and evaluated using the Sokhotski-Plemelj theorem:

$$\int_0^1 \frac{dx}{x-1+i0^+} + \int_1^a \frac{dx}{x-1+i0^+} = \int_{-1}^{a-1} \frac{dy}{y+i0^+} = \mathcal{P} \int_{-1}^{a-1} \frac{dy}{y} - i\pi, \quad (4.37)$$

$$= \ln(a-1) - i\pi.$$

The same holds for the integrals in the results (4.32) and (4.36) for $\tilde{\mathcal{M}}_{V4,UV}^\lambda$ and $\tilde{\mathcal{M}}_{A4,UV}^\lambda$, respectively.

With the above manipulation, we are finally in a position to add (4.31) and (4.34) to the contribution from the quark field-strength renormalization (3.114), yielding:

$$\begin{aligned} & \tilde{\mathcal{M}}_{V1,UV}^\lambda + \tilde{\mathcal{M}}_{A1,UV}^\lambda + \mathcal{Z}_{UV} \tilde{\mathcal{M}}_{LO1}^\lambda \\ &= \tilde{\mathcal{M}}_{LO1}^\lambda \frac{\alpha_s C_F}{\pi} \left\{ \frac{3}{4} \frac{p_0^+ q^+}{(p_0^+)^2 + (p_1^+)^2} \left(-i\pi + \ln \frac{q^+}{p_1^+} \right) \right. \\ & \quad + \ln \frac{\Delta_{UV}}{4\pi e^{-\gamma_E} \mu_R^2} \left(\frac{3}{4} - \frac{1}{2} \ln \frac{p_0^+}{k_{\min}^+} - \frac{1}{2} \ln \frac{p_1^+}{k_{\min}^+} \right) \\ & \quad \left. - \frac{11}{8} + \frac{9}{4} \frac{p_1^+ p_0^+}{(p_0^+)^2 + (p_1^+)^2} - \frac{3}{4} \frac{p_1^+ q^+}{(p_0^+)^2 + (p_1^+)^2} \ln \frac{q^+}{p_0^+} \right\}, \end{aligned} \quad (4.38)$$

and similarly for (4.32) and (4.36):

$$\begin{aligned} & \tilde{\mathcal{M}}_{V4,UV}^\lambda + \tilde{\mathcal{M}}_{A4,UV}^\lambda + \mathcal{Z}_{UV} \tilde{\mathcal{M}}_{LO2}^\lambda \\ &= \tilde{\mathcal{M}}_{LO2}^\lambda \frac{\alpha_s C_F}{\pi} \left\{ \frac{3}{4} \frac{p_0^+ q^+}{(p_0^+)^2 + (p_1^+)^2} \left(-i\pi + \ln \frac{q^+}{p_1^+} \right) \right. \\ & \quad + \ln \frac{\Delta_{UV}}{4\pi e^{-\gamma_E} \mu_R^2} \left(\frac{3}{4} - \frac{1}{2} \ln \frac{p_0^+}{k_{\min}^+} - \frac{1}{2} \ln \frac{p_1^+}{k_{\min}^+} \right) \\ & \quad \left. - \frac{11}{8} + \frac{9}{4} \frac{p_1^+ p_0^+}{(p_0^+)^2 + (p_1^+)^2} - \frac{3}{4} \frac{p_1^+ q^+}{(p_0^+)^2 + (p_1^+)^2} \ln \frac{q^+}{p_0^+} \right\}. \end{aligned} \quad (4.39)$$

Hence, we have proven that, also in the case of a transversely polarized photon, the total virtual contribution to the cross section is free from UV divergences. Just like in the longitudinal case, however, there are rapidity divergences left, which will be treated in section 8.

Note that, in this section, all our expressions are proportional to one of the two leading-order amplitudes. We have chosen to keep these amplitudes defined in D dimensions. However, we have checked that, when factorizing the leading-order amplitudes out in $D = 4$ dimensions instead, the extra finite terms that appear all compensate each other. One, therefore, obtains exactly the same result irrespective of the precise procedure followed, which is an interesting nontrivial check of our calculation.

³Note that, whenever necessary, we consistently assign a positive infinitesimal imaginary part to the gluon plus-momentum.

4.3 Contribution to the cross section due to ultraviolet counterterms

Collecting our results (4.19) and (4.20) for the sum of the UV counterterms, and applying the definition (2.6), we eventually obtain the following contribution to the cross section in case of a longitudinally polarized photon:

$$d\sigma_{\text{UV}}^{\text{L}} = d\sigma_{\text{LO}}^{\text{L}} \frac{\alpha_s C_F}{\pi} \left[\left(-\frac{3}{2} + \ln \frac{p_1^+}{k_{\text{min}}^+} + \ln \frac{p_0^+}{k_{\text{min}}^+} \right) \ln \frac{4\pi e^{-\gamma_E} \mu_R^2}{\Delta_{\text{UV}}} - \frac{1}{2} \right]. \quad (4.40)$$

Similarly, (4.38) and (4.39) can be combined into:

$$d\sigma_{\text{UV}}^{\text{T}} = d\sigma_{\text{LO}}^{\text{T}} \frac{\alpha_s C_F}{\pi} \left[\left(-\frac{3}{2} + \ln \frac{p_1^+}{k_{\text{min}}^+} + \ln \frac{p_0^+}{k_{\text{min}}^+} \right) \ln \frac{4\pi e^{-\gamma_E} \mu_R^2}{\Delta_{\text{UV}}} + \frac{3}{2} \frac{p_0^+ q^+}{(p_0^+)^2 + (p_1^+)^2} \left(-i\pi + \ln \frac{q^+}{p_1^+} + 3 \frac{p_1^+}{q^+} - \frac{p_1^+}{p_0^+} \ln \frac{q^+}{p_0^+} \right) - \frac{11}{4} \right]. \quad (4.41)$$

5 Real next-to-leading order corrections

In this section, we present the amplitudes for the real NLO corrections. One should be very careful to note that, due to momentum conservation, the plus-momentum of the incoming quark is equal to

$$p_{0R}^+ = p_1^+ + q^+ + p_3^+. \quad (5.1)$$

We denote this quantity with an additional index R , to avoid confusion with the same momentum component $p_0^+ = p_1^+ + q^+$ in leading-order and virtual amplitudes. This distinction also allows us to introduce both p_{0R}^+ and p_0^+ in many of the expressions below, where $p_{0R}^+ = p_0^+ + p_3^+$.

5.1 Initial-state radiation

Diagram IS1. The reduced amplitudes corresponding to graph IS1 in figure 8 read:

$$\begin{aligned} \tilde{\mathcal{M}}_{\text{IS1}}^{0\eta} &= -\frac{p_0^+ \mathbf{P}_\perp^2 - p_1^+ M^2}{p_0^+ \mathbf{P}_\perp^2 + p_1^+ M^2} \frac{1}{M} \frac{p_3^+}{p_{0R}^+} \mathcal{S}^{\eta\bar{\eta}} \left(1 + \frac{2p_0^+}{p_3^+} \right) \\ &\quad \times \int_{\mathbf{x}, \mathbf{z}} iA^{\bar{\eta}}(\mathbf{x} - \mathbf{z}) e^{-i\mathbf{k}_\perp \cdot \mathbf{x}} e^{-i\mathbf{p}_3 \cdot \mathbf{z}} (U_{\mathbf{x}} U_{\mathbf{z}}^\dagger t^c U_{\mathbf{z}} - t^c), \end{aligned} \quad (5.2)$$

and:

$$\begin{aligned} \tilde{\mathcal{M}}_{\text{IS1}}^{\lambda\eta} &= \frac{q^+ \mathbf{P}_\perp^{\lambda\bar{\lambda}}}{p_0^+ \mathbf{P}_\perp^2 + p_1^+ M^2} \frac{p_3^+}{p_{0R}^+} \mathcal{S}^{\lambda\bar{\lambda}} \left(1 + \frac{2p_1^+}{q^+} \right) \mathcal{S}^{\eta\bar{\eta}} \left(1 + \frac{2p_0^+}{p_3^+} \right) \\ &\quad \times \int_{\mathbf{x}, \mathbf{z}} iA^{\bar{\eta}}(\mathbf{x} - \mathbf{z}) e^{-i\mathbf{k}_\perp \cdot \mathbf{x}} e^{-i\mathbf{p}_3 \cdot \mathbf{z}} (U_{\mathbf{x}} U_{\mathbf{z}}^\dagger t^c U_{\mathbf{z}} - t^c). \end{aligned} \quad (5.3)$$

Diagram IS2. The amplitude for diagram IS2, when the photon is longitudinally polarized, reads:

$$\begin{aligned} \tilde{\mathcal{M}}_{\text{IS2}}^{0\eta} &= \frac{1}{M} \mathcal{S}^{\eta\bar{\eta}} \left(1 + \frac{2p_0^+}{p_3^+} \right) \frac{p_3^+}{p_{0R}^+} \\ &\quad \times \int \frac{\ell^{\bar{\eta}}}{\ell^2} \frac{p_3^+ (q^+ \ell + p_0^+ \mathbf{q})^2 - p_1^+ p_3^+ p_0^+ M^2}{p_3^+ (q^+ \ell + p_0^+ \mathbf{q})^2 + p_1^+ q^+ p_{0R}^+ \ell^2 + p_1^+ p_3^+ p_0^+ M^2} \\ &\quad \times \int_{\mathbf{x}, \mathbf{z}} e^{-i\ell \cdot (\mathbf{x} - \mathbf{z})} e^{-i\mathbf{k}_\perp \cdot \mathbf{x}} e^{-i\mathbf{p}_3 \cdot \mathbf{z}} (U_{\mathbf{x}} U_{\mathbf{z}}^\dagger t^c U_{\mathbf{z}} - t^c). \end{aligned} \quad (5.4)$$

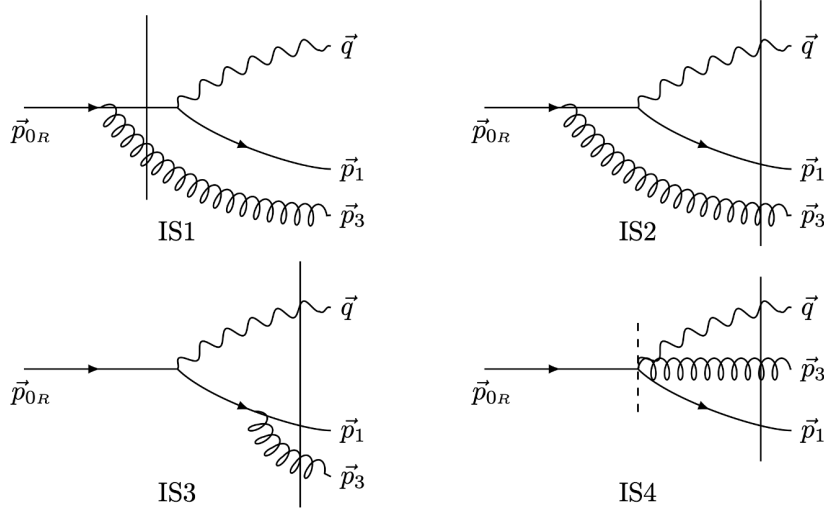


Figure 8. The four diagrams corresponding to real gluon emission in the initial state.

In the transverse case, we obtain:

$$\begin{aligned}
 \tilde{\mathcal{M}}_{\text{IS2}}^{\lambda\eta} &= \frac{q^+(p_3^+)^2}{p_{0R}^+} \mathcal{S}^{\lambda\bar{\lambda}} \left(1 + \frac{2p_1^+}{q^+}\right) \mathcal{S}^{\eta\bar{\eta}} \left(1 + \frac{2p_0^+}{p_3^+}\right) \\
 &\times \int_{\mathbf{x}, \mathbf{z}} \int_{\ell} e^{-i\ell \cdot (\mathbf{x} - \mathbf{z})} \frac{\ell^{\bar{\eta}}}{\ell^2} \frac{q^+ \ell^{\bar{\lambda}} + p_0^+ \mathbf{q}^{\bar{\lambda}}}{p_3^+ (q^+ \ell + p_0^+ \mathbf{q})^2 + p_1^+ q^+ p_{0R}^+ \ell^2 + p_1^+ p_3^+ p_0^+ M^2} \\
 &\times e^{-i\mathbf{k}_{\perp} \cdot \mathbf{x}} e^{-i\mathbf{p}_3 \cdot \mathbf{z}} (U_{\mathbf{x}} U_{\mathbf{z}}^{\dagger} t^c U_{\mathbf{z}} - t^c).
 \end{aligned} \tag{5.5}$$

In the above expressions, we have used the definition:

$$\Delta_{\text{IS}} \equiv \frac{p_1^+ p_3^+}{q^+ (p_1^+ + p_3^+)^2} (p_{0R}^+ \mathbf{q}^2 + (p_1^+ + p_3^+) M^2). \tag{5.6}$$

Diagram IS3. The amplitudes for the production of a longitudinally or transversely polarized virtual photon read, respectively:

$$\begin{aligned}
 \tilde{\mathcal{M}}_{\text{IS3}}^{0\eta} &= \frac{p_{0R}^+ \mathbf{q}^2 - (p_1^+ + p_3^+) M^2}{p_{0R}^+ \mathbf{q}^2 + (p_1^+ + p_3^+) M^2} \frac{1}{M} \frac{p_3^+}{p_1^+ + p_3^+} \mathcal{S}^{\eta\bar{\eta}} \left(1 + \frac{2p_1^+}{p_3^+}\right) \\
 &\times \int_{\mathbf{x}, \mathbf{z}} iA^{\bar{\eta}}(\mathbf{x} - \mathbf{z}, \Delta_{\text{IS}}) e^{\frac{i p_3^+}{p_1^+ + p_3^+} \mathbf{q} \cdot (\mathbf{x} - \mathbf{z})} e^{-i\mathbf{k}_{\perp} \cdot \mathbf{x}} e^{-i\mathbf{p}_3 \cdot \mathbf{z}} (U_{\mathbf{x}} U_{\mathbf{z}}^{\dagger} t^c U_{\mathbf{z}} - t^c),
 \end{aligned} \tag{5.7}$$

and:

$$\begin{aligned}
 \tilde{\mathcal{M}}_{\text{IS3}}^{\lambda\eta} &= \frac{q^+ \mathbf{q}^{\bar{\lambda}}}{p_{0R}^+ \mathbf{q}^2 + (p_1^+ + p_3^+) M^2} \frac{p_3^+}{p_1^+ + p_3^+} \mathcal{S}^{\eta\bar{\eta}} \left(1 + \frac{2p_1^+}{p_3^+}\right) \mathcal{S}^{\lambda\bar{\lambda}} \left(1 + 2\frac{p_1^+ + p_3^+}{q^+}\right) \\
 &\times \int_{\mathbf{x}, \mathbf{z}} iA^{\bar{\eta}}(\mathbf{x} - \mathbf{z}, \Delta_{\text{IS}}) e^{\frac{i p_3^+}{p_1^+ + p_3^+} \mathbf{q} \cdot (\mathbf{x} - \mathbf{z})} e^{-i\mathbf{k}_{\perp} \cdot \mathbf{x}} e^{-i\mathbf{p}_3 \cdot \mathbf{z}} (U_{\mathbf{x}} U_{\mathbf{z}}^{\dagger} t^c U_{\mathbf{z}} - t^c).
 \end{aligned} \tag{5.8}$$

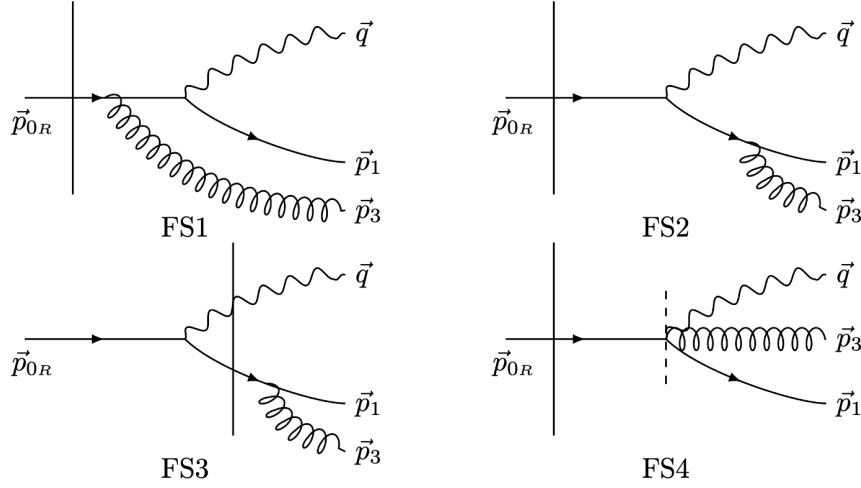


Figure 9. The four diagrams corresponding to real gluon emission in the final state.

Diagram IS4. Finally, for the instantaneous $q \rightarrow \gamma^* g q$ splitting, we obtain the following result for the longitudinally resp. transversely polarized amplitudes:

$$\begin{aligned}
 \tilde{\mathcal{M}}_{\text{IS4}}^{0\eta} &= \frac{-p_1^+ p_3^+}{(p_1^+ + p_3^+)M} \int_{\mathbf{x}, \mathbf{z}} \left[\frac{q^+}{p_1^+ p_0^+} iA^i(\mathbf{x} - \mathbf{z}, \Delta_{\text{IS}}) (\delta^{i\eta} + i\sigma^{i\eta}) \right. \\
 &\quad \left. + \frac{2p_0^+ + p_3^+}{p_0^+ (p_1^+ + p_3^+)} \mathbf{q}^i \mathcal{K}(\mathbf{x} - \mathbf{z}, \Delta_{\text{IS}}) \left(\delta^{i\eta} + \frac{p_3^+}{2p_0^+ + p_3^+} i\sigma^{i\eta} \right) \right] \\
 &\quad \times e^{i\frac{p_3^+}{p_1^+ + p_3^+} \mathbf{q} \cdot (\mathbf{x} - \mathbf{z})} e^{-i\mathbf{k}_\perp \cdot \mathbf{x}} e^{-i\mathbf{p}_3 \cdot \mathbf{z}} (U_{\mathbf{x}} U_{\mathbf{z}}^\dagger t^c U_{\mathbf{z}} - t^c),
 \end{aligned} \tag{5.9}$$

and:

$$\begin{aligned}
 \tilde{\mathcal{M}}_{\text{IS4}}^{\lambda\eta} &= \frac{-p_1^+ p_3^+}{p_1^+ + p_3^+} \left[\left(\frac{1}{p_1^+ + p_3^+} + \frac{1}{p_0^+} \right) \delta^{\eta\lambda} + \left(\frac{1}{p_1^+ + p_3^+} - \frac{1}{p_0^+} \right) i\sigma^{\eta\lambda} \right] \\
 &\quad \times \int_{\mathbf{x}, \mathbf{z}} \mathcal{K}(\mathbf{x} - \mathbf{z}, \Delta_{\text{IS}}) e^{i\frac{p_3^+}{p_1^+ + p_3^+} \mathbf{q} \cdot (\mathbf{x} - \mathbf{z})} e^{-i\mathbf{k}_\perp \cdot \mathbf{x}} e^{-i\mathbf{p}_3 \cdot \mathbf{z}} (U_{\mathbf{x}} U_{\mathbf{z}}^\dagger t^c U_{\mathbf{z}} - t^c).
 \end{aligned} \tag{5.10}$$

5.2 Final-state radiation

Diagram FS1. The amplitude corresponding to the first final-state radiation diagram in figure 9 gives, in the longitudinally polarized case:

$$\begin{aligned}
 \tilde{\mathcal{M}}_{\text{FS1}}^{0\eta} &= \frac{p_0^+ \mathbf{P}_\perp^2 - p_1^+ M^2}{p_0^+ \mathbf{P}_\perp^2 + p_1^+ M^2} \frac{1}{M} \frac{p_3^+}{p_0^+} \mathcal{S}^{\eta\bar{\eta}} \left(1 + \frac{2p_0^+}{p_3^+} \right) \\
 &\quad \times \frac{\left(\mathbf{p}_3 - \frac{p_3^+}{p_0^+} \mathbf{k}_\perp \right)^{\bar{\eta}}}{\left(\mathbf{p}_3 - \frac{p_3^+}{p_0^+} \mathbf{k}_\perp \right)^2 + \Delta_{\text{FS}}} \int_{\mathbf{x}} e^{-i\mathbf{x} \cdot (\mathbf{q} + \mathbf{p}_1 + \mathbf{p}_3)} t^c (U_{\mathbf{x}} - 1),
 \end{aligned} \tag{5.11}$$

and when the photon is transversely polarized:

$$\begin{aligned} \tilde{\mathcal{M}}_{\text{FS1}}^{\lambda\eta} &= -\frac{q^+ \mathbf{P}_\perp^\lambda}{p_0^+ \mathbf{P}_\perp^2 + p_1^+ M^2} \frac{p_3^+}{p_0^+} \mathcal{S}^{\lambda\bar{\lambda}} \left(1 + \frac{2p_1^+}{q^+}\right) \mathcal{S}^{\eta\bar{\eta}} \left(1 + \frac{2p_0^+}{p_3^+}\right) \\ &\quad \times \frac{\left(\mathbf{p}_3 - \frac{p_3^+}{p_0^+} \mathbf{k}_\perp\right)^{\bar{\eta}}}{\left(\mathbf{p}_3 - \frac{p_3^+}{p_0^+} \mathbf{k}_\perp\right)^2 + \Delta_{\text{FS}}} \int_{\mathbf{x}} e^{-i\mathbf{x}\cdot(\mathbf{q}+\mathbf{p}_1+\mathbf{p}_3)} t^c(U_{\mathbf{x}} - 1). \end{aligned} \quad (5.12)$$

In the above, we have introduced:

$$\Delta_{\text{FS}} \equiv \frac{p_3^+ p_{0R}^+}{p_1^+ q^+ p_0^+} (p_0^+ \mathbf{P}_\perp^2 + p_1^+ M^2). \quad (5.13)$$

For later purposes (for instance the high-energy resummation in section 8), it can be convenient to go to transverse coordinate space, writing (obtained by inverting (A.3)):

$$\begin{aligned} \frac{\left(\mathbf{p}_3 - \frac{p_3^+}{p_0^+} \mathbf{k}_\perp\right)^{\bar{\eta}}}{\left(\mathbf{p}_3 - \frac{p_3^+}{p_0^+} \mathbf{k}_\perp\right)^2 + \Delta_{\text{FS}}} e^{-i\mathbf{p}_3\cdot\mathbf{x}} &= \frac{\left(\mathbf{p}_3 - \frac{p_3^+}{p_0^+} \mathbf{k}_\perp\right)^{\bar{\eta}}}{\left(\mathbf{p}_3 - \frac{p_3^+}{p_0^+} \mathbf{k}_\perp\right)^2 + \Delta_{\text{FS}}} e^{-i\left(\mathbf{p}_3 - \frac{p_3^+}{p_0^+} \mathbf{k}_\perp\right)\cdot\mathbf{x}} e^{-i\frac{p_3^+}{p_0^+} \mathbf{k}_\perp\cdot\mathbf{x}}, \\ &= e^{-i\frac{p_3^+}{p_0^+} \mathbf{k}_\perp\cdot\mathbf{x}} \int_{\mathbf{z}} e^{-i\left(\mathbf{p}_3 - \frac{p_3^+}{p_0^+} \mathbf{k}_\perp\right)\cdot\mathbf{z}} iA^{\bar{\eta}}(\mathbf{x} - \mathbf{z}, \Delta_{\text{FS}}) \end{aligned} \quad (5.14)$$

such that:

$$\begin{aligned} \tilde{\mathcal{M}}_{\text{FS1}}^{0\eta} &= \frac{p_0^+ \mathbf{P}_\perp^2 - p_1^+ M^2}{p_0^+ \mathbf{P}_\perp^2 + p_1^+ M^2} \frac{1}{M} \frac{p_3^+}{p_0^+} \mathcal{S}^{\eta\bar{\eta}} \left(1 + \frac{2p_0^+}{p_3^+}\right) \\ &\quad \times \int_{\mathbf{x}, \mathbf{z}} e^{-i\left(\mathbf{p}_3 - \frac{p_3^+}{p_0^+} \mathbf{k}_\perp\right)\cdot\mathbf{z}} e^{-i\frac{p_3^+}{p_0^+} \mathbf{k}_\perp\cdot\mathbf{x}} e^{-i\mathbf{k}_\perp\cdot\mathbf{x}} iA^{\bar{\eta}}(\mathbf{x} - \mathbf{z}, \Delta_{\text{FS}}) t^c(U_{\mathbf{x}} - 1), \end{aligned} \quad (5.15)$$

and:

$$\begin{aligned} \tilde{\mathcal{M}}_{\text{FS1}}^{\lambda\eta} &= -\frac{q^+ \mathbf{P}_\perp^\lambda}{p_0^+ \mathbf{P}_\perp^2 + p_1^+ M^2} \frac{p_3^+}{p_0^+} \mathcal{S}^{\lambda\bar{\lambda}} \left(1 + \frac{2p_1^+}{q^+}\right) \mathcal{S}^{\eta\bar{\eta}} \left(1 + \frac{2p_0^+}{p_3^+}\right) \\ &\quad \times \int_{\mathbf{x}, \mathbf{z}} e^{-i\left(\mathbf{p}_3 - \frac{p_3^+}{p_0^+} \mathbf{k}_\perp\right)\cdot\mathbf{z}} e^{-i\frac{p_3^+}{p_0^+} \mathbf{k}_\perp\cdot\mathbf{x}} e^{-i\mathbf{k}_\perp\cdot\mathbf{x}} iA^{\bar{\eta}}(\mathbf{x} - \mathbf{z}, \Delta_{\text{FS}}) t^c(U_{\mathbf{x}} - 1). \end{aligned} \quad (5.16)$$

Diagram FS2. The amplitudes read:

$$\begin{aligned} \tilde{\mathcal{M}}_{\text{FS2}}^{0\eta} &= \frac{1}{M} \frac{p_3^+}{p_1^+} \mathcal{S}^{\eta\bar{\eta}} \left(1 + \frac{2p_1^+}{p_3^+}\right) \\ &\quad \times \frac{\mathbf{p}_3^{\bar{\eta}} - \frac{p_3^+}{p_1^+} \mathbf{p}_1^{\bar{\eta}}}{\left(\mathbf{p}_3 - \frac{p_3^+}{p_1^+} \mathbf{p}_1\right)^2} \frac{\left(\mathbf{p}_3 + \mathbf{p}_1 - \frac{p_1^+ + p_3^+}{q^+} \mathbf{q}\right)^2 - \frac{p_{0R}^+ (p_1^+ + p_3^+)}{(q^+)^2} M^2}{\frac{p_1^+ p_{0R}^+}{q^+ p_3^+} \left(\mathbf{p}_3 - \frac{p_3^+}{p_1^+} \mathbf{p}_1\right)^2 + \left(\mathbf{p}_3 + \mathbf{p}_1 - \frac{p_1^+ + p_3^+}{q^+} \mathbf{q}\right)^2 + \frac{p_{0R}^+ (p_1^+ + p_3^+)}{(q^+)^2} M^2} \\ &\quad \times \int_{\mathbf{x}} e^{-i\mathbf{x}\cdot(\mathbf{q}+\mathbf{p}_1+\mathbf{p}_3)} t^c(U_{\mathbf{x}} - 1), \end{aligned} \quad (5.17)$$

and:

$$\begin{aligned}
 \tilde{\mathcal{M}}_{\text{FS2}}^{\lambda\eta} &= -\frac{p_3^+}{p_1^+} \mathcal{S}^{\eta\bar{\eta}} \left(1 + \frac{2p_1^+}{p_3^+}\right) \mathcal{S}^{\lambda\bar{\lambda}} \left(1 + \frac{2(p_1^+ + p_3^+)}{q^+}\right) \\
 &\times \frac{\mathbf{p}_3^{\bar{\eta}} - \frac{p_3^+}{p_1^+} \mathbf{p}_1^{\bar{\eta}}}{\left(\mathbf{p}_3 - \frac{p_3^+}{p_1^+} \mathbf{p}_1\right)^2} \frac{\mathbf{p}_3^{\bar{\lambda}} + \mathbf{p}_1^{\bar{\lambda}} - \frac{p_1^+ + p_3^+}{q^+} \mathbf{q}^{\bar{\lambda}}}{\frac{p_1^+ p_{0R}^+}{q^+ p_3^+} \left(\mathbf{p}_3 - \frac{p_3^+}{p_1^+} \mathbf{p}_1\right)^2 + \left(\mathbf{p}_3 + \mathbf{p}_1 - \frac{p_1^+ + p_3^+}{q^+} \mathbf{q}\right)^2 + \frac{p_{0R}^+ (p_1^+ + p_3^+)}{(q^+)^2} M^2} \\
 &\times \int_{\mathbf{x}} e^{-i \cdot (\mathbf{q} + \mathbf{p}_1 + \mathbf{p}_3) \cdot \mathbf{x}} t^c (U_{\mathbf{x}} - 1).
 \end{aligned} \tag{5.18}$$

Diagram FS3. The amplitudes corresponding to Feynman graph FS3 (figure 9) for the emission of a longitudinally or transversely polarized photon read, respectively:

$$\begin{aligned}
 \tilde{\mathcal{M}}_{\text{FS3}}^{0\eta} &= -\frac{1}{M} \frac{p_{0R}^+ \mathbf{q}^2 - (p_1^+ + p_3^+) M^2}{p_{0R}^+ \mathbf{q}^2 + (p_1^+ + p_3^+) M^2} \frac{p_3^+}{p_1^+} \mathcal{S}^{\eta\bar{\eta}} \left(1 + \frac{2p_1^+}{p_3^+}\right) \\
 &\times \frac{\mathbf{p}_3^{\bar{\eta}} - \frac{p_3^+}{p_1^+} \mathbf{p}_1^{\bar{\eta}}}{\left(\mathbf{p}_3 - \frac{p_3^+}{p_1^+} \mathbf{p}_1\right)^2} \int_{\mathbf{x}} e^{-i \mathbf{x} \cdot (\mathbf{q} + \mathbf{p}_1 + \mathbf{p}_3)} t^c (U_{\mathbf{x}} - 1),
 \end{aligned} \tag{5.19}$$

and:

$$\begin{aligned}
 \tilde{\mathcal{M}}_{\text{FS3}}^{\lambda\eta} &= \frac{-q^+ \mathbf{q}^{\bar{\lambda}}}{p_{0R}^+ \mathbf{q}^2 + (p_1^+ + p_3^+) M^2} \frac{\mathbf{p}_3^{\bar{\eta}} - \frac{p_3^+}{p_1^+} \mathbf{p}_1^{\bar{\eta}}}{\left(\mathbf{p}_3 - \frac{p_3^+}{p_1^+} \mathbf{p}_1\right)^2} \\
 &\times \frac{p_3^+}{p_1^+} \mathcal{S}^{\eta\bar{\eta}} \left(1 + \frac{2p_1^+}{p_3^+}\right) \mathcal{S}^{\lambda\bar{\lambda}} \left(1 + \frac{2(p_1^+ + p_3^+)}{q^+}\right) \\
 &\times \int_{\mathbf{x}} e^{-i \mathbf{x} \cdot (\mathbf{q} + \mathbf{p}_1 + \mathbf{p}_3)} t^c (U_{\mathbf{x}} - 1).
 \end{aligned} \tag{5.20}$$

With the help of the relation:

$$\frac{\mathbf{p}_3^{\bar{\eta}} - \frac{p_3^+}{p_1^+} \mathbf{p}_1^{\bar{\eta}}}{\left(\mathbf{p}_3 - \frac{p_3^+}{p_1^+} \mathbf{p}_1\right)^2} e^{-i \mathbf{x} \cdot \mathbf{p}_3} = e^{-i \frac{p_3^+}{p_1^+} \mathbf{p}_1 \cdot \mathbf{x}} \int_{\mathbf{z}} e^{-i \left(\mathbf{p}_3 - \frac{p_3^+}{p_1^+} \mathbf{p}_1\right) \cdot \mathbf{z}} i A^{\bar{\eta}}(\mathbf{x} - \mathbf{z}), \tag{5.21}$$

the above amplitudes can also be cast in coordinate space, yielding:

$$\begin{aligned}
 \tilde{\mathcal{M}}_{\text{FS3}}^{0\eta} &= -\frac{1}{M} \frac{p_{0R}^+ \mathbf{q}^2 - (p_1^+ + p_3^+) M^2}{p_{0R}^+ \mathbf{q}^2 + (p_1^+ + p_3^+) M^2} \frac{p_3^+}{p_1^+} \mathcal{S}^{\eta\bar{\eta}} \left(1 + \frac{2p_1^+}{p_3^+}\right) \\
 &\times \int_{\mathbf{x}, \mathbf{z}} e^{-i \left(\mathbf{p}_3 - \frac{p_3^+}{p_1^+} \mathbf{p}_1\right) \cdot \mathbf{z}} e^{-i \frac{p_3^+}{p_1^+} \mathbf{p}_1 \cdot \mathbf{x}} e^{-i \mathbf{k}_{\perp} \cdot \mathbf{x}} i A^{\bar{\eta}}(\mathbf{x} - \mathbf{z}) t^c (U_{\mathbf{x}} - 1),
 \end{aligned} \tag{5.22}$$

and:

$$\begin{aligned}
 \tilde{\mathcal{M}}_{\text{FS3}}^{\lambda\eta} &= \frac{-q^+ \mathbf{q}^{\bar{\lambda}}}{p_{0R}^+ \mathbf{q}^2 + (p_1^+ + p_3^+) M^2} \frac{p_3^+}{p_1^+} \mathcal{S}^{\eta\bar{\eta}} \left(1 + \frac{2p_1^+}{p_3^+}\right) \mathcal{S}^{\lambda\bar{\lambda}} \left(1 + \frac{2(p_1^+ + p_3^+)}{q^+}\right) \\
 &\times \int_{\mathbf{x}, \mathbf{z}} e^{-i \left(\mathbf{p}_3 - \frac{p_3^+}{p_1^+} \mathbf{p}_1\right) \cdot \mathbf{z}} e^{-i \frac{p_3^+}{p_1^+} \mathbf{p}_1 \cdot \mathbf{x}} e^{-i \mathbf{k}_{\perp} \cdot \mathbf{x}} i A^{\bar{\eta}}(\mathbf{x} - \mathbf{z}) t^c (U_{\mathbf{x}} - 1).
 \end{aligned} \tag{5.23}$$

Diagram FS4. The last diagrams we consider correspond to the instantaneous $q \rightarrow q\gamma^*g$ splitting after the initial quark has interacted with the shockwave. In the longitudinal case, we find:

$$\begin{aligned} \tilde{\mathcal{M}}_{\text{FS4}}^{0\eta} = & -\frac{1}{M} \frac{p_3^+ p_{0R}^+}{p_0^+} \frac{1}{\left(\mathbf{p}_3 - \frac{p_3^+}{p_0^+} \mathbf{k}_\perp\right)^2 + \Delta_{\text{FS}}} \left[\frac{q^+}{p_{0R}^+ (p_1^+ + p_3^+)} \left(\mathbf{p}_3 - \frac{p_3^+}{p_0^+} \mathbf{k}_\perp\right)^{\bar{\eta}} (\delta^{\bar{\eta}\eta} - i\sigma^{\bar{\eta}\eta}) \right. \\ & \left. + \frac{2p_1^+ + p_3^+}{p_1^+ (p_1^+ + p_3^+)} \mathbf{P}_\perp^{\bar{\eta}} \left(\delta^{\bar{\eta}\eta} + \frac{p_3^+}{2p_1^+ + p_3^+} i\sigma^{\bar{\eta}\eta} \right) \right] \int_{\mathbf{x}} e^{-i\mathbf{x} \cdot (\mathbf{q} + \mathbf{p}_1 + \mathbf{p}_3)} t^c (U_{\mathbf{x}} - 1), \end{aligned} \quad (5.24)$$

while we obtain for the emission of a transversely polarized virtual photon:

$$\begin{aligned} \tilde{\mathcal{M}}_{\text{FS4}}^{\lambda\eta} = & \frac{p_3^+ p_{0R}^+}{p_0^+} \frac{1}{\left(\mathbf{p}_3 - \frac{p_3^+}{p_0^+} \mathbf{k}_\perp\right)^2 + \Delta_{\text{FS}}} \left[\left(\frac{1}{p_1^+ + p_3^+} + \frac{1}{p_0^+} \right) \delta^{\eta\lambda} \right. \\ & \left. + i\sigma^{\eta\lambda} \left(\frac{1}{p_1^+ + p_3^+} - \frac{1}{p_0^+} \right) \right] \int_{\mathbf{x}} e^{-i\mathbf{x} \cdot (\mathbf{q} + \mathbf{p}_1 + \mathbf{p}_3)} t^c (U_{\mathbf{x}} - 1). \end{aligned} \quad (5.25)$$

For later purposes, it can be useful to write:

$$\begin{aligned} \frac{1}{\left(\mathbf{p}_3 - \frac{p_3^+}{p_0^+} \mathbf{k}_\perp\right)^2 + \Delta_{\text{FS}}} e^{-i\mathbf{p}_3 \cdot \mathbf{x}} = & \frac{1}{\left(\mathbf{p}_3 - \frac{p_3^+}{p_0^+} \mathbf{k}_\perp\right)^2 + \Delta_{\text{FS}}} e^{-i\left(\mathbf{p}_3 - \frac{p_3^+}{p_0^+} \mathbf{k}_\perp\right) \cdot \mathbf{x}} e^{-i\frac{p_3^+}{p_0^+} \mathbf{k}_\perp \cdot \mathbf{x}}, \\ = & e^{-i\frac{p_3^+}{p_0^+} \mathbf{k}_\perp \cdot \mathbf{x}} \int_{\mathbf{z}} e^{-i\left(\mathbf{p}_3 - \frac{p_3^+}{p_0^+} \mathbf{k}_\perp\right) \cdot \mathbf{z}} \mathcal{K}(\mathbf{x} - \mathbf{z}, \Delta_{\text{FS}}), \end{aligned} \quad (5.26)$$

such that:

$$\begin{aligned} \tilde{\mathcal{M}}_{\text{FS4}}^{0\eta} = & -\frac{1}{M} \frac{p_3^+ p_{0R}^+}{p_0^+} \left[\frac{q^+}{p_{0R}^+ (p_1^+ + p_3^+)} \left(\mathbf{p}_3 - \frac{p_3^+}{p_0^+} \mathbf{k}_\perp\right)^{\bar{\eta}} (\delta^{\bar{\eta}\eta} - i\sigma^{\bar{\eta}\eta}) \right. \\ & \left. + \frac{2p_1^+ + p_3^+}{p_1^+ (p_1^+ + p_3^+)} \mathbf{P}_\perp^{\bar{\eta}} \left(\delta^{\bar{\eta}\eta} + \frac{p_3^+}{2p_1^+ + p_3^+} i\sigma^{\bar{\eta}\eta} \right) \right] \\ & \times e^{-i\frac{p_3^+}{p_0^+} \mathbf{k}_\perp \cdot \mathbf{x}} \int_{\mathbf{x}, \mathbf{z}} e^{-i\left(\mathbf{p}_3 - \frac{p_3^+}{p_0^+} \mathbf{k}_\perp\right) \cdot \mathbf{z}} \mathcal{K}(\mathbf{x} - \mathbf{z}, \Delta_{\text{FS}}) \int_{\mathbf{x}} e^{-i\mathbf{k}_\perp \cdot \mathbf{x}} t^c (U_{\mathbf{x}} - 1), \end{aligned} \quad (5.27)$$

and:

$$\begin{aligned} \tilde{\mathcal{M}}_{\text{FS4}}^{\lambda\eta} = & \frac{p_3^+ p_{0R}^+}{p_0^+} \left[\left(\frac{1}{p_1^+ + p_3^+} + \frac{1}{p_0^+} \right) \delta^{\eta\lambda} + i\sigma^{\eta\lambda} \left(\frac{1}{p_1^+ + p_3^+} - \frac{1}{p_0^+} \right) \right] \\ & \times e^{-i\frac{p_3^+}{p_0^+} \mathbf{k}_\perp \cdot \mathbf{x}} \int_{\mathbf{x}, \mathbf{z}} e^{-i\left(\mathbf{p}_3 - \frac{p_3^+}{p_0^+} \mathbf{k}_\perp\right) \cdot \mathbf{z}} \mathcal{K}(\mathbf{x} - \mathbf{z}, \Delta_{\text{FS}}) \int_{\mathbf{x}} e^{-i\mathbf{k}_\perp \cdot \mathbf{x}} t^c (U_{\mathbf{x}} - 1). \end{aligned} \quad (5.28)$$

6 Infrared safety in the initial state

In this section, we show that two of the initial-state radiation diagrams (figure 8), namely IS1 and IS2, lead to infrared divergences on the level of the cross section, i.e. after squaring

and integrating over the outgoing gluon. These divergences stem from the kinematic region in which the gluon, radiated from the incoming quark, is collinear to its emitter. First, we will evaluate the divergent integrals over the transverse momentum \mathbf{p}_3 of the gluon using dimensional regularization. The collinear singularities will be parameterized by the poles ϵ_{coll} . We shall then demonstrate how these poles can be absorbed into the DGLAP evolution equations of the incoming quark.

6.1 Collinear divergences from initial-state radiation

Real corrections to the NLO cross section are obtained by computing the $2 \rightarrow 3$ partonic amplitudes, multiplying them with their complex conjugate, and integrating the additional parton out (see below, subsection 6.2). When considering the initial-state radiation amplitudes $\mathcal{M}_{\text{IS1}}^{0\eta}$ (5.2) and $\mathcal{M}_{\text{IS2}}^{0\eta}$ (5.4), we obtain after promoting the reduced amplitudes to the full ones according to formula (2.47), multiplying them with their complex conjugate, and integrating over the gluon transverse momentum:

$$\begin{aligned} \int_{\mathbf{p}_3} \left| \mathcal{M}_{\text{IS1}}^{0\eta} + \mathcal{M}_{\text{IS2}}^{0\eta} \right|^2 &= \frac{g_{\text{em}}^2 g_s^2 N_c C_F}{M^2} \left(\frac{p_3^+}{p_{0R}^+} \right)^2 8p_1^+ p_{0R}^+ \left(\left(1 + \frac{2p_0^+}{p_3^+} \right)^2 + D - 3 \right) \\ &\times \int_{\mathbf{x}, \mathbf{x}'} \int_{\ell} \frac{1}{\ell^2} e^{-i\ell \cdot (\mathbf{x} - \mathbf{x}')} \left(-\frac{p_0^+ \mathbf{P}_\perp^2 - p_1^+ M^2}{p_0^+ \mathbf{P}_\perp^2 + p_1^+ M^2} \right. \\ &+ \left. \frac{p_3^+ (q^+ \ell + p_0^+ \mathbf{q})^2 - p_0^+ p_1^+ p_3^+ M^2}{p_3^+ (q^+ \ell + p_0^+ \mathbf{q})^2 + p_1^+ q^+ p_{0R}^+ \ell^2 + p_0^+ p_1^+ p_3^+ M^2} \right)^2 \\ &\times e^{-i\mathbf{k}_\perp \cdot (\mathbf{x} - \mathbf{x}')} (s_{\mathbf{x}\mathbf{x}'} + 1). \end{aligned} \tag{6.1}$$

Power counting teaches us that the integral over the transverse momentum of the gluon with respect to its emitter contains a collinear divergence:⁴

$$\int_{\ell} \frac{1}{\ell^2} e^{-i\ell \cdot (\mathbf{x} - \mathbf{x}')} = -\frac{1}{4\pi} \left(\frac{1}{\epsilon_{\text{coll}}} + \gamma_E + \ln(\mu^2 \pi (\mathbf{x} - \mathbf{x}')^2) \right) + \mathcal{O}(\epsilon_{\text{coll}}), \tag{6.2}$$

which is easily proven with the help of the Schwinger trick (A.1). Therefore, in the collinear limit $\ell \rightarrow 0$, the third line in formula (6.1) can be approximated by:

$$\frac{p_3^+ (q^+ \ell + p_0^+ \mathbf{q})^2 - p_0^+ p_1^+ p_3^+ M^2}{p_3^+ (q^+ \ell + p_0^+ \mathbf{q})^2 + p_1^+ q^+ p_{0R}^+ \ell^2 + p_1^+ p_3^+ p_0^+ M^2} \rightarrow \frac{p_0^+ \mathbf{q}^2 - p_1^+ M^2}{p_0^+ \mathbf{q}^2 + p_1^+ M^2}. \tag{6.3}$$

With these simplifications, the collinearly divergent part of eq. (6.1) can be rewritten as:⁵

$$\begin{aligned} \int_{\mathbf{p}_3} \left| \mathcal{M}_{\text{IS1}}^{(0,\lambda)\eta} + \mathcal{M}_{\text{IS2}}^{(0,\lambda)\eta} \right|^2 &\stackrel{\text{coll.}}{=} |\mathcal{M}_{\text{LO}}^{0,\lambda}|^2 \times -\alpha_s C_F \left(\frac{1}{\epsilon_{\text{coll}}} + \gamma_E + \ln(\mu^2 \pi (\mathbf{x} - \mathbf{x}')^2) \right) \\ &\times \frac{(p_3^+)^2}{p_0^+ p_{0R}^+} \left(\left(1 + \frac{2p_0^+}{p_3^+} \right)^2 + D - 3 \right). \end{aligned} \tag{6.4}$$

⁴Ultraviolet divergences $\ell^2 \rightarrow \infty$ are cut off by the phase.

⁵Of course, the above notation is somewhat symbolic, as the square of the leading order part $|\mathcal{M}_{\text{LO}}|^2$ still contains the integrals over \mathbf{x} and \mathbf{x}' , which also appear in the logarithm.

It is easily verified that the above result also holds in the case of a transversely polarized virtual photon, hence the index $(0, \lambda)$. This implies that we have extracted a universal collinear factor, which is independent of the details of the leading-order process. It is, therefore, natural to associate it with quantum fluctuations of the incoming quark before it participates in the hard process. Indeed, in the next section we demonstrate that the collinear pole can be absorbed into the DGLAP evolution of the quark PDF.

6.2 From parton to hadron level

On the partonic level, the amplitudes for the real NLO corrections are transformed into contributions to the cross section using the following formula:

$$d\hat{\sigma}_{\text{real}} = \frac{1}{2p_{0R}^+} \text{PS}(\vec{p}_1, \vec{q}, \vec{p}_3) 2\pi \delta(p_{0R}^+ - p_1^+ - q^+ - p_3^+) \frac{1}{D-2} |\mathcal{M}_{\text{real}}|^2. \quad (6.5)$$

As discussed in section 2, the partonic cross section needs to be transformed into a hadronic one by convolving with the leading-order quark PDF $f_q^{(0)}$ and taking the CGC average:

$$d\sigma_{\text{real}} = \int \frac{dp_{0R}^+}{p_p^+} f_q^{(0)} \left(\frac{x_p}{\xi} \right) \langle d\hat{\sigma}_{\text{real}} \rangle, \quad (6.6)$$

where $x_p = p_0^+/p_p^+$ according to the leading-order definition of projectile quark momentum fraction, and where we have introduced $\xi = p_0^+/p_{0R}^+$. Finally, the radiated gluon is integrated out in order to obtain the real radiative corrections to the full NLO cross section:

$$d\sigma_{\text{NLO}} = d\sigma_{\text{LO}} + d\sigma_{\text{virtual}} + \mu^{4-D} \int d^{D-1} \vec{p}_3 \frac{d\sigma_{\text{real}}}{d^{D-1} p_3}. \quad (6.7)$$

We shall now apply the procedure above to transform eq. (6.4) into a contribution to the NLO cross section. Promoting (6.4) to a part of the partonic cross section, performing the convolution with the PDF, and averaging over the semiclassical background fields, we find:⁶

$$\begin{aligned} \mu^{4-D} \int d^{D-1} \vec{p}_3 \frac{d\sigma_{\text{IS1,2}}}{d^{D-1} p_3} \text{coll} &\equiv \int \frac{dp_{0R}^+}{p_p^+} f_q^{(0)} \left(\frac{x_p}{\xi} \right) \int_{k_{\min}^+} \frac{dp_3^+}{(2\pi)^{D-3} 2p_3^+} \left(\frac{p_3^+}{p_{0R}^+} \right)^2 \left(\left(1 + \frac{2p_0^+}{p_3^+} \right)^2 + D - 3 \right) \\ &\times \frac{1}{2p_0^+} \int \text{PS}(\vec{p}_1, \vec{q}) 2\pi \delta(p_{0R}^+ - p_1^+ - q^+ - p_3^+) \frac{1}{D-2} \langle |\mathcal{M}_{\text{LO}}|^2 \rangle \\ &\times -\alpha_s C_F \left(\frac{1}{\epsilon_{\text{coll}}} + \gamma_E + \ln(\mu^2 \pi (\mathbf{x} - \mathbf{x}')^2) \right). \end{aligned} \quad (6.8)$$

Changing the integration variable from the gluon plus-momentum to ξ using the relation $p_3^+ = p_0^+ \frac{1-\xi}{\xi}$, and with $d\xi/\xi = dp_3^+/p_{0R}^+$, we finally obtain:

$$\begin{aligned} \mu^{4-D} \int d^{D-1} \vec{p}_3 \frac{d\sigma_{\text{IS1,2}}}{d^{D-1} p_3} \text{coll} &\equiv \int_{x_p}^{p_0^+/(p_0^+ + k_{\min}^+)} d\xi \frac{1+\xi^2}{1-\xi} \frac{x_p}{\xi} f_q^{(0)} \left(\frac{x_p}{\xi} \right) \\ &\times \frac{1}{2(p_0^+)^2} \int \text{PS}(\vec{p}_1, \vec{q}) \frac{1}{2} \langle |\mathcal{M}_{\text{LO}}|^2 \rangle \\ &\times -\alpha_s C_F \left(\frac{1}{\epsilon_{\text{coll}}} + \gamma_E + \ln(\mu^2 \pi (\mathbf{x} - \mathbf{x}')^2) \right). \end{aligned} \quad (6.9)$$

⁶Note that we do not distinguish anymore between the polarization states of the virtual photon, since the collinear initial-state radiation is insensitive to them.

The upper bound $p_0^+/(p_0^+ + k_{\min}^+) > \xi$ in the integral stems from the rapidity cutoff $p_3^+ > k_{\min}^+$, while the requirement $\xi > x_p$ comes from the domain of the PDF. To cast it in a form in which one can recognize DGLAP, let us start by splitting up the integration over ξ :

$$\begin{aligned} & \int_{x_p}^{p_0^+/(p_0^+ + k_{\min}^+)} d\xi \frac{1 + \xi^2}{1 - \xi} \frac{x_p}{\xi} f_q^{(0)}\left(\frac{x_p}{\xi}\right) \\ &= \left(\int_{x_p}^1 d\xi + \int_1^{p_0^+/(p_0^+ + k_{\min}^+)} d\xi \right) \frac{1 + \xi^2}{1 - \xi} \frac{x_p}{\xi} f_q^{(0)}\left(\frac{x_p}{\xi}\right). \end{aligned} \quad (6.10)$$

The next step is to make use of the definition of the plus-distribution:

$$\int_z^1 d\xi \frac{f(\xi)}{(1 - \xi)_+} \equiv \int_z^1 d\xi \frac{f(\xi) - f(1)}{1 - \xi} - f(1) \int_0^z \frac{d\xi}{1 - \xi}, \quad (6.11)$$

using which the first integration in (6.10) can be written as:

$$\int_{x_p}^1 d\xi \frac{1 + \xi^2}{1 - \xi} \frac{x_p}{\xi} f_q^{(0)}\left(\frac{x_p}{\xi}\right) = \int_{x_p}^1 d\xi \frac{1 + \xi^2}{(1 - \xi)_+} \frac{x_p}{\xi} f_q^{(0)}\left(\frac{x_p}{\xi}\right) + x_p f_q^{(0)}(x_p) \int_0^1 d\xi \frac{2}{1 - \xi}. \quad (6.12)$$

The second integral in (6.10) is the one that contains the divergence for $p_3^+ \rightarrow 0$, or equivalently, $\xi \rightarrow 1$. In this limit, one can write:

$$\int_1^{p_0^+/(p_0^+ + k_{\min}^+)} d\xi \frac{1 + \xi^2}{1 - \xi} \frac{x_p}{\xi} f_q^{(0)}\left(\frac{x_p}{\xi}\right) \simeq x_p f_q^{(0)}(x_p) \int_1^{p_0^+/(p_0^+ + k_{\min}^+)} d\xi \frac{2}{1 - \xi}. \quad (6.13)$$

Combining (6.12) and (6.13), eq. (6.10) eventually becomes:

$$\begin{aligned} & \int_{x_p}^{p_0^+/(p_0^+ + k_{\min}^+)} d\xi \frac{1 + \xi^2}{1 - \xi} \frac{x_p}{\xi} f_q^{(0)}\left(\frac{x_p}{\xi}\right) \\ &= \int_{x_p}^1 d\xi \frac{1 + \xi^2}{(1 - \xi)_+} \frac{x_p}{\xi} f_q^{(0)}\left(\frac{x_p}{\xi}\right) + x_p f_q^{(0)}(x_p) \int_0^{p_0^+/(p_0^+ + k_{\min}^+)} d\xi \frac{2}{1 - \xi}, \\ &= \int_{x_p}^1 d\xi \left(\frac{1 + \xi^2}{(1 - \xi)_+} + \frac{3}{2} \delta(1 - \xi) \right) \frac{x_p}{\xi} f_q^{(0)}\left(\frac{x_p}{\xi}\right) + \left(-\frac{3}{2} + 2 \ln \frac{p_0^+}{k_{\min}^+} \right) x_p f_q^{(0)}(x_p). \end{aligned} \quad (6.14)$$

In the last line of the above formula, one can recognize the Altarelli-Parisi $q \rightarrow q$ splitting function:

$$P_{qq}^{(0)}(\xi) = C_F \left(\frac{1 + \xi^2}{(1 - \xi)_+} + \frac{3}{2} \delta(1 - \xi) \right). \quad (6.15)$$

We, therefore, have shown that eq. (6.9) can be rewritten as:

$$\begin{aligned} & \mu^{4-D} \int d^{D-1} \vec{p}_3 \frac{d\sigma_{\text{IS1,2}}}{d^{D-1} p_3} \stackrel{\text{coll}}{=} \left[\int_{x_p}^1 d\xi P_{qq}^{(0)}(\xi) \frac{x_p}{\xi} f_q^{(0)}\left(\frac{x_p}{\xi}\right) + C_F \left(-\frac{3}{2} + 2 \ln \frac{p_0^+}{k_{\min}^+} \right) x_p f_q^{(0)}(x_p) \right] \\ & \quad \times \frac{1}{2(p_0^+)^2} \int \text{PS}(\vec{p}_1, \vec{q}) \frac{1}{2} \langle |\mathcal{M}_{\text{LO}}|^2 \rangle \\ & \quad \times -\alpha_s \left(\frac{1}{\epsilon_{\text{coll}}} + \gamma_E + \ln(\mu^2 \pi(\mathbf{x} - \mathbf{x}')^2) \right). \end{aligned} \quad (6.16)$$

The above pole, stemming from real gluon radiation in the initial-state, is not the first collinear singularity we have encountered in this work. Remember that in subsection 3.6, we discovered collinear poles stemming from the quark field-strength renormalization:

$$\begin{aligned}
 (\mathcal{Z}_{\text{IS}} + \mathcal{Z}_{\text{IS}}^\dagger) d\sigma_{\text{LO}} &= \alpha_s C_F \left(\frac{1}{\epsilon_{\text{coll}}} + \ln \frac{\mu^2}{\mu_R^2} \right) \left(-\frac{3}{2} + 2 \ln \frac{p_0^+}{k_{\text{min}}^+} \right) \\
 &\times x_p f_q^{(0)}(x_p) \frac{1}{2(p_0^+)^2} \int \text{PS}(\vec{p}_1, \vec{q}) \frac{1}{2} \langle |\mathcal{M}_{\text{LO}}|^2 \rangle.
 \end{aligned} \tag{6.17}$$

Adding (6.16) and (6.17), one obtains:

$$\begin{aligned}
 &\mu^{4-D} \int d^{D-1} \vec{p}_3 \left. \frac{d\sigma_{\text{IS1,2}}}{d^{D-1} p_3} \right|_{\text{coll.}} + (\mathcal{Z}_{\text{IS}} + \mathcal{Z}_{\text{IS}}^\dagger) d\sigma_{\text{LO}} \\
 &= \frac{1}{2(p_0^+)^2} \int \text{PS}(\vec{p}_1, \vec{q}) \frac{1}{2} \langle |\mathcal{M}_{\text{LO}}|^2 \rangle \\
 &\times \left[-\alpha_s \left(\frac{1}{\epsilon_{\text{coll}}} + \gamma_E + \ln(\mu^2 \pi(\mathbf{x} - \mathbf{x}')^2) \right) \int_{x_p}^1 d\xi P_{qq}^{(0)}(\xi) \frac{x_p}{\xi} f_q^{(0)} \left(\frac{x_p}{\xi} \right) \right. \\
 &\left. + \alpha_s C_F \left(\ln \frac{e^{-\gamma_E}}{\mu_R^2 \pi(\mathbf{x} - \mathbf{x}')^2} \right) \left(-\frac{3}{2} + 2 \ln \frac{p_0^+}{k_{\text{min}}^+} \right) x_p f_q^{(0)}(x_p) \right].
 \end{aligned} \tag{6.18}$$

In the above equation, the only collinear singularity left is proportional to the leading-order squared amplitude times the quark PDF convolved with the Altarelli-Parisi splitting function. The final step is to notice that the ($\overline{\text{MS}}$ -) quark PDF at NLO: $f_q^{(1)}$, is related to the leading order one $f_q^{(0)}$ as follows [81]:⁷

$$\begin{aligned}
 x_p f_q^{(1)}(x_p, \mu^2) &= x_p f_q^{(0)}(x_p) \\
 &- \left(\frac{1}{\epsilon_{\text{coll}}} - \gamma_E + \ln 4\pi \right) \frac{\alpha_s}{2\pi} \int_{x_p}^1 \frac{d\xi}{\xi} P_{qq}^{(0)}(\xi) x_p f_q^{(0)} \left(\frac{x_p}{\xi} \right) + \mathcal{O}(\alpha_s^2).
 \end{aligned} \tag{6.19}$$

Therefore, we can rewrite the LO cross section as:

$$\begin{aligned}
 d\sigma_{\text{LO}} &= d\sigma_{\text{LO+DGLAP}} + \left(\frac{1}{\epsilon_{\text{coll}}} - \gamma_E + \ln 4\pi \right) \frac{\alpha_s}{2\pi} \int_{x_p}^1 \frac{d\xi}{\xi} P_{qq}^{(0)}(\xi) x_p f_q^{(0)} \left(\frac{x_p}{\xi} \right) \\
 &\times \frac{2\pi}{2(p_0^+)^2} \int \text{PS}(\vec{p}_1, \vec{q}) \frac{1}{D-2} \langle |\mathcal{M}_{\text{LO}}|^2 \rangle,
 \end{aligned} \tag{6.20}$$

where we defined $d\sigma_{\text{LO+DGLAP}}$ as the leading-order cross section convolved with the NLO quark PDF:

$$d\sigma_{\text{LO+DGLAP}} = x_p f_q^{(1)}(x_p, \mu^2) \frac{2\pi}{2(p_0^+)^2} \int \text{PS}(\vec{p}_1, \vec{q}) \frac{1}{D-2} \langle |\mathcal{M}_{\text{LO}}|^2 \rangle. \tag{6.21}$$

Adding (6.18) and (6.20), we finally obtain:

$$d\sigma_{\text{LO}} + \mu^{4-D} \int d^{D-1} \vec{p}_3 \left. \frac{d\sigma_{\text{IS1,2}}}{d^{D-1} p_3} \right|_{\text{coll.}} + (\mathcal{Z}_{\text{IS}} + \mathcal{Z}_{\text{IS}}^\dagger) d\sigma_{\text{LO}} = d\sigma_{\text{LO+DGLAP}} + d\sigma_{\text{IS}}, \tag{6.22}$$

⁷In principle, eq. (6.19) contains an additional term proportional to the gluon PDF. The corresponding collinear pole should cancel with initial-state radiation in the $g + A \rightarrow \gamma^* + q + \bar{q}$ contribution to the cross section. The analysis of the gluon channel is left for future work, see also the discussion in the conclusions 10.

with:

$$\begin{aligned}
 d\sigma_{\text{IS}} \equiv & \alpha_s \left[\ln \frac{c_0^2}{\mu^2(\mathbf{x} - \mathbf{x}')^2} \int_{x_p}^1 d\xi P_{qq}^{(0)}(\xi) \frac{x_p}{\xi} f_q^{(0)}\left(\frac{x_p}{\xi}\right) \right. \\
 & + C_F \left(\ln \frac{e^{-\gamma_E}}{\mu_R^2 \pi(\mathbf{x} - \mathbf{x}')^2} \right) \left(-\frac{3}{2} + 2 \ln \frac{p_0^+}{k_{\text{min}}^+} \right) x_p f_q^{(0)}(x_p) \left. \right] \\
 & \times \frac{1}{2(p_0^+)^2} \int \text{PS}(\vec{p}_1, \vec{q}) \frac{1}{2} \langle |\mathcal{M}_{\text{LO}}|^2 \rangle,
 \end{aligned} \tag{6.23}$$

where $c_0 \equiv 2e^{-\gamma_E}$. The above result proves that, at least at NLO accuracy, the hybrid dilute-dense factorization Ansatz employed in this work holds, as a collinear PDF is sufficient to absorb all collinear singularities stemming from initial-state radiation.

7 Infrared safety in the final state

7.1 Jet algorithm

For the leading-order and virtual contributions to the cross section, the outgoing quark can be trivially related to the jet which it will initiate. Indeed, it is sufficient to assume that the jet will be centered around the outgoing quark, such that $\vec{p}_{\text{jet}} = \vec{p}_1$. However, for the real next-to-leading order corrections, this is not true anymore. Instead, we need to specify what we mean by a jet, using a specific jet algorithm. This algorithm allows one to distinguish the case in which the quark and the gluon are grouped inside the same jet and the reaction hence has a similar topology as the leading-order one, from the situation where both the quark and the gluon each initiate a separate jet. Since our main purpose here is to prove final-state infrared safety, we can limit ourselves to the following straightforward algorithm: the outgoing quark and gluon are grouped inside the same jet when their momenta satisfy the condition:

$$\frac{p_1^+ + p_3^+}{|\mathbf{p}_1 + \mathbf{p}_3|} \left| \frac{\mathbf{p}_1}{p_1^+} - \frac{\mathbf{p}_3}{p_3^+} \right| < R. \tag{7.1}$$

The parameter R is known as the jet radius parameter and is bounded by $0 < R < 1$. Moreover, for our purposes it is sufficient to work in the so-called narrow-jet limit $R \rightarrow 0$, suppressing all positive powers of R in the calculation.⁸ In practice, this means that there is only a single configuration where the quark and gluon are part of the same jet, namely when the gluon is radiated collinearly to the quark in the final state. Note that, in this work, we always consider the case where the observed jet is initiated by the quark and the gluon is integrated out, whether the latter forms its own jet or belongs to the quark one. For later phenomenological applications, our intermediate $q + A \rightarrow \gamma^* + q + g$ results can be directly used to calculate the contribution to the cross section where the observed jet stems from the gluon, while the quark initiates its own jet that stays undetected. In addition, if desired, it always remains possible to employ a more sophisticated jet algorithm.

In our calculation, it turns out that \mathcal{M}_{FS2} and \mathcal{M}_{FS3} are the only amplitudes that lead (always on the level of the cross section) to final-state collinear divergences. They are,

⁸We note that, in this limit, our jet definition becomes equivalent to the Cambridge/Aachen algorithm [82, 83].

therefore, the only amplitudes contributing to the configuration in which the quark and gluon are paired inside the same jet, due to the abovementioned narrow-jet limit we consider. Let us add and square them, starting with the transverse case (eqs. (5.18) resp. (5.20)):

$$\begin{aligned}
 |\mathcal{M}_{\text{FS}2+3}^\lambda|^2 &= g_{\text{em}}^2 g_s^2 C_F N_c \left(\frac{p_3^+}{p_1^+}\right)^2 8p_1^+ p_{0R}^+ \left(\left(1 + \frac{2p_1^+}{p_3^+}\right)^2 + D - 3 \right) \left(\left(1 + 2\frac{p_1^+ + p_3^+}{q^+}\right)^2 + D - 3 \right) \\
 &\quad \times \frac{1}{\left(\mathbf{p}_3 - \frac{p_3^+}{p_1^+} \mathbf{p}_1\right)^2} \left[\frac{p_3^+}{p_0^+} \frac{\mathbf{q} - \frac{q^+}{p_1^+ + p_3^+} (\mathbf{p}_1 + \mathbf{p}_3)}{\left(\mathbf{p}_3 - \frac{p_3^+}{p_0^+} \mathbf{k}_\perp\right)^2 + \Delta_{\text{FS}}} - \frac{q^+ \mathbf{q}}{p_{0R}^+ \mathbf{q}^2 + (p_1^+ + p_3^+) M^2} \right]^2 \\
 &\quad \times \int_{\mathbf{x}, \mathbf{x}'} e^{-i(\mathbf{q} + \mathbf{p}_1 + \mathbf{p}_3) \cdot (\mathbf{x} - \mathbf{x}')} (s_{\mathbf{x}\mathbf{x}'} + 1), \tag{7.2}
 \end{aligned}$$

where the spinor trace was evaluated with the help of the relations in section B. Similarly, in the longitudinal case (eqs. (5.17) resp. (5.19)):

$$\begin{aligned}
 |\mathcal{M}_{\text{FS}2+3}^0|^2 &= g_{\text{em}}^2 g_s^2 C_F N_c \left(\frac{p_3^+}{p_1^+}\right)^2 8p_1^+ p_{0R}^+ \left(\left(1 + \frac{2p_1^+}{p_3^+}\right)^2 + D - 3 \right) \frac{1}{M^2} \frac{1}{\left(\mathbf{p}_3 - \frac{p_3^+}{p_1^+} \mathbf{p}_1\right)^2} \\
 &\quad \times \left[\frac{p_{0R}^+ p_3^+}{q^+ p_0^+} \frac{\left(\frac{(p_1^+ + p_3^+) \mathbf{q} - q^+ (\mathbf{p}_1 + \mathbf{p}_3)}{p_{0R}^+ (p_1^+ + p_3^+)}\right)^2 - M^2}{\left(\mathbf{p}_3 - \frac{p_3^+}{p_0^+} \mathbf{k}_\perp\right)^2 + \Delta_{\text{FS}}} - \frac{p_{0R}^+ \mathbf{q}^2 - (p_1^+ + p_3^+) M^2}{p_{0R}^+ \mathbf{q}^2 + (p_1^+ + p_3^+) M^2} \right]^2 \\
 &\quad \times \int_{\mathbf{x}, \mathbf{x}'} e^{-i(\mathbf{q} + \mathbf{p}_1 + \mathbf{p}_3) \cdot (\mathbf{x} - \mathbf{x}')} (s_{\mathbf{x}\mathbf{x}'} + 1). \tag{7.3}
 \end{aligned}$$

Indeed, from the structure of the above expressions it is clear that both of them contain a divergence in the limit $p_1^+ \mathbf{p}_3 - p_3^+ \mathbf{p}_1 \rightarrow 0$, i.e. when the gluon is radiated collinearly to its parent quark.

7.2 Gluon inside the jet

Let us first consider the case when the quark and the gluon are grouped inside the same jet. Integrating over the gluon momentum, the jet algorithm (7.1) is then imposed by adding the following step function to the integrand:

$$\theta_{\text{in}}(\vec{p}_1, \vec{p}_3) = \theta \left((\mathbf{p}_1 + \mathbf{p}_3)^2 R^2 - (p_1^+ + p_3^+)^2 \left(\frac{\mathbf{p}_1}{p_1^+} - \frac{\mathbf{p}_3}{p_3^+} \right)^2 \right). \tag{7.4}$$

Moreover, the quark momentum \vec{p}_1 is not the correct physical parameter anymore, but rather we should work with the jet momentum $\vec{p}_j \equiv \vec{p}_1 + \vec{p}_3$. With the help of the intermediate relations

$$\begin{aligned}
 &\frac{1}{\left(\mathbf{p}_3 - \frac{p_3^+}{k_1^+} \mathbf{k}_\perp\right)^2 + \Delta_{\text{FS}}} \xrightarrow{\vec{p}_1 \rightarrow \vec{p}_j - \vec{p}_3} \frac{(p_j^+ - p_3^+)(q^+ + p_j^+ - p_3^+)}{(p_j^+ + q^+) p_j^+} \\
 &\quad \times \frac{1}{\left(\mathbf{p}_3 - \frac{p_3^+}{p_j^+} \mathbf{p}_j\right)^2 + \frac{p_3^+ (p_j^+ - p_3^+)}{(p_j^+)^2 q^+} \left((p_j^+ + q^+) \mathbf{P}_{j\perp}^2 + p_j^+ M^2 \right)}, \tag{7.5}
 \end{aligned}$$

and

$$\left(\mathbf{p}_3 - \frac{p_3^+}{p_1^+} \mathbf{p}_1\right)^2 \bar{p}_1 \rightarrow \bar{p}_j - \bar{p}_3 \left(\frac{p_j^+}{p_j^+ - p_3^+}\right)^2 \left(\mathbf{p}_3 - \frac{p_3^+}{p_j^+} \mathbf{p}_j\right)^2, \quad (7.6)$$

one then obtains:

$$\begin{aligned} & \int_{\mathbf{p}_3} |\mathcal{M}_{\text{FS}2+3}^\lambda|^2 \theta_{\text{in}}(\vec{p}_1, \vec{p}_3) \\ & \bar{p}_1 \rightarrow \bar{p}_j - \bar{p}_3 g_{\text{em}}^2 g_s^2 C_F N_c \left(\frac{p_3^+}{p_j^+}\right)^2 8(p_j^+ - p_3^+)(p_j^+ + q^+) \left(\left(2\frac{p_j^+}{p_3^+} - 1\right)^2 + D - 3\right) \left(\left(1 + 2\frac{p_j^+}{q^+}\right)^2 + D - 3\right) \\ & \times \int_{\ell} \frac{1}{\ell^2} \left[\frac{(p_j^+ - p_3^+) p_3^+}{(p_j^+)^2} \frac{\mathbf{P}_{j\perp}}{\ell^2 + \frac{p_3^+(p_j^+ - p_3^+)}{(p_j^+)^2 q^+} ((p_j^+ + q^+) \mathbf{P}_{j\perp}^2 + p_j^+ M^2)} + \frac{q^+ \mathbf{q}}{p_0^+ \mathbf{q}^2 + p_j^+ M^2} \right]^2 \\ & \times \theta\left(\frac{(p_3^+)^2 (p_j^+ - p_3^+)^2}{(p_j^+)^4} \mathbf{P}_j^2 R^2 - \ell^2\right) \int_{\mathbf{x}, \mathbf{x}'} e^{-i(\mathbf{q} + \mathbf{p}_j) \cdot (\mathbf{x} - \mathbf{x}')} (s_{\mathbf{x}\mathbf{x}'} + 1). \end{aligned} \quad (7.7)$$

In the above expression, we changed the integration variable from \mathbf{p}_3 to $\ell \equiv \mathbf{p}_3 - \frac{p_3^+}{p_j^+} \mathbf{p}_j$ and introduced the analogues of the momentum combinations (2.30):

$$\mathbf{P}_{j\perp} \equiv \frac{q^+ \mathbf{p}_j - p_j^+ \mathbf{q}}{q^+ + p_j^+} \quad \text{and} \quad \mathbf{k}_{j\perp} \equiv \mathbf{p}_j + \mathbf{q}. \quad (7.8)$$

Similarly, in the longitudinally polarized case, we have:

$$\begin{aligned} & \int_{\mathbf{p}_3} |\mathcal{M}_{\text{FS}2+3}^0|^2 \theta_{\text{in}}(\vec{p}_1, \vec{p}_3) \\ & \bar{p}_1 \rightarrow \bar{p}_j - \bar{p}_3 \frac{g_{\text{em}}^2 g_s^2 C_F N_c 8(p_j^+ - p_3^+)(p_j^+ + q^+) \left(\left(1 + \frac{2(p_j^+ - p_3^+)}{p_3^+}\right)^2 + D - 3\right) \left(\frac{p_3^+}{p_j^+}\right)^2}{M^2} \\ & \times \int_{\ell} \frac{1}{\ell^2} \left[\frac{p_3^+ (p_j^+ - p_3^+)}{q^+ (p_j^+)^2} \frac{p_0^+ \mathbf{P}_{j\perp}^2 - p_j^+ M^2}{\ell^2 + \frac{p_3^+(p_j^+ - p_3^+)}{(p_j^+)^2 q^+} (p_0^+ \mathbf{P}_{j\perp}^2 + p_j^+ M^2)} - \frac{p_0^+ \mathbf{q}^2 - p_j^+ M^2}{p_0^+ \mathbf{q}^2 + p_j^+ M^2} \right]^2 \\ & \times \theta\left(\frac{(p_3^+)^2 (p_j^+ - p_3^+)^2}{(p_j^+)^4} \mathbf{P}_j^2 R^2 - \ell^2\right) \int_{\mathbf{x}, \mathbf{x}'} e^{-i(\mathbf{q} + \mathbf{p}_j) \cdot (\mathbf{x} - \mathbf{x}')} (s_{\mathbf{x}\mathbf{x}'} + 1). \end{aligned} \quad (7.9)$$

The transverse integrals in eq. (7.7) can be evaluated with the help of the following identities, which are easily proven in dimensional regularization:

$$\begin{aligned} \mu^{4-D} \int \frac{d^{D-2} \ell}{(2\pi)^{D-2}} \frac{\theta(\mathbf{b} - \ell)}{\ell^2} &= -\frac{1}{4\pi} \left[\frac{1}{\epsilon_{\text{coll}}} + \ln\left(\frac{4\pi e^{-\gamma_E} \mu^2}{b^2}\right) \right] + \mathcal{O}(b, \epsilon_{\text{coll}}), \\ \mu^{4-D} \int \frac{d^{D-2} \ell}{(2\pi)^{D-2}} \frac{\theta(\mathbf{b} - \ell)}{\ell^2 (\ell^2 + m)} &= -\frac{1}{4\pi m} \left[\frac{1}{\epsilon_{\text{coll}}} + \ln\left(\frac{4\pi e^{-\gamma_E} \mu^2}{b^2}\right) \right] + \mathcal{O}(b, \epsilon_{\text{coll}}), \\ \mu^{4-D} \int \frac{d^{D-2} \ell}{(2\pi)^{D-2}} \frac{\theta(\mathbf{b} - \ell)}{\ell^2 (\ell^2 + m)^2} &= -\frac{1}{4\pi m^2} \left[\frac{1}{\epsilon_{\text{coll}}} + \ln\left(\frac{4\pi e^{-\gamma_E} \mu^2}{b^2}\right) \right] + \mathcal{O}(b, \epsilon_{\text{coll}}), \end{aligned} \quad (7.10)$$

where we remind the reader that we work in the narrow-cone approximation $R \rightarrow 0$, keeping only negative power-like or logarithmic dependencies on R . We also expand $D - 3 = 1 - 2\epsilon_{\text{coll}}$ from the Dirac structure $(2\frac{p_j^+}{p_3^+} - 1)^2 + D - 3$. In both the transverse (7.7)

and longitudinally (7.9) polarized case, we obtain a result proportional to the corresponding leading-order amplitude:

$$\begin{aligned}
 & \int_{\mathbf{p}_3} |\mathcal{M}_{\text{FS}2+3}^{0,\lambda}|^2 \theta_{\text{in}}(\vec{p}_1, \vec{p}_3) \\
 &= |\mathcal{M}_{\text{LO}}^{0,\lambda}|^2 \times -\alpha_s C_F \left[\frac{1}{\epsilon_{\text{coll}}} + \ln \left(\frac{4\pi e^{-\gamma_E} \mu^2 (p_j^+)^4}{(p_3^+)^2 (p_j^+ - p_3^+)^2 \mathbf{p}_j^2 R^2} \right) - \frac{(p_3^+)^2}{(p_j^+)^2 + (p_j^+ - p_3^+)^2} \right] \\
 & \quad \times \left(\frac{p_3^+}{p_j^+} \right)^2 \frac{(p_j^+ - p_3^+)}{p_j^+} \left(\left(2 \frac{p_j^+}{p_3^+} - 1 \right)^2 + 1 \right) + \mathcal{O}(\epsilon_{\text{coll}}).
 \end{aligned} \tag{7.11}$$

Note that, in the transverse case, the structure $(1+2\frac{p_j^+}{q^+})^2 + D - 3$ is absorbed into $|\mathcal{M}_{\text{LO}1+2}^{\text{T}}|^2$, which hence stays D -dimensional.

The next step is to integrate over the gluon plus-momentum. However, due to the shift $\vec{p}_1 \rightarrow \vec{p}_j - \vec{p}_3$ dictated by the jet algorithm, an additional dependence on p_3^+ is introduced on the level of the cross section:

$$\begin{aligned}
 d\sigma_{\text{in}}^{\text{T,L}} &= \mu^{3(4-D)} \int \frac{dp_3^+ d^{D-2}\mathbf{p}_3}{(2\pi)^{D-1} 2p_3^+} \frac{1}{2p_{0R}^+} \frac{dp_1^+ d^{D-2}\mathbf{p}_1}{(2\pi)^{D-1} 2p_1^+} \frac{dq^+ d^{D-2}\mathbf{q}}{(2\pi)^{D-1} 2q^+} \\
 & \quad \times 2\pi \delta(p_{0R}^+ - p_1^+ - q^+ - p_3^+) \frac{1}{D-2} |\mathcal{M}_{\text{FS}2+3}^{0,\lambda}|^2 \theta_{\text{in}}(\vec{p}_1, \vec{p}_3), \\
 & \quad \xrightarrow{\vec{p}_1 \rightarrow \vec{p}_j - \vec{p}_3} \mu^{3(4-D)} \int \frac{dp_3^+ d^{D-2}\mathbf{p}_3}{(2\pi)^{D-1} 2p_3^+} \frac{1}{2p_0^+} \frac{dp_j^+ d^{D-2}\mathbf{p}_j}{(2\pi)^{D-1} 2(p_j^+ - p_3^+)} \frac{dq^+ d^{D-2}\mathbf{q}}{(2\pi)^{D-1} 2q^+} \\
 & \quad \times 2\pi \delta(p_0^+ - p_j^+ - q^+) \frac{1}{D-2} |\mathcal{M}_{\text{FS}2+3}^{0,\lambda}|^2 \theta_{\text{in}}(\vec{p}_j - \vec{p}_3, \vec{p}_3), \\
 &= \mu^{2(4-D)} \frac{1}{2p_0^+} \frac{dp_j^+ d^{D-2}\mathbf{p}_j}{(2\pi)^{D-1} 2p_j^+} \frac{dq^+ d^{D-2}\mathbf{q}}{(2\pi)^{D-1} 2q^+} 2\pi \delta(p_0^+ - p_j^+ - q^+) \frac{1}{D-2} \\
 & \quad \times \int \frac{dp_3^+}{(2\pi)^{D-3} 2p_3^+} \frac{p_j^+}{(p_j^+ - p_3^+)} \int_{\mathbf{p}_3} |\mathcal{M}_{\text{FS}2+3}^{0,\lambda}|^2 \theta_{\text{in}}(\vec{p}_j - \vec{p}_3, \vec{p}_3).
 \end{aligned} \tag{7.12}$$

Evaluating the plus-momentum integral, regularizing the $p_3^+ \rightarrow 0$ pole with the cutoff k_{min}^+ , we finally obtain:

$$d\sigma_{\text{in}}^{\text{T,L}} = d\sigma_{\text{LO,jet}}^{\text{T,L}} \frac{\alpha_s C_F}{\pi} \left[\left(\frac{1}{\epsilon_{\text{coll}}} + \ln \left(\frac{4\pi e^{-\gamma_E} \mu^2}{\mathbf{p}_j^2 R^2} \right) \right) \left(\frac{3}{4} - \ln \frac{p_j^+}{k_{\text{min}}^+} \right) + \frac{13}{4} - \frac{\pi^2}{3} - \ln^2 \frac{p_j^+}{k_{\text{min}}^+} \right], \tag{7.13}$$

where $d\sigma_{\text{LO,jet}}^{\text{T,L}}$ is the leading-order cross section in terms of the jet instead of the quark. Adding the above result to the ‘final-state’ part of the field-strength renormalization corrections (3.114), which stem from virtual diagrams hence we can directly identify the quark momentum with the jet one:

$$d\sigma_{\mathcal{Z}_{\text{FS}}} = d\sigma_{\text{LO}} \frac{\alpha_s C_F}{\pi} \left(\frac{1}{\epsilon_{\text{coll}}} + \ln \frac{\mu^2}{\mu_R^2} \right) \left(-\frac{3}{4} + \ln \frac{p_j^+}{k_{\text{min}}^+} \right), \tag{7.14}$$

we obtain:

$$d\sigma_{\text{in}} + d\sigma_{\mathcal{Z}_{\text{FS}}} = d\sigma_{\text{LO}} \times \frac{\alpha_s C_F}{\pi} \left[\ln \left(\frac{4\pi e^{-\gamma_E} \mu^2}{\mathbf{p}_j^2 R^2} \right) \left(\frac{3}{4} - \ln \frac{p_j^+}{k_{\text{min}}^+} \right) + \frac{13}{4} - \frac{\pi^2}{3} - \ln^2 \frac{p_j^+}{k_{\text{min}}^+} \right]. \tag{7.15}$$

We omitted the labels indicating the photon polarization since the above result does not depend on it. The above expression is an important result, demonstrating the cancellation of final-state collinear divergencies in our cross section. There is, however, one loose end in the form of a double logarithm in the rapidity cutoff k_{\min}^+ . Since high-energy resummation only involves single large logarithms, this term is unphysical and needs to cancel in the final cross section. In the next subsection, we will show that the unphysical double logarithm cancels when adding the contribution of a soft gluon just outside the jet.

7.3 Gluon outside the jet

In the scenario where the gluon and its parent quark each form a distinct jet, the quark momentum can be directly identified with the one of the jet: $\vec{p}_j = \vec{p}_1$. The jet function, to be added inside the integral over gluon plus-momentum, becomes:

$$\begin{aligned}
 1 - \theta_{\text{in}}(\vec{p}_1 \rightarrow \vec{p}_j, \vec{p}_3) &= \theta \left((p_j^+ + p_3^+)^2 \left(\frac{\mathbf{p}_j}{p_j^+} - \frac{\mathbf{p}_3}{p_3^+} \right)^2 - (\mathbf{p}_j + \mathbf{p}_3)^2 R^2 \right), \\
 &= \theta \left(\ell^2 - \left(\frac{p_3^+}{p_j^+ + p_3^+} \right)^2 \left(\ell + \frac{p_3^+ + p_j^+}{p_j^+} \mathbf{p}_j \right)^2 R^2 \right), \\
 &\approx \theta \left(\ell^2 - \left(\frac{p_3^+}{p_j^+} \right)^2 \mathbf{p}_j^2 R^2 \right),
 \end{aligned} \tag{7.16}$$

where we introduced $\ell \equiv \mathbf{p}_3 - \frac{p_3^+}{p_j^+} \mathbf{p}_j$ and where the equality in the last line holds in the narrow-jet limit $R \rightarrow 0$. Integrating over the gluon momentum in (7.2) then gives:

$$\begin{aligned}
 &\int \text{PS}(\vec{p}_3) |\mathcal{M}_{\text{FS}2+3}^{\lambda\eta}|^2 (1 - \theta_{\text{in}}(\vec{p}_1, \vec{p}_3)) \\
 &= g_{\text{em}}^2 \alpha_s C_F N_c \int \frac{dp_3^+}{p_3^+} \int_{\ell} \frac{1}{\ell^2} \left[\frac{p_3^+}{p_0^+} \frac{q^+}{p_j^+ + p_3^+} \frac{\ell + \frac{p_0^+ p_j^+ + p_3^+}{q^+} \mathbf{P}_{\perp}}{\left(\ell + \frac{p_3^+}{p_j^+} \mathbf{P}_{\perp} \right)^2 + \Delta_{\text{FS}}} + \frac{q^+ \mathbf{q}}{p_{0R}^+ \mathbf{q}^2 + (p_j^+ + p_3^+) M^2} \right]^2 \\
 &\quad \times \theta \left(\ell^2 - \left(\frac{p_3^+}{p_j^+} \right)^2 \mathbf{p}_j^2 R^2 \right) \left(\frac{p_3^+}{p_j^+} \right)^2 \delta p_j^+ p_{0R}^+ \left(\left(1 + \frac{2p_j^+}{p_3^+} \right)^2 + 1 \right) \left(\left(1 + 2 \frac{p_j^+ + p_3^+}{q^+} \right)^2 + 1 \right) \\
 &\quad \times \int_{\mathbf{x}, \mathbf{x}'} e^{-i \left(\ell + \frac{p_3^+}{p_j^+} \mathbf{P}_{\perp} + \frac{p_{0R}^+}{p_0^+} \mathbf{k}_{\perp} \right) \cdot (\mathbf{x} - \mathbf{x}')} (s_{\mathbf{x}\mathbf{x}'} + 1).
 \end{aligned} \tag{7.17}$$

From experience [50], we expect that a similar unphysical double logarithm as the one in eq. (7.15) will appear from the phase-space integration over the gluon, in the kinematical region where the latter is just outside the jet with small plus-momentum, i.e. when simultaneously:

$$\ell = \mathbf{p}_3 - \frac{p_3^+}{p_j^+} \mathbf{p}_j \rightarrow 0 \quad \text{and} \quad p_3^+ \rightarrow 0. \tag{7.18}$$

In this regime, eq. (7.17) can be approximated by:

$$\begin{aligned}
& \lim_{\text{soft}} \int \text{PS}(\vec{p}_3) |\mathcal{M}_{\text{FS}2+3}|^2 (1 - \theta_{\text{in}}(\vec{p}_1, \vec{p}_3)) \\
&= |\mathcal{M}_{\text{LO}}|^2 4\alpha_s C_F \int_{k_{\text{min}}^+}^{+\infty} \frac{dp_3^+}{p_3^+} \int_{\ell} \frac{e^{-i\ell \cdot (\mathbf{x} - \mathbf{x}')}}{\ell^2} \theta \left(\ell^2 - \left(\frac{p_3^+}{p_j^+} \right)^2 \mathbf{p}_j^2 R^2 \right), \\
&= |\mathcal{M}_{\text{LO}}|^2 \frac{\alpha_s C_F}{\pi} \left(2 \ln \frac{p_j^+}{k_{\text{min}}^+} \ln \frac{c_0}{R|\mathbf{p}_j||\mathbf{x} - \mathbf{x}'|} + \ln^2 \frac{p_j^+}{k_{\text{min}}^+} \right),
\end{aligned} \tag{7.19}$$

where we used the identity:

$$\int_{\ell} \frac{e^{-i\ell \cdot \mathbf{x}}}{\ell^2} \theta(\ell^2 - \mathbf{b}^2) = \frac{1}{2\pi} \int_b^{\infty} \frac{d\ell}{\ell} J_0(\ell|\mathbf{x}|) = \frac{1}{2\pi} \ln \frac{c_0}{b|\mathbf{x}|}, \tag{7.20}$$

and where we suppressed the polarization labels since the same relation holds in the longitudinal case. Like everywhere in this work, we parameterized divergences in the limit of vanishing gluon plus-momentum with the cutoff k_{min}^+ . Promoting the result (7.19) to the cross-section level and adding it to eq. (7.15), we end up with:

$$\begin{aligned}
d\sigma_{\text{jet}} &\equiv d\sigma_{\text{in}} + d\sigma_{\mathcal{Z}_{\text{FS}}} + d\sigma_{\text{out,soft}} \\
&= d\sigma_{\text{LO}} \times \frac{\alpha_s C_F}{\pi} \left[\frac{3}{4} \ln \left(\frac{4\pi e^{-\gamma_E} \mu_R^2}{\mathbf{p}_j^2 R^2} \right) + \frac{13}{4} - \frac{\pi^2}{3} + \ln \frac{p_j^+}{k_{\text{min}}^+} \ln \frac{c_0}{2\pi \mu_R^2 (\mathbf{x} - \mathbf{x}')^2} \right],
\end{aligned} \tag{7.21}$$

in which the pathological double logarithm has cancelled.

8 High-energy resummation

In sections 4, 6, and 7, we have demonstrated that the different ultraviolet- and collinear divergences encountered in our calculation all cancel or, in the case of initial-state collinear poles, can be absorbed into the DGLAP evolution of the incoming quark. We are now in a position to treat the remaining high-energy or rapidity divergences, which either stem from the $k_3^+ \rightarrow 0$ limit in the gluon loop for virtual diagrams, either from the $p_3^+ \rightarrow 0$ limit in the gluon phase-space integration of real next-to-leading order contributions to the cross section. In both cases, the divergences are regularized with a cutoff k_{min}^+ and come in the form of single large logarithms.⁹ To be more precise, let us formally separate the integral over gluon plus-momentum in the (fixed-order) NLO cross section as follows:

$$d\sigma_{\text{NLO}} = \int_{k_{\text{min}}^+}^{+\infty} \frac{dp_3^+}{p_3^+} d\tilde{\sigma}_{\text{NLO}}. \tag{8.1}$$

Of course, p_3^+ is further constrained by delta functions or Heaviside step functions inside $\tilde{\sigma}_{\text{NLO}}$. Introducing the high-energy factorization scale k_f^+ , we can rewrite the equation above:

$$d\sigma_{\text{NLO}} = \int_{k_{\text{min}}^+}^{k_f^+} \frac{dp_3^+}{p_3^+} \hat{H}_{\text{JIMWLK}} d\sigma_{\text{LO}} + \int_0^{+\infty} \frac{dp_3^+}{p_3^+} \left(d\tilde{\sigma}_{\text{NLO}} - \theta(k_f^+ - p_3^+) \hat{H}_{\text{JIMWLK}} d\sigma_{\text{LO}} \right) \tag{8.2}$$

⁹We refer the reader to [84] for a discussion on choosing the value of k_{min}^+ .

where \hat{H}_{JIMWLK} is the JIMWLK Hamiltonian, acting on the target averages in the leading-order cross section. We will show in the following subsections that the above subtraction method works, namely that all the rapidity-divergent contributions in our NLO cross section can be combined into the first term of the above equation, such that the second term is a completely finite rapidity-subtracted cross section that does not depend on k_{min}^+ anymore. But first, we will argue that the first term in (8.2) is the first step in the JIMWLK evolution of the leading-order cross section. Indeed, at fixed leading order, the target average of the Wilson-line structure in the LO cross section 2.46 does not contain any evolution, hence we label it with a zero:

$$\langle s_{\mathbf{x}\mathbf{x}'} + 1 \rangle_0. \tag{8.3}$$

In the standard ‘naive’ approach that we use here [84], JIMWLK is used as an evolution equation for the target averages with the factorization scale k_f^+ , resumming the leading high-energy logarithms $Y_f^+ \equiv \ln(k_f^+/k_{\text{min}}^+)$ as follows:

$$\partial_{Y_f^+} \langle s_{\mathbf{x}\mathbf{x}'} + 1 \rangle_{Y_f^+} = \langle \hat{H}_{\text{JIMWLK}}(s_{\mathbf{x}\mathbf{x}'} + 1) \rangle_{Y_f^+}. \tag{8.4}$$

Integrating the above equation, we obtain:

$$\begin{aligned} \langle s_{\mathbf{x}\mathbf{x}'} + 1 \rangle_{Y_f^+} &= \langle s_{\mathbf{x}\mathbf{x}'} + 1 \rangle_0 + \int_0^{Y_f^+} dY^+ \langle \hat{H}_{\text{JIMWLK}}(s_{\mathbf{x}\mathbf{x}'} + 1) \rangle_{Y^+}, \\ &= \langle s_{\mathbf{x}\mathbf{x}'} + 1 \rangle_0 + Y_f^+ \langle \hat{H}_{\text{JIMWLK}}(s_{\mathbf{x}\mathbf{x}'} + 1) \rangle + \mathcal{O}(\alpha_s^2). \end{aligned} \tag{8.5}$$

In the last line, we have performed a fixed-order perturbative expansion in α_s . The JIMWLK Hamiltonian is of order α_s , and the dependence of the target average on the rapidity scale is not specified since it is a higher-order effect. We can, therefore, write the analogue of eq. (6.20):

$$d\sigma_{\text{LO}} = d\sigma_{\text{LO}+\text{JIMWLK}} - \ln \frac{k_f^+}{k_{\text{min}}^+} \hat{H}_{\text{JIMWLK}} d\sigma_{\text{LO}}. \tag{8.6}$$

Combining eqs. (8.6) and (8.2), one then obtains the final result:

$$d\sigma_{\text{LO}} + d\sigma_{\text{NLO}} = d\sigma_{\text{LO}+\text{JIMWLK}} + \int_0^{+\infty} \frac{dp_3^+}{p_3^+} \left(d\tilde{\sigma}_{\text{NLO}} - \theta(k_f^+ - p_3^+) \hat{H}_{\text{JIMWLK}} d\sigma_{\text{LO}} \right). \tag{8.7}$$

In the remainder of this section, we will explicitly demonstrate that the procedure outlined above works, analyzing all the different sources of rapidity divergences in our calculation. We end this subsection with the explicit action of the JIMWLK Hamiltonian on the dipole operator:

$$\hat{H}_{\text{JIMWLK}} \langle s_{\mathbf{x}\mathbf{x}'} + 1 \rangle = - \frac{\alpha_s N_c}{2\pi^2} \int_{\mathbf{z}} \frac{(\mathbf{x} - \mathbf{x}')^2}{(\mathbf{x} - \mathbf{z})^2 (\mathbf{x}' - \mathbf{z})^2} \langle s_{\mathbf{x}'\mathbf{x}} - s_{\mathbf{z}\mathbf{x}} s_{\mathbf{x}'\mathbf{z}} \rangle. \tag{8.8}$$

8.1 Leftovers from ultraviolet- and collinear subtractions

In section 4, we have demonstrated how the sum of the different UV counterterms in the virtual amplitudes yields a result which is free from any UV poles. There are, however, still

rapidity divergences left, regularized by the cutoff k_{\min}^+ . On the level of the cross section, we have for the longitudinally polarized photon (4.40):

$$d\sigma_{UV}^L = d\sigma_{LO}^L \times \frac{\alpha_s C_F}{\pi} \left[\left(-\frac{3}{2} + \ln \frac{p_1^+}{k_{\min}^+} + \ln \frac{p_0^+}{k_{\min}^+} \right) \ln \frac{4\pi e^{-\gamma_E} \mu_R^2}{\Delta_{UV}} - \frac{1}{2} \right]. \quad (8.9)$$

Following the usual high-energy resummation procedure, we will extract from above cross section the terms enhanced by a large rapidity or high-energy logarithm, and cut off the (implicit) integration over the gluon plus-momentum at the rapidity factorization scale k_f^+ :

$$\lim_{k^+ \rightarrow 0} d\sigma_{UV}^L = d\sigma_{LO}^L \times \ln \frac{k_f^+}{k_{\min}^+} \times \frac{2\alpha_s C_F}{\pi} \ln \frac{4\pi e^{-\gamma_E} \mu_R^2}{\Delta_{UV}}. \quad (8.10)$$

We obtain the same result when the photon is transversely polarized (4.41):

$$\lim_{k^+ \rightarrow 0} d\sigma_{UV}^T = d\sigma_{LO}^T \times \ln \frac{k_f^+}{k_{\min}^+} \times \frac{2\alpha_s C_F}{\pi} \ln \frac{4\pi e^{-\gamma_E} \mu_R^2}{\Delta_{UV}}. \quad (8.11)$$

Let us now turn to the real NLO corrections that contributed to the DGLAP evolution of the incoming quark (6.22). Keeping only the high-energy logarithms, we find:

$$\lim_{k^+ \rightarrow 0} d\sigma_{IS} = d\sigma_{LO} \times \ln \frac{k_f^+}{k_{\min}^+} \times \frac{\alpha_s C_F}{\pi} \ln \frac{e^{-\gamma_E}}{\mu_R^2 \pi (\mathbf{x} - \mathbf{x}')^2}. \quad (8.12)$$

irrespective of the polarization of the photon.

Finally, there are leftover rapidity logarithms after the cancellation of collinear divergences in the final state by the jet algorithm (7.21), namely:

$$\lim_{k^+ \rightarrow 0} d\sigma_{\text{jet}} = d\sigma_{LO} \times \ln \frac{k_f^+}{k_{\min}^+} \times \frac{\alpha_s C_F}{\pi} \ln \frac{c_0}{2\pi \mu_R^2 (\mathbf{x} - \mathbf{x}')^2}. \quad (8.13)$$

Adding (8.10) or (8.11) to (8.12) and (8.13), we obtain both for transverse and longitudinally polarized photons:

$$\lim_{k^+ \rightarrow 0} \left(d\sigma_{UV} + d\sigma_{IS} + d\sigma_{\text{jet}} \right) = d\sigma_{LO} \times \ln \frac{k_f^+}{k_{\min}^+} \times \frac{2\alpha_s C_F}{\pi} \ln \frac{c_0^2}{\Delta_{UV} (\mathbf{x} - \mathbf{x}')^2}. \quad (8.14)$$

It is worth remarking that, in the above result, the arbitrary scale μ_R stemming from the quark field-strength renormalization has cancelled. This is not surprising, since eq. (8.14) contains all contributions (UV, IS, FS and their conjugates) from the one-loop result for \mathcal{Z} (3.114), which is itself independent from μ_R .

8.2 Virtual contributions

We will show in the following section (see eq. (9.17)) that, although individually they are divergent in the limit of vanishing gluon plus-momentum, the sums of the UV-subtracted amplitudes $\tilde{\mathcal{M}}_{SE1,\text{sub}}^{0,\lambda} + \tilde{\mathcal{M}}_{V1,\text{sub}}^{0,\lambda}$ and $\tilde{\mathcal{M}}_{SE4,\text{sub}}^{0,\lambda} + \tilde{\mathcal{M}}_{V4,\text{sub}}^{0,\lambda}$ do not contribute any rapidity logarithms to the cross section, nor is there any dependence on the factorization scale k_f^+ . Moreover, the high-energy logarithms stemming from the field-strength renormalization diagrams (3.114) were already taken into account in the previous subsection. It is, then,

very easy to see that the only virtual diagrams left with a high-energy logarithm are the subtracted diagrams $\tilde{\mathcal{M}}_{\text{SE2,sub}}^{0,\lambda}$ in eqs. (3.14) and (3.15), and $\tilde{\mathcal{M}}_{\text{SE3,sub}}^{0,\lambda}$ in eqs. (3.20) and (3.21). Indeed, using that in the limit $k^+ \rightarrow 0$ the Dirac structure (3.3) becomes:

$$\lim_{k^+ \rightarrow 0} \mathcal{S}_{\text{SE}}^{\bar{\eta}\eta'}(p_0^+) = -4 \left(\frac{p_0^+}{k^+} \right)^2 \delta^{\bar{\eta}\eta'}, \quad (8.15)$$

we obtain

$$\begin{aligned} \lim_{k^+ \rightarrow 0} \tilde{\mathcal{M}}_{\text{SE2,sub}}^0 &= 4\alpha_s \frac{1}{M} \frac{p_0^+ \mathbf{P}_\perp^2 - p_1^+ M^2}{p_0^+ \mathbf{P}_\perp^2 + p_1^+ M^2} \int_{k_{\min}^+}^{p_0^+} \frac{dk^+}{k^+} \\ &\times \int_{\mathbf{x}} e^{-i\mathbf{k}_\perp \cdot \mathbf{x}} \left[\int_{\mathbf{z}} A^i(\mathbf{x} - \mathbf{z}) A^i(\mathbf{x} - \mathbf{z}) (t^c U_{\mathbf{x}} U_{\mathbf{z}}^\dagger t^c U_{\mathbf{z}} - C_F) \right. \\ &\left. - \mathcal{A}_0(\Delta_{UV}) C_F (U_{\mathbf{x}} - 1) \right], \end{aligned} \quad (8.16)$$

and:

$$\begin{aligned} \lim_{k^+ \rightarrow 0} \tilde{\mathcal{M}}_{\text{SE2,sub}}^\lambda &= -4\alpha_s \frac{q^+ \mathbf{P}_\perp^{\bar{\lambda}}}{p_0^+ \mathbf{P}_\perp^2 + p_1^+ M^2} \mathcal{S}_{\text{LO}}^{\lambda\bar{\lambda}} \int_{k_{\min}^+}^{p_0^+} \frac{dk^+}{k^+} \\ &\times \int_{\mathbf{x}} e^{-i\mathbf{k}_\perp \cdot \mathbf{x}} \left[\int_{\mathbf{z}} A^i(\mathbf{x} - \mathbf{z}) A^i(\mathbf{x} - \mathbf{z}) (t^c U_{\mathbf{x}} U_{\mathbf{z}}^\dagger t^c U_{\mathbf{z}} - C_F) \right. \\ &\left. - \mathcal{A}_0(\Delta_{UV}) C_F (U_{\mathbf{x}} - 1) \right]. \end{aligned} \quad (8.17)$$

as well as:

$$\begin{aligned} \lim_{k^+ \rightarrow 0} \tilde{\mathcal{M}}_{\text{SE3,sub}}^0 &= -4\alpha_s \frac{p_0^+ \mathbf{q}^2 - p_1^+ M^2}{p_0^+ \mathbf{q}^2 + p_1^+ M^2} \frac{1}{M} \int_{k_{\min}^+}^{p_1^+} \frac{dk^+}{k^+} \\ &\times \int_{\mathbf{x}} e^{-i\mathbf{k}_\perp \cdot \mathbf{x}} \left[\int_{\mathbf{z}} A^i(\mathbf{x} - \mathbf{z}) A^i(\mathbf{x} - \mathbf{z}) (t^c U_{\mathbf{x}} U_{\mathbf{z}}^\dagger t^c U_{\mathbf{z}} - C_F) \right. \\ &\left. - \mathcal{A}_0(\Delta_{UV}) C_F (U_{\mathbf{x}} - 1) \right], \end{aligned} \quad (8.18)$$

and:

$$\begin{aligned} \lim_{k^+ \rightarrow 0} \tilde{\mathcal{M}}_{\text{SE3,sub}}^\lambda &= -4\alpha_s \frac{q^+ \mathbf{q}^{\bar{\lambda}}}{p_0^+ \mathbf{q}^2 + p_1^+ M^2} \mathcal{S}_{\text{LO}}^{\lambda\bar{\lambda}} \int_{k_{\min}^+}^{p_1^+} \frac{dk^+}{k^+} \\ &\times \int_{\mathbf{x}} e^{-i\mathbf{k}_\perp \cdot \mathbf{x}} \left[\int_{\mathbf{z}} A^i(\mathbf{x} - \mathbf{z}) A^i(\mathbf{x} - \mathbf{z}) (t^c U_{\mathbf{x}} U_{\mathbf{z}}^\dagger t^c U_{\mathbf{z}} - C_F) \right. \\ &\left. - \mathcal{A}_0(\Delta_{UV}) C_F (U_{\mathbf{x}} - 1) \right]. \end{aligned} \quad (8.19)$$

Cutting off the logarithmic integral over k^+ at the rapidity factorization scale k_f^+ , the above amplitudes contribute as follows to the cross section:

$$\begin{aligned} \lim_{k^+ \rightarrow 0} d\sigma_{\text{SE2+3}} &= \frac{d\sigma_{\text{LO}}}{s_{\mathbf{x}\mathbf{x}'} + 1} \times \ln \frac{k_f^+}{k_{\text{min}}^+} \\ &\times 4\alpha_s \left[\frac{1}{2} \int_{\mathbf{z}} \left(A^i(\mathbf{x} - \mathbf{z}) A^i(\mathbf{x} - \mathbf{z}) + A^i(\mathbf{x}' - \mathbf{z}) A^i(\mathbf{x}' - \mathbf{z}) \right) \right. \\ &\left. \times \left(N_c s_{\mathbf{x}\mathbf{z}} s_{\mathbf{z}\mathbf{x}'} - \frac{1}{N_c} s_{\mathbf{x}\mathbf{x}'} + 2C_F \right) - \mathcal{A}_0(\Delta_{\text{UV}}) 2C_F (s_{\mathbf{x}\mathbf{x}'} + 1) \right]. \end{aligned} \quad (8.20)$$

8.3 Real contributions

The real contributions to JIMWLK that were not yet taken into account in subsection 8.1 stem from the interferences between the initial-state radiation amplitudes \mathcal{M}_{IS1} and \mathcal{M}_{IS3} (5.2), (5.3), (5.7), and (5.8) on the one hand, and the final-state amplitudes \mathcal{M}_{FS1} and \mathcal{M}_{FS3} (5.15), (5.16), (5.22) and (5.23) on the other.

One obtains in the longitudinal case:

$$\begin{aligned} \lim_{k^+ \rightarrow 0} \tilde{\mathcal{M}}_{\text{IS1+3}}^{0\eta} &= -\frac{2}{M} \left(\frac{p_0^+ \mathbf{P}_\perp^2 - p_1^+ M^2}{p_0^+ \mathbf{P}_\perp^2 + p_1^+ M^2} - \frac{p_0^+ \mathbf{q}^2 - p_1^+ M^2}{p_0^+ \mathbf{q}^2 + p_1^+ M^2} \right) \\ &\times \int_{\mathbf{x}, \mathbf{z}} iA^\eta(\mathbf{x} - \mathbf{z}) e^{-i\mathbf{k}_\perp \cdot \mathbf{x}} e^{-i\mathbf{p}_3 \cdot \mathbf{z}} (U_{\mathbf{x}} U_{\mathbf{z}}^\dagger t^c U_{\mathbf{z}} - t^c), \end{aligned} \quad (8.21)$$

and

$$\begin{aligned} \lim_{k^+ \rightarrow 0} \tilde{\mathcal{M}}_{\text{FS1+3}}^{0\eta} &= \frac{2}{M} \left(\frac{p_0^+ \mathbf{P}_\perp^2 - p_1^+ M^2}{p_0^+ \mathbf{P}_\perp^2 + p_1^+ M^2} - \frac{p_0^+ \mathbf{q}^2 - p_1^+ M^2}{p_0^+ \mathbf{q}^2 + p_1^+ M^2} \right) \\ &\times \int_{\mathbf{x}, \mathbf{z}} e^{-i\mathbf{p}_3 \cdot \mathbf{z}} e^{-i\mathbf{k}_\perp \cdot \mathbf{x}} iA^\eta(\mathbf{x} - \mathbf{z}) t^c (U_{\mathbf{x}} - 1). \end{aligned} \quad (8.22)$$

Similarly, when the photon is transversely polarized:

$$\begin{aligned} \lim_{k^+ \rightarrow 0} \tilde{\mathcal{M}}_{\text{IS1+3}}^{\lambda\eta} &= 2\mathcal{S}^{\lambda\bar{\lambda}} \left(1 + 2\frac{p_1^+}{q^+} \right) \left(\frac{q^+ \mathbf{P}_\perp^{\bar{\lambda}}}{p_0^+ \mathbf{P}_\perp^2 + p_1^+ M^2} + \frac{q^+ \mathbf{q}^{\bar{\lambda}}}{p_0^+ \mathbf{q}^2 + p_1^+ M^2} \right) \\ &\times \int_{\mathbf{x}, \mathbf{z}} iA^\eta(\mathbf{x} - \mathbf{z}) e^{-i\mathbf{k}_\perp \cdot \mathbf{x}} e^{-i\mathbf{p}_3 \cdot \mathbf{z}} (U_{\mathbf{x}} U_{\mathbf{z}}^\dagger t^c U_{\mathbf{z}} - t^c), \end{aligned} \quad (8.23)$$

$$\begin{aligned} \lim_{k^+ \rightarrow 0} \tilde{\mathcal{M}}_{\text{FS1+3}}^{\lambda\eta} &= -2\mathcal{S}^{\lambda\bar{\lambda}} \left(1 + \frac{2p_1^+}{q^+} \right) \left(\frac{q^+ \mathbf{P}_\perp^{\bar{\lambda}}}{p_0^+ \mathbf{P}_\perp^2 + p_1^+ M^2} + \frac{q^+ \mathbf{q}^{\bar{\lambda}}}{p_0^+ \mathbf{q}^2 + p_1^+ M^2} \right) \\ &\times \int_{\mathbf{x}, \mathbf{z}} e^{-i\mathbf{p}_3 \cdot \mathbf{z}} e^{-i\mathbf{k}_\perp \cdot \mathbf{x}} iA^\eta(\mathbf{x} - \mathbf{z}) t^c (U_{\mathbf{x}} - 1). \end{aligned} \quad (8.24)$$

On the level of the cross section, the interference term due to the above amplitudes is, independently of the photon polarization:

$$\begin{aligned} \lim_{k^+ \rightarrow 0} d\sigma_{\text{IS-FS}} &= \frac{d\sigma_{\text{LO}}}{s_{\mathbf{x}\mathbf{x}'} + 1} \times \ln \frac{k_f^+}{k_{\text{min}}^+} \times 4\alpha_s \int_{\mathbf{z}} A^i(\mathbf{x} - \mathbf{z}) A^i(\mathbf{x}' - \mathbf{z}) \\ &\times \left(\frac{1}{N_c} s_{\mathbf{x}\mathbf{x}'} - N_c s_{\mathbf{x}\mathbf{z}} s_{\mathbf{z}\mathbf{x}'} - 2C_F \right). \end{aligned} \quad (8.25)$$

8.4 JIMWLK

We can now, finally, add the intermediate results (8.14), (8.20), and (8.25):

$$\begin{aligned}
 & \lim_{k^+ \rightarrow 0} \left(d\sigma_{UV} + d\sigma_{IS} + d\sigma_{\text{jet}} + d\sigma_{\text{SE2+3}} + d\sigma_{\text{IS-FS}} \right) \\
 &= \frac{d\sigma_{\text{LO}}}{s_{\mathbf{x}\mathbf{x}'} + 1} \times \ln \frac{k_f^+}{k_{\text{min}}^+} \times 4\alpha_s \left[\frac{1}{2} \int_{\mathbf{z}} \left(A^i(\mathbf{x} - \mathbf{z}) A^i(\mathbf{x} - \mathbf{z}) + A^i(\mathbf{x}' - \mathbf{z}) A^i(\mathbf{x}' - \mathbf{z}) \right) \right. \\
 & \quad \times \left(N_c s_{\mathbf{x}\mathbf{z}} s_{\mathbf{z}\mathbf{x}'} - \frac{1}{N_c} s_{\mathbf{x}\mathbf{x}'} + 2C_F \right) \\
 & \quad + \int_{\mathbf{z}} A^i(\mathbf{x} - \mathbf{z}) A^i(\mathbf{x}' - \mathbf{z}) \left(\frac{1}{N_c} s_{\mathbf{x}\mathbf{x}'} - N_c s_{\mathbf{x}\mathbf{z}} s_{\mathbf{z}\mathbf{x}'} - 2C_F \right) \\
 & \quad \left. + \left(\frac{1}{4\pi} \ln \frac{c_0^2}{\Delta_{UV}(\mathbf{x} - \mathbf{x}')^2} - \mathcal{A}_0(\Delta_{UV}) \right) 2C_F (s_{\mathbf{x}\mathbf{x}'} + 1) \right]. \tag{8.26}
 \end{aligned}$$

The terms in the last line of the above expression can be combined into:

$$\begin{aligned}
 \frac{1}{4\pi} \ln \frac{c_0^2}{\Delta_{UV}(\mathbf{x} - \mathbf{x}')^2} - \mathcal{A}_0(\Delta_{UV}) &= -\frac{1}{4\pi} \left(\frac{1}{\epsilon_{UV}} - \gamma_E + \ln \frac{4\pi\mu^2}{\Delta_{UV}} - \ln \frac{c_0^2}{\Delta_{UV}(\mathbf{x} - \mathbf{x}')^2} \right), \\
 &= -\frac{1}{4\pi} \left(\frac{1}{\epsilon_{UV}} + \gamma_E + \ln \pi\mu^2(\mathbf{x} - \mathbf{x}')^2 \right), \tag{8.27}
 \end{aligned}$$

where we used the expansion (A.8) of \mathcal{A}_0 . But in this result one recognizes:

$$\begin{aligned}
 & -\frac{1}{4\pi} \left(\frac{1}{\epsilon_{UV}} + \gamma_E + \ln \pi\mu^2(\mathbf{x} - \mathbf{x}')^2 \right) \\
 &= \int_{\ell} \frac{e^{-i\ell \cdot (\mathbf{x} - \mathbf{x}')}}{\ell^2} = \int_{\mathbf{z}} A^i(\mathbf{x} - \mathbf{z}) A^i(\mathbf{x}' - \mathbf{z}), \tag{8.28}
 \end{aligned}$$

such that

$$\begin{aligned}
 & \lim_{k^+ \rightarrow 0} \left(d\sigma_{UV} + d\sigma_{IS} + d\sigma_{\text{jet}} + d\sigma_{\text{SE2+3}} + d\sigma_{\text{IS-FS}} \right) \\
 &= \frac{d\sigma_{\text{LO}}}{s_{\mathbf{x}\mathbf{x}'} + 1} \times \ln \frac{k_f^+}{k_{\text{min}}^+} \times 4\alpha_s \left[\frac{1}{2} \int_{\mathbf{z}} \left(A^i(\mathbf{x} - \mathbf{z}) A^i(\mathbf{x} - \mathbf{z}) + A^i(\mathbf{x}' - \mathbf{z}) A^i(\mathbf{x}' - \mathbf{z}) \right) \right. \\
 & \quad \left. \times \left(N_c s_{\mathbf{x}\mathbf{z}} s_{\mathbf{z}\mathbf{x}'} - \frac{1}{N_c} s_{\mathbf{x}\mathbf{x}'} + 2C_F \right) + \int_{\mathbf{z}} A^i(\mathbf{x} - \mathbf{z}) A^i(\mathbf{x}' - \mathbf{z}) N_c (s_{\mathbf{x}\mathbf{x}'} - s_{\mathbf{x}\mathbf{z}} s_{\mathbf{z}\mathbf{x}'}) \right]. \tag{8.29}
 \end{aligned}$$

Setting $\mathbf{x} = \mathbf{x}'$ in (8.28), we obtain a scaleless integral which in dimensional regularization is, of course, equal to zero:

$$\int_{\mathbf{z}} A^i(\mathbf{x} - \mathbf{z}) A^i(\mathbf{x} - \mathbf{z}) = \int_{\ell} \frac{1}{\ell^2} = 0. \tag{8.30}$$

We are, therefore, allowed to subtract from (8.29) the following vanishing contribution:

$$\int_{\mathbf{z}} \left(A^i(\mathbf{x} - \mathbf{z}) A^i(\mathbf{x} - \mathbf{z}) + A^i(\mathbf{x}' - \mathbf{z}) A^i(\mathbf{x}' - \mathbf{z}) \right) C_F (s_{\mathbf{x}\mathbf{x}'} + 1) = 0, \tag{8.31}$$

which gives:

$$\begin{aligned}
 & \lim_{k^+ \rightarrow 0} \left(d\sigma_{UV} + d\sigma_{IS} + d\sigma_{\text{jet}} + d\sigma_{\text{SE2+3}} + d\sigma_{\text{IS-FS}} \right) \\
 &= \frac{d\sigma_{\text{LO}}}{s_{\mathbf{x}\mathbf{x}'} + 1} \times \ln \frac{k_f^+}{k_{\text{min}}^+} (s_{\mathbf{x}\mathbf{x}'} - s_{\mathbf{x}\mathbf{z}} s_{\mathbf{z}\mathbf{x}'}) \\
 & \quad \times 4\alpha_s N_c \int_{\mathbf{z}} \left(A^i(\mathbf{x} - \mathbf{z}) A^i(\mathbf{x}' - \mathbf{z}) - \frac{1}{2} A^i(\mathbf{x} - \mathbf{z}) A^i(\mathbf{x} - \mathbf{z}) - \frac{1}{2} A^i(\mathbf{x}' - \mathbf{z}) A^i(\mathbf{x}' - \mathbf{z}) \right). \tag{8.32}
 \end{aligned}$$

The final step is to recognize the integration over Weizsäcker-Williams fields, in the last line, as the BK kernel:

$$\begin{aligned} & \int_{\mathbf{z}} \left(A^i(\mathbf{x} - \mathbf{z}) A^i(\mathbf{x}' - \mathbf{z}) - \frac{1}{2} A^i(\mathbf{x} - \mathbf{z}) A^i(\mathbf{x} - \mathbf{z}) - \frac{1}{2} A^i(\mathbf{x}' - \mathbf{z}) A^i(\mathbf{x}' - \mathbf{z}) \right) \\ &= -\frac{1}{8\pi^2} \int_{\mathbf{z}} \frac{(\mathbf{x} - \mathbf{x}')^2}{(\mathbf{x} - \mathbf{z})^2 (\mathbf{x}' - \mathbf{z})^2}, \end{aligned} \quad (8.33)$$

such that we recover the JIMWLK evolution of a dipole (8.8):

$$\begin{aligned} & \lim_{k^+ \rightarrow 0} \left(d\sigma_{UV} + d\sigma_{IS} + d\sigma_{\text{jet}} + d\sigma_{\text{SE2+3}} + d\sigma_{\text{IS-FS}} \right) \\ &= \frac{d\sigma_{\text{LO}}}{s_{\mathbf{x}\mathbf{x}'} + 1} \times \ln \frac{k_f^+}{k_{\text{min}}^+} \times -\frac{\alpha_s N_c}{2\pi^2} \int_{\mathbf{z}} \frac{(\mathbf{x} - \mathbf{x}')^2}{(\mathbf{x} - \mathbf{z})^2 (\mathbf{x}' - \mathbf{z})^2} (s_{\mathbf{x}\mathbf{x}'} - s_{\mathbf{x}\mathbf{z}} s_{\mathbf{z}\mathbf{x}'}) \\ &= \ln \frac{k_f^+}{k_{\text{min}}^+} \times \hat{H}_{\text{JIMWLK}} d\sigma_{\text{LO}}. \end{aligned} \quad (8.34)$$

Hence, we have proven the validity of eq. (8.2), namely that all the rapidity-divergent NLO contributions combine into the JIMWLK Hamiltonian acting on the LO cross section. Therefore, they can be subtracted and absorbed into the JIMWLK evolution of the latter, according to eq. (8.7).

Some subtleties. We have asserted in subsection 8.3 that only interferences between initial- and final-state gluon emissions needed to be calculated, the other contributions to JIMWLK from real NLO corrections already being accounted for in subsection 8.1. Let us take a closer look at this statement.

First, the squared amplitudes $|\mathcal{M}_{\text{IS1}}|^2$ and $|\mathcal{M}_{\text{FS3}}|^2$ cause collinear initial- and final state divergences when integrating over the gluon momentum. Therefore, we have separately analyzed them in sections 6 and 7 in the context of DGLAP and the jet definition, respectively, and showed how these collinear poles cancel. The leftovers of these procedures still contain rapidity divergences that are, indeed, taken into account via eq. (8.14).

More subtle, however, are the cases of squared amplitudes $|\mathcal{M}_{\text{IS3}}|^2$ and $|\mathcal{M}_{\text{FS1}}|^2$, as well as the interference terms $2\text{Re}\mathcal{M}_{\text{IS1}}^\dagger \mathcal{M}_{\text{IS3}}$ and $2\text{Re}\mathcal{M}_{\text{FS1}}^\dagger \mathcal{M}_{\text{FS3}}$. They do not contribute to DGLAP or to the jet function and hence are not taken into account in subsection 8.1. Moreover, at first sight they seem to be missing from (8.34). To solve this puzzle, we should revisit sections 6 and 7, where we were not able to evaluate the transverse integrations in amplitudes \mathcal{M}_{IS2} and \mathcal{M}_{FS2} exactly and, instead, devised an approximation to extract their collinear behavior. For definiteness, let us look again at amplitude $\tilde{\mathcal{M}}_{\text{IS2}}^0$ (the other cases are similar):

$$\begin{aligned} \tilde{\mathcal{M}}_{\text{IS2}}^{0\eta} &= \frac{1}{M} \mathcal{S}^{\eta\bar{\eta}} \left(1 + \frac{2p_0^+}{p_3^+} \right) \frac{p_3^+}{p_{0R}^+} \\ &\times \int_{\ell} \frac{\ell^{\bar{\eta}}}{\ell^2} \frac{p_3^+ (q^+ \ell + p_0^+ \mathbf{q})^2 - p_1^+ p_3^+ p_0^+ M^2}{p_3^+ (q^+ \ell + p_0^+ \mathbf{q})^2 + p_1^+ q^+ p_{0R}^+ \ell^2 + p_1^+ p_3^+ p_0^+ M^2} \\ &\times \int_{\mathbf{x}, \mathbf{z}} e^{-i\ell \cdot (\mathbf{x} - \mathbf{z})} e^{-i\mathbf{k}_\perp \cdot \mathbf{x}} e^{-i\mathbf{p}_3 \cdot \mathbf{z}} (U_{\mathbf{x}} U_{\mathbf{z}}^\dagger t^c U_{\mathbf{z}} - t^c). \end{aligned} \quad (8.35)$$

Clearly, this amplitude will not lead to rapidity divergences, since it disappears in the limit $p_3^+ \rightarrow 0$. Introducing the transformation $\ell = p_3^+ / q^+ \tilde{\ell}$ and only then taking the limit $p_3^+ \rightarrow 0$ allows us to study the kinematics where all components of the gluon momentum tend to zero simultaneously (the ‘genuine soft’ limit $\vec{p}_3 \rightarrow 0$, see e.g., [50]):

$$\begin{aligned} \lim_{\vec{p}_3 \rightarrow 0} \tilde{\mathcal{M}}_{\text{IS2}}^{0\eta} &= \lim_{p_3^+ \rightarrow 0} \frac{1}{M} \mathcal{S}^{\eta\bar{\eta}} \left(1 + \frac{2p_0^+}{p_3^+} \right) \frac{p_3^+}{p_{0R}^+} \\ &\times \int_{\tilde{\ell}} \frac{\tilde{\ell}^{\bar{\eta}} p_3^+}{\tilde{\ell}^2 q^+} \frac{(p_3^+ \tilde{\ell} + p_0^+ \mathbf{q})^2 - p_1^+ p_0^+ M^2}{(p_3^+ \tilde{\ell} + p_0^+ \mathbf{q})^2 + p_1^+ p_3^+ p_{0R}^+ \tilde{\ell}^2 / q^+ + p_1^+ p_0^+ M^2} \\ &\times \int_{\mathbf{x}, \mathbf{z}} e^{-i \frac{p_3^+}{q^+} \tilde{\ell} \cdot (\mathbf{x} - \mathbf{z})} e^{-i \mathbf{k}_\perp \cdot \mathbf{x}} e^{-i \mathbf{p}_3 \cdot \mathbf{z}} (U_{\mathbf{x}} U_{\mathbf{z}}^\dagger t^c U_{\mathbf{z}} - t^c) = 0. \end{aligned} \quad (8.36)$$

It follows that $\tilde{\mathcal{M}}_{\text{IS2}}^0$ cannot generate logarithmic divergences of the form $\ln p^+ / k_{\min}^+$: neither rapidity ones, nor genuine soft ones. However, in the approximation (6.3), we have set $\ell \rightarrow 0$ inside the integrand to extract the collinear behavior:

$$\begin{aligned} \tilde{\mathcal{M}}_{\text{IS2}}^{0\eta} \Big|_{\text{coll.}} &= \frac{1}{M} \frac{p_0^+ \mathbf{q}^2 - p_1^+ M^2}{p_0^+ \mathbf{q}^2 + p_1^+ M^2} \mathcal{S}^{\eta\bar{\eta}} \left(1 + \frac{2p_0^+}{p_3^+} \right) \frac{p_3^+}{p_{0R}^+} \\ &\times \int_{\mathbf{x}, \mathbf{z}} \int_{\ell} \frac{\ell^{\bar{\eta}}}{\ell^2} e^{-i \ell \cdot (\mathbf{x} - \mathbf{z})} e^{-i \mathbf{k}_\perp \cdot \mathbf{x}} e^{-i \mathbf{p}_3 \cdot \mathbf{z}} (U_{\mathbf{x}} U_{\mathbf{z}}^\dagger t^c U_{\mathbf{z}} - t^c). \end{aligned} \quad (8.37)$$

But the above expression *does* lead to a rapidity divergence, in particular, exactly the same as the one from amplitude $\mathcal{M}_{\text{IS3}}^{0\eta}$:

$$\lim_{p_3^+ \rightarrow 0} \mathcal{M}_{\text{IS2}}^{0\eta} \Big|_{\text{coll.}} = \lim_{p_3^+ \rightarrow 0} \mathcal{M}_{\text{IS3}}^{0\eta}. \quad (8.38)$$

Thus, the reason that, in section 8.3, we only need to consider the interference terms $\mathcal{M}_{\text{IS1+3}}^\dagger \mathcal{M}_{\text{FS1+3}} + \text{c.c.}$, is because all the rapidity divergences from $|\mathcal{M}_{\text{IS1+3}}|^2$ and $|\mathcal{M}_{\text{FS1+3}}|^2$ are accounted for in eq. (8.14). The rapidity-divergent squared amplitudes $|\mathcal{M}_{\text{IS1}}|^2$ and $|\mathcal{M}_{\text{FS3}}|^2$ contribute directly, while the contributions from the others, namely $|\mathcal{M}_{\text{IS3}}|^2$, $|\mathcal{M}_{\text{FS1}}|^2$, $\mathcal{M}_{\text{IS1}}^\dagger \mathcal{M}_{\text{IS3}}$, and $\mathcal{M}_{\text{FS1}}^\dagger \mathcal{M}_{\text{FS3}}$ are *mimicked* by the artificially large logarithmic terms in $|\mathcal{M}_{\text{IS2}}|^2 \Big|_{\text{coll.}}$, $|\mathcal{M}_{\text{FS2}}|^2 \Big|_{\text{coll.}}$, $\mathcal{M}_{\text{IS1}}^\dagger \mathcal{M}_{\text{IS2}} \Big|_{\text{coll.}}$, and $\mathcal{M}_{\text{FS1}}^\dagger \mathcal{M}_{\text{FS2}} \Big|_{\text{coll.}}$.

9 Next-to-leading order cross section

We are now ready to present the full NLO cross section for our process. It is given by the following sum of separately finite contributions:

$$d\sigma_{\text{LO+NLO}}^{pA \rightarrow \gamma^* + \text{jet} + X} = d\sigma_{\text{LO+DGLAP+JIMWLK}} + d\sigma_{\text{jet}} + d\sigma_{\text{IS}} + d\sigma_{\text{virtual}} + d\sigma_{\text{real}}. \quad (9.1)$$

The first part of the cross section 9.1 is the leading-order one, eq. (2.46), where the quark PDF is evolved at least one step with DGLAP (6.21), and where the target average of the dipole is evolved at least one step with JIMWLK (8.6). For all the other terms, it is understood that the subtraction of high-energy leading logarithms has been performed according to (8.7) in the previous section.

The term $d\sigma_{\text{jet}}$ (7.21), after performing the rapidity subtraction, reads:

$$d\sigma_{\text{jet}} = d\sigma_{\text{LO, jet}} \frac{\alpha_s C_F}{\pi} \left[\frac{3}{4} \ln \left(\frac{4\pi e^{-\gamma_E} \mu_R^2}{\mathbf{p}_j^2 R^2} \right) + \frac{13}{4} - \frac{\pi^2}{3} + \ln \frac{p_j^+}{k_f^+} \ln \frac{c_0}{2\pi \mu_R^2 (\mathbf{x} - \mathbf{x}')^2} \right]. \quad (9.2)$$

As explained in section 7, all scenarios in which the quark and gluon are paired in the same jet are taken into account by the above contribution. Therefore, in the remaining terms of eq. (9.1) we should always identify the quark momentum with the one of the jet.

The contribution to $d\sigma_{\text{IS}}$ is obtained after subtracting the large high-energy logarithm from (6.23):

$$\begin{aligned} d\sigma_{\text{IS}} &= \frac{1}{2(p_0^+)^2} \int \text{PS}(\vec{p}_1, \vec{q}) \frac{1}{2} \langle |\mathcal{M}_{\text{LO}}|^2 \rangle \\ &\times \alpha_s \left[\ln \frac{c_0^2}{\mu^2 (\mathbf{x} - \mathbf{x}')^2} \int_{x_p}^1 d\xi P_{qq}^{(0)}(\xi) \frac{x_p}{\xi} f_q^{(0)} \left(\frac{x_p}{\xi} \right) \right. \\ &\left. + C_F \left(\ln \frac{e^{-\gamma_E}}{\mu_R^2 \pi (\mathbf{x} - \mathbf{x}')^2} \right) \left(-\frac{3}{2} + 2 \ln \frac{p_0^+}{k_f^+} \right) x_p f_q^{(0)}(x_p) \right] \Big|_{\vec{p}_1 = \vec{p}_j}. \end{aligned} \quad (9.3)$$

The term $d\sigma_{\text{virtual}}$, the finite leftovers of the virtual diagrams are collected after cancelling the UV divergences, and after absorbing the collinear divergences inside the jet definition and the DGLAP evolution. Moreover, the rapidity subtraction procedure has been performed explicitly, hence a residual dependence on the rapidity factorization scale k_f^+ is left. The result reads, for the longitudinally polarized virtual photon:

$$\begin{aligned} d\sigma_{\text{virtual}}^{\text{L}} &= x_p f_q^{(0)}(x_p) \frac{2\pi}{2(p_0^+)^2} \text{PS}(\vec{p}_1, \vec{q}) \frac{1}{2} \\ &\times \text{Tr} \left\langle \mathcal{M}_{\text{LO}}^{0\dagger} \left[\mathcal{M}_{\text{SE1,sub}}^0 \Big|_{\text{finite}} + \mathcal{M}_{\text{SE2,sub}}^0 + \mathcal{M}_{\text{SE3,sub}}^0 + \mathcal{M}_{\text{SE4,sub}}^0 \Big|_{\text{finite}} \right. \right. \\ &+ \left(\mathcal{M}_{\text{SE1,sub}}^0 + \mathcal{M}_{\text{V1,sub}}^0 \right) \Big|_{1/k^+} + \mathcal{M}_{\text{V1,sub}}^0 \Big|_{\text{finite}} + \mathcal{M}_{\text{V2,sub}}^0 \Big|_{\text{finite}} \\ &+ \mathcal{M}_{\text{V3,sub}}^0 + \mathcal{M}_{\text{V4,sub}}^0 + \mathcal{M}_{\text{A1,sub}}^0 \Big|_{\text{finite}} + \mathcal{M}_{\text{A2,sub}}^0 \Big|_{\text{finite}} \\ &+ \left(\mathcal{M}_{\text{V1,sub}}^0 + \mathcal{M}_{\text{A1,sub}}^0 \right) \Big|_{\text{spurious}} + \left(\mathcal{M}_{\text{V2,sub}}^0 + \mathcal{M}_{\text{A2,sub}}^0 \right) \Big|_{\text{spurious}} \\ &+ \mathcal{M}_{\text{A3,sub}}^0 + \mathcal{M}_{\text{A4,sub}}^0 + \mathcal{M}_{\text{Q1,sub}}^0 + \mathcal{M}_{\text{Q2,sub}}^0 + \mathcal{M}_{\text{Q3,sub}}^0 \\ &\left. + \mathcal{M}_{\text{I1,sub}}^0 + \mathcal{M}_{\text{I2,sub}}^0 + \mathcal{M}_{\text{I3,sub}}^0 + \mathcal{M}_{\text{I4,sub}}^0 \right] + \text{c.c.} \Big|_{\vec{p}_1 = \vec{p}_j}. \end{aligned} \quad (9.4)$$

The explicit expressions for the different contributions are presented in subsection 9.1.1. In the transversely polarized case, the ‘virtual’ cross section is given by:

$$\begin{aligned} d\sigma_{\text{virtual}}^{\text{T}} &= x_p f_q^{(0)}(x_p) \frac{2\pi}{2(p_0^+)^2} \text{PS}(\vec{p}_1, \vec{q}) \frac{1}{2} \\ &\times \text{Tr} \left\langle \mathcal{M}_{\text{LO}}^{\lambda\dagger} \left[\mathcal{M}_{\text{SE1,sub}}^\lambda \Big|_{\text{finite}} + \mathcal{M}_{\text{SE2,sub}}^\lambda + \mathcal{M}_{\text{SE3,sub}}^\lambda + \mathcal{M}_{\text{SE4,sub}}^\lambda \Big|_{\text{finite}} \right. \right. \\ &+ \left(\mathcal{M}_{\text{SE1,sub}}^\lambda + \mathcal{M}_{\text{V1,sub}}^\lambda \right) \Big|_{1/k^+} + \mathcal{M}_{\text{V1,sub}}^\lambda \Big|_{\text{finite}} \\ &+ \mathcal{M}_{\text{V2}}^\lambda + \mathcal{M}_{\text{V3}}^\lambda + \mathcal{M}_{\text{V4,sub}}^\lambda \Big|_{\text{finite}} + \mathcal{M}_{\text{A1,sub}}^\lambda + \mathcal{M}_{\text{A2}}^\lambda + \mathcal{M}_{\text{A3}}^\lambda + \mathcal{M}_{\text{A4,sub}}^\lambda \\ &\left. + \mathcal{M}_{\text{Q2}}^\lambda + \mathcal{M}_{\text{I2}}^\lambda + \mathcal{M}_{\text{I3}}^\lambda \right] + \text{c.c.} \Big|_{\vec{p}_1 = \vec{p}_j}, \end{aligned} \quad (9.5)$$

where the expressions for the various terms are listed in subsection 9.1.2.

The last term in eq. (9.1), $d\sigma_{\text{real}}$, collects those contributions from real radiative corrections that were not yet absorbed into $d\sigma_{\text{jet}}$ or $d\sigma_{\text{IS}}$, and has the same structure irregardless of the photon polarization, which is why the polarization labels are omitted:

$$\begin{aligned}
 d\sigma_{\text{real}} = & x_{pR} f_q^{(0)}(x_{pR}) \frac{2\pi}{2(p_1^+ + q^+ + p_3^+)^2} \text{PS}(\vec{p}_1, \vec{q}) \int \frac{dp_3^+}{4\pi p_3^+} \frac{1}{2} \\
 & \times \int_{\mathbf{p}_3} \text{Tr} \left\langle \left| \mathcal{M}_{\text{IS2,finite}}^\eta \right|^2 + 2\text{Re}(\mathcal{M}_{\text{IS1}}^{\eta\dagger} \mathcal{M}_{\text{IS2,finite}}^\eta) + 2\text{Re}(\mathcal{M}_{\text{IS2,coll}}^{\eta\dagger} \mathcal{M}_{\text{IS2,finite}}^\eta) \right. \\
 & + \left| \mathcal{M}_{\text{IS3+4}}^\eta \right|^2 + 2\text{Re}(\mathcal{M}_{\text{IS1+2}}^{\eta\dagger} \mathcal{M}_{\text{IS3+4}}^\eta) \\
 & + \left| \mathcal{M}_{\text{FS2+3}}^\eta \right|_{\text{out-soft}}^2 + \left| \mathcal{M}_{\text{FS1+4}}^\eta \right|^2 + 2\text{Re}(\mathcal{M}_{\text{FS2+3}}^{\eta\dagger} \mathcal{M}_{\text{FS1+4}}^\eta) \\
 & \left. + 2\text{Re}(\mathcal{M}_{\text{IS1+2}}^{\eta\dagger} \mathcal{M}_{\text{FS1+4}}^\eta + \mathcal{M}_{\text{IS1+2}}^{\eta\dagger} \mathcal{M}_{\text{FS2+3}}^\eta + \mathcal{M}_{\text{IS3+4}}^{\eta\dagger} \mathcal{M}_{\text{FS1+4}}^\eta + \mathcal{M}_{\text{IS3+4}}^{\eta\dagger} \mathcal{M}_{\text{FS2+3}}^\eta) \right\rangle \Big|_{\vec{p}_1 = \vec{p}_j}. \tag{9.6}
 \end{aligned}$$

The explicit expressions of the terms above are listed in subsections 9.2.1 and 9.2.2 for the longitudinal resp. transversely polarized case. Note that, for the real radiative corrections, the longitudinal momentum fraction of the incoming quark with respect to the proton is $x_{pR} = (p_1^+ + q^+ + p_3^+)/p_p^+$. The requirement $x_{pR} \leq 1$ leads to the upper bound $p_3^+ \leq p_p^+ - p_1^+ - q^+$, which is implicit in all the gluon plus-momentum integrations in 9.2.1 and 9.2.2. Moreover, unless explicitly indicated, p_3^+ can be safely integrated over down to zero.

In the following subsections, we present the results for the different terms in eqs. (9.4), (9.5), and (9.6). It is interesting to remark that, despite the complexity of this calculation, most of the result only depends on two simple sets of color operators, namely:

$$(s_{\mathbf{x}\mathbf{x}'} + 1) \quad \text{and} \quad \left(\frac{N_c^2}{2} s_{\mathbf{x}\mathbf{z}} s_{\mathbf{z}\mathbf{x}'} - \frac{1}{2} s_{\mathbf{x}\mathbf{x}'} + C_F N_c \right). \tag{9.7}$$

The exceptions to this rule are eqs. (9.34), (9.37), (9.61), and (9.63), due to the virtual amplitudes \mathcal{M}_{A3} and \mathcal{M}_{Q2} , which also include a quadrupole:

$$\left(\frac{N_c^2}{2} s_{\mathbf{x}_1\mathbf{x}_2} s_{\mathbf{x}_3\mathbf{x}'} - \frac{1}{2} Q_{\mathbf{x}_1\mathbf{x}'\mathbf{x}_3\mathbf{x}_2} + C_F N_c \right). \tag{9.8}$$

Our result logarithmically depends on three factorization scales, μ^2 , k_f^+ , and μ_R^2 , which should be chosen in such a way that leftover logarithms are small. The first scale, μ^2 , stems from the dimensional renormalization of the ultraviolet- and collinear divergences. The standard approach is to choose it to be equal to the typical hard scale in the process, for instance a combination of the virtuality M^2 of the photon and the transverse-momentum vector \mathbf{P}_\perp^2 . The rapidity factorization scale k_f^+ should be independent of the center-of-mass energy and of the target kinematics [84]. A sensible choice could be $k_f^+ = p_j^+ q^+ / p_0^+$. Finally, μ_R^2 is an artificial scale associated with the quark field-strength renormalization, and can be adjusted at will. A fine choice is $\mu_R^2 = \mu^2 / (4\pi e^{-\gamma_E})$, which leads to some simplifications in $d\sigma_{\text{jet}}$ and $d\sigma_{\text{IS}}$.

9.1 Virtual contributions

9.1.1 Longitudinal polarization

Self-energy corrections. Diagrams $\tilde{\mathcal{M}}_{\text{SE1,sub}}^0$ (3.6) and $\tilde{\mathcal{M}}_{\text{SE4,sub}}^0$ (3.24) can be split up in a finite part and a part that is divergent for $k^+ \rightarrow 0$:

$$\begin{aligned}
 \tilde{\mathcal{M}}_{\text{SE1,sub}}^0 &= \tilde{\mathcal{M}}_{\text{LO1}}^0 \frac{\alpha_s C_F}{\pi} \left[\int_0^{p_0^+} dk^+ \frac{k^+ - 2p_0^+}{2(p_0^+)^2} + \int_{k_{\min}^+}^{p_0^+} \frac{dk^+}{k^+} \right] \ln \frac{\Delta_P}{\Delta_{UV}}, \\
 &= \tilde{\mathcal{M}}_{\text{SE1,sub}}^0 \Big|_{\text{finite}} + \tilde{\mathcal{M}}_{\text{SE1,sub}}^0 \Big|_{1/k^+}, \\
 \tilde{\mathcal{M}}_{\text{SE4,sub}}^0 &= \tilde{\mathcal{M}}_{\text{LO2}}^0 \frac{\alpha_s C_F}{\pi} \left[\int_0^{p_1^+} dk^+ \frac{k^+ - 2p_1^+}{2(p_1^+)^2} + \int_{k_{\min}^+}^{p_1^+} \frac{dk^+}{k^+} \right] \ln \frac{\Delta_q}{\Delta_{UV}}, \\
 &= \tilde{\mathcal{M}}_{\text{SE4,sub}}^0 \Big|_{\text{finite}} + \tilde{\mathcal{M}}_{\text{SE4,sub}}^0 \Big|_{1/k^+}.
 \end{aligned} \tag{9.9}$$

Making use of the following identities (see [85]), valid for $a \geq c > 0$:

$$\begin{aligned}
 \int_0^c dx \ln(x(a-x)) &= -2c + a \ln a - (a-c) \ln(a-c) + c \ln c, \\
 \int_0^c dx x \ln(x(a-x)) &= \frac{1}{2} \left(-c(a+c) + a^2 \ln a + c^2 \ln c + (c^2 - a^2) \ln(a-c) \right),
 \end{aligned} \tag{9.10}$$

the finite integrals over the gluon plus-momentum can be evaluated, yielding:

$$\begin{aligned}
 \tilde{\mathcal{M}}_{\text{SE1,sub}}^0 \Big|_{\text{finite}} &= \tilde{\mathcal{M}}_{\text{LO1}}^0 \frac{\alpha_s C_F}{\pi} \times -\frac{3}{4} \left(-i\pi + 2 \ln \frac{p_0^+}{p_1^+} - 2 + \ln \frac{p_1^+ (p_0^+ \mathbf{P}_\perp^2 + p_1^+ M^2)}{p_0^+ q^+ \Delta_{UV}} \right), \\
 \tilde{\mathcal{M}}_{\text{SE4,sub}}^0 \Big|_{\text{finite}} &= \tilde{\mathcal{M}}_{\text{LO2}}^{0,\lambda} \frac{\alpha_s C_F}{\pi} \times -\frac{3}{4} \left(\ln \frac{p_0^+ \mathbf{q}^2 + p_1^+ M^2}{q^+ \Delta_{UV}} - 2 \right).
 \end{aligned} \tag{9.11}$$

Hence, we obtain the following virtual contributions to the cross section:

$$\begin{aligned}
 \text{Tr } \mathcal{M}_{\text{LO}}^{0\dagger} \mathcal{M}_{\text{SE1,sub}}^0 \Big|_{\text{finite}} &= \text{Tr } (\mathcal{M}_{\text{LO}}^{0\dagger} \mathcal{M}_{\text{LO1}}^0) \frac{\alpha_s C_F}{\pi} \\
 &\quad \times -\frac{3}{4} \left(-i\pi + 2 \ln \frac{p_0^+}{p_1^+} - 2 + \ln \frac{p_1^+ (p_0^+ \mathbf{P}_\perp^2 + p_1^+ M^2)}{p_0^+ q^+ \Delta_{UV}} \right),
 \end{aligned} \tag{9.12}$$

and:

$$\text{Tr } \mathcal{M}_{\text{LO}}^{0\dagger} \mathcal{M}_{\text{SE4,sub}}^0 \Big|_{\text{finite}} = \text{Tr } (\mathcal{M}_{\text{LO}}^{0\dagger} \mathcal{M}_{\text{LO2}}^0) \frac{\alpha_s C_F}{\pi} \times -\frac{3}{4} \left(\ln \frac{p_0^+ \mathbf{q}^2 + p_1^+ M^2}{q^+ \Delta_{UV}} - 2 \right). \tag{9.13}$$

We will show below that the contributions $\tilde{\mathcal{M}}_{\text{SE1,sub}}^0 \Big|_{1/k^+}$ and $\tilde{\mathcal{M}}_{\text{SE4,sub}}^0 \Big|_{1/k^+}$ nicely combine with similar contributions from the vertex corrections. First, let us write down the contributions from the amplitude $\tilde{\mathcal{M}}_{\text{SE2,sub}}^0$ (3.14), which reads after subtracting the high-energy

logarithms and multiplying with the leading-order amplitude:¹⁰

$$\begin{aligned}
 & \text{Tr } \mathcal{M}_{\text{LO}}^{0\dagger} \mathcal{M}_{\text{SE2,sub}}^0 \\
 &= \frac{g_{\text{em}}^2 \alpha_s}{M^2} 8 p_1^+ p_0^+ \left(\frac{p_0^+ \mathbf{P}_\perp^2 - p_1^+ M^2}{p_0^+ \mathbf{P}_\perp^2 + p_1^+ M^2} - \frac{p_0^+ \mathbf{q}^2 - p_1^+ M^2}{p_0^+ \mathbf{q}^2 + p_1^+ M^2} \right) \frac{p_0^+ \mathbf{P}_\perp^2 - p_1^+ M^2}{p_0^+ \mathbf{P}_\perp^2 + p_1^+ M^2} \\
 & \times \int_{\mathbf{x}, \mathbf{x}'} e^{-i \mathbf{k}_\perp \cdot (\mathbf{x} - \mathbf{x}')} \left\{ \int_{k_{\text{min}}^+}^{p_0^+} \frac{dk^+}{k^+} \left(\frac{k^+}{p_0^+} \right)^2 \left(\left(1 - \frac{2p_0^+}{k^+} \right)^2 + 1 \right) \right. \\
 & \times \left[\int_{\mathbf{z}} A^i(\mathbf{x} - \mathbf{z}) A^i(\mathbf{x} - \mathbf{z}, \Delta_{\text{P}}) e^{i \frac{k^+}{p_0^+} \mathbf{k}_\perp \cdot (\mathbf{x} - \mathbf{z})} \left(\frac{N_c^2}{2} s_{\mathbf{xz}} s_{\mathbf{zx}'} - \frac{1}{2} s_{\mathbf{xx}'} + C_F N_c \right) \right. \\
 & \left. \left. - \mathcal{A}_0(\Delta_{\text{UV}}) C_F N_c (s_{\mathbf{xx}'} + 1) \right] \right. \\
 & \left. - 4 \int_{k_{\text{min}}^+}^{k_f^+} \frac{dk^+}{k^+} \left[\int_{\mathbf{z}} A^i(\mathbf{x} - \mathbf{z}) A^i(\mathbf{x} - \mathbf{z}) \left(\frac{N_c^2}{2} s_{\mathbf{xz}} s_{\mathbf{zx}'} - \frac{1}{2} s_{\mathbf{xx}'} + C_F N_c \right) \right. \right. \\
 & \left. \left. - \mathcal{A}_0(\Delta_{\text{UV}}) C_F N_c (s_{\mathbf{xx}'} + 1) \right] \right\}. \tag{9.14}
 \end{aligned}$$

Similarly, $\tilde{\mathcal{M}}_{\text{SE3,sub}}^0$ (3.20) leads to the contribution:

$$\begin{aligned}
 & \text{Tr } \mathcal{M}_{\text{LO}}^{0\dagger} \mathcal{M}_{\text{SE3,sub}}^0 \\
 &= \frac{g_{\text{em}}^2 \alpha_s}{M^2} 8 p_1^+ p_0^+ \left(\frac{p_0^+ \mathbf{P}_\perp^2 - p_1^+ M^2}{p_0^+ \mathbf{P}_\perp^2 + p_1^+ M^2} - \frac{p_0^+ \mathbf{q}^2 - p_1^+ M^2}{p_0^+ \mathbf{q}^2 + p_1^+ M^2} \right) \left(- \frac{p_0^+ \mathbf{q}^2 - p_1^+ M^2}{p_0^+ \mathbf{q}^2 + p_1^+ M^2} \right) \\
 & \times \int_{\mathbf{x}, \mathbf{x}'} e^{-i \mathbf{k}_\perp \cdot (\mathbf{x} - \mathbf{x}')} \left\{ \int_{k_{\text{min}}^+}^{p_1^+} \frac{dk^+}{k^+} \left(\frac{k^+}{p_1^+} \right)^2 \left(\left(1 - \frac{2p_1^+}{k^+} \right)^2 + 1 \right) \right. \\
 & \times \left[\int_{\mathbf{z}} A^i(\mathbf{x} - \mathbf{z}) A^i(\mathbf{x} - \mathbf{z}, \Delta_{\text{q}}) e^{i \frac{k^+}{p_1^+} \mathbf{k}_\perp \cdot (\mathbf{x} - \mathbf{z})} \left(\frac{N_c^2}{2} s_{\mathbf{xz}} s_{\mathbf{zx}'} - \frac{1}{2} s_{\mathbf{xx}'} + C_F N_c \right) \right. \\
 & \left. \left. - \mathcal{A}_0(\Delta_{\text{UV}}) C_F N_c (s_{\mathbf{xx}'} + 1) \right] \right. \\
 & \left. - 4 \int_{k_{\text{min}}^+}^{k_f^+} \frac{dk^+}{k^+} \left[\int_{\mathbf{z}} A^i(\mathbf{x} - \mathbf{z}) A^i(\mathbf{x} - \mathbf{z}) \left(\frac{N_c^2}{2} s_{\mathbf{xz}} s_{\mathbf{zx}'} - \frac{1}{2} s_{\mathbf{xx}'} + C_F N_c \right) \right. \right. \\
 & \left. \left. - \mathcal{A}_0(\Delta_{\text{UV}}) C_F N_c (s_{\mathbf{xx}'} + 1) \right] \right\}. \tag{9.15}
 \end{aligned}$$

Vertex corrections. The parts from $\tilde{\mathcal{M}}_{\text{V1,sub}}^0$ (3.32) and $\tilde{\mathcal{M}}_{\text{V4,sub}}^0$ (3.53) that contain rapidity divergences are:

$$\begin{aligned}
 \mathcal{M}_{\text{V1,sub}}^0 \Big|_{1/k^+} &= \mathcal{M}_{\text{LO1}}^0 \frac{\alpha_s C_F}{\pi} \int_{k_{\text{min}}^+}^{p_1^+} \frac{dk^+}{k^+} \ln \frac{\Delta_{\text{UV}}}{\Delta_{\text{P}}}, \\
 \mathcal{M}_{\text{V4,sub}}^0 \Big|_{1/k^+} &= \mathcal{M}_{\text{LO2}}^0 \frac{\alpha_s C_F}{\pi} \int_{k_{\text{min}}^+}^{p_1^+} \frac{dk^+}{k^+} \ln \frac{\Delta_{\text{UV}}}{\Delta_{\text{q}}}. \tag{9.16}
 \end{aligned}$$

¹⁰Since the high-energy subtraction is explicitly carried out, k_{min}^+ can, in principle, be set to zero in the result below.

When combining them with their counterparts from diagrams SE1 and SE4 (9.9), and multiplying with the leading-order amplitude, we obtain:

$$\begin{aligned} \text{Tr} \mathcal{M}_{\text{LO}}^{0\dagger} \left(\mathcal{M}_{\text{SE4,sub}}^0 + \mathcal{M}_{\text{V4,sub}}^0 \right) \Big|_{1/k^+} &= 0, \\ \text{Tr} \mathcal{M}_{\text{LO}}^{0\dagger} \left(\mathcal{M}_{\text{SE1,sub}}^0 + \mathcal{M}_{\text{V1,sub}}^0 \right) \Big|_{1/k^+} &= \text{Tr} \mathcal{M}_{\text{LO}}^{0\dagger} \mathcal{M}_{\text{LO1}}^0 \frac{\alpha_s C_F}{\pi} \int_{p_1^+}^{p_0^+} \frac{dk^+}{k^+} \ln \frac{\Delta_{\text{P}}}{\Delta_{\text{UV}}}. \end{aligned} \quad (9.17)$$

The plus-momentum integral in the latter expression can be evaluated explicitly, and yields:

$$\begin{aligned} &\text{Tr} \mathcal{M}_{\text{LO}}^{0\dagger} \left(\mathcal{M}_{\text{SE1,sub}}^0 + \mathcal{M}_{\text{V1,sub}}^0 \right) \Big|_{1/k^+} \\ &= \text{Tr} \mathcal{M}_{\text{LO}}^{0\dagger} \mathcal{M}_{\text{LO1}}^0 \frac{\alpha_s C_F}{\pi} \left[\ln \frac{p_0^+}{p_1^+} \left(-i\pi + \ln \frac{p_1^+ (p_0^+ \mathbf{P}_\perp^2 + p_1^+ M^2)}{p_0^+ q^+ \Delta_{\text{UV}}} \right) \right. \\ &\quad \left. + \frac{1}{2} \ln^2 \frac{p_0^+}{p_1^+} + \ln \frac{p_0^+}{p_1^+} \ln \frac{q^+}{p_1^+} - \text{Li}_2 \frac{q^+}{p_0^+} \right], \end{aligned} \quad (9.18)$$

with Li_2 the dilogarithm, and where we used the identity (see [85]):

$$\int_b^c \frac{dx}{x} \ln(x(a-x)) = \frac{1}{2} \ln^2 c - \frac{1}{2} \ln^2 b + \ln a \ln \frac{c}{b} - \text{Li}_2 \frac{c}{a} + \text{Li}_2 \frac{b}{a}. \quad (9.19)$$

Two parts are left of $\tilde{\mathcal{M}}_{\text{V1,sub}}^0$ after subtracting the rapidity-divergent part (9.16), namely:

$$\begin{aligned} &\text{Tr} \mathcal{M}_{\text{LO}}^{0\dagger} \mathcal{M}_{\text{V1,sub}}^0 \Big|_{\text{finite}} \\ &= \text{Tr} \mathcal{M}_{\text{LO}}^{0\dagger} \mathcal{M}_{\text{LO1}}^0 \frac{\alpha_s C_F}{\pi} \left\{ \frac{2p_0^+ + p_1^+}{4p_0^+} \left(-i\pi + \ln \frac{p_1^+ (p_0^+ \mathbf{P}_\perp^2 + p_1^+ M^2)}{p_0^+ q^+ \Delta_{\text{UV}}} \right) \right. \\ &\quad - \frac{3}{4} \frac{p_0^+ + p_1^+}{p_0^+} + \frac{p_0^+ + 2p_1^+}{4p_1^+} \ln \frac{p_0^+}{p_1^+} - \frac{q^+ (p_0^+ + p_1^+)}{4p_1^+ p_0^+} \ln \frac{q^+}{p_1^+} \\ &\quad - \frac{M^2 \mathbf{P}_\perp^2}{p_0^+ \mathbf{P}_\perp^2 - p_1^+ M^2} \int_0^{p_1^+} \frac{dk^+}{k^+} \frac{(k^+)^4}{p_0^+ (p_1^+)^2} \left(\left(2 \frac{p_1^+}{k^+} - 1 \right) \left(2 \frac{p_0^+}{k^+} - 1 \right) + 1 \right) \\ &\quad \left. \times 2\pi \mathcal{B}_1 \left(0, \Delta_{\text{P}}, \frac{k^+}{p_1^+} \mathbf{P}_\perp \right) \right\}, \end{aligned} \quad (9.20)$$

and:

$$\begin{aligned} \text{Tr} \mathcal{M}_{\text{LO}}^{0\dagger} \mathcal{M}_{\text{V1,sub}}^0 \Big|_{\text{spurious}} &= \text{Tr} \mathcal{M}_{\text{LO}}^{0\dagger} \mathcal{M}_{\text{LO1}}^0 \frac{\alpha_s C_F}{4\pi} \frac{p_0^+ \mathbf{P}_\perp^2 + p_1^+ M^2}{p_0^+ \mathbf{P}_\perp^2 - p_1^+ M^2} \\ &\quad \times \int_0^{p_1^+} \frac{dk^+}{k^+} \frac{(k^+)^3 q^+}{(p_0^+)^2 p_1^+ (p_1^+ - k^+)} \left(\left(2 \frac{p_1^+}{k^+} - 1 \right) \left(2 \frac{p_0^+}{k^+} - 1 \right) + 1 \right) \ln \frac{\Delta_{\text{UV}}}{\Delta_{\text{P}}}. \end{aligned} \quad (9.21)$$

This last contribution still contains an unphysical divergence for $k^+ \rightarrow p_1^+$. We will show in the next paragraph that it cancels with a similar spurious pole in $\tilde{\mathcal{M}}_{\text{A1,sub}}^0$. Also the next vertex correction $\mathcal{M}_{\text{V2,sub}}^0$ (3.41) contains both a finite and an unphysical divergent contribution to the cross section, and also here it will cancel with a similar contribution

from $\mathcal{M}_{A2,\text{sub}}^0$. The finite and ‘spurious’ parts from $\mathcal{M}_{V2,\text{sub}}^0$ result in:

$$\begin{aligned}
 \text{Tr}\mathcal{M}_{\text{LO}}^{0\dagger}\mathcal{M}_{V2,\text{sub}}^0\Big|_{\text{finite}} &= \frac{g_{\text{em}}^2\alpha_s}{M^2}8p_1^+p_0^+\left(\frac{p_0^+\mathbf{P}_\perp^2-p_1^+M^2}{p_0^+\mathbf{P}_\perp^2+p_1^+M^2}-\frac{p_0^+\mathbf{q}^2-p_1^+M^2}{p_0^+\mathbf{q}^2+p_1^+M^2}\right) \\
 &\times\int_0^{p_1^+}\frac{dk^+}{k^+}\frac{(k^+)^3q^+}{(p_0^+)^2p_1^+(p_1^+-k^+)}\mathcal{S}_V^{\bar{\eta}0\eta'} \\
 &\times\left[\int_{\mathbf{x},\mathbf{z}}iA^{\eta'}(\mathbf{x}-\mathbf{z})\int_\ell\frac{\ell^{\bar{\eta}}}{\ell^2}\frac{e^{i\left(\ell+\frac{k^+}{p_1^+}\mathbf{P}_\perp\right)\cdot(\mathbf{x}-\mathbf{z})}}{\left(\ell+\frac{k^+}{p_1^+}\mathbf{P}_\perp\right)^2+\Delta_{\mathbf{P}}}\right. \\
 &\times\left(\left(\ell-\frac{p_0^+(p_1^+-k^+)}{q^+}\mathbf{P}_\perp\right)^2-\frac{(p_1^+-k^+)(p_0^+-k^+)}{(q^+)^2}M^2\right) \\
 &\left.\times e^{-i\mathbf{k}_\perp\cdot\left(\frac{p_0^+-k^+}{p_0^+}\mathbf{x}+\frac{k^+}{p_0^+}\mathbf{z}\right)}\left(\frac{N_c^2}{2}s_{\mathbf{xz}}s_{\mathbf{zx}'}-\frac{1}{2}s_{\mathbf{xx}'}+C_F N_c\right)\right], \tag{9.22}
 \end{aligned}$$

and:

$$\begin{aligned}
 \text{Tr}\mathcal{M}_{\text{LO}}^{0\dagger}\mathcal{M}_{V2,\text{sub}}^0\Big|_{\text{spurious}} &= \frac{g_{\text{em}}^2\alpha_s}{M^2}8p_1^+p_0^+\left(\frac{p_0^+\mathbf{P}_\perp^2-p_1^+M^2}{p_0^+\mathbf{P}_\perp^2+p_1^+M^2}-\frac{p_0^+\mathbf{q}^2-p_1^+M^2}{p_0^+\mathbf{q}^2+p_1^+M^2}\right) \\
 &\times\int_0^{p_1^+}\frac{dk^+}{k^+}\frac{(k^+)^3q^+}{(p_0^+)^2p_1^+(p_1^+-k^+)}\left(\left(2\frac{p_1^+}{k^+}-1\right)\left(2\frac{p_0^+}{k^+}-1\right)+1\right) \\
 &\times\mathcal{A}_0(\Delta_{UV})\int_{\mathbf{x},\mathbf{x}'}e^{-i\mathbf{k}_\perp\cdot(\mathbf{x}-\mathbf{x}')}C_F N_c(s_{\mathbf{xx}'}+1). \tag{9.23}
 \end{aligned}$$

The last two vertex-correction amplitudes $\mathcal{M}_{V3,\text{sub}}^0$ (3.47) and $\mathcal{M}_{V4,\text{sub}}^0$ (3.53) lead to the following contributions to the cross section:

$$\begin{aligned}
 \text{Tr}\mathcal{M}_{\text{LO}}^{0\dagger}\mathcal{M}_{V3,\text{sub}}^0 &= -g_{\text{em}}^2\alpha_s8p_1^+p_0^+\left(\frac{p_0^+\mathbf{P}_\perp^2-p_1^+M^2}{p_0^+\mathbf{P}_\perp^2+p_1^+M^2}-\frac{p_0^+\mathbf{q}^2-p_1^+M^2}{p_0^+\mathbf{q}^2+p_1^+M^2}\right)\frac{1}{M^2} \\
 &\times\int_{\mathbf{x},\mathbf{x}'}e^{-i\mathbf{k}_\perp\cdot(\mathbf{x}-\mathbf{x}')} \int_0^{p_1^+}\frac{dk^+}{k^+}\frac{(k^+)^3q^+}{(p_1^+)^2p_0^+(p_0^+-k^+)}\mathcal{S}_V^{\bar{\eta}0\eta'} \\
 &\times\left[\int_{\mathbf{z}}iA^{\bar{\eta}}(\mathbf{x}-\mathbf{z})\int_\ell\frac{\ell^{\eta'}}{\ell^2}\frac{e^{i\left(\ell+\frac{k^+}{p_1^+}\mathbf{q}\right)\cdot(\mathbf{z}-\mathbf{x})}}{\left(\ell+\frac{k^+}{p_1^+}\mathbf{q}\right)^2+\Delta_{\mathbf{q}}}\right. \\
 &\times\left(\left(\ell+\frac{p_0^+-k^+}{q^+}\mathbf{q}\right)^2-\frac{(p_1^+-k^+)(p_0^+-k^+)}{(q^+)^2}M^2\right) \\
 &\times e^{\frac{i k^+}{p_1^+}\mathbf{k}_\perp\cdot(\mathbf{x}-\mathbf{z})}\left(\frac{N_c^2}{2}s_{\mathbf{xz}}s_{\mathbf{zx}'}-\frac{1}{2}s_{\mathbf{xx}'}+C_F N_c\right) \\
 &\left.+\frac{\delta\bar{\eta}'}{2}\mathcal{A}_0(\Delta_{UV})C_F N_c(s_{\mathbf{xx}'}+1)\right], \tag{9.24}
 \end{aligned}$$

and:

$$\begin{aligned}
 \text{Tr} \mathcal{M}_{\text{LO}}^{0\dagger} \mathcal{M}_{\text{V4,sub}}^0 &= \text{Tr} \mathcal{M}_{\text{LO}}^{0\dagger} \mathcal{M}_{\text{LO}2}^0 \frac{\alpha_s C_F}{\pi} \left\{ -\frac{2p_0^+ + p_1^+}{2p_0^+} \left(1 + \frac{1}{2} \ln \frac{q^+ \Delta_{\text{UV}}}{p_0^+ \mathbf{q}^2 + p_1^+ M^2} \right) \right. \\
 &\quad \times \frac{-1}{p_0^+ \mathbf{q}^2 - p_1^+ M^2} \left[-\frac{q^+ (p_1^+ + 2p_0^+ \ln p_0^+ / q^+)}{4p_1^+ p_0^+} (p_0^+ \mathbf{q}^2 + p_1^+ M^2) \ln \frac{q^+ \Delta_{\text{UV}}}{(p_0^+ \mathbf{q}^2 + p_1^+ M^2)} \right. \\
 &\quad \left. \left. + \frac{q^+}{6p_0^+} \left(-3 + \frac{p_0^+}{p_1^+} \pi^2 + \frac{3}{2} \frac{p_0^+}{p_1^+} \ln \frac{q^+}{p_0^+} \left(4i\pi - 3 \ln \frac{q^+}{p_1^+} - \ln \frac{p_0^+}{p_1^+} \right) - 6 \frac{p_0^+}{p_1^+} \text{Li}_2 \frac{p_0^+}{q^+} \right) \right] \right. \\
 &\quad \left. - \int_0^{p_1^+} \frac{dk^+}{k^+} \frac{4(k^+)^2 ((k^+)^2 + 2p_1^+ p_0^+ - k^+ (p_0^+ + p_1^+))}{p_1^+ (p_0^+)^2} \mathbf{q}^2 M^2 \pi \mathcal{B}_1(0, \Delta_{\mathbf{q}}, \frac{k^+}{p_1^+} \mathbf{q}) \right\}. \tag{9.25}
 \end{aligned}$$

Antiquark vertex corrections. As already announced in the previous paragraph, $\tilde{\mathcal{M}}_{\text{A1,sub}}^0$ (3.59) can be split in both a finite and a divergent contribution to the cross section:

$$\begin{aligned}
 \text{Tr} \mathcal{M}_{\text{LO}}^{0\dagger} \mathcal{M}_{\text{A1,sub}}^0 \Big|_{\text{finite}} &= \text{Tr} (\mathcal{M}_{\text{LO}}^0 \mathcal{M}_{\text{LO}1}^0) \frac{\alpha_s C_F}{\pi} \int_{p_1^+}^{p_0^+} \frac{dk^+}{k^+} \frac{k^+ p_1^+ (p_0^+ - k^+)}{p_0^+ q^+} \left(\left(2 \frac{p_1^+}{k^+} - 1 \right) \left(2 \frac{p_0^+}{k^+} - 1 \right) + 1 \right) \\
 &\quad \times \frac{-1}{p_0^+ \mathbf{P}_\perp^2 - p_1^+ M^2} \left\{ \frac{M^2 p_1^+}{2} \left[\left(\frac{7p_0^+ + p_1^+}{p_0^+} - \frac{2(p_0^+ + 3p_1^+)}{q^+} \ln \frac{p_0^+}{p_1^+} \right) (-i\pi + \ln \frac{\Delta_{\text{UV}}}{M^2}) \right. \right. \\
 &\quad \left. \left. + 6 + 2 \frac{p_1^+}{p_0^+} + 4 \frac{p_0^+ + p_1^+}{q^+} \ln \frac{p_0^+}{p_1^+} \right. \right. \\
 &\quad \left. \left. + 2 \frac{p_0^+ + 3p_1^+}{q^+} \left(-\frac{\pi^2}{6} + \ln^2 \frac{p_0^+}{p_1^+} + 3 \ln \frac{p_0^+}{p_1^+} \ln \frac{q^+}{p_1^+} + \text{Li}_2 \frac{q^+}{p_1^+} + \text{Li}_2 \frac{p_1^+}{p_0^+} \right) \right] \right. \\
 &\quad \left. - 2M^2 \Delta_{\text{P}} \pi \mathcal{B}_0(\Delta_{\text{P}}, \hat{M}^2, \frac{p_0^+ - k^+}{q^+} \mathbf{P}_\perp) \right. \\
 &\quad \left. + 2 \frac{k^+}{p_1^+} \frac{p_0^+ - k^+}{q^+} M^2 \mathbf{P}_\perp^2 \pi \mathcal{B}_1(\Delta_{\text{P}}, \hat{M}^2, \frac{p_0^+ - k^+}{q^+} \mathbf{P}_\perp) \right\}. \tag{9.26}
 \end{aligned}$$

and:

$$\begin{aligned}
 \text{Tr} \mathcal{M}_{\text{LO}}^{0\dagger} \mathcal{M}_{\text{A1,sub}}^0 \Big|_{\text{spurious}} &= \text{Tr} \mathcal{M}_{\text{LO}}^{0\dagger} \mathcal{M}_{\text{LO}1}^0 \frac{\alpha_s C_F}{\pi} \frac{p_0^+ \mathbf{P}_\perp^2 + p_1^+ M^2}{p_0^+ \mathbf{P}_\perp^2 - p_1^+ M^2} \\
 &\quad \times \int_{p_1^+}^{p_0^+} \frac{dk^+}{k^+} \frac{(k^+)^2 (p_0^+ - k^+)}{(p_0^+)^2 (p_1^+ - k^+)} \left(\left(2 \frac{p_1^+}{k^+} - 1 \right) \left(2 \frac{p_0^+}{k^+} - 1 \right) + 1 \right) \frac{1}{4} \ln \frac{\Delta_{\text{UV}}}{\Delta_{\text{P}}}. \tag{9.27}
 \end{aligned}$$

Combining eqs. (9.27) and (9.21), we see that the pathological plus-momentum integrals can be combined and evaluated with the help of the Sokhotski-Plemelj theorem:

$$\begin{aligned}
 &\left[\int_0^{p_1^+} \frac{dk^+}{k^+} \frac{(k^+)^3 q^+}{(p_0^+)^2 p_1^+ (p_1^+ - k^+)} + \int_{p_1^+}^{p_0^+} \frac{dk^+}{k^+} \frac{(k^+)^2 (p_0^+ - k^+)}{(p_0^+)^2 (p_1^+ - k^+)} \right] \left(\left(2 \frac{p_1^+}{k^+} - 1 \right) \left(2 \frac{p_0^+}{k^+} - 1 \right) + 1 \right) \\
 &= \frac{q^+ (2p_0^+ - p_1^+)}{(p_0^+)^2} - \frac{q^+ (3p_0^+ - p_1^+)}{(p_0^+)^2} + 4 \ln \frac{p_0^+}{p_1^+} - \frac{2q^+}{p_0^+} \int_0^{p_0^+} \frac{dk^+}{k^+ - p_1^+ + i0^+} \\
 &= 4 \ln \frac{p_0^+}{p_1^+} - \frac{2q^+}{p_0^+} \left(\frac{1}{2} - i\pi + \ln \frac{q^+}{p_1^+} \right), \tag{9.28}
 \end{aligned}$$

and:

$$\begin{aligned}
 & \left[\int_0^{p_1^+} \frac{dk^+}{k^+} \frac{(k^+)^3 q^+}{(p_0^+)^2 p_1^+ (p_1^+ - k^+)} + \int_{p_1^+}^{p_0^+} \frac{dk^+}{k^+} \frac{(k^+)^2 (p_0^+ - k^+)}{(p_0^+)^2 (p_1^+ - k^+)} \right] \\
 & \times \left(\left(2 \frac{p_1^+}{k^+} - 1 \right) \left(2 \frac{p_0^+}{k^+} - 1 \right) + 1 \right) \ln \frac{k^+ (p_0^+ - k^+)}{(p_1^+)^2} \\
 & = \frac{3q^+}{p_0^+} + \frac{p_0^+ - 4p_1^+}{p_1^+} \ln \frac{p_0^+}{p_1^+} + \frac{(p_1^+)^2 - (p_0^+)^2}{p_0^+ p_1^+} \ln \frac{q^+}{p_1^+} + 2 \ln^2 \frac{p_0^+}{p_1^+} + 4 \ln \frac{p_0^+}{p_1^+} \ln \frac{q^+}{p_1^+} \\
 & \quad - 4 \text{Li}_2 \frac{q^+}{p_0^+} - \frac{2q^+}{p_0^+} \left(\ln^2 \frac{q^+}{p_1^+} + \text{Li}_2 \left(-\frac{p_1^+}{q^+} \right) - \text{Li}_2 \left(-\frac{q^+}{p_1^+} \right) + i\pi \ln \frac{q^+}{p_1^+} \right).
 \end{aligned} \tag{9.29}$$

We end up with the well-behaved result:

$$\begin{aligned}
 & \text{Tr} \mathcal{M}_{\text{LO}}^{0\dagger} \left(\mathcal{M}_{\text{V1,sub}}^0 + \mathcal{M}_{\text{A1,sub}}^0 \right) \Big|_{\text{spurious}} \\
 & = \text{Tr} \mathcal{M}_{\text{LO}}^{0\dagger} \mathcal{M}_{\text{LO1}}^0 \frac{\alpha_s C_F p_0^+ \mathbf{P}_\perp^2 + p_1^+ M^2}{4\pi p_0^+ \mathbf{P}_\perp^2 - p_1^+ M^2} \\
 & \quad \times \left[\left(4 \ln \frac{p_0^+}{p_1^+} - \frac{2q^+}{p_0^+} \left(\frac{1}{2} + i\pi + \ln \frac{q^+}{p_1^+} \right) \right) \left(i\pi + \ln \frac{p_0^+ q^+ \Delta_{\text{UV}}}{p_1^+ (p_0^+ \mathbf{P}_\perp^2 + p_1^+ M^2)} \right) \right. \\
 & \quad - \frac{3q^+}{p_0^+} - \frac{p_0^+ - 4p_1^+}{p_1^+} \ln \frac{p_0^+}{p_1^+} - \frac{(p_1^+)^2 - (p_0^+)^2}{p_0^+ p_1^+} \ln \frac{q^+}{p_1^+} - 2 \ln^2 \frac{p_0^+}{p_1^+} - 4 \ln \frac{p_0^+}{p_1^+} \ln \frac{q^+}{p_1^+} \\
 & \quad \left. + 4 \text{Li}_2 \frac{q^+}{p_0^+} + \frac{2q^+}{p_0^+} \left(\ln^2 \frac{q^+}{p_1^+} + \text{Li}_2 \left(-\frac{p_1^+}{q^+} \right) - \text{Li}_2 \left(-\frac{q^+}{p_1^+} \right) + i\pi \ln \frac{q^+}{p_1^+} \right) \right].
 \end{aligned} \tag{9.30}$$

Similarly, for amplitude $\mathcal{M}_{\text{A2,sub}}^0$ (3.65), we find the finite part:

$$\begin{aligned}
 \text{Tr} \mathcal{M}_{\text{LO}}^{0\dagger} \mathcal{M}_{\text{A2,sub}}^0 \Big|_{\text{finite}} & = g_{\text{em}}^2 \alpha_s 8 p_1^+ p_0^+ \left(\frac{p_0^+ \mathbf{P}_\perp^2 - p_1^+ M^2}{p_0^+ \mathbf{P}_\perp^2 + p_1^+ M^2} - \frac{p_0^+ \mathbf{q}^2 - p_1^+ M^2}{p_0^+ \mathbf{q}^2 + p_1^+ M^2} \right) \frac{1}{M^2} \\
 & \quad \times - \int_{p_1^+}^{p_0^+} \frac{dk^+}{k^+} \frac{(k^+)^2 (p_0^+ - k^+)}{(p_0^+)^2 (p_1^+ - k^+)} \mathcal{S}_V^{\bar{\eta} 0 \eta'} \int_{\mathbf{x}, \mathbf{x}'} e^{-i \mathbf{k}_\perp \cdot (\mathbf{x} - \mathbf{x}')} \\
 & \quad \times \int_{\mathbf{z}} i A^{\eta'}(\mathbf{x} - \mathbf{z}) \int_{\ell} e^{-i \ell \cdot (\mathbf{x} - \mathbf{z})} \frac{\ell^{\bar{\eta}} + \frac{k^+}{p_1^+} \mathbf{P}_\perp^{\bar{\eta}} \left(\ell + \frac{p_0^+ - k^+}{q^+} \mathbf{P}_\perp \right)^2 - \hat{M}^2}{\ell^2 + \Delta_{\text{P}} \left(\ell + \frac{p_0^+ - k^+}{q^+} \mathbf{P}_\perp \right)^2 + \hat{M}^2} \\
 & \quad \times e^{\frac{k^+}{p_0^+} \mathbf{k}_\perp \cdot (\mathbf{x} - \mathbf{z})} \left(\frac{N_c^2}{2} s_{\mathbf{z}\mathbf{z}'} s_{\mathbf{z}\mathbf{x}'} - \frac{1}{2} s_{\mathbf{x}\mathbf{x}'} + C_F N_c \right),
 \end{aligned} \tag{9.31}$$

while the term with the spurious singularity for $k^+ \rightarrow p_1^+$ is:

$$\begin{aligned}
 \text{Tr} \mathcal{M}_{\text{LO}}^{0\dagger} \mathcal{M}_{\text{A2,sub}}^0 \Big|_{\text{spurious}} & = g_{\text{em}}^2 \alpha_s 8 p_1^+ p_0^+ \left(\frac{p_0^+ \mathbf{P}_\perp^2 - p_1^+ M^2}{p_0^+ \mathbf{P}_\perp^2 + p_1^+ M^2} - \frac{p_0^+ \mathbf{q}^2 - p_1^+ M^2}{p_0^+ \mathbf{q}^2 + p_1^+ M^2} \right) \frac{1}{M^2} \\
 & \quad \times \int_{p_1^+}^{p_0^+} \frac{dk^+}{k^+} \frac{(k^+)^2 (p_0^+ - k^+)}{(p_0^+)^2 (p_1^+ - k^+)} \left(\left(2 \frac{p_1^+}{k^+} - 1 \right) \left(2 \frac{p_0^+}{k^+} - 1 \right) + 1 \right) \\
 & \quad \times \mathcal{A}_0(\Delta_{\text{UV}}) \int_{\mathbf{x}, \mathbf{x}'} e^{-i \mathbf{k}_\perp \cdot (\mathbf{x} - \mathbf{x}')} C_F N_c (s_{\mathbf{x}\mathbf{x}'} + 1).
 \end{aligned} \tag{9.32}$$

Combining the above with (9.23) and applying (9.28):

$$\begin{aligned}
 & \text{Tr} \mathcal{M}_{\text{LO}}^{0\dagger} \left(\mathcal{M}_{V2,\text{sub}}^0 + \mathcal{M}_{A2,\text{sub}}^0 \right) \Big|_{\text{spurious}} \\
 &= \frac{g_{\text{em}}^2 \alpha_s}{M^2} 8p_1^+ p_0^+ \left(\frac{p_0^+ \mathbf{P}_\perp^2 - p_1^+ M^2}{p_0^+ \mathbf{P}_\perp^2 + p_1^+ M^2} - \frac{p_0^+ \mathbf{q}^2 - p_1^+ M^2}{p_0^+ \mathbf{q}^2 + p_1^+ M^2} \right) \\
 & \quad \times \left(4 \ln \frac{p_0^+}{p_1^+} - \frac{2q^+}{p_0^+} \left(\frac{1}{2} - i\pi + \ln \frac{q^+}{p_1^+} \right) \right) \mathcal{A}_0(\Delta_{\text{UV}}) \int_{\mathbf{x}, \mathbf{x}'} e^{-i\mathbf{k}_\perp \cdot (\mathbf{x} - \mathbf{x}')} C_F N_c (s_{\mathbf{x}\mathbf{x}'} + 1).
 \end{aligned} \tag{9.33}$$

The next contribution is due to amplitude $\mathcal{M}_{A3,\text{sub}}^0$ (3.69):

$$\begin{aligned}
 \text{Tr} \mathcal{M}_{\text{LO}}^{0\dagger} \mathcal{M}_{A3,\text{sub}}^0 &= \frac{g_{\text{em}}^2 \alpha_s}{M^2} 8p_1^+ p_0^+ \left(\frac{p_0^+ \mathbf{P}_\perp^2 - p_1^+ M^2}{p_0^+ \mathbf{P}_\perp^2 + p_1^+ M^2} - \frac{p_0^+ \mathbf{q}^2 - p_1^+ M^2}{p_0^+ \mathbf{q}^2 + p_1^+ M^2} \right) \\
 & \quad \times \left\{ \mathcal{S}_V^{\bar{\eta}0\eta'} \int_{p_1^+}^{p_0^+} \frac{dk^+}{k^+} \frac{k^+(p_0^+ - k^+)}{q^+ p_0^+} \int_{\mathbf{x}_1, \mathbf{x}_2, \mathbf{x}_3} 2\hat{M}^2 \mathcal{K}(\mathbf{x}_1 - \mathbf{x}_2, \hat{M}^2) \right. \\
 & \quad \times \int_{\ell, \ell_2} e^{-i\ell \cdot \mathbf{x}_{12}} e^{-i\ell_2 \cdot \mathbf{x}_{23}} \frac{\ell^{\eta'}}{\ell^2} \frac{\ell^{\bar{\eta}} - \frac{k^+}{p_1^+} \ell_2^{\bar{\eta}}}{\left(\ell - \frac{p_0^+ - k^+}{q^+} \ell_2 \right)^2 - \frac{p_0^+(p_0^+ - k^+)(p_1^+ - k^+)}{p_1^+(q^+)^2} \ell_2^2} \\
 & \quad \times e^{-i\mathbf{p}_1 \cdot \mathbf{x}_3} e^{-i\mathbf{q} \cdot \left(\frac{p_0^+ - k^+}{q^+} \mathbf{x}_1 - \frac{p_1^+ - k^+}{q^+} \mathbf{x}_2 \right)} \left(\frac{N_c^2}{2} s_{\mathbf{x}_3 \mathbf{x}'} s_{\mathbf{x}_1 \mathbf{x}_2} - \frac{1}{2} Q_{\mathbf{x}_1 \mathbf{x}' \mathbf{x}_3 \mathbf{x}_2} + C_F N_c \right) \\
 & \quad \left. - \left(\frac{7p_0^+ + p_1^+}{p_0^+} + 2 \frac{p_0^+ + 3p_1^+}{q^+} \ln \frac{p_1^+}{p_0^+} \right) \mathcal{A}_0(\Delta_{\text{UV}}) \int_{\mathbf{x}, \mathbf{x}'} e^{-i\mathbf{k}_\perp \cdot (\mathbf{x} - \mathbf{x}')} C_F N_c (s_{\mathbf{x}\mathbf{x}'} + 1) \right\}.
 \end{aligned} \tag{9.34}$$

Finally, from eq. (3.75):

$$\begin{aligned}
 \text{Tr} \mathcal{M}_{\text{LO}}^{0\dagger} \mathcal{M}_{A4,\text{sub}}^0 &= \text{Tr} \mathcal{M}_{\text{LO}}^{0\dagger} \mathcal{M}_{\text{LO}2}^0 \frac{\alpha_s C_F}{\pi} \\
 & \quad \times \left[\left(\frac{7}{4} + \frac{p_1^+}{4p_0^+} - \frac{2(p_0^+ + 3p_1^+)}{4q^+} \ln \frac{p_0^+}{p_1^+} \right) \ln \frac{(q^+)^2 \Delta_{\text{UV}}}{p_0^+ p_1^+ \mathbf{q}^2} + \frac{3p_0^+ + p_1^+}{2p_0^+} - \frac{7p_0^+ + p_1^+}{2p_0^+} \ln \frac{q^+}{p_1^+} \right. \\
 & \quad - \frac{p_0^+ + p_1^+ + (p_0^+ + 3p_1^+) \ln \frac{q^+}{p_1^+}}{q^+} \ln \frac{p_0^+}{p_1^+} - \frac{p_0^+ + 3p_1^+}{2q^+} \left(\text{Li}_2 \left(-\frac{q^+}{p_1^+} \right) - \text{Li}_2 \frac{q^+}{p_0^+} \right) \\
 & \quad \left. + \int_{p_1^+}^{p_0^+} \frac{dk^+}{k^+} \frac{(k^+)^2 (p_0^+ - k^+)^2}{p_1^+ p_0^+ (q^+)^2} \left(\left(2 \frac{p_1^+}{k^+} - 1 \right) \left(2 \frac{p_0^+}{k^+} - 1 \right) + 1 \right) \mathbf{q}^2 \pi \mathcal{B}_1 \left(0, \hat{Q}^2, \frac{p_0^+ - k^+}{q^+} \mathbf{q} \right) \right].
 \end{aligned} \tag{9.35}$$

Instantaneous four-fermion interaction. We obtain the following finite cross-section contributions from amplitudes (3.81), (3.86), and (3.92):

$$\begin{aligned}
 \text{Tr} \mathcal{M}_{\text{LO}}^{0\dagger} \mathcal{M}_{Q1,\text{sub}}^0 &= \text{Tr} \mathcal{M}_{\text{LO}}^{0\dagger} \mathcal{M}_{\text{LO}1}^0 \\
 & \quad \times \frac{\alpha_s C_F}{\pi} \frac{M^2}{p_0^+ \mathbf{P}_\perp^2 - p_1^+ M^2} \frac{2p_1^+}{q^+} \left[\left(2q^+ - (p_0^+ + p_1^+) \ln \frac{p_0^+}{p_1^+} \right) \left(i\pi + \ln \frac{\Delta_{\text{UV}}}{M^2} \right) \right. \\
 & \quad \left. + 2q^+ + (p_0^+ + p_1^+) \left(\ln \frac{p_0^+}{p_1^+} + \text{Li}_2 \left(-\frac{q^+}{p_1^+} \right) - \text{Li}_2 \left(\frac{q^+}{p_0^+} \right) \right) \right],
 \end{aligned} \tag{9.36}$$

and:

$$\begin{aligned}
 & \text{Tr } \mathcal{M}_{\text{LO}}^{0\dagger} \mathcal{M}_{\text{Q2,sub}}^0 \\
 &= g_{\text{em}}^2 \left(\frac{p_0^+ \mathbf{P}_\perp^2 - p_1^+ M^2}{p_0^+ \mathbf{P}_\perp^2 + p_1^+ M^2} - \frac{p_0^+ \mathbf{q}^2 - p_1^+ M^2}{p_0^+ \mathbf{q}^2 + p_1^+ M^2} \right) 8p_1^+ p_0^+ \\
 & \times \frac{4\alpha_s}{M^2} \left[\int_0^{q^+} d\ell_1^+ \frac{1}{(p_0^+ - \ell_1^+)^2} \frac{p_1^+ \ell_1^+}{p_1^+ + \ell_1^+} \right. \\
 & \times \int_{\mathbf{x}_1, \mathbf{x}_2, \mathbf{x}_3} \int_\ell e^{-i\ell \cdot \mathbf{x}_{12}} \frac{\ell^2 + \frac{\ell_1^+(q^+ - \ell_1^+)}{(q^+)^2} M^2}{\ell^2 - \frac{\ell_1^+(q^+ - \ell_1^+)}{(q^+)^2} M^2} \int_{\ell_1, \ell_4} \frac{e^{i\ell_1 \cdot \mathbf{x}_{13}} e^{i\ell_4 \cdot \mathbf{x}_{23}}}{\left(\ell_1 + \frac{\ell_1^+}{\ell_1^+ + p_1^+} \ell_4 \right)^2 + \frac{p_1^+ \ell_1^+ p_0^+ \ell_4^2}{(q^+ - \ell_1^+)(p_1^+ + \ell_1^+)^2}} \\
 & \times e^{-i\mathbf{q} \cdot \left(\frac{q^+ - \ell_1^+}{q^+} \mathbf{x}_2 + \frac{\ell_1^+}{q^+} \mathbf{x}_1 \right)} e^{-i\mathbf{p}_1 \cdot \mathbf{x}_3} \int_{\mathbf{x}'} e^{i\mathbf{k}_\perp \cdot \mathbf{x}'} \left(\frac{N_c^2}{2} s_{\mathbf{x}_1 \mathbf{x}_2} s_{\mathbf{x}_3 \mathbf{x}'} - \frac{1}{2} Q_{\mathbf{x}_1 \mathbf{x}' \mathbf{x}_3 \mathbf{x}_2} + C_F N_c \right) \\
 & \left. + \left(2 - \frac{(p_0^+ + p_1^+)}{q^+} \ln \frac{p_0^+}{p_1^+} \right) \mathcal{A}_0(\Delta_{\text{UV}}) \int_{\mathbf{x}, \mathbf{x}'} e^{-i\mathbf{k}_\perp \cdot (\mathbf{x} - \mathbf{x}')} C_F N_c (s_{\mathbf{x}\mathbf{x}'} + 1) \right], \tag{9.37}
 \end{aligned}$$

and finally:

$$\begin{aligned}
 \text{Tr } \mathcal{M}_{\text{LO}}^{0\dagger} \mathcal{M}_{\text{Q3,sub}}^0 &= \text{Tr } \mathcal{M}_{\text{LO}}^{0\dagger} \mathcal{M}_{\text{LO2}}^0 \\
 & \times \frac{\alpha_s C_F}{\pi} \left[\left(-2 + \frac{p_0^+ + p_1^+}{q^+} \ln \frac{p_0^+}{p_1^+} \right) \ln \frac{p_1^+ \Delta_{\text{UV}}}{p_0^+ \mathbf{q}^2} \right. \\
 & \left. - 2 + \left(2 \frac{p_0^+}{q^+} - 1 \right) \left(\ln \left(\frac{p_1^+}{p_0^+} \right) \left(1 + i\pi + \ln \frac{p_0^+ p_1^+}{(q^+)^2} \right) - \text{Li}_2 \left(\frac{p_1^+}{p_0^+} \right) + \text{Li}_2 \left(\frac{p_0^+}{p_1^+} \right) \right) \right]. \tag{9.38}
 \end{aligned}$$

To obtain the expression in the last line of the above result, we made use of the identity:

$$\begin{aligned}
 & - \int_0^1 dx \frac{x(1-x)}{(c-x)^2} \ln(x(1-x) - i0^+) \\
 &= -2 + (2c-1) \left[\ln \left(\frac{c-1}{c} \right) \left(1 + i\pi + \ln c(c-1) \right) - \text{Li}_2 \left(\frac{c-1}{c} \right) + \text{Li}_2 \left(\frac{c}{c-1} \right) \right] \tag{9.39}
 \end{aligned}$$

for $c > 1$.

Instantaneous $gq\gamma q$ interaction. Here, we list the four contributions to the cross section due to the amplitudes (3.96), (3.101), (3.106), and (3.110) with an instantaneous $gq\gamma q$ interaction. They are all finite. The first one is:

$$\begin{aligned}
 & \text{Tr } \mathcal{M}_{\text{LO}}^{0\dagger} \mathcal{M}_{\text{I1,sub}}^0 \\
 &= \frac{g_{\text{em}}^2 N_c}{M^2} 8p_1^+ p_0^+ \left(\frac{p_0^+ \mathbf{P}_\perp^2 - p_1^+ M^2}{p_0^+ \mathbf{P}_\perp^2 + p_1^+ M^2} - \frac{p_0^+ \mathbf{q}^2 - p_1^+ M^2}{p_0^+ \mathbf{q}^2 + p_1^+ M^2} \right) \int_{\mathbf{x}, \mathbf{x}'} e^{-i\mathbf{k}_\perp \cdot (\mathbf{x} - \mathbf{x}')} (s_{\mathbf{x}\mathbf{x}'} + 1) \\
 & \times \frac{\alpha_s C_F}{\pi} \frac{q^+}{2p_0^+} \left[\left(\ln \frac{q^+}{p_1^+} - i\pi \right) \left(i\pi + \ln \frac{p_0^+ \Delta_{\text{UV}}}{p_0^+ \mathbf{P}_\perp^2 + p_1^+ M^2} \right) - \text{Li}_2 \left(-\frac{p_1^+}{q^+} \right) + \text{Li}_2 \left(-\frac{q^+}{p_1^+} \right) \right], \tag{9.40}
 \end{aligned}$$

and the second:

$$\begin{aligned}
& \text{Tr} \mathcal{M}_{\text{LO}}^{0\dagger} \mathcal{M}_{\text{I2,sub}}^0 \\
&= \frac{g_{\text{em}}^2}{M^2} 8p_1^+ p_0^+ \left(\frac{p_0^+ \mathbf{P}_\perp^2 - p_1^+ M^2}{p_0^+ \mathbf{P}_\perp^2 + p_1^+ M^2} - \frac{p_0^+ \mathbf{q}^2 - p_1^+ M^2}{p_0^+ \mathbf{q}^2 + p_1^+ M^2} \right) \int_{\mathbf{x}, \mathbf{x}'} e^{-i\mathbf{k}_\perp \cdot (\mathbf{x} - \mathbf{x}')} \\
&\quad \times \alpha_s \int_0^{p_0^+} \frac{dk^+}{k^+} \frac{k^+}{p_0^+} \left[\frac{k^+}{p_0^+} \frac{p_0^+ - k^+}{p_1^+ - k^+} \int_{\mathbf{z}} iA^i(\mathbf{x} - \mathbf{z}) \right. \\
&\quad \times \left(\frac{q^+ iA^i(\mathbf{x} - \mathbf{z}, \Delta_{\text{P}})}{p_0^+ - k^+} \frac{2p_0^+}{k^+} - \frac{2p_1^+ - k^+}{p_1^+} \mathbf{P}_\perp^i \mathcal{K}(\mathbf{x} - \mathbf{z}, \Delta_{\text{P}}) \left(\frac{2p_0^+}{k^+} - 1 + \frac{k^+}{2p_1^+ - k^+} \right) \right) \\
&\quad \left. \times e^{i \frac{k^+}{p_0^+} \mathbf{k}_\perp \cdot (\mathbf{x} - \mathbf{z})} \left(\frac{N_c^2}{2} s_{\mathbf{xz}} s_{\mathbf{zx}'} - \frac{1}{2} s_{\mathbf{xx}'} + C_F N_c \right) + \frac{2q^+}{k^+ - p_1^+} \mathcal{A}_0(\Delta_{\text{UV}}) C_F N_c (s_{\mathbf{xx}'} + 1) \right]. \tag{9.41}
\end{aligned}$$

Moreover, we have:

$$\begin{aligned}
& \text{Tr} \mathcal{M}_{\text{LO}}^{0\dagger} \mathcal{M}_{\text{I3,sub}}^0 \\
&= \frac{g_{\text{em}}^2}{M^2} 8p_1^+ p_0^+ \left(\frac{p_0^+ \mathbf{P}_\perp^2 - p_1^+ M^2}{p_0^+ \mathbf{P}_\perp^2 + p_1^+ M^2} - \frac{p_0^+ \mathbf{q}^2 - p_1^+ M^2}{p_0^+ \mathbf{q}^2 + p_1^+ M^2} \right) \int_{\mathbf{x}, \mathbf{x}'} e^{-i\mathbf{k}_\perp \cdot (\mathbf{x} - \mathbf{x}')} \\
&\quad \times \alpha_s \int_0^{p_1^+} \frac{dk^+}{p_0^+ - k^+} \left[\int_{\mathbf{z}} \frac{k^+ (p_1^+ - k^+)}{(p_1^+)^2} iA^i(\mathbf{x} - \mathbf{z}) \right. \\
&\quad \times \left(-\frac{2p_1^+}{k^+} \frac{q^+ iA^i(\mathbf{x} - \mathbf{z}, \Delta_{\text{q}})}{p_1^+ - k^+} + \frac{k^+}{p_1^+} \mathbf{q}^i \mathcal{K}(\mathbf{x} - \mathbf{z}, \Delta_{\text{P}}) \left(\frac{2p_0^+ - k^+}{k^+} \left(1 - \frac{2p_1^+}{k^+} \right) - 1 \right) \right) \\
&\quad \left. \times e^{i \frac{k^+}{p_1^+} \mathbf{k}_\perp \cdot (\mathbf{x} - \mathbf{z})} \left(\frac{N_c^2}{2} s_{\mathbf{xz}} s_{\mathbf{zx}'} - \frac{1}{2} s_{\mathbf{xx}'} + C_F N_c \right) - \frac{2q^+}{p_1^+} \mathcal{A}_0(\Delta_{\text{UV}}) C_F N_c (s_{\mathbf{xx}'} + 1) \right], \tag{9.42}
\end{aligned}$$

and finally:

$$\begin{aligned}
\text{Tr} \mathcal{M}_{\text{LO}}^{0\dagger} \mathcal{M}_{\text{I4,sub}}^0 &= \frac{g_{\text{em}}^2 N_c}{M^2} 8p_1^+ p_0^+ \left(\frac{p_0^+ \mathbf{P}_\perp^2 - p_1^+ M^2}{p_0^+ \mathbf{P}_\perp^2 + p_1^+ M^2} - \frac{p_0^+ \mathbf{q}^2 - p_1^+ M^2}{p_0^+ \mathbf{q}^2 + p_1^+ M^2} \right) \\
&\quad \times \frac{\alpha_s C_F}{\pi} \frac{q^+}{2p_1^+} \left(\ln \frac{q^+}{p_0^+} \ln \frac{q^+ \Delta_{\text{UV}}}{p_0^+ \mathbf{q}^2 + p_1^+ M^2} - \text{Li}_2 \left(\frac{p_1^+}{p_0^+} \right) + \text{Li}_2 \left(-\frac{p_1^+}{q^+} \right) \right) \\
&\quad \times \int_{\mathbf{x}, \mathbf{x}'} e^{-i\mathbf{k}_\perp \cdot (\mathbf{x} - \mathbf{x}')} (s_{\mathbf{xx}'} + 1), \tag{9.43}
\end{aligned}$$

9.1.2 Transverse polarization

Self-energy corrections. The contributions $\text{Tr} \mathcal{M}_{\text{LO}}^{\lambda\dagger} \mathcal{M}_{\text{SE1,sub}}^\lambda \Big|_{\text{finite}}$ and $\text{Tr} \mathcal{M}_{\text{LO}}^{\lambda\dagger} \mathcal{M}_{\text{SE4,sub}}^\lambda \Big|_{\text{finite}}$ are the same as their counterparts (9.12) and (9.13) after changing the polarization of the leading-order amplitudes which they are proportional to. A similar principle holds for amplitudes and $\mathcal{M}_{\text{SE2,sub}}^\lambda$ (3.15) and $\mathcal{M}_{\text{SE3,sub}}^\lambda$ (3.21), but here the LO amplitudes cannot

be completely factorized out. We, therefore, present the expressions explicitly:

$$\begin{aligned}
 \text{Tr} \mathcal{M}_{\text{LO}}^{\lambda\dagger} \mathcal{M}_{\text{SE2,sub}}^\lambda &= g_{\text{em}}^2 \alpha_s 8 p_1^+ p_0^+ \left(\frac{q^+ \mathbf{P}_\perp^\lambda}{p_0^+ \mathbf{P}_\perp^2 + p_1^+ M^2} + \frac{q^+ \mathbf{q}^\lambda}{p_0^+ \mathbf{q}^2 + p_1^+ M^2} \right) \frac{q^+ \mathbf{P}_\perp^\lambda}{p_0^+ \mathbf{P}_\perp^2 + p_1^+ M^2} \\
 &\times \left(\left(1 + 2 \frac{p_1^+}{q^+} \right)^2 + 1 \right) \int_{\mathbf{x}, \mathbf{x}'} e^{-i \mathbf{k}_\perp \cdot (\mathbf{x} - \mathbf{x}')} \left\{ \int_{k_{\text{min}}^+}^{p_0^+} \frac{dk^+}{k^+} \left(\frac{k^+}{p_0^+} \right)^2 \left(\left(1 - \frac{2p_0^+}{k^+} \right)^2 + 1 \right) \right. \\
 &\times \left[\int_{\mathbf{z}} e^{i \frac{k^+}{p_0^+} \mathbf{k}_\perp \cdot (\mathbf{x} - \mathbf{z})} A^i(\mathbf{x} - \mathbf{z}) A^i(\mathbf{x} - \mathbf{z}, \Delta_{\text{P}}) \left(\frac{N_c^2}{2} s_{\mathbf{xz}} s_{\mathbf{zx}'} - \frac{1}{2} s_{\mathbf{xx}'} + C_F N_c \right) \right. \\
 &\left. \left. - \mathcal{A}_0(\Delta_{\text{UV}}) C_F N_c (s_{\mathbf{xx}'} + 1) \right] \right. \\
 &\left. - 4 \int_{k_{\text{min}}^+}^{k_f^+} \frac{dk^+}{k^+} \left[\int_{\mathbf{z}} A^i(\mathbf{x} - \mathbf{z}) A^i(\mathbf{x} - \mathbf{z}) \left(\frac{N_c^2}{2} s_{\mathbf{xz}} s_{\mathbf{zx}'} - \frac{1}{2} s_{\mathbf{xx}'} + C_F N_c \right) \right. \right. \\
 &\left. \left. - \mathcal{A}_0(\Delta_{\text{UV}}) C_F N_c (s_{\mathbf{xx}'} + 1) \right] \right\}, \tag{9.44}
 \end{aligned}$$

and:

$$\begin{aligned}
 \text{Tr} \mathcal{M}_{\text{LO}}^{\lambda\dagger} \mathcal{M}_{\text{SE3,sub}}^\lambda &= g_{\text{em}}^2 \alpha_s 8 p_1^+ p_0^+ \left(\frac{q^+ \mathbf{P}_\perp^\lambda}{p_0^+ \mathbf{P}_\perp^2 + p_1^+ M^2} + \frac{q^+ \mathbf{q}^\lambda}{p_0^+ \mathbf{q}^2 + p_1^+ M^2} \right) \frac{q^+ \mathbf{q}^\lambda}{p_0^+ \mathbf{q}^2 + p_1^+ M^2} \\
 &\times \left(\left(1 + 2 \frac{p_1^+}{q^+} \right)^2 + 1 \right) \int_{\mathbf{x}, \mathbf{x}'} e^{-i \mathbf{k}_\perp \cdot (\mathbf{x} - \mathbf{x}')} \left\{ \int_{k_{\text{min}}^+}^{p_1^+} \frac{dk^+}{k^+} \left(\frac{k^+}{p_1^+} \right)^2 \left(\left(1 - \frac{2p_1^+}{k^+} \right)^2 + 1 \right) \right. \\
 &\times \left[\int_{\mathbf{z}} e^{i \frac{k^+}{p_1^+} \mathbf{k}_\perp \cdot (\mathbf{x} - \mathbf{z})} A^i(\mathbf{x} - \mathbf{z}) A^i(\mathbf{x} - \mathbf{z}, \Delta_{\text{q}}) \left(\frac{N_c^2}{2} s_{\mathbf{xz}} s_{\mathbf{zx}'} - \frac{1}{2} s_{\mathbf{xx}'} + C_F N_c \right) \right. \\
 &\left. \left. - \mathcal{A}_0(\Delta_{\text{UV}}) C_F N_c (s_{\mathbf{xx}'} + 1) \right] \right. \\
 &\left. - 4 \int_{k_{\text{min}}^+}^{k_f^+} \frac{dk^+}{k^+} \left[\int_{\mathbf{z}} A^i(\mathbf{x} - \mathbf{z}) A^i(\mathbf{x} - \mathbf{z}) \left(\frac{N_c^2}{2} s_{\mathbf{xz}} s_{\mathbf{zx}'} - \frac{1}{2} s_{\mathbf{xx}'} + C_F N_c \right) \right. \right. \\
 &\left. \left. - \mathcal{A}_0(\Delta_{\text{UV}}) C_F N_c (s_{\mathbf{xx}'} + 1) \right] \right\}. \tag{9.45}
 \end{aligned}$$

Vertex corrections. In an attempt to make the expressions below a bit more compact, we introduce the following notation for the spinor trace over the Dirac structures, evaluated with the help of identity (B.11)

$$\begin{aligned}
 &\text{Tr} \left(\bar{u}_G(p_0^+) \gamma^+ \mathcal{S}^{\lambda\lambda'} \left(1 + \frac{2p_1^+}{q^+} \right)^\dagger u_G(p_1^+) \bar{u}_G(p_1^+) \gamma^+ \mathcal{S}_V^{\bar{\eta}\lambda\eta'} u_G(p_0^+) \right) \\
 &= -8 p_0^+ p_1^+ \left[\mathcal{E}_V \delta^{\bar{\eta}\eta'} \delta^{\lambda\lambda'} + \mathcal{O}_V \epsilon^{\bar{\eta}\eta'} \epsilon^{\lambda\lambda'} \right], \tag{9.46}
 \end{aligned}$$

with:

$$\begin{aligned}
 \mathcal{E}_V &\equiv \left(\left(1 + \frac{2p_1^+}{q^+} \right) \left(2 \frac{k^+ - p_1^+}{q^+} - 1 \right) - 1 \right) \left(\left(2 \frac{p_1^+}{k^+} - 1 \right) \left(1 - 2 \frac{p_0^+}{k^+} \right) - 1 \right), \\
 \mathcal{O}_V &\equiv 4 \frac{(p_0^+ + p_1^+ - k^+)^2}{k^+ q^+}. \tag{9.47}
 \end{aligned}$$

We can show that the UV-subtracted vertex corrections $\mathcal{M}_{V1,\text{sub}}^\lambda$ (3.33) and $\mathcal{M}_{V4,\text{sub}}^\lambda$ (3.54) contribute as follows to the cross section:

$$\begin{aligned}
 & \text{Tr } \mathcal{M}_{\text{LO}}^{\lambda\dagger} \mathcal{M}_{V1,\text{sub}}^\lambda \\
 &= \text{Tr } \mathcal{M}_{\text{LO}}^{\lambda\dagger} \mathcal{M}_{\text{LO1}}^\lambda \frac{\alpha_s C_F}{\pi} \frac{1}{2} \frac{(q^+)^2}{(p_0^+)^2 + (p_1^+)^2} \\
 & \times \left\{ 2 \frac{(p_0^+)^2 + (p_1^+)^2}{(q^+)^2} \int_{k_{\min}^+}^{p_1^+} \frac{dk^+}{k^+} \ln \frac{\Delta_{\text{UV}}}{\Delta_{\text{P}}} + 2 \int_0^{p_1^+} dk^+ \frac{k^+ - 2p_1^+ - q^+}{(q^+)^2} \ln \frac{\Delta_{\text{UV}}}{\Delta_{\text{P}}} \right. \\
 & + \int_0^{p_1^+} dk^+ \left(\frac{k^+}{p_1^+(p_0^+ - k^+)} \left(\frac{k^+}{p_1^+} \right)^2 \mathbf{P}_\perp^2 \right. \\
 & \left. \left. + 4 \frac{(p_1^+)^2 + (p_0^+ - k^+)^2}{p_1^+ q^+ (p_0^+ - k^+)} \left(\Delta_{\text{P}} + \left(\frac{k^+}{p_1^+} \right)^2 \mathbf{P}_\perp^2 \right) \right) \pi \mathcal{B}_1(0, \Delta_{\text{P}}, \frac{k^+}{p_1^+} \mathbf{P}_\perp) \right\}, \tag{9.48}
 \end{aligned}$$

and:

$$\begin{aligned}
 \text{Tr } \mathcal{M}_{\text{LO}}^{\lambda\dagger} \mathcal{M}_{V4,\text{sub}}^\lambda &= \text{Tr } \mathcal{M}_{\text{LO}}^{\lambda\dagger} \mathcal{M}_{\text{LO2}}^\lambda \frac{\alpha_s C_F}{\pi} \frac{1}{2} \frac{(q^+)^2}{(p_0^+)^2 + (p_1^+)^2} \\
 & \times \left\{ 2 \frac{(p_0^+)^2 + (p_1^+)^2}{(q^+)^2} \int_{k_{\min}^+}^{p_1^+} \frac{dk^+}{k^+} \ln \frac{\Delta_{\text{UV}}}{\Delta_{\text{q}}} + 2 \int_0^{p_1^+} dk^+ \frac{k^+ - p_0^+ - p_1^+}{(q^+)^2} \ln \frac{\Delta_{\text{UV}}}{\Delta_{\text{q}}} \right. \\
 & + 4 \int_0^{p_1^+} dk^+ \left[\frac{(p_0^+ + p_1^+ - k^+)^2}{p_0^+ q^+ (p_1^+ - k^+)} \left(\frac{k^+}{p_1^+} \right)^2 \mathbf{q}^2 \right. \\
 & \left. \left. + \frac{(p_0^+)^2 + (p_1^+ - k^+)^2}{q^+ p_0^+ (p_1^+ - k^+)} \left(\Delta_{\text{q}} + \left(\frac{k^+}{p_1^+} \right)^2 \mathbf{q}^2 \right) \right] \pi \mathcal{B}_1(0, \Delta_{\text{q}}, \frac{k^+}{p_1^+} \mathbf{q}) \right\}. \tag{9.49}
 \end{aligned}$$

The second lines of the above two expressions contain the rapidity-divergent parts. These terms nicely combine with the similar parts of $\mathcal{M}_{\text{SE1},\text{sub}}^\lambda|_{1/k^+}$ into completely finite expressions that are independent of the rapidity factorization scale. Indeed, we have:

$$\text{Tr } \mathcal{M}_{\text{LO}}^{\lambda\dagger} \mathcal{M}_{V1,\text{sub}}^\lambda \Big|_{1/k^+} = \text{Tr } \mathcal{M}_{\text{LO}}^{\lambda\dagger} \mathcal{M}_{\text{LO1}}^\lambda \frac{\alpha_s C_F}{\pi} \int_{k_{\min}^+}^{p_1^+} \frac{dk^+}{k^+} \ln \frac{\Delta_{\text{UV}}}{\Delta_{\text{P}}}, \tag{9.50}$$

but also:

$$\text{Tr } \mathcal{M}_{\text{LO}}^{\lambda\dagger} \mathcal{M}_{\text{SE1},\text{sub}}^\lambda \Big|_{1/k^+} = \text{Tr } \mathcal{M}_{\text{LO}}^{\lambda\dagger} \mathcal{M}_{\text{LO1}}^\lambda \frac{\alpha_s C_F}{\pi} \int_{k_{\min}^+}^{p_0^+} \frac{dk^+}{k^+} \ln \frac{\Delta_{\text{P}}}{\Delta_{\text{UV}}}. \tag{9.51}$$

Their sum is:

$$\begin{aligned}
 & \text{Tr } \mathcal{M}_{\text{LO}}^{\lambda\dagger} \left(\mathcal{M}_{\text{SE1},\text{sub}}^\lambda + \mathcal{M}_{V1,\text{sub}}^\lambda \right) \Big|_{1/k^+} \\
 &= \text{Tr } \mathcal{M}_{\text{LO}}^{\lambda\dagger} \mathcal{M}_{\text{LO1}}^\lambda \frac{\alpha_s C_F}{\pi} \int_{p_1^+}^{p_0^+} \frac{dk^+}{k^+} \ln \frac{\Delta_{\text{P}}}{\Delta_{\text{UV}}}, \\
 &= \text{Tr } \mathcal{M}_{\text{LO}}^{\lambda\dagger} \mathcal{M}_{\text{LO1}}^\lambda \frac{\alpha_s C_F}{\pi} \\
 & \times \left[\ln \frac{p_0^+}{p_1^+} \left(i\pi + \ln \frac{p_0^+ q^+ \Delta_{\text{P}}}{p_1^+ (p_0^+ \mathbf{P}_\perp^2 + p_1^+ M^2)} \right) - \ln \frac{p_0^+}{p_1^+} \ln \frac{q^+}{p_1^+} - \frac{1}{2} \ln^2 \frac{p_0^+}{p_1^+} + \text{Li}_2 \frac{q^+}{p_0^+} \right], \tag{9.52}
 \end{aligned}$$

in which all dependence on the rapidity cutoff or the rapidity factorization scale has disappeared. Likewise:

$$\text{Tr } \mathcal{M}_{\text{LO}}^{\lambda\dagger} \mathcal{M}_{\text{V4,sub}}^\lambda \Big|_{1/k^+} = \text{Tr } \mathcal{M}_{\text{LO}}^{\lambda\dagger} \mathcal{M}_{\text{LO2}}^\lambda \frac{\alpha_s C_F}{\pi} \int_{k_{\text{min}}^+}^{p_1^+} \frac{dk^+}{k^+} \ln \frac{\Delta_{\text{UV}}}{\Delta_{\text{q}}}, \quad (9.53)$$

cancels with:

$$\begin{aligned} \text{Tr } \mathcal{M}_{\text{LO}}^{\lambda\dagger} \mathcal{M}_{\text{SE2,sub}}^\lambda \Big|_{1/k^+} &= \text{Tr } \mathcal{M}_{\text{LO}}^{\lambda\dagger} \mathcal{M}_{\text{LO2}}^\lambda \frac{\alpha_s C_F}{\pi} \int_{k_{\text{min}}^+}^{p_1^+} \frac{dk^+}{k^+} \ln \frac{\Delta_{\text{q}}}{\Delta_{\text{UV}}}, \\ &= - \text{Tr } \mathcal{M}_{\text{LO}}^{\lambda\dagger} \mathcal{M}_{\text{V4,sub}}^\lambda \Big|_{1/k^+}. \end{aligned} \quad (9.54)$$

The completely finite leftovers of (9.48) and (9.49) are:

$$\begin{aligned} &\text{Tr } \mathcal{M}_{\text{LO}}^{\lambda\dagger} \mathcal{M}_{\text{V1,sub}}^\lambda \Big|_{\text{finite}} \\ &= \text{Tr } \mathcal{M}_{\text{LO}}^{\lambda\dagger} \mathcal{M}_{\text{LO1}}^\lambda \frac{\alpha_s C_F}{\pi} \frac{1}{2} \frac{(q^+)^2}{(p_0^+)^2 + (p_1^+)^2} \\ &\quad \times \left\{ - \frac{p_1^+(2p_0^+ + p_1^+)}{(q^+)^2} \left(i\pi + \ln \frac{p_0^+ q^+ \Delta_{\text{P}}}{p_1^+ (p_0^+ \mathbf{P}_\perp^2 + p_1^+ M^2)} \right) \right. \\ &\quad - \frac{3p_1^+(p_0^+ + p_1^+) + ((p_0^+)^2 - (p_1^+)^2) \ln \frac{q^+}{p_1^+} - p_0^+(p_0^+ + 2p_1^+) \ln \frac{p_0^+}{p_1^+}}{(q^+)^2} \\ &\quad + \int_0^{p_1^+} dk^+ \left(\frac{k^+}{p_1^+(p_0^+ - k^+)} \left(\frac{k^+}{p_1^+} \right)^2 \mathbf{P}_\perp^2 \right. \\ &\quad \left. \left. + 4 \frac{(p_1^+)^2 + (p_0^+ - k^+)^2}{p_1^+ q^+ (p_0^+ - k^+)} \left(\Delta_{\text{P}} + \left(\frac{k^+}{p_1^+} \right)^2 \mathbf{P}_\perp^2 \right) \right) \pi \mathcal{B}_1 \left(0, \Delta_{\text{P}}, \frac{k^+}{p_1^+} \mathbf{P}_\perp \right) \right\}, \end{aligned} \quad (9.55)$$

and:

$$\begin{aligned} &\text{Tr } \mathcal{M}_{\text{LO}}^{\lambda\dagger} \mathcal{M}_{\text{V4,sub}}^\lambda \Big|_{\text{finite}} \\ &= \text{Tr } \mathcal{M}_{\text{LO}}^{\lambda\dagger} \mathcal{M}_{\text{LO2}}^\lambda \frac{\alpha_s C_F}{\pi} \frac{1}{2} \frac{(q^+)^2}{(p_0^+)^2 + (p_1^+)^2} \\ &\quad \times \left\{ - \frac{p_1^+(2p_0^+ + p_1^+)}{(q^+)^2} \ln \frac{q^+ \Delta_{\text{UV}}}{p_0^+ \mathbf{q}^2 + p_1^+ M^2} - \frac{2p_1^+(2p_0^+ + p_1^+)}{(q^+)^2} \right. \\ &\quad + 4 \int_0^{p_1^+} dk^+ \left[\frac{(p_0^+ + p_1^+ - k^+)^2}{p_0^+ q^+ (p_1^+ - k^+)} \left(\frac{k^+}{p_1^+} \right)^2 \mathbf{q}^2 \right. \\ &\quad \left. \left. + \frac{(p_0^+)^2 + (p_1^+ - k^+)^2}{q^+ p_0^+ (p_1^+ - k^+)} \left(\Delta_{\text{q}} + \left(\frac{k^+}{p_1^+} \right)^2 \mathbf{q}^2 \right) \right] \pi \mathcal{B}_1 \left(0, \Delta_{\text{q}}, \frac{k^+}{p_1^+} \mathbf{q} \right) \right\}. \end{aligned} \quad (9.56)$$

The other contributions to the cross section stem from the vertex correction amplitudes (3.42) and (3.48), which have never exhibited any divergence to begin with:

$$\begin{aligned} &\text{Tr } \mathcal{M}_{\text{LO}}^{\lambda\dagger} \mathcal{M}_{\text{V2}}^\lambda \\ &= g_{\text{em}}^2 \alpha_s 8 p_0^+ p_1^+ \left(\frac{q^+ \mathbf{P}_\perp^{\lambda'}}{p_0^+ \mathbf{P}_\perp^2 + p_1^+ M^2} + \frac{q^+ \mathbf{q}^{\lambda'}}{p_0^+ \mathbf{q}^2 + p_1^+ M^2} \right) \int_0^{p_1^+} \frac{dk^+}{k^+} \frac{q^+ (k^+)^3}{p_1^+ (p_0^+)^2 (p_1^+ - k^+)} \end{aligned}$$

$$\begin{aligned}
 & \times \left[\left(\left(1 + \frac{2p_1^+}{q^+} \right) \left(2 \frac{k^+ - p_1^+}{q^+} - 1 \right) - 1 \right) \left(\left(2 \frac{p_1^+}{k^+} - 1 \right) \left(1 - 2 \frac{p_0^+}{k^+} \right) - 1 \right) \delta^{\bar{\eta}\eta'} \delta^{\bar{\lambda}\lambda'} \right. \\
 & \left. + 4 \frac{(p_0^+ + p_1^+ - k^+)^2}{k^+ q^+} \epsilon^{\bar{\eta}\eta'} \epsilon^{\bar{\lambda}\lambda'} \right] \\
 & \times \int_{\mathbf{x}, \mathbf{x}', \mathbf{z}} i A^{\eta'}(\mathbf{x} - \mathbf{z}) \int_{\ell} e^{i\ell \cdot (\mathbf{x} - \mathbf{z})} \frac{\ell^{\bar{\eta}} - \frac{k^+}{p_1^+} \mathbf{P}_{\perp}^{\bar{\eta}}}{\left(\ell - \frac{k^+}{p_1^+} \mathbf{P}_{\perp} \right)^2} \frac{\ell^{\bar{\lambda}} - \frac{p_0^+ - k^+}{q^+} \mathbf{P}_{\perp}^{\bar{\lambda}}}{\ell^2 + \Delta_{\text{P}}} \\
 & \times e^{-i\mathbf{k}_{\perp} \cdot (\mathbf{x} - \mathbf{x}')} e^{-i\mathbf{k}_{\perp} \cdot (\mathbf{x} - \mathbf{z})} \left(\frac{N_c^2}{2} s_{\mathbf{x}\mathbf{z}} s_{\mathbf{z}\mathbf{x}'} - \frac{1}{2} s_{\mathbf{x}\mathbf{x}'} + C_F N_c \right), \tag{9.57}
 \end{aligned}$$

and similarly:

$$\begin{aligned}
 & \text{Tr} \mathcal{M}_{\text{LO}}^{\lambda\dagger} \mathcal{M}_{\text{V3}}^{\lambda} \\
 & = g_{\text{ew}}^2 \alpha_s 8 p_0^+ p_1^+ \left(\frac{q^+ \mathbf{P}_{\perp}^{\lambda'}}{p_0^+ \mathbf{P}_{\perp}^2 + p_1^+ M^2} + \frac{q^+ \mathbf{q}^{\lambda'}}{p_0^+ \mathbf{q}^2 + p_1^+ M^2} \right) \int_0^{p_1^+} \frac{dk^+}{k^+} \frac{q^+(k^+)^3}{p_0^+ (p_1^+)^2 (p_0^+ - k^+)} \\
 & \times \left[\left(\left(1 + \frac{2p_1^+}{q^+} \right) \left(2 \frac{k^+ - p_1^+}{q^+} - 1 \right) - 1 \right) \left(\left(2 \frac{p_1^+}{k^+} - 1 \right) \left(1 - 2 \frac{p_0^+}{k^+} \right) - 1 \right) \delta^{\bar{\eta}\eta'} \delta^{\bar{\lambda}\lambda'} \right. \\
 & \left. + 4 \frac{(p_0^+ + p_1^+ - k^+)^2}{k^+ q^+} \epsilon^{\bar{\eta}\eta'} \epsilon^{\bar{\lambda}\lambda'} \right] \\
 & \times \int_{\mathbf{x}, \mathbf{x}', \mathbf{z}} i A^{\bar{\eta}}(\mathbf{z} - \mathbf{x}) \int_{\ell} e^{-i\ell \cdot (\mathbf{x} - \mathbf{z})} \frac{\ell^{\eta'}}{\ell^2} \frac{\ell^{\bar{\lambda}} + \frac{p_0^+ - k^+}{q^+} \mathbf{q}^{\bar{\lambda}}}{\left(\ell + \frac{k^+}{p_1^+} \mathbf{q} \right)^2 + \Delta_{\text{q}}} \\
 & \times e^{\frac{k^+}{p_1^+} \mathbf{p}_1 \cdot (\mathbf{x} - \mathbf{z})} e^{-i\mathbf{k}_{\perp} \cdot (\mathbf{x} - \mathbf{x}')} \left(\frac{N_c^2}{2} s_{\mathbf{x}\mathbf{z}} s_{\mathbf{z}\mathbf{x}'} - \frac{1}{2} s_{\mathbf{x}\mathbf{x}'} + C_F N_c \right). \tag{9.58}
 \end{aligned}$$

Antiquark vertex corrections. The contribution to the cross section coming from the UV-subtracted amplitude $\mathcal{M}_{\text{A1,sub}}^{\lambda}$ (3.60) is given by the following, quite complicated, formula:

$$\begin{aligned}
 & \text{Tr} \mathcal{M}_{\text{LO}}^{\lambda\dagger} \mathcal{M}_{\text{A1,sub}}^{\lambda} \\
 & = \text{Tr} \mathcal{M}_{\text{LO}}^{\lambda\dagger} \mathcal{M}_{\text{LO1}}^{\lambda} \times \frac{1}{2} \frac{(q^+)^2}{(p_1^+)^2 + (p_0^+)^2} \frac{\alpha_s C_F}{\pi} \\
 & \times \left\{ \frac{-q^+(2p_0^+ + q^+) + 2((p_1^+)^2 + (p_0^+)^2) \ln(p_0^+/p_1^+)}{2(q^+)^2} \left(-i\pi + \ln \frac{\Delta_{\text{UV}}}{M^2} \right) \right. \\
 & + \frac{(p_1^+)^2 + (p_0^+)^2}{(q^+)^2} \left(-\frac{\pi^2}{6} + \ln^2 \frac{p_0^+}{p_1^+} + 3 \ln \frac{p_0^+}{p_1^+} \ln \frac{q^+}{p_1^+} + \text{Li}_2 \left(-\frac{q^+}{p_1^+} \right) + \text{Li}_2 \left(\frac{p_1^+}{p_0^+} \right) \right) \\
 & - \frac{2p_0^+ + q^+}{q^+} \left(-1 + 2 \ln \frac{q^+}{p_1^+} \right) \\
 & + \int_{p_1^+}^{p_0^+} \frac{dk^+}{k^+} \frac{k^+ p_1^+}{p_0^+ (p_1^+ - k^+)} \left(-\frac{p_0^+ - k^+}{q^+} \mathcal{E}_{\text{V}} + \frac{k^+}{p_1^+} \mathcal{O}_{\text{V}} \right) \Delta_{\text{P}} \pi \mathcal{B}_0(\Delta_{\text{P}}, \hat{M}^2, \frac{p_0^+ - k^+}{q^+} \mathbf{P}_{\perp}) \\
 & + \int_{p_1^+}^{p_0^+} \frac{dk^+}{k^+} \frac{k^+ p_1^+}{p_0^+ (p_1^+ - k^+)} \frac{k^+ (p_0^+ - k^+)}{2p_1^+ (q^+)^2} \left(\frac{2p_1^+ (p_0^+ - k^+) - k^+ q^+}{p_0^+ p_1^+} (p_0^+ \mathbf{P}_{\perp}^2 + p_1^+ M^2) \right)
 \end{aligned}$$

$$\begin{aligned}
& + \left((p_0^+ - k^+) \mathbf{P}_\perp^2 - (p_1^+ - k^+) M^2 \right) \mathcal{E}_V \pi \mathcal{B}_1(\Delta_P, \hat{M}^2, \frac{p_0^+ - k^+}{q^+} \mathbf{P}_\perp) \\
& + \left. \int_{p_1^+}^{p_0^+} \frac{dk^+}{k^+} \frac{(k^+)^2}{p_0^+(2p_1^+ - k^+)} \left(\Delta_P - \hat{M}^2 - \left(\frac{p_0^+ - k^+}{q^+} \mathbf{P}_\perp \right)^2 \right) \mathcal{O}_V \pi \mathcal{B}_1(\Delta_P, \hat{M}^2, \frac{p_0^+ - k^+}{q^+} \mathbf{P}_\perp) \right\}.
\end{aligned} \tag{9.59}$$

The contribution due to the, finite, diagram A2 (3.62) reads:

$$\begin{aligned}
\text{Tr} \mathcal{M}_{\text{LO}}^{\lambda\dagger} \mathcal{M}_{\text{A2}}^\lambda & = g_{\text{em}}^2 \alpha_s \delta p_1^+ p_0^+ \left(\frac{q^+ \mathbf{P}_\perp^{\lambda'}}{p_0^+ \mathbf{P}_\perp^2 + p_1^+ M^2} + \frac{q^+ \mathbf{q}^{\lambda'}}{p_0^+ \mathbf{q}^2 + p_1^+ M^2} \right) \\
& \times \int_{p_1^+}^{p_0^+} \frac{dk^+}{k^+} \frac{(k^+)^2 (p_0^+ - k^+)}{(p_0^+)^2 (p_1^+ - k^+)} \left[\mathcal{E}_V \delta^{\bar{\eta}\eta'} \delta^{\bar{\lambda}\lambda'} + \mathcal{O}_V \epsilon^{\bar{\eta}\eta'} \epsilon^{\bar{\lambda}\lambda'} \right] \\
& \times \int_{\mathbf{x}, \mathbf{x}', \mathbf{z}} i A^{\eta'}(\mathbf{x} - \mathbf{z}) \int_{\ell} e^{-i\ell \cdot (\mathbf{x} - \mathbf{z})} \frac{\ell^{\bar{\eta}} + \frac{k^+}{p_1^+} \mathbf{P}_\perp^{\bar{\eta}}}{\ell^2 + \Delta_P} \frac{\left(\ell^{\bar{\lambda}} + \frac{p_0^+ - k^+}{q^+} \mathbf{P}_\perp^{\bar{\lambda}} \right)}{\left(\ell + \frac{p_0^+ - k^+}{q^+} \mathbf{P}_\perp \right)^2 + \hat{M}^2} \\
& \times e^{i\mathbf{k}_\perp \cdot (\mathbf{x} - \mathbf{x}')} e^{i \frac{k^+}{p_0^+} \mathbf{k}_\perp \cdot (\mathbf{x} - \mathbf{z})} \left(\frac{N_c^2}{2} s_{\mathbf{xz}} s_{\mathbf{zx}'} - \frac{1}{2} s_{\mathbf{xx}'} + C_F N_c \right).
\end{aligned} \tag{9.60}$$

Amplitude $\mathcal{M}_{\text{A3}}^\lambda$ (3.67), which did not exhibit any divergences either, yields the following term:

$$\begin{aligned}
\text{Tr} \mathcal{M}_{\text{LO}}^{\lambda\dagger} \mathcal{M}_{\text{A3}}^\lambda & = g_{\text{ew}}^2 \alpha_s \delta p_0^+ p_1^+ \left(\frac{q^+ \mathbf{P}_\perp^{\lambda'}}{p_0^+ \mathbf{P}_\perp^2 + p_1^+ M^2} + \frac{q^+ \mathbf{q}^{\lambda'}}{p_0^+ \mathbf{q}^2 + p_1^+ M^2} \right) \\
& \times \int_{p_1^+}^{p_0^+} \frac{dk^+}{k^+} \frac{k^+ (p_0^+ - k^+)}{q^+ p_0^+} \left[\mathcal{E}_V \delta^{\bar{\eta}\eta'} \delta^{\bar{\lambda}\lambda'} + \mathcal{O}_V \epsilon^{\bar{\eta}\eta'} \epsilon^{\bar{\lambda}\lambda'} \right] \int_{\mathbf{x}_1, \mathbf{x}_2, \mathbf{x}_3, \mathbf{x}'} i A^{\bar{\lambda}}(\mathbf{x}_1 - \mathbf{x}_2, \hat{M}^2) \\
& \times \int_{\mathbf{k}, \ell} e^{-i\mathbf{k} \cdot \mathbf{x}_{12}} e^{-i\ell \cdot \mathbf{x}_{23}} \frac{\mathbf{k}^{\eta'}}{k^2} \frac{\left(\mathbf{k}^{\bar{\eta}} - \frac{k^+}{p_1^+} \ell^{\bar{\eta}} \right)}{\left(\mathbf{k} - \frac{p_0^+ - k^+}{q^+} \ell \right)^2 - \frac{p_0^+ (p_0^+ - k^+) (p_1^+ - k^+)}{p_1^+ (q^+)^2} \ell^2} \\
& \times e^{i\mathbf{k}_\perp \cdot \mathbf{x}'} e^{-i\mathbf{p}_1 \cdot \mathbf{x}_3} e^{-i\mathbf{q} \cdot \left(\frac{p_0^+ - k^+}{q^+} \mathbf{x}_1 - \frac{p_1^+ - k^+}{q^+} \mathbf{x}_2 \right)} \left(\frac{N_c^2}{2} s_{\mathbf{x}_1 \mathbf{x}_2} s_{\mathbf{x}_3 \mathbf{x}'} - \frac{1}{2} Q_{\mathbf{x}_1 \mathbf{x}' \mathbf{x}_3 \mathbf{x}_2} + C_F N_c \right).
\end{aligned} \tag{9.61}$$

Finally, the contribution due to the UV-subtracted amplitude $\mathcal{M}_{\text{A4,sub}}^\lambda$ in eq. (3.76) is given by:

$$\begin{aligned}
\text{Tr} \mathcal{M}_{\text{LO}}^{\lambda\dagger} \mathcal{M}_{\text{A4,sub}}^\lambda & = \text{Tr} \mathcal{M}_{\text{LO}}^{\lambda\dagger} \mathcal{M}_{\text{LO2}}^\lambda \times \frac{1}{2} \frac{(q^+)^2}{(p_1^+)^2 + (p_0^+)^2} \frac{\alpha_s C_F}{\pi} \\
& \times \left\{ \frac{-q^+ (2p_0^+ + q^+) + 2((p_1^+)^2 + (p_0^+)^2) \ln(p_0^+/p_1^+)}{2(q^+)^2} \ln \frac{p_1^+ \Delta_{\text{UV}}}{p_0^+ \mathbf{q}^2} \right. \\
& + \frac{(p_1^+)^2 + (p_0^+)^2}{(q^+)^2} \left(-\frac{\pi^2}{6} + \ln^2 \frac{p_0^+}{p_1^+} + 3 \ln \frac{p_0^+}{p_1^+} \ln \frac{q^+}{p_1^+} + \text{Li}_2 \left(-\frac{q^+}{p_1^+} \right) + \text{Li}_2 \left(\frac{p_1^+}{p_0^+} \right) \right) \\
& \left. - \frac{2p_0^+ + q^+}{q^+} \left(-1 + 2 \ln \frac{q^+}{p_1^+} \right) \right\}
\end{aligned}$$

$$\begin{aligned}
& - \int_{p_1^+}^{p_0^+} \frac{dk^+}{k^+} \frac{(k^+)^2}{2p_0^+(p_1^+ - k^+)} \left[\left(\hat{Q}^2 - \left(\frac{p_0^+ - k^+}{q^+} \mathbf{q} \right)^2 \right) \mathcal{E}_V + \frac{k^+(p_0^+ - k^+)}{p_1^+ q^+} \mathbf{q}^2 \mathcal{O}_V \right] \\
& \times \pi \mathcal{B}_1(0, \hat{Q}^2, \frac{p_0^+ - k^+}{q^+} \mathbf{q}) \Big\}. \tag{9.62}
\end{aligned}$$

Instantaneous interactions. We conclude this overview of virtual NLO contributions to the cross section with those coming from instantaneous interactions. For a transversely polarized photon, only a couple of them are nonzero: the first one is \mathcal{M}_{Q2}^λ (3.83) due to the four-fermion vertex. We have:

$$\begin{aligned}
\text{Tr} \mathcal{M}_{\text{LO}}^{\lambda\dagger} \mathcal{M}_{Q2}^\lambda &= g_{\text{ew}}^2 \alpha_s 8p_1^+ p_0^+ \left(\frac{q^+ \mathbf{P}_\perp^i}{p_0^+ \mathbf{P}_\perp^2 + p_1^+ M^2} + \frac{q^+ \mathbf{q}^i}{p_0^+ \mathbf{q}^2 + p_1^+ M^2} \right) \\
&\times \int_0^{q^+} dk^+ \frac{4}{(p_0^+ - k^+)^2} \frac{p_1^+ k^+}{p_1^+ + k^+} \left(\left(1 + \frac{2p_1^+}{q^+} \right) \left(\frac{2k^+}{q^+} - 1 \right) + 1 \right) \\
&\times \int_{\mathbf{x}_1, \mathbf{x}_2, \mathbf{x}_3, \mathbf{x}'} iA^i(\mathbf{x}_{12}, \tilde{M}^2) \\
&\times \int_{\ell_1, \ell_2} \frac{e^{i\ell_1 \cdot \mathbf{x}_{13}} e^{i\ell_2 \cdot \mathbf{x}_{23}}}{\left(\ell_1 + \frac{k^+}{k^+ + p_1^+} \ell_2 \right)^2 + \frac{p_1^+ k^+ p_0^+ \ell_2^2}{(q^+ - k^+)(p_1^+ + k^+)^2}} \\
&\times e^{i\mathbf{k}_\perp \cdot \mathbf{x}'} e^{-i\mathbf{q} \cdot \left(\frac{q^+ - k^+}{q^+} \mathbf{x}_2 + \frac{k^+}{q^+} \mathbf{x}_1 \right)} e^{-i\mathbf{p}_1 \cdot \mathbf{x}_3} \\
&\times \left(\frac{N_c^2}{2} s_{\mathbf{x}_1 \mathbf{x}_2} s_{\mathbf{x}_3 \mathbf{x}'} - \frac{1}{2} Q_{\mathbf{x}_1 \mathbf{x}' \mathbf{x}_3 \mathbf{x}_2} + C_F N_c \right). \tag{9.63}
\end{aligned}$$

The non-vanishing contributions due to the instantaneous $gq\gamma q$ vertex, eq. (3.98) and (3.103), read:

$$\begin{aligned}
\text{Tr} \mathcal{M}_{\text{LO}}^{\lambda\dagger} \mathcal{M}_{12}^\lambda &= -g_{\text{ew}}^2 \alpha_s 8p_1^+ p_0^+ \left(\frac{q^+ \mathbf{P}_\perp^i}{p_0^+ \mathbf{P}_\perp^2 + p_1^+ M^2} + \frac{q^+ \mathbf{q}^i}{p_0^+ \mathbf{q}^2 + p_1^+ M^2} \right) \\
&\times 4 \int_0^{p_0^+} \frac{dk^+}{k^+} \left(\frac{k^+}{p_0^+} \right)^2 (p_0^+ - k^+) \frac{p_0^+ \left((p_1^+)^2 + (p_0^+)^2 \right) + p_1^+ k^+ (k^+ - p_0^+ - p_1^+)}{k^+ q^+ p_0^+ (p_1^+ - k^+)} \\
&\times \int_{\mathbf{x}, \mathbf{x}', \mathbf{z}} iA^i(\mathbf{x} - \mathbf{z}) \mathcal{K}(\mathbf{x} - \mathbf{z}, \Delta_P) e^{i\mathbf{k}_\perp \cdot (\mathbf{x} - \mathbf{x}')} e^{i\frac{k^+}{p_0^+} \mathbf{k}_\perp \cdot (\mathbf{x} - \mathbf{z})} \left(\frac{N_c^2}{2} s_{\mathbf{x}\mathbf{z}} s_{\mathbf{z}\mathbf{x}'} - \frac{1}{2} s_{\mathbf{x}\mathbf{x}'} + C_F N_c \right), \tag{9.64}
\end{aligned}$$

and:

$$\begin{aligned}
\text{Tr} \mathcal{M}_{\text{LO}}^{\lambda\dagger} \mathcal{M}_{13}^\lambda &= -g_{\text{ew}}^2 \alpha_s 8p_1^+ p_0^+ \left(\frac{q^+ \mathbf{P}_\perp^i}{p_0^+ \mathbf{P}_\perp^2 + p_1^+ M^2} + \frac{q^+ \mathbf{q}^i}{p_0^+ \mathbf{q}^2 + p_1^+ M^2} \right) \\
&\times \int_0^{p_1^+} dk^+ \frac{2(k^+ - p_1^+) \left(q^+ (k^+)^2 - k^+ (p_0^+ + p_1^+)^2 + 2p_1^+ \left((p_0^+)^2 + (p_1^+)^2 \right) \right)}{(p_1^+)^3 q^+ (p_0^+ - k^+)} \\
&\times \int_{\mathbf{x}, \mathbf{x}', \mathbf{z}} iA^i(\mathbf{x} - \mathbf{z}) \mathcal{K}(\mathbf{x} - \mathbf{z}, \Delta_P) e^{i\mathbf{k}_\perp \cdot (\mathbf{x} - \mathbf{x}')} e^{i\frac{k^+}{p_1^+} \mathbf{k}_\perp \cdot (\mathbf{x} - \mathbf{z})} \left(\frac{N_c^2}{2} s_{\mathbf{x}\mathbf{z}} s_{\mathbf{z}\mathbf{x}'} - \frac{1}{2} s_{\mathbf{x}\mathbf{x}'} + C_F N_c \right). \tag{9.65}
\end{aligned}$$

9.2 Real NLO corrections

9.2.1 Longitudinal polarization

Initial-state radiation. During the analysis of initial-state radiation in section 6, we have extracted the part of amplitude $\mathcal{M}_{\text{IS2}}^{0\eta}$ (5.4) that, upon squaring or multiplying with

amplitude $\mathcal{M}_{\text{IS1}}^{0\eta}$ (5.2), leads to collinear divergences. The collinear-safe leftovers yield the following finite contribution to the cross section:

$$\begin{aligned}
 & \int \text{PS}(\vec{p}_3) \text{Tr} \left(2\text{Re}(\mathcal{M}_{\text{IS1}}^{0\eta\dagger} \mathcal{M}_{\text{IS2,finite}}^{0\eta}) + 2\text{Re}(\mathcal{M}_{\text{IS2,coll}}^{0\eta\dagger} \mathcal{M}_{\text{IS2,finite}}^{0\eta}) + \left| \mathcal{M}_{\text{IS2,finite}}^{0\eta} \right|^2 \right) \\
 &= \frac{g_{em}^2 \alpha_s N_c C_F}{M^2} 8p_1^+ p_0^+ \text{Re} \int_{\mathbf{x}, \mathbf{x}'} \int_{\ell} \frac{1}{\ell^2} e^{-i\ell \cdot (\mathbf{x} - \mathbf{x}')} e^{-i\mathbf{k}_\perp \cdot (\mathbf{x} - \mathbf{x}')} (s_{\mathbf{x}'\mathbf{x}} + 1) \\
 & \times \left\{ \int_{k_{\min}^+}^{+\infty} \frac{dp_3^+}{p_3^+} \left(\frac{p_3^+}{p_{0R}^+} \right)^2 \frac{p_{0R}^+}{p_0^+} \left(\left(1 + \frac{2p_0^+}{p_3^+} \right)^2 + 1 \right) \right. \\
 & \times \left[-2 \frac{p_0^+ \mathbf{P}_\perp^2 - p_1^+ M^2}{p_0^+ \mathbf{P}_\perp^2 + p_1^+ M^2} + \frac{p_0^+ \mathbf{q}^2 - p_1^+ M^2}{p_0^+ \mathbf{q}^2 + p_1^+ M^2} \right. \\
 & \left. \left. + \frac{p_3^+ (q^+ \ell + p_0^+ \mathbf{q})^2 - p_0^+ p_1^+ p_3^+ M^2}{p_3^+ (q^+ \ell + p_0^+ \mathbf{q})^2 + p_1^+ q^+ p_{0R}^+ \ell^2 + p_0^+ p_1^+ p_3^+ M^2} \right] \right. \\
 & \times \left(\frac{p_3^+ (q^+ \ell + p_0^+ \mathbf{q})^2 - p_0^+ p_1^+ p_3^+ M^2}{p_3^+ (q^+ \ell + p_0^+ \mathbf{q})^2 + p_1^+ q^+ p_{0R}^+ \ell^2 + p_0^+ p_1^+ p_3^+ M^2} - \frac{p_0^+ \mathbf{q}^2 - p_1^+ M^2}{p_0^+ \mathbf{q}^2 + p_1^+ M^2} \right) \\
 & \left. + 4 \int_{k_{\min}^+}^{k_f^+} \frac{dp_3^+}{p_3^+} \left(-2 \frac{p_0^+ \mathbf{P}_\perp^2 - p_1^+ M^2}{p_0^+ \mathbf{P}_\perp^2 + p_1^+ M^2} + \frac{p_0^+ \mathbf{q}^2 - p_1^+ M^2}{p_0^+ \mathbf{q}^2 + p_1^+ M^2} \right) \frac{p_0^+ \mathbf{q}^2 - p_1^+ M^2}{p_0^+ \mathbf{q}^2 + p_1^+ M^2} \right\}. \tag{9.66}
 \end{aligned}$$

Diagrams $\mathcal{M}_{\text{IS3}}^{0\eta}$ (5.7) and $\mathcal{M}_{\text{IS4}}^{0\eta}$ (5.9) never lead to collinear singularities. Their sum, multiplied with its complex conjugate, traced and integrated over the gluon transverse momentum, reads:

$$\begin{aligned}
 & \int \text{PS}(\vec{p}_3) \text{Tr} \left| \mathcal{M}_{\text{IS3+4}}^{0\eta} \right|^2 = \frac{g_{em}^2 \alpha_s C_F N_c}{M^2} 8p_1^+ p_0^+ \int_{\mathbf{x}, \mathbf{x}'} e^{-i\mathbf{k}_\perp \cdot (\mathbf{x} - \mathbf{x}')} (s_{\mathbf{x}\mathbf{x}'} + 1) \\
 & \times \left\{ \int_{k_{\min}^+}^{+\infty} \frac{dp_3^+}{p_3^+} \left(\frac{p_3^+}{p_1^+ + p_3^+} \right)^2 \frac{p_{0R}^+}{p_0^+} e^{i \frac{p_3^+}{p_1^+ + p_3^+} \mathbf{q} \cdot (\mathbf{x} - \mathbf{x}')} \right. \\
 & \times \left[\left(\left(\frac{p_{0R}^+ \mathbf{q}^2 - (p_1^+ + p_3^+) M^2}{p_{0R}^+ \mathbf{q}^2 + (p_1^+ + p_3^+) M^2} \right)^2 \left(\left(1 + \frac{2p_1^+}{p_3^+} \right)^2 + 1 \right) \right. \right. \\
 & \left. \left. - \frac{4q^+ (p_1^+ + p_3^+) p_{0R}^+ \mathbf{q}^2 - (p_1^+ + p_3^+) M^2}{p_3^+ p_0^+ p_{0R}^+ \mathbf{q}^2 + (p_1^+ + p_3^+) M^2} + 2 \left(\frac{q^+}{p_0^+} \right)^2 \right) \mathcal{K}(\mathbf{x} - \mathbf{x}', \Delta_{\text{IS}}) \right. \\
 & \left. + 2 \frac{(p_1^+)^2 ((p_0^+)^2 + (p_1^+ + p_3^+)^2)}{(p_0^+)^2 (p_1^+ + p_3^+)^2} \mathbf{q}^2 \int_{\ell} \frac{e^{i\ell \cdot (\mathbf{x} - \mathbf{x}')}}{(\ell^2 + \Delta_{\text{IS}})^2} \right. \\
 & \left. + \frac{4p_1^+ (p_0^+ + p_3^+)}{p_0^+ (p_1^+ + p_3^+)} \int_{\ell} \frac{\mathbf{q} \cdot \ell}{(\ell^2 + \Delta_{\text{IS}})^2} e^{-i\ell \cdot (\mathbf{x} - \mathbf{x}')} \right. \\
 & \left. \times \left(\frac{p_{0R}^+ \mathbf{q}^2 - (p_1^+ + p_3^+) M^2}{p_{0R}^+ \mathbf{q}^2 + (p_1^+ + p_3^+) M^2} \frac{2(p_1^+)^2 + (2p_1^+ + p_3^+)(q^+ + p_3^+)}{p_3^+ p_{0R}^+} - \frac{q^+}{p_0^+} \right) \right] \\
 & \left. - 4 \int_{k_{\min}^+}^{k_f^+} \frac{dp_3^+}{p_3^+} \left(\frac{p_0^+ \mathbf{q}^2 - p_1^+ M^2}{p_0^+ \mathbf{q}^2 + p_1^+ M^2} \right)^2 \int_{\ell} \frac{e^{i\ell \cdot (\mathbf{x} - \mathbf{x}')}}{\ell^2} \right\}. \tag{9.67}
 \end{aligned}$$

Note that the integrals that appear in the above formula have analytical solutions in terms of Macdonald functions, which are easily obtained using the Schwinger trick together

with formula (A.5):

$$\begin{aligned} \mathcal{K}(\mathbf{x}, \Delta) &= \frac{1}{2\pi} K_0(\sqrt{\mathbf{x}^2 \Delta}), \\ \int_{\ell} \frac{e^{i\ell \cdot \mathbf{x}}}{(\ell^2 + \Delta)^2} &= \frac{1}{4\pi} \sqrt{\frac{\mathbf{x}^2}{\Delta}} K_1(\sqrt{\mathbf{x}^2 \Delta}), \\ \int_{\ell} \frac{\ell^i e^{i\ell \cdot \mathbf{x}}}{(\ell^2 + \Delta)^2} &= \frac{1}{4\pi} \frac{\mathbf{x}^i}{\sqrt{\mathbf{x}^2 \Delta}} \left(K_1(\sqrt{\mathbf{x}^2 \Delta}) - \frac{1}{2} \sqrt{\mathbf{x}^2 \Delta} K_0(\sqrt{\mathbf{x}^2 \Delta}) - \frac{1}{2} \sqrt{\mathbf{x}^2 \Delta} K_2(\sqrt{\mathbf{x}^2 \Delta}) \right). \end{aligned} \quad (9.68)$$

Moreover, we have a contribution from the following interference term:

$$\begin{aligned} &\int \text{PS}(\vec{p}_3) \text{Tr} 2\text{Re}(\mathcal{M}_{\text{IS}1+2}^{0\eta\dagger} \mathcal{M}_{\text{IS}3+4}^{0\eta}) \\ &= \frac{g_{\text{em}}^2 \alpha_s C_F N_c}{M^2} 8p_1^+ p_0^+ 2\text{Re} \int_{\mathbf{x}, \mathbf{x}'} e^{-i\mathbf{k}_{\perp} \cdot (\mathbf{x} - \mathbf{x}')} (s_{\mathbf{x}\mathbf{x}'} + 1) \\ &\quad \times \left\{ \int_{k_{\text{min}}^+}^{+\infty} \frac{dp_3^+}{p_3^+} \frac{p_3^+}{p_0^+} \frac{p_3^+}{p_1^+ + p_3^+} \int_{\mathbf{z}} e^{i\frac{p_3^+}{p_1^+ + p_3^+} \mathbf{q} \cdot (\mathbf{x} - \mathbf{z})} \int_{\ell_2} \frac{1}{\ell_2^2 + \Delta_{\text{IS}}} e^{-i\ell_2 \cdot (\mathbf{x} - \mathbf{z})} \int_{\ell} \frac{\ell^i}{\ell^2} e^{i\ell \cdot (\mathbf{x}' - \mathbf{z})} \right. \\ &\quad \times \left[-\frac{p_0^+ \mathbf{P}_{\perp}^2 - p_1^+ M^2}{p_0^+ \mathbf{P}_{\perp}^2 + p_1^+ M^2} + \frac{p_3^+ (q^+ \ell + p_0^+ \mathbf{q})^2 - p_3^+ p_1^+ p_0^+ M^2}{p_3^+ (q^+ \ell + p_0^+ \mathbf{q})^2 + p_1^+ q^+ p_{0R}^+ \ell^2 + p_1^+ p_3^+ p_0^+ M^2} \right] \\ &\quad \times \left[\left(\frac{p_{0R}^+ \mathbf{q}^2 - (p_1^+ + p_3^+) M^2}{p_{0R}^+ \mathbf{q}^2 + (p_1^+ + p_3^+) M^2} \left(\left(1 + \frac{2p_0^+}{p_3^+} \right) \left(1 + \frac{2p_1^+}{p_3^+} \right) + 1 \right) - \frac{q^+ 2(p_0^+ + p_3^+)}{p_0^+ p_3^+} \right) \ell_2^i \right. \\ &\quad \left. - \frac{2p_1^+ ((p_0^+)^2 + (p_3^+ + p_0^+)^2)}{p_3^+ p_0^+ (p_1^+ + p_3^+)} \mathbf{q}^i \right] \\ &\quad \left. + 4 \int_{k_{\text{min}}^+}^{k_f^+} \frac{dp_3^+}{p_3^+} \frac{p_0^+ \mathbf{P}_{\perp}^2 - p_1^+ M^2}{p_0^+ \mathbf{P}_{\perp}^2 + p_1^+ M^2} \frac{p_0^+ \mathbf{q}^2 - p_1^+ M^2}{p_0^+ \mathbf{q}^2 + p_1^+ M^2} \int_{\ell} \frac{e^{-i\ell \cdot (\mathbf{x} - \mathbf{x}')}}{\ell^2} \right\}. \end{aligned} \quad (9.69)$$

Final-state radiation. In section 7, we analyzed the collinear divergences in final-state radiation, and noted that the amplitudes $\mathcal{M}_{\text{FS}2}^{0\eta}$ (5.17) and $\mathcal{M}_{\text{FS}3}^{0\eta}$ (5.19) exhibit collinear-like behavior even when the gluon and the quark are not grouped inside the same jet. Indeed, even though the jet definition cuts off the collinear pole in this ‘outside-jet’ configuration, it still leads to logarithms that combine with the ‘inside-jet’ contributions. We have extracted the part of $\mathcal{M}_{\text{FS}2}^{0\eta}$ responsible for these ‘outside-jet’ logarithms. What is left after this extraction, as well as its interference with $\mathcal{M}_{\text{FS}3}^{0\eta}$, is completely finite. This results in the following, finite, contribution to the cross section:

$$\begin{aligned} &\int \text{PS}(\vec{p}_3) \left| \mathcal{M}_{\text{FS}2+3}^{0\eta} \right|^2 (1 - \theta_{\text{in}}(\vec{p}_1, \vec{p}_3)) - \lim_{\text{soft}} \int \text{PS}(\vec{p}_3) \left| \mathcal{M}_{\text{FS}2+3}^{0\eta} \right|^2 (1 - \theta_{\text{in}}(\vec{p}_1, \vec{p}_3)) \\ &= \frac{g_{\text{em}}^2 \alpha_s N_c C_F}{M^2} 8p_1^+ p_0^+ \int_{\mathbf{x}, \mathbf{x}'} e^{-i\mathbf{k}_{\perp} \cdot (\mathbf{x} - \mathbf{x}')} (s_{\mathbf{x}\mathbf{x}'} + 1) \\ &\quad \left\{ \int_{k_{\text{min}}^+}^{+\infty} \frac{dp_3^+}{p_3^+} \left(\frac{p_3^+}{p_1^+} \right)^2 \frac{p_{0R}^+}{p_0^+} \left(\left(1 + \frac{2p_1^+}{p_3^+} \right)^2 + 1 \right) \right. \\ &\quad \times \int_{\ell} \frac{1}{\ell^2} e^{-i(\ell + \frac{p_3^+}{p_1^+} \mathbf{P}_{\perp} + \frac{p_3^+}{p_0^+} \mathbf{k}_{\perp}) \cdot (\mathbf{x} - \mathbf{x}')} \theta \left(\ell^2 - \left(\frac{p_3^+}{p_1^+} \right)^2 \mathbf{P}_1^2 R^2 \right) \end{aligned}$$

$$\begin{aligned}
 & \times \left(\frac{p_{0R}^+ p_3^+}{q^+ p_0^+} \frac{(p_1^+ q^+ \ell + p_0^+ (p_1^+ + p_3^+) \mathbf{P}_\perp)^2}{p_{0R}^+ (p_1^+ + p_3^+) (p_1^+)^2} - M^2 - \frac{p_{0R}^+ \mathbf{q}^2 - (p_1^+ + p_3^+) M^2}{p_{0R}^+ \mathbf{q}^2 + (p_1^+ + p_3^+) M^2} \right)^2 \\
 & - \left(\frac{p_0^+ \mathbf{P}_\perp^2 - p_1^+ M^2}{p_0^+ \mathbf{P}_\perp^2 + p_1^+ M^2} - \frac{p_0^+ \mathbf{q}^2 - p_1^+ M^2}{p_0^+ \mathbf{q}^2 + p_1^+ M^2} \right)^2 4 \int_{k_{\min}^+}^{+\infty} \frac{dp_3^+}{p_3^+} \int_{\ell} \frac{e^{-i\ell \cdot (\mathbf{x} - \mathbf{x}')}}{\ell^2} \theta \left(\ell^2 - \left(\frac{p_3^+}{p_1^+} \right)^2 \mathbf{p}_1^2 R^2 \right) \\
 & + 4 \int_{k_{\min}^+}^{k_f^+} \frac{dp_3^+}{p_3^+} \left[\left(\frac{p_0^+ \mathbf{P}_\perp^2 - p_1^+ M^2}{p_0^+ \mathbf{P}_\perp^2 + p_1^+ M^2} \right)^2 - 2 \frac{p_0^+ \mathbf{P}_\perp^2 - p_1^+ M^2}{p_0^+ \mathbf{P}_\perp^2 + p_1^+ M^2} \frac{p_0^+ \mathbf{q}^2 - p_1^+ M^2}{p_0^+ \mathbf{q}^2 + p_1^+ M^2} \right] \int_{\ell} \frac{e^{-i\ell \cdot (\mathbf{x} - \mathbf{x}')}}{\ell^2} \Big\} \quad (9.70)
 \end{aligned}$$

Moreover, we have the following finite contributions to the cross section stemming from real final-state radiation amplitudes $\mathcal{M}_{\text{FS1}}^{0\eta}$ (5.11) and $\mathcal{M}_{\text{FS4}}^{0\eta}$ (5.28):

$$\begin{aligned}
 & \int \text{PS}(\vec{p}_3) \text{Tr} |\mathcal{M}_{\text{FS1+4}}^{0\eta}|^2 \\
 & = \frac{g_{\text{em}}^2 \alpha_s N_c C_F}{M^2} 8 p_1^+ p_0^+ \int_{\mathbf{x}, \mathbf{x}'} e^{-i\mathbf{k}_\perp \cdot (\mathbf{x} - \mathbf{x}')} (s_{\mathbf{x}\mathbf{x}'} + 1) \\
 & \quad \times \left\{ \int_{k_{\min}^+}^{+\infty} \frac{dp_3^+}{p_3^+} \left(\frac{p_3^+}{p_0^+} \right)^2 \frac{p_{0R}^+}{p_0^+} e^{-i\frac{p_3^+}{p_0^+} \mathbf{k}_\perp \cdot \mathbf{x}} \left[\left(\frac{p_0^+ \mathbf{P}_\perp^2 - p_1^+ M^2}{p_0^+ \mathbf{P}_\perp^2 + p_1^+ M^2} \right)^2 \left(\left(1 + \frac{2p_0^+}{p_3^+} \right)^2 + 1 \right) \right. \right. \\
 & \quad + 2 \left(\frac{q^+}{p_1^+ + p_3^+} \right)^2 + \frac{4q^+ p_0^+}{p_3^+ (p_1^+ + p_3^+)} \frac{p_0^+ \mathbf{P}_\perp^2 - p_1^+ M^2}{p_0^+ \mathbf{P}_\perp^2 + p_1^+ M^2} \Big] \mathcal{K}(\mathbf{x} - \mathbf{x}', \Delta_{\text{FS}}) \\
 & \quad + \frac{2(p_{0R}^+)^2 ((p_1^+)^2 + (p_1^+ + p_3^+)^2)}{(p_1^+)^2 (p_1^+ + p_3^+)^2} \mathbf{P}_\perp^2 \int_{\ell} \frac{e^{i\ell \cdot (\mathbf{x} - \mathbf{x}')}}{(\ell^2 + \Delta_{\text{FS}})^2} \\
 & \quad + \frac{4p_{0R}^+}{p_1^+ + p_3^+} \left(\frac{p_0^+ \mathbf{P}_\perp^2 - p_1^+ M^2}{p_0^+ \mathbf{P}_\perp^2 + p_1^+ M^2} \frac{2(p_1^+)^2 + (2p_1^+ + p_3^+)(p_3^+ + q^+)}{p_1^+ p_3^+} - \frac{q^+}{p_1^+ + p_3^+} \right) \\
 & \quad \times \int_{\ell} \frac{\mathbf{P}_\perp \cdot \ell}{(\ell^2 + \Delta_{\text{FS}})^2} e^{-i\ell \cdot (\mathbf{x} - \mathbf{x}')} \Big] \\
 & \quad \left. - 4 \int_{k_{\min}^+}^{k_f^+} \frac{dp_3^+}{p_3^+} \left(\frac{p_0^+ \mathbf{P}_\perp^2 - p_1^+ M^2}{p_0^+ \mathbf{P}_\perp^2 + p_1^+ M^2} \right)^2 \int_{\ell} \frac{e^{i\ell \cdot (\mathbf{x} - \mathbf{x}')}}{\ell^2} \right\}, \quad (9.71)
 \end{aligned}$$

and:

$$\begin{aligned}
 & \int \text{PS}(\vec{p}_3) \text{Tr} 2\text{Re}(\mathcal{M}_{\text{FS2+3}}^{0\eta\dagger} \mathcal{M}_{\text{FS1+4}}^{0\eta}) \\
 & = \frac{g_{\text{em}}^2 \alpha_s N_c C_F}{M^2} 8 p_1^+ p_0^+ 2\text{Re} \int_{\mathbf{x}, \mathbf{x}'} e^{-i\mathbf{k}_\perp \cdot (\mathbf{x} - \mathbf{x}')} (s_{\mathbf{x}\mathbf{x}'} + 1) \\
 & \quad \times \left\{ \int_{k_{\min}^+}^{+\infty} \frac{dp_3^+}{p_3^+} \int_{\mathbf{z}} \frac{(p_3^+)^2}{p_1^+ p_0^+} \frac{p_{0R}^+}{p_0^+} e^{-i\frac{p_3^+}{p_0^+} \mathbf{k}_\perp \cdot (\mathbf{x} - \mathbf{z})} \int_{\mathbf{p}_3} e^{i\mathbf{p}_3 \cdot (\mathbf{x}' - \mathbf{z})} \right. \\
 & \quad \times \frac{\mathbf{p}_3 - \frac{p_3^+}{p_1^+} \mathbf{p}_1}{\left(\mathbf{p}_3 - \frac{p_3^+}{p_1^+} \mathbf{p}_1 \right)^2} \left[\frac{p_3^+ \left(\mathbf{p}_3 + \mathbf{p}_1 - \frac{p_1^+ + p_3^+}{q^+} \mathbf{q} \right)^2 - p_3^+ \frac{p_{0R}^+ (p_1^+ + p_3^+)}{(q^+)^2} M^2}{\frac{p_1^+ p_{0R}^+}{q^+} \left(\mathbf{p}_3 - \frac{p_3^+}{p_1^+} \mathbf{p}_1 \right)^2 + p_3^+ \left(\mathbf{p}_3 + \mathbf{p}_1 - \frac{p_1^+ + p_3^+}{q^+} \mathbf{q} \right)^2 + p_3^+ \frac{p_{0R}^+ (p_1^+ + p_3^+)}{(q^+)^2} M^2} \right. \\
 & \quad \left. \left. - \frac{p_{0R}^+ \mathbf{q}^2 - (p_1^+ + p_3^+) M^2}{p_{0R}^+ \mathbf{q}^2 + (p_1^+ + p_3^+) M^2} \right] \right\}
 \end{aligned}$$

$$\begin{aligned}
 & \times \left[\left(\frac{p_0^+ \mathbf{P}_\perp^2 - p_1^+ M^2}{p_0^+ \mathbf{P}_\perp^2 + p_1^+ M^2} \left(\left(1 + \frac{2p_1^+}{p_3^+} \right) \left(1 + \frac{2p_0^+}{p_3^+} \right) + 1 \right) - \frac{q^+}{p_1^+ + p_3^+} \frac{2p_1^+}{p_3^+} \right) iA^i(\mathbf{x} - \mathbf{z}, \Delta_{\text{FS}}) \right. \\
 & \left. - p_{0R}^+ \frac{2p_1^+ + p_3^+}{p_1^+(p_1^+ + p_3^+)} \mathcal{K}(\mathbf{x} - \mathbf{z}, \Delta_{\text{FS}}) \mathbf{P}_\perp^i \left(1 + \frac{2p_1^+}{p_3^+} + \frac{p_3^+}{2p_1^+ + p_3^+} \right) \right] \\
 & + 4 \int_{k_{\min}^+}^{k_f^+} \frac{dp_3^+}{p_3^+} \frac{p_0^+ \mathbf{q}^2 - p_1^+ M^2}{p_0^+ \mathbf{q}^2 + p_1^+ M^2} \frac{p_0^+ \mathbf{P}_\perp^2 - p_1^+ M^2}{p_0^+ \mathbf{P}_\perp^2 + p_1^+ M^2} \int_{\ell} \frac{e^{i\ell \cdot (\mathbf{x} - \mathbf{x}')}}{\ell^2} \Bigg\}. \tag{9.72}
 \end{aligned}$$

Initial-final state radiation interference. Finally, in our calculation, the interference between initial- and final state radiation never leads to collinear divergences, although it constitutes an important contribution to the high-energy resummation. We have:

$$\begin{aligned}
 & \int \text{PS}(\vec{p}_3) \text{Tr} 2\text{Re}(\mathcal{M}_{\text{IS1+2}}^{0\eta\dagger} \mathcal{M}_{\text{FS1+4}}^{0\eta}) \\
 & = \frac{g_{\text{em}}^2 \alpha_s}{M^2} 8p_1^+ p_0^+ 2\text{Re} \int_{\mathbf{x}, \mathbf{x}', \mathbf{z}} e^{-i\mathbf{k}_\perp \cdot (\mathbf{x} - \mathbf{x}')} \left(\frac{N_c^2}{2} s_{\mathbf{xz}} s_{\mathbf{zx}'} - \frac{1}{2} s_{\mathbf{xx}'} + C_F N_c \right) \\
 & \times \left\{ \int_{k_{\min}^+}^{+\infty} \frac{dp_3^+}{p_3^+} \left(\frac{p_3^+}{p_0^+} \right)^2 \int_{\mathbf{p}_3} \frac{e^{-i\mathbf{p}_3 \cdot (\mathbf{x} - \mathbf{z})}}{\left(\mathbf{p}_3 - \frac{p_3^+}{p_0^+} \mathbf{k}_\perp \right)^2 + \Delta_{\text{FS}}} \int_{\ell} \frac{\ell^j}{\ell^2} e^{i\ell \cdot (\mathbf{x}' - \mathbf{z})} \right. \\
 & \times \left[- \frac{p_0^+ \mathbf{P}_\perp^2 - p_1^+ M^2}{p_0^+ \mathbf{P}_\perp^2 + p_1^+ M^2} + \frac{p_3^+ (q^+ \ell + p_0^+ \mathbf{q})^2 - p_1^+ p_0^+ p_3^+ M^2}{p_3^+ (q^+ \ell + p_0^+ \mathbf{q})^2 + p_1^+ q^+ p_{0R}^+ \ell^2 + p_1^+ p_3^+ p_0^+ M^2} \right] \\
 & \times \left[\left(\frac{p_0^+ \mathbf{P}_\perp^2 - p_1^+ M^2}{p_0^+ \mathbf{P}_\perp^2 + p_1^+ M^2} \left(\left(1 + \frac{2p_0^+}{p_3^+} \right)^2 + 1 \right) - \frac{q^+}{p_1^+ + p_3^+} \frac{2p_0^+}{p_3^+} \right) \left(\mathbf{p}_3 - \frac{p_3^+}{p_0^+} \mathbf{k}_\perp \right)^j \right. \\
 & \left. - p_{0R}^+ \frac{2p_1^+ + p_3^+}{p_1^+(p_1^+ + p_3^+)} \mathbf{P}_\perp^j \left(1 + \frac{2p_0^+}{p_3^+} + \frac{p_3^+}{2p_1^+ + p_3^+} \right) \right] \\
 & \left. + 4 \int_{k_{\min}^+}^{k_f^+} \frac{dp_3^+}{p_3^+} \left(\frac{p_0^+ \mathbf{P}_\perp^2 - p_1^+ M^2}{p_0^+ \mathbf{P}_\perp^2 + p_1^+ M^2} \right)^2 A^i(\mathbf{x} - \mathbf{z}) A^i(\mathbf{x}' - \mathbf{z}) \right\}. \tag{9.73}
 \end{aligned}$$

Moreover:

$$\begin{aligned}
 & \int \text{PS}(\vec{p}_3) \text{Tr} 2\text{Re}(\mathcal{M}_{\text{IS1+2}}^{0\eta\dagger} \mathcal{M}_{\text{FS2+3}}^{0\eta}) \\
 & = \frac{g_{\text{em}}^2 \alpha_s}{M^2} 8p_1^+ p_0^+ 2\text{Re} \int_{\mathbf{x}, \mathbf{x}', \mathbf{z}} e^{i\mathbf{k}_\perp \cdot (\mathbf{x} - \mathbf{x}')} \left(\frac{N_c^2}{2} s_{\mathbf{xz}} s_{\mathbf{zx}'} - \frac{1}{2} s_{\mathbf{xx}'} + C_F N_c \right) \\
 & \times \left\{ \int_{k_{\min}^+}^{+\infty} \frac{dp_3^+}{p_3^+} \frac{p_3^+}{p_0^+} \frac{p_3^+}{p_1^+} \left(\left(1 + \frac{2p_0^+}{p_3^+} \right) \left(1 + \frac{2p_1^+}{p_3^+} \right) + 1 \right) \right. \\
 & \times \int_{\mathbf{p}_3} e^{-i\mathbf{p}_3 \cdot (\mathbf{x} - \mathbf{z})} \frac{\mathbf{p}_3^i - \frac{p_3^+}{p_1^+} \mathbf{p}_1^i}{\left(\mathbf{p}_3 - \frac{p_3^+}{p_1^+} \mathbf{p}_1 \right)^2} \int_{\ell} e^{i\ell \cdot (\mathbf{x}' - \mathbf{z})} \frac{\ell^i}{\ell^2} \\
 & \times \left[- \frac{p_0^+ \mathbf{P}_\perp^2 - p_1^+ M^2}{p_0^+ \mathbf{P}_\perp^2 + p_1^+ M^2} + \frac{p_3^+ (q^+ \ell + p_0^+ \mathbf{q})^2 - p_1^+ p_3^+ p_0^+ M^2}{p_1^+ q^+ p_{0R}^+ \ell^2 + p_3^+ (q^+ \ell + p_0^+ \mathbf{q})^2 + p_1^+ p_3^+ p_0^+ M^2} \right] \\
 & \times \left[\frac{p_3^+ \left(\mathbf{p}_3 + \mathbf{p}_1 - \frac{p_1^+ + p_3^+}{q^+} \mathbf{q} \right)^2 - p_3^+ \frac{p_{0R}^+ (p_1^+ + p_3^+)}{(q^+)^2} M^2}{\frac{p_1^+ p_{0R}^+}{q^+} \left(\mathbf{p}_3 - \frac{p_3^+}{p_1^+} \mathbf{p}_1 \right)^2 + p_3^+ \left(\mathbf{p}_3 + \mathbf{p}_1 - \frac{p_1^+ + p_3^+}{q^+} \mathbf{q} \right)^2 + p_3^+ \frac{p_{0R}^+ (p_1^+ + p_3^+)}{(q^+)^2} M^2} - \frac{p_{0R}^+ \mathbf{q}^2 - (p_1^+ + p_3^+) M^2}{p_{0R}^+ \mathbf{q}^2 + (p_1^+ + p_3^+) M^2} \right] \\
 & \left. - 4 \int_{k_{\min}^+}^{k_f^+} \frac{dp_3^+}{p_3^+} \frac{p_0^+ \mathbf{P}_\perp^2 - p_1^+ M^2}{p_0^+ \mathbf{P}_\perp^2 + p_1^+ M^2} \frac{p_0^+ \mathbf{q}^2 - p_1^+ M^2}{p_0^+ \mathbf{q}^2 + p_1^+ M^2} A^i(\mathbf{x} - \mathbf{z}) A^i(\mathbf{x}' - \mathbf{z}) \right\}. \tag{9.74}
 \end{aligned}$$

Furthermore:

$$\begin{aligned}
 & \int \text{PS}(\vec{p}_3) \text{Tr} 2\text{Re}(\mathcal{M}_{\text{IS}3+4}^{0\eta\dagger} \mathcal{M}_{\text{FS}1+4}^{0\eta}) \\
 &= \frac{g_{\text{em}}^2 \alpha_s}{M^2} 8p_1^+ p_0^+ 2\text{Re} \int_{\mathbf{x}, \mathbf{x}', \mathbf{z}} e^{-i\mathbf{k}_\perp \cdot (\mathbf{x} - \mathbf{x}')} \left(\frac{N_c^2}{2} s_{\mathbf{x}\mathbf{z}} s_{\mathbf{z}\mathbf{x}'} - \frac{1}{2} s_{\mathbf{x}\mathbf{x}'} + C_F N_c \right) \\
 & \times \left\{ \int_{k_{\text{min}}^+}^{+\infty} \frac{dp_3^+}{p_3^+} \frac{p_{0R}^+}{p_1^+ + p_3^+} \left(\frac{p_3^+}{p_0^+} \right)^2 e^{-i\frac{p_3^+}{p_1^+ + p_3^+} \mathbf{q} \cdot (\mathbf{x}' - \mathbf{z})} e^{-i\frac{p_3^+}{p_0^+} \mathbf{k}_\perp \cdot (\mathbf{x} - \mathbf{z})} \right. \\
 & \times \left[\left(\frac{p_{0R}^+ \mathbf{q}^2 - (p_1^+ + p_3^+) M^2}{p_{0R}^+ \mathbf{q}^2 + (p_1^+ + p_3^+) M^2} \frac{p_0^+ \mathbf{P}_\perp^2 - p_1^+ M^2}{p_0^+ \mathbf{P}_\perp^2 + p_1^+ M^2} \left(\left(1 + \frac{2p_1^+}{p_3^+} \right) \left(1 + \frac{2p_0^+}{p_3^+} \right) + 1 \right) \right. \right. \\
 & \left. \left. - 2 \frac{p_0^+ + p_3^+}{p_3^+} \frac{q^+}{p_0^+} \frac{p_0^+ \mathbf{P}_\perp^2 - p_1^+ M^2}{p_0^+ \mathbf{P}_\perp^2 + p_1^+ M^2} - \frac{2p_1^+}{p_3^+} \frac{q^+}{p_1^+ + p_3^+} \frac{p_{0R}^+ \mathbf{q}^2 - (p_1^+ + p_3^+) M^2}{p_{0R}^+ \mathbf{q}^2 + (p_1^+ + p_3^+) M^2} \right) \right. \\
 & \times A^i(\mathbf{x}' - \mathbf{z}, \Delta_{\text{IS}}) A^i(\mathbf{x} - \mathbf{z}, \Delta_{\text{FS}}) \\
 & \left. + 2 \frac{p_{0R}^+}{p_1^+} \left(\frac{p_{0R}^+ \mathbf{q}^2 - (p_1^+ + p_3^+) M^2}{p_{0R}^+ \mathbf{q}^2 + (p_1^+ + p_3^+) M^2} \frac{(p_1^+)^2 + (p_1^+ + p_3^+)^2}{p_3^+ (p_1^+ + p_3^+)} - \frac{q^+}{p_0^+} \right) \right. \\
 & \times \mathbf{P}_\perp^i A^i(\mathbf{x}' - \mathbf{z}, \Delta_{\text{IS}}) \mathcal{K}(\mathbf{x} - \mathbf{z}, \Delta_{\text{FS}}) \\
 & \left. - \frac{2p_1^+}{p_1^+ + p_3^+} \left(\frac{p_0^+ \mathbf{P}_\perp^2 - p_1^+ M^2}{p_0^+ \mathbf{P}_\perp^2 + p_1^+ M^2} \frac{2(p_0^+)^2 + p_3^+ (p_3^+ + 2p_0^+)}{p_3^+ p_0^+} - \frac{q^+}{p_1^+ + p_3^+} \right) \right. \\
 & \times \mathbf{q}^i A^i(\mathbf{x} - \mathbf{z}, \Delta_{\text{FS}}) \mathcal{K}(\mathbf{x}' - \mathbf{z}, \Delta_{\text{IS}}) \\
 & \left. + \frac{2p_{0R}^+ (2p_1^+ p_{0R}^+ + p_3^+ q^+)}{p_0^+ (p_1^+ + p_3^+)^2} \mathbf{q} \cdot \mathbf{P}_\perp \times \mathcal{K}(\mathbf{x}' - \mathbf{z}, \Delta_{\text{IS}}) \mathcal{K}(\mathbf{x} - \mathbf{z}, \Delta_{\text{FS}}) \right] \\
 & \left. - 4 \int_{k_{\text{min}}^+}^{k_f^+} \frac{dp_3^+}{p_3^+} \frac{p_0^+ \mathbf{q}^2 - p_1^+ M^2}{p_0^+ \mathbf{q}^2 + p_1^+ M^2} \frac{p_0^+ \mathbf{P}_\perp^2 - p_1^+ M^2}{p_0^+ \mathbf{P}_\perp^2 + p_1^+ M^2} A^i(\mathbf{x}' - \mathbf{z}) A^i(\mathbf{x} - \mathbf{z}) \right\}. \tag{9.75}
 \end{aligned}$$

The final contribution is:

$$\begin{aligned}
 & \int \text{PS}(\vec{p}_3) \text{Tr} 2\text{Re}(\mathcal{M}_{\text{IS}3+4}^{0\eta\dagger} \mathcal{M}_{\text{FS}2+3}^{0\eta}) \\
 &= \frac{g_{\text{em}}^2 \alpha_s}{M^2} 8p_1^+ p_0^+ 2\text{Re} \int_{\mathbf{x}, \mathbf{x}', \mathbf{z}} e^{-i\mathbf{k}_\perp \cdot (\mathbf{x} - \mathbf{x}')} \left(\frac{N_c^2}{2} s_{\mathbf{x}\mathbf{z}} s_{\mathbf{z}\mathbf{x}'} - \frac{1}{2} s_{\mathbf{x}\mathbf{x}'} + C_F N_c \right) \\
 & \times \left\{ \int_{k_{\text{min}}^+}^{+\infty} \frac{dp_3^+}{p_3^+} \frac{p_3^+}{p_1^+ + p_3^+} \frac{p_3^+}{p_1^+} \frac{p_{0R}^+}{p_0^+} e^{-i\frac{p_3^+}{p_1^+ + p_3^+} \mathbf{q} \cdot (\mathbf{x}' - \mathbf{z})} \int_{\mathbf{P}_3} \frac{\mathbf{P}_3^j - \frac{p_3^+}{p_1^+} \mathbf{P}_1^j}{\left(\mathbf{P}_3 - \frac{p_3^+}{p_1^+} \mathbf{P}_1 \right)^2} e^{-i\mathbf{P}_3 \cdot (\mathbf{x} - \mathbf{z})} \right. \\
 & \times \left[\left(-\frac{p_{0R}^+ \mathbf{q}^2 - (p_1^+ + p_3^+) M^2}{p_{0R}^+ \mathbf{q}^2 + (p_1^+ + p_3^+) M^2} \left(\left(1 + \frac{2p_1^+}{p_3^+} \right)^2 + 1 \right) + 2 \frac{q^+}{p_0^+} \frac{p_1^+ + p_3^+}{p_3^+} \right) i A^j(\mathbf{x}' - \mathbf{z}, \Delta_{\text{IS}}) \right. \\
 & \left. - p_1^+ \frac{2p_0^+ + p_3^+}{p_0^+ (p_1^+ + p_3^+)} \mathbf{q}^j \mathcal{K}(\mathbf{x}' - \mathbf{z}, \Delta_{\text{IS}}) \left(1 + \frac{2p_1^+}{p_3^+} + \frac{p_3^+}{2p_0^+ + p_3^+} \right) \right] \\
 & \times \left[\frac{p_3^+ \left(\mathbf{P}_3 + \mathbf{P}_1 - \frac{p_1^+ + p_3^+}{q^+} \mathbf{q} \right)^2 - p_3^+ \frac{p_{0R}^+ (p_1^+ + p_3^+)}{(q^+)^2} M^2}{\frac{p_1^+ p_{0R}^+}{q^+} \left(\mathbf{P}_3 - \frac{p_3^+}{p_1^+} \mathbf{P}_1 \right)^2 + p_3^+ \left(\mathbf{P}_3 + \mathbf{P}_1 - \frac{p_1^+ + p_3^+}{q^+} \mathbf{q} \right)^2 + p_3^+ \frac{p_{0R}^+ (p_1^+ + p_3^+)}{(q^+)^2} M^2} \right. \\
 & \left. - \frac{p_{0R}^+ \mathbf{q}^2 - (p_1^+ + p_3^+) M^2}{p_{0R}^+ \mathbf{q}^2 + (p_1^+ + p_3^+) M^2} \right] + 4 \int_{k_{\text{min}}^+}^{k_f^+} \frac{dp_3^+}{p_3^+} \left(\frac{p_0^+ \mathbf{q}^2 - p_1^+ M^2}{p_0^+ \mathbf{q}^2 + p_1^+ M^2} \right)^2 A^i(\mathbf{x}' - \mathbf{z}) A^i(\mathbf{x} - \mathbf{z}) \left\}. \tag{9.76}
 \end{aligned}$$

9.2.2 Transverse polarization

Initial-state radiation. Firstly, we have the finite leftovers of the initial-state diagrams (eqs. (5.3) and (5.5)) that constituted the real part of the DGLAP equations:

$$\begin{aligned}
 & \int \text{PS}(\vec{p}_3) \text{Tr} \left(2\text{Re}(\mathcal{M}_{\text{IS1}}^{\lambda\eta\dagger} \mathcal{M}_{\text{IS2,finite}}^{\lambda\eta}) + 2\text{Re}(\mathcal{M}_{\text{IS2,coll}}^{\lambda\eta\dagger} \mathcal{M}_{\text{IS2,finite}}^{\lambda\eta}) + \left| \mathcal{M}_{\text{IS2,finite}}^{\lambda\eta} \right|^2 \right) \\
 &= g_{em}^2 \alpha_s N_c C_F 8 p_0^+ p_1^+ \left(\left(1 + \frac{2p_1^+}{q^+}\right)^2 + 1 \right) \int_{\mathbf{x}, \mathbf{x}'} e^{-i\mathbf{k}_\perp \cdot (\mathbf{x} - \mathbf{x}')} (s_{\mathbf{x}'\mathbf{x}} + 1) \int_{\ell} \frac{e^{-i\ell \cdot (\mathbf{x} - \mathbf{x}')}}{\ell^2} \\
 & \quad \left\{ \int_{k_{\min}^+}^{+\infty} \frac{dp_3^+}{p_3^+} \frac{(p_3^+)^2}{p_{0R}^+ p_0^+} \left(\left(1 + \frac{2p_0^+}{p_3^+}\right)^2 + 1 \right) \right. \\
 & \quad \times \left(2 \frac{q^+ \mathbf{P}_\perp^{\bar{\lambda}}}{p_0^+ \mathbf{P}_\perp^2 + p_1^+ M^2} + \frac{q^+ \mathbf{q}^{\bar{\lambda}}}{p_0^+ \mathbf{q}^2 + p_1^+ M^2} \right. \\
 & \quad \left. \left. + \frac{(q^+)^2 p_3^+ (\ell^{\bar{\lambda}} + \frac{p_0^+}{q^+} \mathbf{q}^{\bar{\lambda}})}{p_3^+ (q^+ \ell + p_0^+ \mathbf{q})^2 + p_1^+ q^+ p_{0R}^+ \ell^2 + p_1^+ p_3^+ p_0^+ M^2} \right) \right. \\
 & \quad \times \left(\frac{(q^+)^2 p_3^+ (\ell^{\bar{\lambda}} + \frac{p_0^+}{q^+} \mathbf{q}^{\bar{\lambda}})}{p_3^+ (q^+ \ell + p_0^+ \mathbf{q})^2 + p_1^+ q^+ p_{0R}^+ \ell^2 + p_1^+ p_3^+ p_0^+ M^2} - \frac{q^+ \mathbf{q}^{\bar{\lambda}}}{p_0^+ \mathbf{q}^2 + p_1^+ M^2} \right) \\
 & \quad \left. \left. + 4 \int_{k_{\min}^+}^{k_f^+} \frac{dp_3^+}{p_3^+} \left(2 \frac{q^+ \mathbf{P}_\perp^{\bar{\lambda}}}{p_0^+ \mathbf{P}_\perp^2 + p_1^+ M^2} + \frac{q^+ \mathbf{q}^{\bar{\lambda}}}{p_0^+ \mathbf{q}^2 + p_1^+ M^2} \right) \frac{q^+ \mathbf{q}^{\bar{\lambda}}}{p_0^+ \mathbf{q}^2 + p_1^+ M^2} \right\}. \tag{9.77}
 \end{aligned}$$

where we used eq. (B.12). Similarly, we obtain for the contribution of amplitudes $\mathcal{M}_{\text{IS3}}^{\lambda\eta}$ (5.8) and $\mathcal{M}_{\text{IS4}}^{\lambda\eta}$ (5.10):

$$\begin{aligned}
 & \int \text{PS}(\vec{p}_3) \text{Tr} \left| \mathcal{M}_{\text{IS3+4}}^{\lambda\eta} \right|^2 \\
 &= g_{em}^2 \alpha_s N_c C_F 8 p_1^+ p_0^+ \int_{\mathbf{x}, \mathbf{x}'} e^{-i\mathbf{k}_\perp \cdot (\mathbf{x} - \mathbf{x}')} (s_{\mathbf{x}\mathbf{x}'} + 1) \\
 & \quad \left\{ \int_{k_{\min}^+}^{+\infty} \frac{dp_3^+}{p_3^+} \left(\frac{p_3^+}{p_1^+ + p_3^+} \right)^2 \frac{p_{0R}^+}{p_0^+} \int_{\mathbf{z}} e^{i \frac{p_3^+}{p_1^+ + p_3^+} \mathbf{q} \cdot (\mathbf{x} - \mathbf{x}')} \right. \\
 & \quad \times \left[\left(\left(1 + \frac{2p_1^+}{p_3^+}\right)^2 + 1 \right) \left(\left(1 + 2 \frac{p_1^+ + p_3^+}{q^+}\right)^2 + 1 \right) \frac{(q^+)^2 \mathbf{q}^2}{(p_{0R}^+ \mathbf{q}^2 + (p_1^+ + p_3^+) M^2)^2} A^i(\mathbf{x} - \mathbf{z}, \Delta_{\text{IS}}) A^i(\mathbf{x}' - \mathbf{z}, \Delta_{\text{IS}}) \right. \\
 & \quad + 4 \left(\frac{p_1^+}{p_0^+ (p_1^+ + p_3^+)} \right)^2 \left((p_0^+)^2 + (p_1^+ + p_3^+)^2 \right) \mathcal{K}(\mathbf{x} - \mathbf{z}, \Delta_{\text{IS}}) \mathcal{K}(\mathbf{x}' - \mathbf{z}, \Delta_{\text{IS}}) \\
 & \quad + \frac{p_1^+ q^+}{p_{0R}^+ \mathbf{q}^2 + (p_1^+ + p_3^+) M^2} \mathbf{q}^i \left(i A^i(\mathbf{x}' - \mathbf{z}, \Delta_{\text{IS}}) \mathcal{K}(\mathbf{x} - \mathbf{z}, \Delta_{\text{IS}}) - i A^i(\mathbf{x} - \mathbf{z}, \Delta_{\text{IS}}) \mathcal{K}(\mathbf{x}' - \mathbf{z}, \Delta_{\text{IS}}) \right) \\
 & \quad \times \left(\left(\frac{1}{p_1^+ + p_3^+} + \frac{1}{p_0^+} \right) \left(\left(1 + \frac{2p_1^+}{p_3^+}\right) \left(1 + 2 \frac{p_1^+ + p_3^+}{q^+}\right) - 1 \right) \right. \\
 & \quad \left. \left. + \left(\frac{1}{p_1^+ + p_3^+} - \frac{1}{p_0^+} \right) \left(\frac{2p_1^+}{p_3^+} - 2 \frac{p_1^+ + p_3^+}{q^+} \right) \right) \right] \\
 & \quad \left. - \left(\left(1 + 2 \frac{p_1^+}{q^+}\right)^2 + 1 \right) 4 \int_{k_{\min}^+}^{k_f^+} \frac{dp_3^+}{p_3^+} \frac{(q^+)^2 \mathbf{q}^2}{(p_0^+ \mathbf{q}^2 + p_1^+ M^2)^2} \int_{\ell} \frac{e^{-i\ell \cdot (\mathbf{x} - \mathbf{x}')}}{\ell^2} \right\} \tag{9.78}
 \end{aligned}$$

Furthermore, the interference terms read, adapting identity (B.11):

$$\begin{aligned}
 & \int \text{PS}(\vec{p}_3) \text{Tr} 2\text{Re}(\mathcal{M}_{\text{IS}1+2}^{\lambda\eta\dagger} \mathcal{M}_{\text{IS}3+4}^{\lambda\eta}) \\
 &= g_{\text{em}}^2 \alpha_s 8p_1^+ p_0^+ 2\text{Re} \int_{\mathbf{x}, \mathbf{x}', \mathbf{z}} e^{-i\mathbf{k}_\perp \cdot (\mathbf{x} - \mathbf{x}')} C_F N_c (s_{\mathbf{x}\mathbf{x}'} + 1) \int_{\ell} e^{i\ell \cdot (\mathbf{x}' - \mathbf{z})} \frac{\ell^{\eta'}}{\ell^2} \\
 & \quad \times \left\{ \int_{k_{\text{min}}^+}^{+\infty} \frac{dp_3^+}{p_3^+} \frac{p_3^+}{p_1^+ + p_3^+} \frac{p_3^+}{p_0^+} e^{i\frac{p_3^+}{p_1^+ + p_3^+} \mathbf{q} \cdot (\mathbf{x} - \mathbf{z})} \right. \\
 & \quad \times \left[\frac{q^+ \mathbf{P}_\perp^{\lambda'}}{p_0^+ \mathbf{P}_\perp^2 + p_1^+ M^2} + \frac{(q^+)^2 p_3^+ \left(\ell^{\lambda'} + \frac{p_0^+}{q^+} \mathbf{q}^{\lambda'} \right)}{p_3^+ (q^+ \ell + p_0^+ \mathbf{q})^2 + p_1^+ q^+ p_{0R}^+ \ell^2 + p_1^+ p_3^+ p_0^+ M^2} \right] \\
 & \quad \times \left[\frac{q^+ \mathbf{q}^{\bar{\lambda}}}{p_{0R}^+ \mathbf{q}^2 + (p_1^+ + p_3^+) M^2} \left(\left(1 + \frac{2p_1^+}{q^+} \right) \left(1 + 2\frac{p_1^+ + p_3^+}{q^+} \right) + 1 \right) \right. \\
 & \quad \times \left(\left(1 + \frac{2p_0^+}{p_3^+} \right) \left(1 + \frac{2p_1^+}{p_3^+} \right) + 1 \right) \delta^{\bar{\lambda}\lambda'} \delta^{\bar{\eta}\eta'} i A^{\bar{\eta}}(\mathbf{x} - \mathbf{z}, \Delta_{\text{IS}}) \\
 & \quad - \frac{\mathbf{q}^{\bar{\lambda}}}{p_{0R}^+ \mathbf{q}^2 + (p_1^+ + p_3^+) M^2} \frac{4(p_0^+ + p_1^+ + p_3^+)^2}{p_3^+} e^{\bar{\lambda}\lambda'} e^{\bar{\eta}\eta'} i A^{\bar{\eta}}(\mathbf{x} - \mathbf{z}, \Delta_{\text{IS}}) \\
 & \quad - \left(\left(\frac{1}{p_1^+ + p_3^+} + \frac{1}{p_0^+} \right) \left(\left(1 + \frac{2p_1^+}{q^+} \right) \left(1 + \frac{2p_0^+}{p_3^+} \right) - 1 \right) \right. \\
 & \quad \left. + \left(\frac{1}{p_1^+ + p_3^+} - \frac{1}{p_0^+} \right) \left(\frac{2p_0^+}{p_3^+} - \frac{2p_1^+}{q^+} \right) \right] p_1^+ \delta^{\lambda'\eta'} \mathcal{K}(\mathbf{x} - \mathbf{z}, \Delta_{\text{IS}}) \left. \right\} \\
 & \quad - 4 \int_{k_{\text{min}}^+}^{k_f^+} \frac{dp_3^+}{p_3^+} \left(\left(1 + \frac{2p_1^+}{q^+} \right)^2 + 1 \right) i A^{\eta'}(\mathbf{x} - \mathbf{z}) \\
 & \quad \times \frac{q^+ \mathbf{P}_\perp^{\lambda'}}{p_0^+ \mathbf{P}_\perp^2 + p_1^+ M^2} \frac{q^+ \mathbf{q}^{\lambda'}}{p_0^+ \mathbf{q}^2 + p_1 M^2} \left. \right\}. \tag{9.79}
 \end{aligned}$$

Final-state radiation. Using identity (B.12), what is left after the analysis in section 7 of collinear final-state divergences from amplitudes $\mathcal{M}_{\text{FS}2}^{\lambda\eta}$ (5.18) and $\mathcal{M}_{\text{FS}3}^{\lambda\eta}$ (5.20) can be cast in the following form:

$$\begin{aligned}
 & \int \text{PS}(\vec{p}_3) |\mathcal{M}_{\text{FS}2+3}^{\lambda\eta}|^2 (1 - \theta_{\text{in}}(\vec{p}_1, \vec{p}_3)) - \lim_{\text{soft}} \int \text{PS}(\vec{p}_3) |\mathcal{M}_{\text{FS}2+3}^{\lambda\eta}|^2 (1 - \theta_{\text{in}}(\vec{p}_1, \vec{p}_3)) \\
 &= g_{\text{em}}^2 \alpha_s C_F N_c 8p_1^+ p_0^+ \int_{\mathbf{x}, \mathbf{x}'} e^{-i\mathbf{k}_\perp \cdot (\mathbf{x} - \mathbf{x}')} (s_{\mathbf{x}\mathbf{x}'} + 1) \\
 & \quad \left\{ \int_{k_{\text{min}}^+}^{+\infty} \frac{dp_3^+}{p_3^+} \int_{\ell} \frac{1}{\ell^2} \left(\frac{p_3^+}{p_0^+} \frac{q^+}{p_1^+ + p_3^+} \frac{\ell + \frac{p_0^+}{p_1^+} \frac{p_1^+ + p_3^+}{q^+} \mathbf{P}_\perp}{\left(\ell + \frac{p_3^+}{p_1^+} \mathbf{P}_\perp \right)^2 + \Delta_{\text{FS}}} + \frac{q^+ \mathbf{q}}{p_{0R}^+ \mathbf{q}^2 + (p_1^+ + p_3^+) M^2} \right)^2 \right. \\
 & \quad \times \theta \left(\ell^2 - \left(\frac{p_3^+}{p_1^+} \right)^2 \mathbf{p}_1^2 R^2 \right) e^{-i \left(\ell + \frac{p_3^+}{p_1^+} \mathbf{P}_\perp + \frac{p_3^+}{p_0^+} \mathbf{k}_\perp \right) \cdot (\mathbf{x} - \mathbf{x}')} \\
 & \quad \times \left(\frac{p_3^+}{p_1^+} \right)^2 \frac{p_{0R}^+}{p_0^+} \left(\left(1 + \frac{2p_1^+}{p_3^+} \right)^2 + 1 \right) \left(\left(1 + 2\frac{p_1^+ + p_3^+}{q^+} \right)^2 + 1 \right) \\
 & \quad - \left(\left(1 + 2\frac{p_1^+}{q^+} \right)^2 + 1 \right) \left(\frac{q^+ \mathbf{P}_\perp}{p_0^+ \mathbf{P}_\perp^2 + p_1^+ M^2} + \frac{q^+ \mathbf{q}}{p_0^+ \mathbf{q}^2 + p_1^+ M^2} \right)^2 \left. \right\}
 \end{aligned}$$

$$\begin{aligned}
& \times 4 \int_{k_{\min}^+}^{+\infty} \frac{dp_3^+}{p_3^+} \int_{\ell} \frac{e^{-i\ell \cdot (\mathbf{x}-\mathbf{x}')}}{\ell^2} \theta\left(\ell^2 - \left(\frac{p_3^+}{p_1^+}\right)^2 \mathbf{P}_1^2 R^2\right) \\
& + 4 \left(\left(1 + 2\frac{p_1^+}{q^+}\right)^2 + 1 \right) \left[\left(\frac{q^+ \mathbf{P}_\perp}{p_0^+ \mathbf{P}_\perp^2 + p_1^+ M^2}\right)^2 + 2 \frac{q^+ \mathbf{P}_\perp^\lambda}{p_0^+ \mathbf{P}_\perp^2 + p_1^+ M^2} \frac{q^+ \mathbf{q}^\lambda}{p_0^+ \mathbf{q}^2 + p_1^+ M^2} \right] \\
& \times \left. \int_{k_{\min}^+}^{k_f^+} \frac{dp_3^+}{p_3^+} \int_{\ell} \frac{e^{-i\ell \cdot (\mathbf{x}-\mathbf{x}')}}{\ell^2} \right\} \tag{9.80}
\end{aligned}$$

Likewise, one obtains for the amplitudes in eqs. (5.20) and (5.25) that never contributed to the jet function:

$$\begin{aligned}
\int \text{PS}(\vec{p}_3) |\mathcal{M}_{\text{FS1+4}}^{\lambda\eta^\dagger}|^2 &= g_{\text{em}}^2 \alpha_s 8 p_1^+ p_0^+ \int_{\mathbf{x}, \mathbf{x}'} e^{i\mathbf{k}_\perp \cdot (\mathbf{x}-\mathbf{x}')} C_F N_c (s_{\mathbf{x}\mathbf{x}'} + 1) \\
& \times \int_{k_{\min}^+}^{+\infty} \frac{dp_3^+}{p_3^+} \left\{ \left(\frac{p_3^+}{p_0^+}\right)^2 \frac{p_{0R}^+}{p_0^+} e^{i\frac{p_3^+}{p_0^+} \mathbf{k}_\perp \cdot (\mathbf{x}-\mathbf{x}')} \right. \\
& \times \left[\left(\frac{q^+ \mathbf{P}_\perp}{p_0^+ \mathbf{P}_\perp^2 + p_1^+ M^2}\right)^2 \left(\left(1 + 2\frac{2p_0^+}{p_3^+}\right)^2 + 1 \right) \left(\left(1 + 2\frac{2p_1^+}{q^+}\right)^2 + 1 \right) \int_{\ell} \frac{\ell^2 e^{-i\ell \cdot (\mathbf{x}-\mathbf{x}')}}{(\ell^2 + \Delta_{\text{FS}})^2} \right. \\
& + 4 \frac{(p_{0R}^+)^2 ((p_1^+ + p_3^+)^2 + (p_0^+)^2)}{(p_1^+ + p_3^+)^2 (p_0^+)^2} \int_{\ell} \frac{e^{-i\ell \cdot (\mathbf{x}-\mathbf{x}')}}{(\ell^2 + \Delta_{\text{FS}})^2} \\
& - 2 \frac{p_{0R}^+ q^+ \mathbf{P}_\perp^i}{p_0^+ \mathbf{P}_\perp^2 + p_1^+ M^2} \int_{\ell} \frac{\ell^i e^{-i\ell \cdot (\mathbf{x}-\mathbf{x}')}}{(\ell^2 + \Delta_{\text{FS}})^2} \\
& \times \left(\left(\frac{1}{p_1^+ + p_3^+} + \frac{1}{p_0^+} \right) \left(\left(1 + 2\frac{2p_0^+}{p_3^+}\right) \left(1 + 2\frac{2p_1^+}{q^+}\right) - 1 \right) \right. \\
& \left. \left. + \left(\frac{2p_0^+}{p_3^+} - \frac{2p_1^+}{q^+} \right) \left(\frac{1}{p_1^+ + p_3^+} - \frac{1}{p_0^+} \right) \right) \right] \\
& \left. - 4 \int_{k_{\min}^+}^{k_f^+} \frac{dp_3^+}{p_3^+} \left(\left(1 + 2\frac{2p_1^+}{q^+}\right)^2 + 1 \right) \left(\frac{q^+ \mathbf{P}_\perp}{p_0^+ \mathbf{P}_\perp^2 + p_1^+ M^2}\right)^2 \int_{\ell} \frac{e^{-i\ell \cdot (\mathbf{x}-\mathbf{x}')}}{\ell^2} \right\}. \tag{9.81}
\end{aligned}$$

Next, we find the following result for the interference terms, using the trace identity (B.11):

$$\begin{aligned}
& \int \text{PS}(\vec{p}_3) \text{Tr} 2\text{Re}(\mathcal{M}_{\text{FS2+3}}^{\lambda\eta^\dagger} \mathcal{M}_{\text{FS1+4}}^{\lambda\eta}) \\
& = -g_{\text{em}}^2 \alpha_s 8 p_1^+ p_0^+ 2\text{Re} \int_{\mathbf{x}, \mathbf{x}', \mathbf{z}} e^{-i\mathbf{k}_\perp \cdot (\mathbf{x}-\mathbf{x}')} C_F N_c (s_{\mathbf{x}\mathbf{x}'} + 1) \\
& \times \left\{ \int_{k_{\min}^+}^{+\infty} \frac{dp_3^+}{p_3^+} \frac{(p_3^+)^2 p_{0R}^+}{(p_0^+)^2 p_1^+} e^{-i\frac{p_3^+}{p_0^+} \mathbf{k}_\perp \cdot (\mathbf{x}-\mathbf{z})} e^{i\frac{p_3^+}{p_1^+} \mathbf{P}_1 \cdot (\mathbf{z}-\mathbf{x}')} \int_{\ell} \frac{\ell^{\eta'} e^{-i\ell \cdot (\mathbf{z}-\mathbf{x}')}}{\ell^2} \right. \\
& \times \left[\frac{p_3^+}{p_0^+} \frac{q^+}{p_1^+ + p_3^+} \frac{\ell^{\lambda'} + \frac{p_0^+}{p_1^+} \frac{p_1^+ + p_3^+}{q^+} \mathbf{P}_\perp^{\lambda'}}{\left(\ell + \frac{p_3^+}{p_1^+} \mathbf{P}_\perp\right)^2 + \Delta_{\text{FS}}} + \frac{q^+ \mathbf{q}^{\lambda'}}{p_{0R}^+ \mathbf{q}^2 + (p_1^+ + p_3^+) M^2} \right] \\
& \times \left[-\frac{q^+ \mathbf{P}_\perp^\lambda}{p_0^+ \mathbf{P}_\perp^2 + p_1^+ M^2} i A^{\bar{\eta}}(\mathbf{x}-\mathbf{z}, \Delta_{\text{FS}}) \left(\left(\left(1 + 2\frac{p_1^+ + p_3^+}{q^+}\right) \left(1 + 2\frac{2p_1^+}{q^+}\right) + 1 \right) \right. \right. \\
& \left. \left. \times \left(\left(1 + 2\frac{2p_1^+}{p_3^+}\right) \left(1 + 2\frac{2p_0^+}{p_3^+}\right) + 1 \right) \delta^{\bar{\eta}\eta'} \delta^{\lambda\lambda'} \right) \right]
\end{aligned}$$

$$\begin{aligned}
 & -4 \frac{(p_0^+ + p_1^+ + p_3^+)^2}{p_3^+ q^+} \epsilon^{\bar{\eta}\eta'} \epsilon^{\bar{\lambda}\lambda'} \\
 & + \delta^{\eta'\lambda'} p_{0R}^+ \mathcal{K}(\mathbf{x} - \mathbf{z}, \Delta_{\text{FS}}) \left(\left(\frac{1}{p_1^+ + p_3^+} + \frac{1}{p_0^+} \right) \left(\left(1 + 2 \frac{p_1^+ + p_3^+}{q^+} \right) \left(1 + \frac{2p_1^+}{p_3^+} \right) - 1 \right) \right. \\
 & \left. + 2 \left(\frac{p_1^+}{p_3^+} - \frac{p_1^+ + p_3^+}{q^+} \right) \left(\frac{1}{p_1^+ + p_3^+} - \frac{1}{p_0^+} \right) \right) \\
 & + 4 \int_{k_{\min}^+}^{+\infty} \frac{dp_3^+}{p_3^+} \left(\left(1 + 2 \frac{p_1^+}{q^+} \right)^2 + 1 \right) \frac{q^+ \mathbf{q}^{\bar{\lambda}}}{p_0^+ \mathbf{q}^2 + p_1^+ M^2} \frac{q^+ \mathbf{P}_{\perp}^{\bar{\lambda}}}{p_0^+ \mathbf{P}_{\perp}^2 + p_1^+ M^2} \int_{\ell} \frac{e^{-i\ell \cdot (\mathbf{x} - \mathbf{x}')}}{\ell^2} \Big\}. \quad (9.82)
 \end{aligned}$$

Initial-final state radiation interference. The last real NLO contributions are due to the interference between initial- and final state radiation in the transversely polarized case:

$$\begin{aligned}
 & \int \text{PS}(\vec{p}_3) \text{Tr} 2\text{Re}(\mathcal{M}_{\text{IS}1+2}^{\lambda\eta\dagger} \mathcal{M}_{\text{FS}1+4}^{\lambda\eta}) \\
 & = g_{\text{em}}^2 \alpha_s 8 p_1^+ p_0^+ 2\text{Re} \int_{\mathbf{x}, \mathbf{x}', \mathbf{z}} e^{-i\mathbf{k}_{\perp} \cdot (\mathbf{x} - \mathbf{x}')} \left(\frac{N_c^2}{2} s_{\mathbf{x}\mathbf{z}} s_{\mathbf{z}\mathbf{x}'} - \frac{1}{2} s_{\mathbf{x}\mathbf{x}'} + C_F N_c \right) \\
 & \times \left\{ \int_{k_{\min}^+}^{+\infty} \frac{dp_3^+}{p_3^+} \left(\frac{p_3^+}{p_0^+} \right)^2 e^{-i\frac{p_3^+}{p_0^+} \mathbf{k}_{\perp} \cdot (\mathbf{x} - \mathbf{z})} \int_{\ell} e^{i\ell \cdot (\mathbf{x}' - \mathbf{z})} \frac{\ell^{\eta'}}{\ell^2} \right. \\
 & \times \left[\frac{q^+ \mathbf{P}_{\perp}^{\lambda'}}{p_0^+ \mathbf{P}_{\perp}^2 + p_1^+ M^2} + \frac{(q^+)^2 p_3^+ \left(\ell^{\lambda'} + \frac{p_0^+}{q^+} \mathbf{q}^{\lambda'} \right)}{p_3^+ (q^+ \ell + p_0^+ \mathbf{q})^2 + p_1^+ q^+ p_{0R}^+ \ell^2 + p_1^+ p_3^+ p_0^+ M^2} \right] \\
 & \times \left[- \frac{q^+ \mathbf{P}_{\perp}^{\bar{\lambda}}}{p_0^+ \mathbf{P}_{\perp}^2 + p_1^+ M^2} i A^{\bar{\eta}}(\mathbf{x} - \mathbf{z}, \Delta_{\text{FS}}) \right. \\
 & \times \left(\left(\left(1 + \frac{2p_1^+}{q^+} \right)^2 + 1 \right) \left(\left(1 + \frac{2p_0^+}{p_3^+} \right)^2 + 1 \right) \delta^{\bar{\eta}\eta'} \delta^{\bar{\lambda}\lambda'} - 4 \left(1 + \frac{2p_1^+}{q^+} \right) \left(1 + \frac{2p_0^+}{p_3^+} \right) \epsilon^{\bar{\eta}\eta'} \epsilon^{\bar{\lambda}\lambda'} \right) \\
 & + \delta^{\eta'\lambda'} p_{0R}^+ \mathcal{K}(\mathbf{x} - \mathbf{z}, \Delta_{\text{FS}}) \left(\left(\frac{1}{p_1^+ + p_3^+} + \frac{1}{p_0^+} \right) \left(\left(1 + \frac{2p_1^+}{q^+} \right) \left(1 + \frac{2p_0^+}{p_3^+} \right) - 1 \right) \right. \\
 & \left. + \left(\frac{2p_0^+}{p_3^+} - \frac{2p_1^+}{q^+} \right) \left(\frac{1}{p_1^+ + p_3^+} - \frac{1}{p_0^+} \right) \right) \\
 & \left. + 4 \int_{k_{\min}^+}^{k_f^+} \frac{dp_3^+}{p_3^+} \left(\left(1 + \frac{2p_1^+}{q^+} \right)^2 + 1 \right) \left(\frac{q^+ \mathbf{P}_{\perp}}{p_0^+ \mathbf{P}_{\perp}^2 + p_1^+ M^2} \right)^2 A^i(\mathbf{x}' - \mathbf{z}) A^i(\mathbf{x} - \mathbf{z}) \right\}, \quad (9.83)
 \end{aligned}$$

where, once again, we relied on (B.12). Moreover, using (B.11):

$$\begin{aligned}
 & \int \text{PS}(\vec{p}_3) \text{Tr} 2\text{Re}(\mathcal{M}_{\text{IS}1+2}^{\lambda\eta\dagger} \mathcal{M}_{\text{FS}2+3}^{\lambda\eta}) \\
 & = -g_{\text{em}}^2 \alpha_s 8 p_1^+ p_0^+ 2\text{Re} \int_{\mathbf{x}, \mathbf{x}', \mathbf{z}} e^{i\mathbf{k}_{\perp} \cdot (\mathbf{x} - \mathbf{x}')} \left(\frac{N_c^2}{2} s_{\mathbf{x}\mathbf{z}} s_{\mathbf{z}\mathbf{x}'} - \frac{1}{2} s_{\mathbf{x}\mathbf{x}'} + C_F N_c \right) \\
 & \times \left\{ \int_{k_{\min}^+}^{+\infty} \frac{dp_3^+}{p_3^+} \frac{p_3^+}{p_1^+} \frac{p_3^+}{p_0^+} e^{-i\frac{p_3^+}{p_1^+} \mathbf{p}_1 \cdot (\mathbf{x} - \mathbf{z})} \int_{\ell} e^{i\ell \cdot (\mathbf{x}' - \mathbf{z})} \frac{\ell^{\eta'}}{\ell^2} \int_{\ell_2} \frac{\ell_2^{\bar{\eta}}}{\ell_2^2} e^{-i\ell_2 \cdot (\mathbf{x} - \mathbf{z})} \right. \\
 & \times \left[\left(\left(1 + \frac{2p_1^+}{q^+} \right) \left(1 + 2 \frac{p_1^+ + p_3^+}{q^+} \right) + 1 \right) \left(\left(1 + \frac{2p_0^+}{p_3^+} \right) \left(1 + \frac{2p_1^+}{p_3^+} \right) + 1 \right) \delta^{\bar{\lambda}\lambda'} \delta^{\bar{\eta}\eta'} \right. \\
 & \left. \left. - 4 \frac{(p_{0R}^+ + p_1^+)^2}{p_3^+ q^+} \epsilon^{\bar{\lambda}\lambda'} \epsilon^{\bar{\eta}\eta'} \right] \right\}
 \end{aligned}$$

$$\begin{aligned}
 & \times \left[\frac{q^+ \mathbf{P}_\perp^{\lambda'}}{p_0^+ \mathbf{P}_\perp^2 + p_1^+ M^2} + \frac{(q^+)^2 p_3^+ \left(\ell^{\lambda'} + \frac{p_0^+}{q^+} \mathbf{q}^{\lambda'} \right)}{p_3^+ (q^+ \ell + p_0^+ \mathbf{q})^2 + p_1^+ q^+ p_{0R}^+ \ell^2 + p_1^+ p_3^+ p_0^+ M^2} \right] \\
 & \times \left[\frac{p_3^+}{p_0^+} \frac{q^+}{p_1^+ + p_3^+} \frac{\ell_2^{\bar{\lambda}} + \frac{p_0^+}{p_1^+} \frac{p_1^+ + p_3^+}{q^+} \mathbf{P}_\perp^{\bar{\lambda}}}{\left(\ell_2 + \frac{p_3^+}{p_1^+} \mathbf{P}_\perp \right)^2 + \Delta_{\text{FS}}} + \frac{q^+ \mathbf{q}^{\bar{\lambda}}}{p_{0R}^+ \mathbf{q}^2 + (p_1^+ + p_3^+) M^2} \right] \\
 & - 4 \int_{k_{\min}^+}^{k_f^+} \frac{dp_3^+}{p_3^+} \left(\left(1 + \frac{2p_1^+}{q^+} \right)^2 + 1 \right) A^i(\mathbf{x}' - \mathbf{z}) A^i(\mathbf{x} - \mathbf{z}) \frac{q^+ \mathbf{P}_\perp^{\bar{\lambda}}}{p_0^+ \mathbf{P}_\perp^2 + p_1^+ M^2} \frac{q^+ \mathbf{q}^{\bar{\lambda}}}{p_0^+ \mathbf{q}^2 + p_1^+ M^2} \Bigg\}, \quad (9.84)
 \end{aligned}$$

and:

$$\begin{aligned}
 & \int \text{PS}(\vec{p}_3) \text{Tr} 2\text{Re}(\mathcal{M}_{\text{IS}3+4}^{\lambda\eta\dagger} \mathcal{M}_{\text{FS}1+4}^{\lambda\eta}) \\
 & = g_{\text{em}}^2 \alpha_s 8 p_1^+ p_0^+ 2\text{Re} \int_{\mathbf{x}, \mathbf{x}', \mathbf{z}} e^{i\mathbf{k}_\perp \cdot (\mathbf{x} - \mathbf{x}')} \left(\frac{N_c^2}{2} s_{\mathbf{x}\mathbf{z}} s_{\mathbf{z}\mathbf{x}'} - \frac{1}{2} s_{\mathbf{x}\mathbf{x}'} + C_F N_c \right) \\
 & \times \left\{ \int_{k_{\min}^+}^{+\infty} \frac{dp_3^+}{p_3^+} \frac{(p_3^+)^2}{p_1^+ + p_3^+} \frac{p_{0R}^+}{(p_0^+)^2} e^{-i \frac{p_3^+}{p_1^+ + p_3^+} \mathbf{q} \cdot (\mathbf{x}' - \mathbf{z})} e^{-i \frac{p_3^+}{p_0^+} \mathbf{k}_\perp \cdot (\mathbf{x} - \mathbf{z})} \right. \\
 & \times \left[\frac{q^+ \mathbf{q}^{\lambda'}}{p_{0R}^+ \mathbf{q}^2 + (p_1^+ + p_3^+) M^2} \frac{q^+ \mathbf{P}_\perp^{\bar{\lambda}}}{p_0^+ \mathbf{P}_\perp^2 + p_1^+ M^2} i A^{\eta'}(\mathbf{x}' - \mathbf{z}, \Delta_{\text{IS}}) i A^{\bar{\eta}}(\mathbf{x} - \mathbf{z}, \Delta_{\text{FS}}) \right. \\
 & \times \left(\left(\left(1 + 2 \frac{p_1^+ + p_3^+}{q^+} \right) \left(1 + \frac{2p_1^+}{q^+} \right) + 1 \right) \left(\left(1 + \frac{2p_1^+}{p_3^+} \right) \left(1 + \frac{2p_0^+}{p_3^+} \right) + 1 \right) \delta^{\bar{\eta}\eta'} \delta^{\bar{\lambda}\lambda'} \right. \\
 & - 4 \frac{(p_{0R}^+ + p_1^+)}{p_3^+ q^+} \epsilon^{\bar{\eta}\eta'} \epsilon^{\bar{\lambda}\lambda'} \Bigg) \\
 & - 4 p_1^+ (p_{0R}^+)^3 \frac{(p_1^+ + p_3^+)^2 + (p_0^+)^2}{(p_1^+ + p_3^+)^2 (p_0^+)^2} \mathcal{K}(\mathbf{x}' - \mathbf{z}, \Delta_{\text{IS}}) \mathcal{K}(\mathbf{x} - \mathbf{z}, \Delta_{\text{FS}}) \\
 & - p_{0R}^+ \frac{q^+ \mathbf{q}^i}{p_{0R}^+ \mathbf{q}^2 + (p_1^+ + p_3^+) M^2} i A^i(\mathbf{x}' - \mathbf{z}, \Delta_{\text{IS}}) \mathcal{K}(\mathbf{x} - \mathbf{z}, \Delta_{\text{FS}}) \\
 & \times \left(\left(\frac{1}{p_1^+ + p_3^+} + \frac{1}{p_0^+} \right) \left(\left(1 + 2 \frac{p_1^+ + p_3^+}{q^+} \right) \left(1 + \frac{2p_1^+}{p_3^+} \right) - 1 \right) \right. \\
 & + 2 \left(\frac{p_1^+}{p_3^+} - \frac{p_1^+ + p_3^+}{q^+} \right) \left(\frac{1}{p_1^+ + p_3^+} - \frac{1}{p_0^+} \right) \Bigg) \\
 & + \frac{p_1^+ q^+ \mathbf{P}_\perp^i}{p_0^+ \mathbf{P}_\perp^2 + p_1^+ M^2} i A^i(\mathbf{x} - \mathbf{z}, \Delta_{\text{FS}}) \mathcal{K}(\mathbf{x}' - \mathbf{z}, \Delta_{\text{IS}}) \\
 & \times \left(\left(\frac{1}{p_1^+ + p_3^+} + \frac{1}{p_0^+} \right) \left(\left(1 + \frac{2p_1^+}{q^+} \right) \left(1 + \frac{2p_0^+}{p_3^+} \right) - 1 \right) \right. \\
 & \left. \left. - 2 \left(\frac{p_1^+}{q^+} - \frac{p_0^+}{p_3^+} \right) \left(\frac{1}{p_1^+ + p_3^+} - \frac{1}{p_0^+} \right) \right) \right] \\
 & + 4 \int_{k_{\min}^+}^{k_f^+} \frac{dp_3^+}{p_3^+} \left(\left(1 + \frac{2p_1^+}{q^+} \right)^2 + 1 \right) \frac{q^+ \mathbf{q}^j}{p_0^+ \mathbf{q}^2 + p_1^+ M^2} \frac{q^+ \mathbf{P}_\perp^j}{p_0^+ \mathbf{P}_\perp^2 + p_1^+ M^2} A^i(\mathbf{x}' - \mathbf{z}) A^i(\mathbf{x} - \mathbf{z}) \Bigg\}. \quad (9.85)
 \end{aligned}$$

The following monstrosity, obtained with the help of identity (B.12), concludes this section:

$$\begin{aligned}
& \int \text{PS}(\vec{p}_3) \text{Tr} 2\text{Re}(\mathcal{M}_{\text{IS}3+4}^{\lambda\eta\dagger} \mathcal{M}_{\text{FS}2+3}^{\lambda\eta}) \\
&= -g_{\text{em}}^2 \alpha_s 8p_1^+ p_0^+ 2\text{Re} \int_{\mathbf{x}, \mathbf{x}', \mathbf{z}} e^{i\mathbf{k}_\perp \cdot (\mathbf{x} - \mathbf{x}')} \left(\frac{N_c^2}{2} s_{\mathbf{x}\mathbf{z}} s_{\mathbf{z}\mathbf{x}'} - \frac{1}{2} s_{\mathbf{x}\mathbf{x}'} + C_F N_c \right) \\
&\times \left\{ \int_{k_{\text{min}}^+}^{+\infty} \frac{dp_3^+}{p_3^+} \frac{p_3^+}{p_1^+} \frac{p_{0R}^+}{p_0^+} \frac{p_3^+}{p_1^+ + p_3^+} e^{-i \frac{p_3^+}{p_1^+ + p_3^+} \mathbf{q} \cdot (\mathbf{x}' - \mathbf{z})} e^{-i \frac{p_3^+}{p_1^+} \mathbf{p}_1 \cdot (\mathbf{x} - \mathbf{z})} \int_{\ell_2} \frac{\ell_2^{\bar{\eta}}}{\ell_2^{\bar{\lambda}}} e^{-i\ell_2 \cdot (\mathbf{x} - \mathbf{z})} \right. \\
&\times \left[\frac{p_3^+}{p_0^+} \frac{q^+}{p_1^+ + p_3^+} \frac{\ell_2^{\bar{\lambda}} + \frac{p_0^+}{p_1^+} \frac{p_1^+ + p_3^+}{q^+} \mathbf{P}_\perp^{\bar{\lambda}}}{\left(\ell_2 + \frac{p_3^+}{p_1^+} \mathbf{P}_\perp \right)^2 + \Delta_{\text{FS}}} + \frac{q^+ \mathbf{q}^{\bar{\lambda}}}{p_{0R}^+ \mathbf{q}^2 + (p_1^+ + p_3^+) M^2} \right] \\
&\times \left[- \frac{q^+ \mathbf{q}^{\lambda'}}{p_{0R}^+ \mathbf{q}^2 + (p_1^+ + p_3^+) M^2} i A^{\eta'}(\mathbf{x}' - \mathbf{z}, \Delta_{\text{IS}}) \right. \\
&\times \left(\left(\left(1 + 2 \frac{p_1^+ + p_3^+}{q^+} \right)^2 + 1 \right) \left(\left(1 + \frac{2p_1^+}{p_3^+} \right)^2 + 1 \right) \delta^{\bar{\lambda}\lambda'} \delta^{\bar{\eta}\eta'} \right. \\
&- 4 \left(1 + 2 \frac{p_1^+ + p_3^+}{q^+} \right) \left(1 + \frac{2p_1^+}{p_3^+} \right) \epsilon^{\bar{\lambda}\lambda'} \epsilon^{\bar{\eta}\eta'} \\
&- p_1^+ \delta^{\bar{\eta}\bar{\lambda}} \mathcal{K}(\mathbf{x}' - \mathbf{z}, \Delta_{\text{IS}}) \left(\left(\frac{1}{p_1^+ + p_3^+} + \frac{1}{p_0^+} \right) \left(\left(1 + \frac{2p_1^+}{p_3^+} \right) \left(1 + 2 \frac{p_1^+ + p_3^+}{q^+} \right) - 1 \right) \right. \\
&- \left. \left. 2 \left(\frac{1}{p_1^+ + p_3^+} - \frac{1}{p_0^+} \right) \left(\frac{p_1^+ + p_3^+}{q^+} - \frac{p_1^+}{p_3^+} \right) \right) \right] \\
&- \left. 4 \int_{k_{\text{min}}^+}^{k_f^+} \frac{dp_3^+}{p_3^+} \left(\left(1 + 2 \frac{p_1^+}{q^+} \right)^2 + 1 \right) \left(\frac{q^+ \mathbf{q}}{p_0^+ \mathbf{q}^2 + p_1^+ M^2} \right)^2 A^i(\mathbf{x}' - \mathbf{z}) A^i(\mathbf{x} - \mathbf{z}) \right\}. \tag{9.86}
\end{aligned}$$

10 Conclusions

We have presented the first next-to-leading order calculation of the cross section for the $p + A \rightarrow \gamma^* + \text{jet} + X$ process within the hybrid dilute-dense formalism. Replacing the electromagnetic coupling constant, the result can be carried over to the production of a Z-boson. The Drell-Yan + jet cross section is obtained trivially by multiplying with the $\gamma^*/Z \rightarrow \ell^+ + \ell^-$ branching ratio, unless angular correlations between both leptons are measured. In that case, the leptons might be sensitive to the interference between the production of a longitudinally or transversely polarized virtual boson, which is not calculated explicitly in this work but can in principle be computed using the intermediate results we have presented here.

It is straightforward to extend this calculation to the production of a Drell-Yan pair in association with a hadron, instead of a jet. In this case, the final-state collinear poles would cancel with the DGLAP evolution of the quark fragmentation function, very similar to the way the initial-state collinear divergences are absorbed into the DGLAP evolution of the PDF.

Furthermore, for phenomenological applications the gluon channel $g + A \rightarrow \gamma^* + q + \bar{q}$ should be included. The representative Feynman diagrams are depicted in figure 10. Assuming the photon has nonvanishing plus-momentum and virtuality, the amplitudes where the incoming gluon interacts with the shockwave are completely finite, as are the amplitudes with instantaneous $g \rightarrow \gamma^* q \bar{q}$ splittings. However, the remaining amplitudes, corresponding to the diagrams where the quark-antiquark pair scatters off the shockwave before or after emitting the photon, are not. Indeed, integrating over the momentum of the antiquark (quark) will yield a singularity when this antiquark (quark) is collinear to its parent gluon. These contributions are proportional to the leading-order amplitudes for the quark (antiquark) channel, where the incoming quark (antiquark) comes from the $g \rightarrow q \bar{q}$ splitting in the DGLAP evolution of the PDF. Indeed, these terms were not taken into account in our analysis in section 6. We leave the gluon channel for future work.

Our result encompasses the NLO cross section for prompt photon plus jet hadroproduction as an important by-product, easily obtained by taking the real photon limit. This process has been studied quite extensively in the literature at leading order [86–91] and is planned to be measured with the proposed forward calorimeter (FoCal) of the ALICE experiment [92, 93]. The next-to-leading cross section we provide will greatly increase the potential of this study.

One of the major motivations behind this work is the prospect of studying the region where the virtual photon and the jet are back-to-back in the transverse plane [94], hence $\mathbf{P}_\perp^2 \gg \mathbf{k}_\perp^2$. In this regime, soft-collinear gluon radiation is expected to lead to large Sudakov logarithms in the ratio $\mathbf{P}_\perp^2/\mathbf{k}_\perp^2$, which need to be resummed. Indeed, in the HEF approach of [66], incorporating Sudakov resummation was observed to be essential to be able to describe LHCb data on $Z + \text{jet}$ production.

It was observed in ref. [95] that in this regime the leading-order cross section factorizes into a convolution of a hard part with the quark PDF and a (dipole-type) gluon transverse momentum dependent (TMD) PDF [96]. Proving such a factorization at next-to-leading order would be much more challenging, complicated amongst others by the emergence of large Sudakov logarithms in the ratio $\mathbf{P}_\perp^2/\mathbf{k}_\perp^2$, which should be absorbed into the Collins-Soper-Sterman [97] evolution of the gluon TMD. However, should the above nontrivial scenario indeed take place, it would be a further confirmation of the CGC and TMD factorization being compatible at one loop. First steps in this direction were taken in [98, 99]. In our recent work [50], we calculated the cross section for dijet photoproduction at NLO in the CGC, and provided the first proof that large Sudakov double logarithms can be extracted in a way consistent with high-energy resummation, under the condition that the latter is kinematically improved. In a series of papers [100–102], complete next-to-leading order TMD factorization was then established for back-to-back dijet production in deep-inelastic scattering in the CGC. We should remark that the study of combined low- x and Sudakov resummation is a very active field, undertaken within several different formalisms, see e.g., [67, 103–132].

Finally, another interesting future direction is the study of the inclusive Drell-Yan process, obtained from our result by integrating the outgoing quark out. This integration, albeit nontrivial, should not lead to new divergences. Experimental data on dilepton pro-

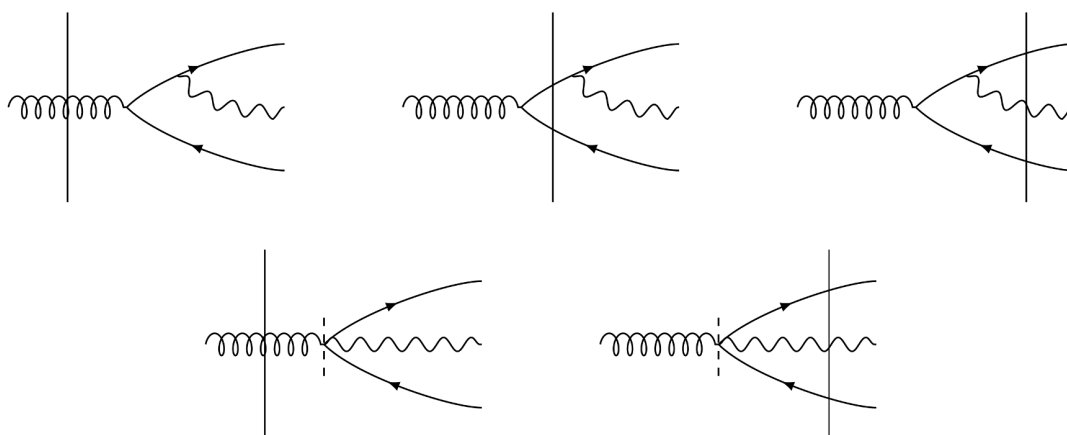


Figure 10. The representative Feynman diagrams for the gluon channel, i.e. the partonic process $g + A \rightarrow \gamma^* + q + \bar{q}$. Only the second and third diagram (and their $q \leftrightarrow \bar{q}$ counterparts) contain a singularity, namely when the antiquark (quark) is integrated out. These contributions can then be viewed as the LO quark channel amplitudes, where the incoming quark is generated from the $g \rightarrow q\bar{q}$ splitting of the gluon PDF. Hence, these collinear divergences should be absorbed into the DGLAP evolution of the LO cross section.

duction at low invariant mass is currently being analyzed by the ATLAS collaboration [133], and at forward rapidities by the LHCb collaboration [134]. Moreover, making use of the intermediate results of our calculation, one could then extend to next-to-leading order the higher-twist analysis of the Drell-Yan structure functions performed in [135–138].

Acknowledgments

First, I am very grateful to Guillaume Beuf for sharing some of his profound insight in LCPT and higher-order calculations with me. Moreover, I would like to thank Valerio Bertone, Daniël Boer, Renaud Boussarie, Francesco Giuli, Cyrille Marquet, and Pierre Van Mechelen for interesting discussions. My work is supported by a postdoctoral fellowship fundamental research of the Research Foundation Flanders (FWO) no. 1233422N.

A Transverse integral identities

A standard tool for evaluating the different transverse integrals in our calculation is the Schwinger trick:

$$\frac{\Gamma(\alpha)}{A^\alpha} = \int_0^\infty dt t^{\alpha-1} e^{-At}, \tag{A.1}$$

using which we find, for instance, the following expressions for the Weizsäcker-Williams field (taking the derivative with respect to \mathbf{x}):

$$iA^i(\mathbf{x}) \equiv \int_{\mathbf{k}} e^{-i\mathbf{k}\cdot\mathbf{x}} \frac{\mathbf{k}^i}{\mathbf{k}^2} = \frac{-i}{2\pi^{\frac{D}{2}-1}} \frac{\mathbf{x}^i}{(\mathbf{x}^2)^{\frac{D}{2}-1}} \Gamma\left(\frac{D}{2} - 1\right) \stackrel{D \rightarrow 4}{=} \frac{-i}{2\pi} \frac{\mathbf{x}^i}{\mathbf{x}^2}, \tag{A.2}$$

and its generalization:

$$\begin{aligned}
 iA^i(\mathbf{x}, \Delta) &\equiv \int_{\mathbf{k}} e^{-i\mathbf{k}\cdot\mathbf{x}} \frac{\mathbf{k}^i}{\mathbf{k}^2 + \Delta}, \\
 &= -i \frac{\mu^{4-D}}{(2\pi)^{\frac{D-2}{2}}} (\sqrt{\Delta})^{\frac{D-2}{2}} \frac{\mathbf{x}^i}{|\mathbf{x}|^{\frac{D-2}{2}}} K_{\frac{D-2}{2}}(\sqrt{\mathbf{x}^2\Delta}), \\
 &\stackrel{D \rightarrow 4}{=} \frac{-i}{2\pi} \frac{\mathbf{x}^i}{|\mathbf{x}|} \sqrt{\Delta} K_1(\sqrt{\mathbf{x}^2\Delta}).
 \end{aligned} \tag{A.3}$$

Note that the generalized Weizsäcker-Williams field satisfies the following identity, for a constant χ :

$$iA^i(\chi\mathbf{x}, \Delta) = \chi^{3-D} iA^i(\mathbf{x}, \chi^2\Delta). \tag{A.4}$$

A second very useful identity is:

$$\int_0^\infty ds s^{\nu-1} e^{-B/s} e^{-Cs} = 2 \left(\frac{B}{C}\right)^{\frac{\nu}{2}} K_{-\nu}(2\sqrt{BC}), \tag{A.5}$$

which we can use to solve, e.g.,

$$\mathcal{K}(\mathbf{x}, \Delta) \equiv \int_{\ell} \frac{e^{i\ell\cdot\mathbf{x}}}{\ell^2 + \Delta} = \frac{\mu^{4-D}}{(2\pi)^{\frac{D-2}{2}}} \left(\frac{\mathbf{x}^2}{\Delta}\right)^{\frac{4-D}{4}} K_{\frac{D-4}{2}}(\sqrt{\mathbf{x}^2\Delta}). \tag{A.6}$$

The above integral is finite when $\Delta \neq 0$, since Δ acts as an infrared regulator, while the phase cuts off ultraviolet divergences. We can, therefore, set $D = 4$ and take the derivative with respect to \mathbf{x} to obtain:

$$\int_{\ell} e^{i\ell\cdot\mathbf{x}} \frac{\ell^2 - \Delta}{\ell^2 + \Delta} = -2\Delta\mathcal{K}(\mathbf{x}, \Delta). \tag{A.7}$$

The following UV-divergent loop integral is omnipresent in our calculation, and is very straightforward to solve (see e.g., [139]) using dimensional regularization with $D = 4 - 2\epsilon_{UV}$:

$$\begin{aligned}
 \mathcal{A}_0(\Delta) &\equiv \int_{\ell} \frac{1}{\ell^2 + \Delta} = \frac{1}{4\pi} \Gamma\left(\frac{4-D}{2}\right) \left(\frac{\Delta}{4\pi\mu^2}\right)^{\frac{D-4}{2}}, \\
 &= \frac{1}{4\pi} \left(\frac{1}{\epsilon_{UV}} - \gamma_E + \ln \frac{4\pi\mu^2}{\Delta}\right) + \mathcal{O}(\epsilon_{UV}).
 \end{aligned} \tag{A.8}$$

Likewise:

$$\begin{aligned}
 \int_{\ell} \frac{\ell^2}{\ell^2 + \Delta} &= -\frac{\mu^{4-D}}{(4\pi)^{\frac{D-2}{2}}} \Gamma\left(\frac{4-D}{2}\right) \Delta^{\frac{D-2}{2}}, \\
 &= -\frac{\Delta}{4\pi} \left(\frac{1}{\epsilon_{UV}} - \gamma_E + \ln \frac{4\pi\mu^2}{\Delta}\right) + \mathcal{O}(\epsilon_{UV}), \\
 &= -\Delta\mathcal{A}_0(\Delta).
 \end{aligned} \tag{A.9}$$

In the virtual amplitudes, we encounter many transverse loop integrals that require a bit more of machinery to tackle them. This machinery is provided by the Passarino-Veltman reduction procedure (ref. [140], see also [33] for a clear outline), using which we obtain the following identities:

$$\int_{\ell} \frac{1}{\ell^2 + \Omega} \frac{1}{(\ell + \mathbf{k})^2 + \Delta} = \mathcal{B}_0(\Omega, \Delta, \mathbf{k}),$$

$$\begin{aligned}
 \int_{\ell} \frac{\ell^i}{\ell^2 + \Omega} \frac{1}{(\ell + \mathbf{k})^2 + \Delta} &\equiv \mathbf{k}^i \mathcal{B}_1(\Omega, \Delta, \mathbf{k}), \\
 &= \frac{\mathbf{k}^i}{2\mathbf{k}^2} \left(\mathcal{A}_0(\Omega) - \mathcal{A}_0(\Delta) + (\Omega - \Delta - \mathbf{k}^2) \mathcal{B}_0(\Omega, \Delta, \mathbf{k}) \right), \\
 \int_{\ell} \frac{\ell^i \ell^j}{\ell^2 + \Omega} \frac{1}{(\ell + \mathbf{k})^2 + \Delta} &= \frac{\mathbf{k}^i \mathbf{k}^j}{\mathbf{k}^2} \frac{1}{D-3} \left(\frac{D-4}{2} \mathcal{A}_0(\Delta) + \Omega \mathcal{B}_0(\Omega, \Delta, \mathbf{k}) \right. \\
 &\quad \left. + \frac{D-2}{2} (\Omega - \Delta - \mathbf{k}^2) \mathcal{B}_1(\Omega, \Delta, \mathbf{k}) \right) + \frac{\delta^{ij}}{D-3} \left(\frac{1}{2} \mathcal{A}_0(\Delta) \right. \\
 &\quad \left. - \Omega \mathcal{B}_0(\Omega, \Delta, \mathbf{k}) - \frac{1}{2} (\Omega - \Delta - \mathbf{k}^2) \mathcal{B}_1(\Omega, \Delta, \mathbf{k}) \right), \\
 \mathbf{k}^j \int_{\ell} \frac{\ell^i \ell^j}{\ell^2 + \Omega} \frac{1}{(\ell + \mathbf{k})^2 + \Delta} &= \frac{\mathbf{k}^i}{2} \left(\mathcal{A}_0(\Delta) + (\Omega - \Delta - \mathbf{k}^2) \mathcal{B}_1(\Omega, \Delta, \mathbf{k}) \right), \\
 \mathcal{B}_0(\Delta, \mathbf{k}) &\equiv \mathcal{B}_0(0, \Delta, \mathbf{k}) = \mathcal{B}_0(\Delta, 0, \mathbf{k}), \\
 \mathcal{B}_0(\Delta) &\equiv \mathcal{B}_0(0, \Delta, 0) = \mathcal{B}_0(\Delta, 0, 0). \tag{A.10}
 \end{aligned}$$

All the above integrals are reduced to combinations of the simple scalar integrals $\mathcal{A}_0(\Delta)$ and $\mathcal{B}_0(\Omega, \Delta, \mathbf{k})$. As already explained above, $\mathcal{A}_0(\Delta)$ is divergent in the ultraviolet. In the limit $\Delta \rightarrow 0$, a second, infrared divergence appears, which exactly cancels the UV one, at least within dimensional regularization. Another way to see this is that $\mathcal{A}_0(0)$ is a scaleless integral:

$$\mathcal{A}_0(0) = \int_{\ell} \frac{1}{\ell^2} = \frac{1}{4\pi} \left(\frac{1}{\epsilon_{\text{UV}}} - \frac{1}{\epsilon_{\text{IR}}} \right) = 0. \tag{A.11}$$

The above property plays a central role in the analysis of field-strength renormalization amplitudes in section 3.6.

From simple power counting it follows that the integral $\mathcal{B}_0(\Omega, \Delta, \mathbf{k})$, defined in the first line of eq. (A.10), is divergent in the infrared when one of its first two arguments tends to zero. Indeed, introducing Feynman parameters (see e.g., [139]):

$$\begin{aligned}
 \frac{1}{A_1^{m_1} A_2^{m_2} \dots A_n^{m_n}} &= \int_0^1 dx_1 \dots dx_n \delta \left(\sum x_i - 1 \right) \frac{x_1^{m_1-1} \cdot x_2^{m_2-1} \cdot \dots \cdot x_n^{m_n-1}}{(x_1 A_1 + x_2 A_2 + \dots + x_n A_n)^{(m_1+m_2+\dots+m_n)}} \\
 &\quad \times \frac{\Gamma(m_1+m_2+\dots+m_n)}{\Gamma(m_1)\Gamma(m_2)\dots\Gamma(m_n)}, \tag{A.12}
 \end{aligned}$$

and writing $D = 4 - 2\epsilon_{\text{IR}}$, we obtain in the $\overline{\text{MS}}$ scheme (where $\mu^2 \rightarrow \mu^2 e^{\gamma_E}/4\pi$):

$$\begin{aligned}
 \mathcal{B}_0(0, \Delta, \mathbf{k}) &= \mu^{4-D} \left(\frac{1}{4\pi} \right)^{\frac{D-2}{2}} \Gamma \left(\frac{6-D}{2} \right) \int_0^1 dx \frac{1}{x^{\frac{6-D}{2}} ((1-x)\mathbf{k}^2 + \Delta)^{\frac{6-D}{2}}}, \\
 &= \frac{1}{4\pi} \frac{-1}{\mathbf{k}^2 + \Delta} \left(\frac{1}{\epsilon_{\text{IR}}} - \ln \frac{\Delta + \mathbf{k}^2}{\mu^2} - {}_2F_1^{(0,0,1,0)} \left(0, 1, 1, \frac{\mathbf{k}^2}{\mathbf{k}^2 + \Delta} \right) \right. \\
 &\quad \left. + {}_2F_1^{(0,1,0,0)} \left(0, 1, 1, \frac{\mathbf{k}^2}{\mathbf{k}^2 + \Delta} \right) - {}_2F_1^{(1,0,0,0)} \left(0, 1, 1, \frac{\mathbf{k}^2}{\mathbf{k}^2 + \Delta} \right) \right) + \mathcal{O}(\epsilon_{\text{IR}}), \\
 &= \mathcal{B}_0(\Delta, 0, \mathbf{k}), \tag{A.13}
 \end{aligned}$$

where ${}_2F_1^{(0,0,1,0)}$ is the derivative of the third argument of the hypergeometric function ${}_2F_1$. The above calculation serves to prove that all the other expressions in (A.10) are finite when either Δ or Ω is zero. For example:

$$\begin{aligned} \lim_{\Omega \rightarrow 0} \mathcal{B}_1(\Omega, \Delta, \mathbf{k}) &= \frac{1}{2\mathbf{k}^2} \left(\mathcal{A}_0(0) - \mathcal{A}_0(\Delta) + (-\Delta - \mathbf{k}^2) \mathcal{B}_0(0, \Delta, \mathbf{k}) \right), \\ &= \frac{1}{2\mathbf{k}^2} \left(\mathcal{A}_0(0) - \mathcal{A}_0(\Delta) + \frac{1}{4\pi} \frac{1}{\epsilon_{\text{IR}}} \right) + \text{finite}, \\ &= \frac{1}{2\mathbf{k}^2} \frac{1}{4\pi} \left(\frac{1}{\epsilon_{\text{UV}}} - \frac{1}{\epsilon_{\text{IR}}} - \frac{1}{\epsilon_{\text{UV}}} + \frac{1}{\epsilon_{\text{IR}}} \right) + \text{finite}. \end{aligned} \quad (\text{A.14})$$

A second useful set of integrals is:

$$\begin{aligned} \int_{\ell} \frac{1}{\ell^2} \frac{1}{\ell^2 + \Delta} \frac{1}{(\ell + \mathbf{k})^2 + \Pi} &= \mathcal{C}_0(\Delta, \Pi, \mathbf{k}), \\ \int_{\ell} \frac{\ell^i}{\ell^2} \frac{1}{\ell^2 + \Delta} \frac{1}{(\ell + \mathbf{k})^2 + \Pi} &= \mathbf{k}^i \mathcal{C}_1(\Delta, \Pi, \mathbf{k}), \\ &= \frac{\mathbf{k}^i}{2\mathbf{k}^2} \left(\mathcal{B}_0(\Delta) - \mathcal{B}_0(\Delta, \Pi, \mathbf{k}) - (\mathbf{k}^2 + \Pi) \mathcal{C}_0(\Delta, \Pi, \mathbf{k}) \right), \\ \mathbf{k}^j \int_{\ell} \frac{\ell^i \ell^j}{\ell^2} \frac{1}{\ell^2 + \Delta} \frac{1}{(\ell + \mathbf{k})^2 + \Pi} &= -\frac{\mathbf{k}^i}{2} \left(\mathcal{B}_1(\Delta, \Pi, \mathbf{k}) + (\mathbf{k}^2 + \Pi) \mathcal{C}_1(\Delta, \Pi, \mathbf{k}) \right), \\ \int_{\ell} \frac{\ell^i \ell^j}{\ell^2} \frac{1}{\ell^2 + \Delta} \frac{1}{(\ell + \mathbf{k})^2 + \Pi} &= \mathcal{C}^{ij}(\Delta, \Pi, \mathbf{k}) = \mathbf{k}^i \mathbf{k}^j \mathcal{C}_{21}(\Delta, \Pi, \mathbf{k}) + \delta^{ij} \mathcal{C}_{22}(\Delta, \Pi, \mathbf{k}), \end{aligned} \quad (\text{A.15})$$

with:

$$\begin{aligned} \mathcal{C}_{22}(\Delta, \Pi, \mathbf{k}) &= \frac{1}{D-3} \left(\frac{1}{2} \mathcal{B}_1(\Delta, \Pi, \mathbf{k}) + \frac{1}{2} (\mathbf{k}^2 + \Pi) \mathcal{C}_1(\Delta, \Pi, \mathbf{k}) + \mathcal{B}_0(\Delta, \Pi, \mathbf{k}) \right), \\ \mathcal{C}_{21}(\Delta, \Pi, \mathbf{k}) &= -\frac{1}{D-3} \frac{1}{\mathbf{k}^2} \left(\mathcal{B}_0(\Delta, \Pi, \mathbf{k}) \right. \\ &\quad \left. + \frac{D-2}{2} \mathcal{B}_1(\Delta, \Pi, \mathbf{k}) + \frac{D-2}{2} (\mathbf{k}^2 + \Pi) \mathcal{C}_1(\Delta, \Pi, \mathbf{k}) \right). \end{aligned} \quad (\text{A.16})$$

Explicitly, we find that:

$$\begin{aligned} \mathcal{C}_0(\Delta, \mathbf{k}) &\equiv \mathcal{C}_0(\Delta, 0, \mathbf{k}) = \mathcal{C}_0(0, \Delta, \mathbf{k}), \\ &= \frac{\mu^{4-D}}{(4\pi)^{\frac{D-2}{2}}} \Gamma\left(\frac{8-D}{2}\right) \int_0^1 dy \int_0^{1-y} dz \frac{1}{(y(1-y)\mathbf{k}^2 + z\Delta)^{\frac{8-D}{2}}}, \\ &= -\frac{1}{\mathbf{k}^2 \Delta} \left(1 + \frac{\Delta}{\mathbf{k}^2 + \Delta} \right) \frac{1}{4\pi \epsilon_{\text{IR}}} + \mathcal{O}(\epsilon_{\text{IR}}^0). \end{aligned} \quad (\text{A.17})$$

We conclude this section with a list of the divergent (either ultraviolet or infrared) parts of transverse integrals commonly encountered in the calculation, in particular in the evaluation of the virtual vertex corrections in section 3.2:

$$\begin{aligned} \mathcal{A}_0(\Delta) &= \int_{\ell} \frac{1}{\ell^2 + \Delta} = \frac{1}{4\pi} \frac{1}{\epsilon_{\text{UV}}} + \mathcal{O}(\epsilon^0), \\ \mathcal{B}_0(\Delta, \mathbf{k}) &= \int_{\ell} \frac{1}{(\ell + \mathbf{k})^2} \frac{1}{\ell^2 + \Delta} = -\frac{1}{\mathbf{k}^2 + \Delta} \frac{1}{4\pi \epsilon_{\text{IR}}} + \mathcal{O}(\epsilon^0), \end{aligned}$$

$$\begin{aligned}
 \mathcal{C}_0(\Delta, \mathbf{k}) &= \int_{\ell} \frac{1}{\ell^2} \frac{1}{(\ell + \mathbf{k})^2} \frac{1}{\ell^2 + \Delta} = \frac{\mathbf{k}^2 + 2\Delta}{\mathbf{k}^2 \Delta} \mathcal{B}_0(\Delta, \mathbf{k}) + \mathcal{O}(\epsilon^0), \\
 \mathbf{k}^i \mathcal{C}_1(\Delta, \mathbf{k}) &= \int_{\ell} \frac{\ell^i}{\ell^2} \frac{1}{(\ell + \mathbf{k})^2} \frac{1}{\ell^2 + \Delta} = -\frac{\mathbf{k}^i}{\mathbf{k}^2} \mathcal{B}_0(\Delta, \mathbf{k}) + \mathcal{O}(\epsilon^0), \\
 \mathcal{C}^{ij}(\Delta, \mathbf{k}) &= \int_{\ell} \frac{\ell^i \ell^j}{\ell^2} \frac{1}{(\ell + \mathbf{k})^2} \frac{1}{\ell^2 + \Delta} = \frac{\mathbf{k}^i \mathbf{k}^j}{\mathbf{k}^2} \mathcal{B}_0(\Delta, \mathbf{k}) + \mathcal{O}(\epsilon^0).
 \end{aligned} \tag{A.18}$$

B Dirac algebra

In this section, we remind the reader of some key gamma matrix identities in transverse $D - 2$ -dimensional Euclidean space.

First, it follows from the definition $\{\gamma^\mu, \gamma^\nu\} = 2g^{\mu\nu} \mathbb{1}_4$ that:

$$\{\gamma^i, \gamma^j\} = -2\delta^{ij} \mathbb{1}_4, \tag{B.1}$$

with the trivial corollary:

$$\gamma^i \gamma^i \mathbb{1}_4 = -(D - 2) \mathbb{1}_4. \tag{B.2}$$

Repeated application of (B.1) brings us to the following important identity:

$$\gamma^i \gamma^j \gamma^k \gamma^l = \gamma^k \gamma^l \gamma^i \gamma^j + 2\delta^{il} \gamma^k \gamma^j - 2\delta^{ik} \gamma^l \gamma^j + 2\delta^{jl} \gamma^i \gamma^k - 2\delta^{jk} \gamma^i \gamma^l. \tag{B.3}$$

The Dirac sigma in $D - 2$ dimensions: $\sigma^{ij} = (i/2)[\gamma^i, \gamma^j]$, can then be shown to satisfy the following commutation relation:

$$[\sigma^{ij}, \sigma^{kl}] = 2i\delta^{il} \sigma^{kj} - 2i\delta^{ik} \sigma^{lj} + 2i\delta^{jl} \sigma^{ik} - 2i\delta^{jk} \sigma^{il}, \tag{B.4}$$

while contracting two Dirac sigmas gives:

$$\sigma^{ij} \sigma^{il} = (D - 3)\delta^{jl} \mathbb{1}_4 + i(D - 4)\sigma^{jl}. \tag{B.5}$$

The following identities will be useful as well:

$$\begin{aligned}
 \sigma^{\eta\eta'} \sigma^{\lambda\bar{\lambda}} \sigma^{\eta\bar{\eta}} &= 2i(D - 3)\delta^{\lambda\bar{\eta}} \delta^{\eta'\bar{\lambda}} - 2(D - 4)\delta^{\lambda\bar{\eta}} \sigma^{\eta'\bar{\lambda}} - 2i\sigma^{\lambda\eta'} \sigma^{\eta\bar{\lambda}} - 2i(D - 3)\delta^{\lambda\bar{\eta}} \delta^{\eta'\lambda} \\
 &\quad + 2(D - 4)\delta^{\lambda\bar{\eta}} \sigma^{\eta'\lambda} - 2i\sigma^{\lambda\eta'} \sigma^{\lambda\bar{\eta}} + (D - 3)\delta^{\eta'\bar{\eta}} \sigma^{\lambda\bar{\lambda}} + i(D - 4)\sigma^{\eta'\bar{\eta}} \sigma^{\lambda\bar{\lambda}},
 \end{aligned} \tag{B.6}$$

and:

$$\sigma^{\eta\bar{\eta}} \sigma^{\lambda\bar{\lambda}} \sigma^{\eta\bar{\eta}} = [(D - 3)(D - 2) - 8(D - 4)] \sigma^{\lambda\bar{\lambda}}. \tag{B.7}$$

Dirac traces can be often simplified using the fact that γ^+ and γ^- commute with the transverse gamma matrices and thus also with σ^{ij} , and then applying the completeness relation

$$u_G^s(q^+) \bar{u}_G^s(q^+) \gamma^+ = 2q^+ \mathcal{P}_G, \tag{B.8}$$

with $\mathcal{P}_G = \gamma^- \gamma^+ / 2$ the projector on good spinors.

Using the above definitions, together with the cyclic permutation property of the spinor trace and the fact that one can reverse the order of gamma matrices inside a trace:

$$\text{Tr}(\gamma^\mu \gamma^\nu \gamma^\rho \dots) = \text{Tr}(\dots \gamma^\rho \gamma^\nu \gamma^\mu), \tag{B.9}$$

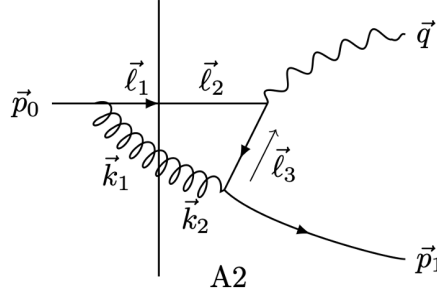


Figure 11. Feynman diagram for the production of a virtual photon and a quark via a gluon-quark-antiquark loop. The virtual gluon and quark scatter off the shockwave.

it is straightforward to establish the identities:

$$\begin{aligned}
 \text{Tr}(\mathcal{P}_G) &= 2, \\
 \text{Tr}(\mathcal{P}_G \sigma^{ij}) &= 0, \\
 \text{Tr}(\mathcal{P}_G \sigma^{ij} \sigma^{kl}) &= 2(\delta^{ik} \delta^{jl} - \delta^{il} \delta^{jk}) \stackrel{D \rightarrow 4}{=} 2\epsilon^{ij} \epsilon^{kl}.
 \end{aligned} \tag{B.10}$$

Moreover, using the above relations as well as the commutation relation (B.4), it is straightforward to prove the following relations:

$$\begin{aligned}
 &\text{Tr}\left\{\mathcal{P}_G(a\delta^{\lambda\lambda'} + i\sigma^{\lambda\lambda'})(b\delta^{\eta\bar{\eta}} - i\sigma^{\eta\bar{\eta}})(c\delta^{\lambda\bar{\lambda}} - i\sigma^{\lambda\bar{\lambda}})(d\delta^{\eta\eta'} - i\sigma^{\eta\eta'})\right\} \\
 &= 2\left[(ac + D - 3)(bd - (D - 3))\delta^{\bar{\eta}\eta'} \delta^{\bar{\lambda}\lambda'}\right. \\
 &\quad \left.+ \left((a + c)(b - d) + (D - 4)(c - a - b - d) + (D - 4)^2\right)\epsilon^{\bar{\eta}\eta'} \epsilon^{\bar{\lambda}\lambda'}\right],
 \end{aligned} \tag{B.11}$$

and:

$$\begin{aligned}
 &\text{Tr}\left\{\mathcal{P}_G(a\delta^{\eta\eta'} + i\sigma^{\eta\eta'})(b\delta^{\lambda\lambda'} + i\sigma^{\lambda\lambda'})(c\delta^{\lambda\bar{\lambda}} - i\sigma^{\lambda\bar{\lambda}})(d\delta^{\eta\bar{\eta}} - i\sigma^{\eta\bar{\eta}})\right\} \\
 &= 2\left[(ad + D - 3)(bc + D - 3)\delta^{\bar{\eta}\eta'} \delta^{\bar{\lambda}\lambda'} - (a + d + D - 4)(b + c - (D - 4))\epsilon^{\bar{\eta}\eta'} \epsilon^{\bar{\lambda}\lambda'}\right].
 \end{aligned} \tag{B.12}$$

C Example calculation

In this section, we describe in full detail the calculation of the amplitude corresponding to the diagram A2, depicted in figure 11. We follow the Bjorken-Kogut-Soper formulation of light-cone perturbation theory [77], and approach the CGC in the spirit of the dipole approach [74, 75]. In particular, we draw heavily from the excellent introduction to LCPT applied to the CGC in the appendix of ref. [33].

We remind the reader that the shockwave is treated as an external static potential. In this background field, we then perturbatively calculate the projectile dynamics, which take place on a much shorter timescale than those of the ‘frozen’ target. The leading-order and virtual amplitudes \mathcal{M} in our calculation are defined as:

$$f\langle \mathbf{q}(\vec{p}_1) \gamma^*(\vec{q}) | \hat{F} - 1 | \mathbf{q}(\vec{p}_0) \rangle_i = 2\pi \delta(p_0^+ - p_1^+ - q^+) \mathcal{M}, \tag{C.1}$$

where $\hat{F} - 1$ is the external potential evaluated between the Fock states of the incoming quark and outgoing quark with a virtual photon or vector boson.

The Fock states appearing in eq. (C.1) are obtained from the perturbative evolution of the asymptotic eigenstates of the free Hamiltonian \hat{H}_0 :

$$\begin{aligned} |\mathbf{q}(\vec{p}_0)\rangle_i &= \hat{U}(0, -\infty)|\mathbf{q}(\vec{p}_0)\rangle, \\ {}_f\langle\mathbf{q}(\vec{p}_1)\gamma^*(\vec{q})| &= \langle\mathbf{q}(\vec{p}_1)\gamma^*(\vec{q})|\hat{U}(+\infty, 0), \end{aligned} \quad (\text{C.2})$$

where $x^+ = 0$ is the space-time position of the shockwave. Next, remember from eq. (2.9) that:

$$\hat{U}(0, -\infty) \equiv \hat{T} \exp\left(-i \int_{-\infty}^0 dx^+ \hat{\mathcal{H}}(x^+)\right), \quad (\text{C.3})$$

where the Hamiltonian has the usual time dependence of the interaction picture:

$$\hat{\mathcal{H}}(x^+) = e^{i\hat{H}_0 x^+} \hat{V} e^{-i\hat{H}_0 x^+}. \quad (\text{C.4})$$

We now obtain:

$$\begin{aligned} \hat{U}(0, -\infty)|\mathbf{q}(\vec{p}_0)\rangle &= |\mathbf{q}(\vec{p}_0)\rangle \\ &\quad -i \int \text{PS}(\vec{\ell}_1, \vec{k}_1) \int_{-\infty}^0 dx^+ \langle\mathbf{q}(\vec{\ell}_1)\mathbf{g}(\vec{k}_1)| e^{i(\ell_1^- + k_1^-)x^+} \hat{V} e^{-ip_0^- x^+} |\mathbf{q}(\vec{p}_0)\rangle \\ &\quad \times |\mathbf{q}(\vec{\ell}_1)\mathbf{g}(\vec{k}_1)\rangle + \mathcal{O}(g_s^2), \\ &= |\mathbf{q}(\vec{p}_0)\rangle + \int \text{PS}(\vec{\ell}_1, \vec{k}_1) \frac{\langle\mathbf{q}(\vec{\ell}_1)\mathbf{g}(\vec{k}_1)|\hat{V}|\mathbf{q}(\vec{p}_0)\rangle}{p_0^- - \ell_1^- - k_1^- + i0^+} |\mathbf{q}(\vec{\ell}_1)\mathbf{g}(\vec{k}_1)\rangle + \mathcal{O}(g_s^2). \end{aligned} \quad (\text{C.5})$$

Likewise, being careful with the time-ordering operator \hat{T} :

$$\begin{aligned} \langle\mathbf{q}(\vec{p}_1)\gamma^*(\vec{q})|\hat{U}(+\infty, 0) &= \langle\mathbf{q}(\vec{p}_1)\gamma^*(\vec{q})| + \int \text{PS}(\vec{\ell}_2, \vec{\ell}_3) \langle\mathbf{q}(\vec{p}_1)\mathbf{q}(\vec{\ell}_2)\bar{\mathbf{q}}(\vec{\ell}_3)| \\ &\quad \times \langle\mathbf{q}(\vec{p}_1)\gamma^*(\vec{q})|\exp\left(-i \int_0^{+\infty} dx^+ \hat{\mathcal{H}}(x^+)\right) |\mathbf{q}(\vec{p}_1)\mathbf{q}(\vec{\ell}_2)\bar{\mathbf{q}}(\vec{\ell}_3)\rangle + (\dots), \\ &= \langle\mathbf{q}(\vec{p}_1)\gamma^*(\vec{q})| + \int \text{PS}(\vec{k}_2, \vec{\ell}_2, \vec{\ell}_3) \langle\mathbf{q}(\vec{\ell}_2)\mathbf{g}(\vec{k}_2)| \\ &\quad \times \langle\mathbf{q}(\vec{p}_1)\gamma^*(\vec{q})|\exp\left(-i \int_0^{+\infty} dx^+ \hat{\mathcal{H}}(x^+)\right) |\mathbf{q}(\vec{p}_1)\mathbf{q}(\vec{\ell}_2)\bar{\mathbf{q}}(\vec{\ell}_3)\rangle \\ &\quad \times \langle\mathbf{q}(\vec{p}_1)\mathbf{q}(\vec{\ell}_2)\bar{\mathbf{q}}(\vec{\ell}_3)|\exp\left(-i \int_0^{x^+} dy^+ \hat{\mathcal{H}}(y^+)\right) |\mathbf{q}(\vec{\ell}_2)\mathbf{g}(\vec{k}_2)\rangle + (\dots), \\ &= \langle\mathbf{q}(\vec{p}_1)\gamma^*(\vec{q})| + \int \text{PS}(\vec{k}_2, \vec{\ell}_2, \vec{\ell}_3) \langle\mathbf{q}(\vec{\ell}_2)\mathbf{g}(\vec{k}_2)| \\ &\quad \times \frac{\langle\mathbf{q}(\vec{p}_1)\gamma^*(\vec{q})|\hat{V}|\mathbf{q}(\vec{p}_1)\mathbf{q}(\vec{\ell}_2)\bar{\mathbf{q}}(\vec{\ell}_3)\rangle}{q^- - \ell_2^- - \ell_3^- + i0^+} \frac{\langle\mathbf{q}(\vec{p}_1)\mathbf{q}(\vec{\ell}_2)\bar{\mathbf{q}}(\vec{\ell}_3)|\hat{V}|\mathbf{q}(\vec{\ell}_2)\mathbf{g}(\vec{k}_2)\rangle}{p_1^+ + q^- - \ell_2^- - k_2^- + i0^+} + (\dots), \end{aligned} \quad (\text{C.6})$$

where (\dots) stands for all other possible diagrams, generated by inserting different intermediate Fock states. Combining (C.1) with (C.5) and (C.6), we obtain:

$$\begin{aligned} {}_f\langle\mathbf{q}(\vec{p}_1)\gamma^*(\vec{q})|\hat{F} - 1|\mathbf{q}(\vec{p}_0)\rangle_i &= \langle\mathbf{q}(\vec{p}_1)\gamma^*(\vec{q})|\hat{F} - 1|\mathbf{q}(\vec{p}_0)\rangle \\ &\quad + \int \text{PS}(\vec{k}_1, \vec{k}_2, \vec{\ell}_1, \vec{\ell}_2, \vec{\ell}_3) \frac{\langle\mathbf{q}(\vec{p}_1)\gamma^*(\vec{q})|\hat{V}|\mathbf{q}(\vec{p}_1)\mathbf{q}(\vec{\ell}_2)\bar{\mathbf{q}}(\vec{\ell}_3)\rangle}{q^- - \ell_2^- - \ell_3^- + i0^+} \\ &\quad \times \frac{\langle\mathbf{q}(\vec{p}_1)\mathbf{q}(\vec{\ell}_2)\bar{\mathbf{q}}(\vec{\ell}_3)|\hat{V}|\mathbf{q}(\vec{\ell}_2)\mathbf{g}(\vec{k}_2)\rangle}{p_1^+ + q^- - \ell_2^- - k_2^- + i0^+} \frac{\langle\mathbf{q}(\vec{\ell}_1)\mathbf{g}(\vec{k}_1)|\hat{V}|\mathbf{q}(\vec{p}_0)\rangle}{p_0^- - \ell_1^- - k_1^- + i0^+} \\ &\quad \times \langle\mathbf{q}(\vec{\ell}_2)\mathbf{g}(\vec{k}_2)|\hat{F} - 1|\mathbf{q}(\vec{\ell}_1)\mathbf{g}(\vec{k}_1)\rangle + (\dots). \end{aligned} \quad (\text{C.7})$$

Neglecting the leading-order part, there are three different numerators to evaluate. The interaction terms of the light-cone Hamiltonian for QCD and QED of interest are:

$$\hat{V} = \int d^{D-3}\vec{x} : g_{\text{em}}\bar{\psi}(\vec{x})\mathcal{A}(\vec{x})\psi(\vec{x}) + g_s t^c \bar{\psi}(\vec{x})\mathcal{A}^c(\vec{x})\psi(\vec{x}) : . \quad (\text{C.8})$$

We then obtain

$$\begin{aligned} \langle \mathbf{q}(\vec{\ell}_1)\mathbf{g}(\vec{k}_1)|\hat{V}|\mathbf{q}(\vec{p}_0)\rangle &= \langle 0|b_{\vec{\ell}_1} a_{\vec{k}_1} \hat{V} b_{\vec{p}_0}^\dagger |0\rangle, \\ &= g_s t^c \int d^{D-3}\vec{x} \langle 0|b_{\vec{\ell}_1} a_{\vec{k}_1} : \bar{\psi}(\vec{x})\mathcal{A}(\vec{x})\psi(\vec{x}) : b_{\vec{p}_0}^\dagger |0\rangle, \\ &= (2\pi)^{D-1} \delta^{(D-1)}(\vec{p}_0 - \vec{\ell}_1 - \vec{k}_1) g_s t^c \bar{u}(\vec{\ell}_1) \not{\epsilon}^*(\vec{k}_2) u(\vec{p}_0). \end{aligned} \quad (\text{C.9})$$

Likewise, the other numerators give:

$$\begin{aligned} \langle \mathbf{q}(\vec{p}_1)\mathbf{q}(\vec{\ell}_2)\bar{\mathbf{q}}(\vec{\ell}_3)|\hat{V}|\mathbf{q}(\vec{\ell}_2)\mathbf{g}(\vec{k}_2)\rangle &= (2\pi)^{D-1} \delta^{(D-1)}(\vec{p}_1 + \vec{\ell}_3 - \vec{k}_2) g_s t^c \bar{u}(\vec{p}_1) \not{\epsilon}(\vec{k}_2) v(\vec{\ell}_3), \\ \langle \mathbf{q}(\vec{p}_1)\gamma^*(\vec{q})|\hat{V}|\mathbf{q}(\vec{p}_1)\mathbf{q}(\vec{\ell}_2)\bar{\mathbf{q}}(\vec{\ell}_3)\rangle &= -(2\pi)^{D-1} \delta^{(D-1)}(\vec{\ell}_2 + \vec{\ell}_3 - \vec{q}) g_{\text{em}} \bar{v}(\vec{\ell}_3) \not{\epsilon}^*(\vec{q}) u(\vec{p}_1). \end{aligned} \quad (\text{C.10})$$

The minus sign in the last line comes from the anticommutation of the fermion field operators. Note that one should be careful to make sure that $\langle \mathbf{q}(\vec{p}_1)\mathbf{q}(\vec{\ell}_2)\bar{\mathbf{q}}(\vec{\ell}_3)|$ and $|\mathbf{q}(\vec{p}_1)\mathbf{q}(\vec{\ell}_2)\bar{\mathbf{q}}(\vec{\ell}_3)\rangle$ are indeed each other's conjugate.¹¹

We will shortly discuss the evaluation of the Dirac algebra, but let us first turn to the interaction of the projectile with the shockwave, encoded in the last line of (C.7). With the help of the (anti-)commutation relations (2.18) we derive the normalization of the Fock states:

$$\langle \mathbf{q}(\vec{\ell}_2)\mathbf{g}(\vec{k}_2)|\mathbf{q}(\vec{\ell}_1)\mathbf{g}(\vec{k}_1)\rangle = 2k_1^+ (2\pi)^{D-1} \delta^{(D-1)}(\vec{k}_1 - \vec{k}_2) 2\ell_1^+ (2\pi)^{D-1} \delta^{(D-1)}(\vec{\ell}_1 - \vec{\ell}_2). \quad (\text{C.11})$$

Moreover, the CGC dictates that, in the eikonal approximation, the shockwave is built from Wilson lines, and, therefore, the action of the external potential becomes:

$$\begin{aligned} \langle \mathbf{q}(\vec{\ell}_2)\mathbf{g}(\vec{k}_2)|\hat{F}|\mathbf{q}(\vec{\ell}_1)\mathbf{g}(\vec{k}_1)\rangle &= 2k_1^+ 2\pi \delta(k_1^+ - k_2^+) 2\ell_1^+ 2\pi \delta(\ell_1^+ - \ell_2^+) \\ &\quad \times \int_{\mathbf{x}, \mathbf{z}} e^{-i\mathbf{x}\cdot(\ell_2 - \ell_1)} e^{-i\mathbf{z}\cdot(\mathbf{k}_2 - \mathbf{k}_1)} U_{\mathbf{x}} W_{\mathbf{z}}^c, \end{aligned} \quad (\text{C.12})$$

where U and W are Wilson lines and the fundamental and adjoint representation, respectively. Filling in the implicit color factors and using the Fierz identity:

$$t^d W^{dc} = U^\dagger t^c U, \quad (\text{C.13})$$

equations (C.11) and (C.12) can be conveniently combined into:

$$\begin{aligned} \langle \mathbf{q}(\vec{\ell}_2)\mathbf{g}(\vec{k}_2)|\hat{F} - 1|\mathbf{q}(\vec{\ell}_1)\mathbf{g}(\vec{k}_1)\rangle &= 2k_1^+ 2\pi \delta(k_1^+ - k_2^+) 2\ell_1^+ 2\pi \delta(\ell_1^+ - \ell_2^+) \\ &\quad \times \int_{\mathbf{x}, \mathbf{z}} e^{-i\mathbf{x}\cdot(\ell_2 - \ell_1)} e^{-i\mathbf{z}\cdot(\mathbf{k}_2 - \mathbf{k}_1)} (t^c U_{\mathbf{x}} U_{\mathbf{z}}^\dagger t^c U_{\mathbf{z}} - C_F), \end{aligned} \quad (\text{C.14})$$

¹¹I am grateful to Guillaume Beuf for pointing me to this possible source of error, which allowed me to identify and correct a sign mistake.

We are now in a position to extract from definition (C.1) the expression for the amplitude \mathcal{M}_{A2} , by plugging the above equation together with (C.9) and (C.10) into (C.7), and using the delta functions to eliminate as many intermediate momenta as possible

$$\begin{aligned} \mathcal{M}_{A2} = & -g_{\text{em}} g_s^2 \int_{p_1^+}^{p_0^+} \frac{dk^+}{2\pi 2k^+} \frac{1}{2\ell_2^+ 2\ell_3^+} \int_{\mathbf{k}_1, \mathbf{k}_2} \frac{\bar{u}(\vec{p}_1) \not{\epsilon}(\vec{k}_2) v(\vec{\ell}_3)}{q^- - \ell_2^- - \ell_3^- + i0^+} \\ & \times \frac{\bar{v}(\vec{\ell}_3) \not{\epsilon}^*(\vec{q}) u(\vec{p}_1)}{p_1^+ + q^- - \ell_2^- - k_2^- + i0^+} \frac{\bar{u}(\vec{\ell}_1) \not{\epsilon}^*(\vec{k}_2) u(\vec{p}_0)}{p_0^- - \ell_1^- - k^- + i0^+} \\ & \times \int_{\mathbf{x}, \mathbf{z}} e^{-i\mathbf{x} \cdot (\ell_2 - \ell_1)} e^{-i\mathbf{z} \cdot (\mathbf{k}_2 - \mathbf{k}_1)} (t^c U_{\mathbf{x}} U_{\mathbf{z}}^\dagger t^c U_{\mathbf{z}} - C_F), \end{aligned} \quad (\text{C.15})$$

where it is understood that

$$\begin{aligned} \vec{\ell}_3 &= \vec{k}_2 - \vec{p}_1, & \vec{\ell}_2 &= \vec{q} + \vec{p}_1 - \vec{k}_2, \\ \vec{\ell}_1 &= \vec{p}_0 - \vec{k}_1, & k^+ &= k_1^+ = k_2^+. \end{aligned} \quad (\text{C.16})$$

Note that the Heaviside theta functions hidden in the phase-space integrations of (C.7) result in upper and lower limits for the integration over the gluon plus momentum.

The above expression can be simplified further by exploiting the properties of the projectors $\mathcal{P}_{G,B}$, such as $u_G = \mathcal{P}_G u_G$, $\bar{u}_G \mathcal{P}_B = 0$, $\gamma^- \mathcal{P}_G = \mathcal{P}_G \gamma^+ = 0$, and the fact that they commute with the transverse gamma matrices: $[\mathcal{P}_{G,B}, \gamma^i] = 0$. A generic spinor product then further simplifies into:

$$\begin{aligned} \bar{u}(\vec{k}_1) \not{\epsilon}(\vec{k}_3) u(\vec{k}_2) &= \bar{u}_G(k_1^+) \left[\gamma^+ \epsilon^-(\vec{k}_3) - \mathbf{k}_1 \cdot \gamma \frac{\gamma^+}{2k_1^+} \gamma \cdot \epsilon(\vec{k}_3) - \gamma \cdot \epsilon(\vec{k}_3) \frac{\gamma^+}{2k_2^+} \mathbf{k}_2 \cdot \gamma \right. \\ & \quad \left. + \mathbf{k}_1 \cdot \gamma \frac{\gamma^+}{2k_1^+} \gamma^- \frac{\gamma^+}{2k_2^+} \mathbf{k}_2 \cdot \gamma \epsilon^+(\vec{k}_3) \right] u_G(k_2^+), \\ &= \bar{u}_G(k_1^+) \gamma^+ \left[\epsilon^-(\vec{k}_3) + \left(\frac{\mathbf{k}_1^i \epsilon^j(\vec{k}_3)}{2k_1^+} + \frac{\epsilon^i(\vec{k}_3) \mathbf{k}_2^j}{2k_2^+} - \epsilon^+(\vec{k}_3) \frac{\mathbf{k}_1^i \mathbf{k}_2^j}{2k_1^+ k_2^+} \right) \gamma^i \gamma^j \right] u_G(k_2^+). \end{aligned} \quad (\text{C.17})$$

Finally, introducing $\sigma^{ij} = (i/2)[\gamma^i, \gamma^j]$ which allows us to write $\gamma^i \gamma^j = -\delta^{ij} - i\sigma^{ij}$, we obtain the expression:

$$\begin{aligned} \bar{u}(\vec{k}_1) \not{\epsilon}(\vec{k}_3) u(\vec{k}_2) &= \bar{u}_G(k_1^+) \gamma^+ \left[\left(\epsilon^-(\vec{k}_3) - \frac{\mathbf{k}_1^i \epsilon^j(\vec{k}_3)}{2k_1^+} - \frac{\epsilon^i(\vec{k}_3) \mathbf{k}_2^j}{2k_2^+} + \epsilon^+(\vec{k}_3) \frac{\mathbf{k}_1^i \mathbf{k}_2^j}{2k_1^+ k_2^+} \right) \delta^{ij} \right. \\ & \quad \left. - i\sigma^{ij} \left(\frac{\mathbf{k}_1^i \epsilon^j(\vec{k}_3)}{2k_1^+} + \frac{\epsilon^i(\vec{k}_3) \mathbf{k}_2^j}{2k_2^+} - \epsilon^+(\vec{k}_3) \frac{\mathbf{k}_1^i \mathbf{k}_2^j}{2k_1^+ k_2^+} \right) \right] u_G(k_2^+). \end{aligned} \quad (\text{C.18})$$

With a suitable choice of polarization vectors, and taking the relation between the different momenta into account, the above formula gives rise to remarkably compact expressions. For instance, returning to amplitude (C.15), we have the numerator:

$$\bar{u}(\vec{\ell}_1 = \vec{p}_0 - \vec{k}_2) \not{\epsilon}_\eta^*(\vec{k}_2) u(\vec{p}_0), \quad (\text{C.19})$$

where $\eta = 1, 2$ is the (transverse) polarization of the gluon. Choosing the polarization vectors for the gluon to be linearly polarized: $\epsilon_\eta^i = \delta^{i\eta}$, we have:

$$\epsilon_\eta^\mu(\vec{k}) = \left(0, \frac{\mathbf{k} \cdot \epsilon_\eta}{k^+}, \epsilon_\eta \right) = \left(0, \frac{\mathbf{k}^\eta}{k^+}, \delta^{i\eta} \right), \quad (\text{C.20})$$

applying (C.18) to the spinor product (C.19) gives:

$$\begin{aligned}
 & \bar{u}(\vec{\ell}_1 = \vec{p}_0 - \vec{k}_1) \not{\epsilon}_\eta^*(\vec{k}_1) u(\vec{p}_0) \\
 &= \bar{u}_G(\ell_1^+) \gamma^+ \left[\left(\frac{\mathbf{k}_1^{\eta'}}{k^+} - \frac{(\mathbf{p}_0 - \mathbf{k}_1)^{\eta'}}{2(p_0^+ - k^+)} - \frac{\mathbf{p}_0^{\eta'}}{2p_0^+} \right) \delta^{\eta\eta'} - i\sigma^{\eta\eta'} \left(\frac{\mathbf{p}_0^{\eta'}}{2p_0^+} - \frac{(\mathbf{p}_0 - \mathbf{k}_1)^{\eta'}}{2(p_0^+ - k^+)} \right) \right] u_G(p_0^+), \\
 &= \frac{p_0^+ \mathbf{k}_1^{\eta'} - k^+ \mathbf{p}_0^{\eta'}}{2p_0^+(p_0^+ - k^+)} \bar{u}_G(\ell_1^+) \gamma^+ \left[\left(2\frac{p_0^+}{k^+} - 1 \right) \delta^{\eta\eta'} - i\sigma^{\eta\eta'} \right] u_G(p_0^+), \\
 &= \frac{p_0^+ \mathbf{k}_1^{\eta'} - k^+ \mathbf{p}_0^{\eta'}}{2p_0^+(p_0^+ - k^+)} \bar{u}_G(\ell_1^+) \gamma^+ \mathcal{S}^{\eta\eta'} \left(2\frac{p_0^+}{k^+} - 1 \right) u_G(p_0^+).
 \end{aligned} \tag{C.21}$$

Likewise:

$$\bar{u}(\vec{p}_1) \not{\epsilon}_\eta(\vec{k}_2) v(\vec{\ell}_3) = -\frac{\ell^{\bar{\eta}} - \frac{k^+}{p_1^+} \mathbf{P}_\perp^{\bar{\eta}}}{2(p_1^+ - k^+)} \bar{u}_G(p_1^+) \gamma^+ \mathcal{S}^{\eta\bar{\eta}} \left(1 - \frac{2p_1^+}{k^+} \right) v_G(\ell_3^+), \tag{C.22}$$

where, for later convenience, we introduced the momentum combination:

$$\boldsymbol{\ell} \equiv \mathbf{k}_2 - \frac{k^+}{p_0^+} \mathbf{k}_\perp. \tag{C.23}$$

The last spinor product in (C.15) involves the external virtual photon. When the latter is transversely polarized, we obtain a similar expression to the ones with a gluon:

$$\begin{aligned}
 \bar{v}_G(\vec{\ell}_3) \not{\epsilon}_\lambda^*(\vec{q}) u_G(\vec{\ell}_2) &= \frac{q^+ \left(\ell^{\bar{\lambda}} - \frac{p_0^+ - k^+}{q^+} \mathbf{P}_\perp^{\bar{\lambda}} \right)}{2(p_1^+ - k^+)(p_0^+ - k^+)} \\
 &\times \bar{v}_G(\ell_3^+) \gamma^+ \mathcal{S}^{\lambda\bar{\lambda}} \left(1 + \frac{2(p_1^+ - k^+)}{q^+} \right) u_G(\ell_2^+).
 \end{aligned} \tag{C.24}$$

However, in the longitudinal case, the spinor product looks quite different:

$$\begin{aligned}
 \bar{v}_G(\vec{\ell}_3) \not{\epsilon}_0^*(\vec{q}) u_G(\vec{\ell}_2) &= \frac{q^+}{2(p_1^+ - k^+)(p_0^+ - k^+)M} \\
 &\times \left[\left(\ell - \frac{p_0^+ - k^+}{q^+} \mathbf{P}_\perp \right)^2 - \hat{M}^2 \right] \bar{v}_G(\ell_3^+) \gamma^+ u_G(\ell_2^+),
 \end{aligned} \tag{C.25}$$

where \hat{M}^2 is defined in (3.27).

Finally, it is convenient to cast the energy denominators in a form dictated by the momentum structure of the spinor products (C.21), (C.22), and (C.24), yielding after some algebra:

$$\begin{aligned}
 \frac{1}{p_0^- - k_1^- - \ell_1^-} &= \frac{-2k^+(p_0^+ - k^+)}{p_0^+ \mathbf{k}_1^2}, \\
 \frac{1}{q^- - \ell_2^- - \ell_3^-} &= \frac{2(p_1^+ - k^+)(p_0^+ - k^+)}{q^+} \frac{1}{\left(\ell - \frac{p_0^+ - k^+}{q^+} \mathbf{P}_\perp \right)^2 + \hat{M}^2}, \\
 \frac{1}{q^- + p_1^- - \ell_2^- - k_2^-} &= \frac{-2k^+(p_0^+ - k^+)}{p_0^+} \frac{1}{\ell^2 + \Delta_{\mathbf{P}}},
 \end{aligned} \tag{C.26}$$

where $\Delta_{\mathbf{P}}$ was defined in equation (3.4).

Gathering our expressions (C.21), (C.22), (C.24), and (C.25) for the numerators, together with the calculation (C.26) of the denominators, using (C.16) and (C.23) to rewrite the phases, we finally obtain:

$$\begin{aligned}
 \mathcal{M}_{A2}^0 &= \frac{1}{M} \int_{p_1^+}^{p_0^+} \frac{dk^+}{2\pi 2k^+} \frac{(k^+)^2 (p_0^+ - k^+)}{(p_0^+)^2 (p_1^+ - k^+)} \mathcal{S}_V^{\bar{\eta}0\eta'} \\
 &\times \int_{\mathbf{x}, \mathbf{z}} \int_{\mathbf{k}_1} \frac{\mathbf{k}_1^{\eta'}}{k_1^2} e^{-i\mathbf{k}_1 \cdot (\mathbf{x} - \mathbf{z})} \int_{\ell} e^{-i\ell \cdot (\mathbf{x} - \mathbf{z})} \frac{\ell^{\bar{\eta}} + \frac{k^+}{p_1^+} \mathbf{P}_{\perp}^{\bar{\eta}}}{\ell^2 + \Delta_P} \frac{\left(\ell + \frac{p_0^+ - k^+}{q^+} \mathbf{P}_{\perp}\right)^2 - \hat{M}^2}{\left(\ell + \frac{p_0^+ - k^+}{q^+} \mathbf{P}_{\perp}\right)^2 + \hat{M}^2} \\
 &\times e^{-i\mathbf{k}_{\perp} \cdot \left(\frac{p_0^+ - k^+}{p_0^+} \mathbf{x} + \frac{k^+}{p_0^+} \mathbf{z}\right)} (t^c U_{\mathbf{x}} U_{\mathbf{z}}^{\dagger} t^c U_{\mathbf{z}} - C_F),
 \end{aligned} \tag{C.27}$$

for the longitudinal polarization, and

$$\begin{aligned}
 \mathcal{M}_{A2}^{\lambda} &= - \int_{p_1^+}^{p_0^+} \frac{dk^+}{2\pi 2k^+} \frac{(k^+)^2 (p_0^+ - k^+)}{(p_0^+)^2 (p_1^+ - k^+)} \mathcal{S}_V^{\bar{\eta}\bar{\lambda}\eta'} \\
 &\times \int_{\mathbf{x}, \mathbf{z}} \int_{\mathbf{k}_1} \frac{\mathbf{k}_1^{\eta'}}{k_1^2} e^{-i\mathbf{k}_1 \cdot (\mathbf{x} - \mathbf{z})} \int_{\ell} e^{-i\ell \cdot (\mathbf{x} - \mathbf{z})} \frac{\ell^{\bar{\eta}} + \frac{k^+}{p_1^+} \mathbf{P}_{\perp}^{\bar{\eta}}}{\ell^2 + \Delta_P} \frac{\left(\ell^{\bar{\lambda}} + \frac{p_0^+ - k^+}{q^+} \mathbf{P}_{\perp}^{\bar{\lambda}}\right)}{\left(\ell + \frac{p_0^+ - k^+}{q^+} \mathbf{P}_{\perp}\right)^2 + \hat{M}^2} \\
 &\times e^{-i\mathbf{k}_{\perp} \cdot \left(\frac{p_0^+ - k^+}{p_0^+} \mathbf{x} + \frac{k^+}{p_0^+} \mathbf{z}\right)} (t^c U_{\mathbf{x}} U_{\mathbf{z}}^{\dagger} t^c U_{\mathbf{z}} - C_F),
 \end{aligned} \tag{C.28}$$

in the transverse case.

D Ultraviolet behavior of amplitude \mathcal{M}_{V2}

To investigate whether the transverse integral in (3.42) exhibits an UV divergence in the $\mathbf{z} \rightarrow \mathbf{x}$ limit, we set $\mathbf{z} = \mathbf{x}$ in the last line, after which \mathbf{z} can be integrated over in the second line. We obtain:

$$\begin{aligned}
 \lim_{\mathbf{z} \rightarrow \mathbf{x}} \tilde{\mathcal{M}}_{V2}^{\lambda} &= \alpha_s C_F \int_{k_{\min}^+}^{p_1^+} \frac{dk^+}{k^+} \frac{(k^+)^3 q^+}{p_1^+ (p_0^+)^2 (p_1^+ - k^+)} \mathcal{S}_V^{\bar{\eta}\bar{\lambda}\eta'} \\
 &\times \int_{\ell} \frac{\ell^{\eta'}}{\ell^2} \frac{\ell^{\bar{\eta}} - \frac{k^+}{p_1^+} \mathbf{P}_{\perp}^{\bar{\eta}}}{\left(\ell - \frac{k^+}{p_1^+} \mathbf{P}_{\perp}\right)^2} \frac{\ell^{\bar{\lambda}} - \frac{p_0^+ - k^+}{q^+} \mathbf{P}_{\perp}^{\bar{\lambda}}}{\ell^2 + \Delta_P} \\
 &\times \int_{\mathbf{x}} e^{-i\mathbf{k}_{\perp} \cdot \mathbf{x}} [U_{\mathbf{x}} - 1].
 \end{aligned} \tag{D.1}$$

The integral over ℓ , which we denote $\mathcal{I}_{V2}^{\eta'\bar{\eta}\lambda}$, contains three open transverse indices. However, when multiplying (3.38) with $\mathcal{M}_{LO}^{\lambda\dagger}$ to obtain the cross section, the trace of the Dirac structures $\mathcal{S}_{LO}^{\lambda\dagger} \mathcal{S}_V^{\bar{\eta}\bar{\lambda}\eta'}$ will yield only the Lorentz structures $\delta^{\bar{\eta}\eta'}$ and $\epsilon^{\bar{\eta}\eta'}$. We will use this knowledge and only calculate the projections $\delta^{\bar{\eta}\eta'} \mathcal{I}_{V2}^{\eta'\bar{\eta}\lambda}$ and $\epsilon^{\bar{\eta}\eta'} \mathcal{I}_{V2}^{\eta'\bar{\eta}\lambda}$, dramatically simplifying the evaluation. Using the identities (A.10) and (A.15), one finds:

$$\begin{aligned}
 \delta^{\bar{\eta}\eta'} \mathcal{I}_{V2}^{\eta'\bar{\eta}\lambda} &= \int_{\ell} \frac{1}{\ell^2} \frac{\ell \cdot \left(\ell - \frac{k^+}{p_1^+} \mathbf{P}_{\perp}\right)}{\left(\ell - \frac{k^+}{p_1^+} \mathbf{P}_{\perp}\right)^2} \frac{\ell^{\bar{\lambda}} - \frac{p_0^+ - k^+}{q^+} \mathbf{P}_{\perp}^{\bar{\lambda}}}{\ell^2 + \Delta_P}, \\
 &= \frac{k^+}{2p_1^+} \mathbf{P}_{\perp}^{\bar{\lambda}} \mathcal{B}_1(0, \Delta_P, \frac{k^+}{p_1^+} \mathbf{P}_{\perp})
 \end{aligned}$$

$$\begin{aligned}
 & -\frac{1}{2} \left(\frac{1}{2} + \frac{p_0^+(p_1^+ - k^+)}{k^+q^+} \right) \frac{k^+}{p_1^+} \mathbf{P}_\perp^\lambda \\
 & \times \left[\mathcal{B}_0(\Delta_P) + \mathcal{B}_0(\Delta_P, \frac{k^+}{p_1^+} \mathbf{P}_\perp) - \left(\frac{k^+}{p_1^+} \right)^2 \mathbf{P}_\perp^2 \mathcal{C}_0(\Delta_P, \frac{k^+}{p_1^+} \mathbf{P}_\perp) \right], \quad (\text{D.2})
 \end{aligned}$$

and

$$\begin{aligned}
 \epsilon^{\bar{\eta}\eta'} \mathcal{I}_{V2}^{\eta'\eta\lambda} &= \epsilon^{\bar{\eta}\eta'} \int \ell \frac{\ell^{\eta'} \ell^{\bar{\eta}} - \frac{k^+}{p_1^+} \mathbf{P}_\perp^{\bar{\eta}}}{\left(\ell - \frac{k^+}{p_1^+} \mathbf{P}_\perp \right)^2} \frac{\ell^{\bar{\lambda}} - \frac{p_0^+ - k^+}{q^+} \mathbf{P}_\perp^{\bar{\lambda}}}{\ell^2 + \Delta_P} \\
 &= \frac{k^+}{p_1^+} \mathbf{P}_\perp^{\bar{\eta}} \epsilon^{\bar{\eta}\lambda} \frac{1}{2} \frac{1}{D-3} \left[\mathcal{B}_1(0, \Delta_P, \frac{k^+}{p_1^+} \mathbf{P}_\perp) \right. \\
 & \quad \left. - \frac{1}{2} \mathcal{B}_0(\Delta_P) - \frac{1}{2} \mathcal{B}_0(\Delta_P, \frac{k^+}{p_1^+} \mathbf{P}_\perp) + \frac{1}{2} \left(\frac{k^+}{p_1^+} \right)^2 \mathbf{P}_\perp^2 \mathcal{C}_0(\Delta_P, \frac{k^+}{p_1^+} \mathbf{P}_\perp) \right]. \quad (\text{D.3})
 \end{aligned}$$

Neither of the above results contain an UV divergence. Moreover, the infrared poles contained in the structures $\mathcal{B}_0(\Delta_P)$, $\mathcal{B}_0(\Delta_P, \frac{k^+}{p_1^+} \mathbf{P}_\perp)$, and $\mathcal{C}_0(\Delta_P, \frac{k^+}{p_1^+} \mathbf{P}_\perp)$ all cancel (see eq. (A.18)). Expressions (D.2) and (D.3) are, therefore, finite.

E Quark field-strength renormalization

We consider a dressed quark Fock state, and expand it perturbatively to first order:

$$|\mathbf{q}(\vec{p}_0)\rangle = \sqrt{\mathcal{Z}} |\mathbf{q}(\vec{p}_0)\rangle_0 + \int \text{PS}(\vec{p}_1, \vec{k}) \frac{{}_0\langle \mathbf{q}(\vec{p}_1), \mathbf{g}(\vec{k}) | \hat{V} | \mathbf{q}(\vec{p}_0) \rangle_0}{p_0^- - k^- - p_1^-} |\mathbf{q}(\vec{p}_1), \mathbf{g}(\vec{k})\rangle_0 + \mathcal{O}(g_s^2). \quad (\text{E.1})$$

The interaction Hamiltonian sandwiched between the bare Fock states yields:

$$\begin{aligned}
 {}_0\langle \mathbf{q}(\vec{p}_1), \mathbf{g}(\vec{k}) | \hat{V} | \mathbf{q}(\vec{p}_0)\rangle_0 &= (2\pi)^{D-1} \delta^{(D-1)}(\vec{p}_0 - \vec{k} - \vec{p}_1) g_s t^c \bar{u}(\vec{p}_1) \not{\epsilon}_\eta^*(\vec{k}) u(\vec{p}_0), \\
 &= (2\pi)^{D-1} \delta^{(D-1)}(\vec{p}_0 - \vec{k} - \vec{p}_1) g_s t^c \\
 & \quad \times \frac{\left(\mathbf{k} - \frac{k^+}{p_0^+} \mathbf{p}_0 \right)^{\bar{\eta}}}{2(p_0^+ - k^+)} \mathcal{S}^{\eta\bar{\eta}} \left(2 \frac{p_0^+}{k^+} - 1 \right), \quad (\text{E.2})
 \end{aligned}$$

while the energy denominator gives:

$$\frac{1}{p_0^- - k^- - p_1^-} = -\frac{2k^+(p_0^+ - k^+)}{p_0^+ \left(\mathbf{k} - \frac{k^+}{p_0^+} \mathbf{p}_0 \right)^2}. \quad (\text{E.3})$$

Combining the above results, we obtain the following result for the first-order expansion of the dressed quark state, temporarily indicating all the spin- and color indices

$$\begin{aligned}
 |\mathbf{q}(\vec{p}_0, s, i)\rangle &= \sqrt{\mathcal{Z}} |\mathbf{q}(\vec{p}_0, s, i)\rangle_0 \\
 & - \sum_{j, \tilde{s}, h, c} \int \text{PS}(\vec{p}_1, \vec{k}) (2\pi)^{D-1} \delta^{(D-1)}(\vec{p}_0 - \vec{k} - \vec{p}_1) \\
 & \quad \times g_s t_{ij}^c \frac{k^+}{p_0^+} \frac{\left(\mathbf{k} - \frac{k^+}{p_0^+} \mathbf{p}_0 \right)^{\bar{\eta}}}{\left(\mathbf{k} - \frac{k^+}{p_0^+} \mathbf{p}_0 \right)^2} \mathcal{S}^{\eta\bar{\eta}} \left(2 \frac{p_0^+}{k^+} - 1 \right) |\mathbf{q}(\vec{p}_1, \tilde{s}, j), \mathbf{g}(\vec{k}, h, c)\rangle_0. \quad (\text{E.4})
 \end{aligned}$$

Per definition, we require the Fock states to be normalized in the sense of a distribution:

$$\langle \mathbf{q}(\vec{p}_0, s', i') | \mathbf{q}(\vec{p}_0, s, i) \rangle = 2p_0^+ \delta_{s's} \delta_{i'i} (2\pi)^{D-1} \delta^{(D-1)}(\vec{p}_0 - \vec{p}'_0), \quad (\text{E.5})$$

or:

$$\frac{1}{2N_c} \sum_{s'i'} \int \text{PS}(\vec{p}_0) \langle \mathbf{q}(\vec{p}'_0, s', i') | \mathbf{q}(\vec{p}_0, s, i) \rangle = 1. \quad (\text{E.6})$$

Since the above is supposed to hold to any order of perturbation theory, we can write:

$$\begin{aligned} 1 &= \mathcal{Z} + \frac{1}{2N_c} \int \text{PS}(\vec{p}_0, \vec{p}_1, \vec{k}, \vec{p}'_1, \vec{k}') (2\pi)^{D-1} \delta^{(D-1)}(\vec{p}_0 - \vec{k} - \vec{p}_1) \\ &\quad \times (2\pi)^{D-1} \delta^{(D-1)}(\vec{p}'_0 - \vec{k}' - \vec{p}'_1) g_s^2 \text{Tr}(t^c t^c) \frac{k^+ k'^+}{p_0^+ p_0'^+} \\ &\quad \times \frac{\left(\mathbf{k} - \frac{k^+}{p_0^+} \mathbf{p}_0\right)^{\bar{\eta}} \left(\mathbf{k}' - \frac{k'^+}{p_0'^+} \mathbf{p}'_0\right)^{\bar{\eta}'}}{\left(\mathbf{k} - \frac{k^+}{p_0^+} \mathbf{p}_0\right)^2 \left(\mathbf{k}' - \frac{k'^+}{p_0'^+} \mathbf{p}'_0\right)^2} \mathcal{S}^{\eta\eta'} \left(2\frac{p_0'^+}{k'^+} - 1\right) \mathcal{S}^{\bar{\eta}\bar{\eta}'} \left(2\frac{p_0^+}{k^+} - 1\right) \\ &\quad \times {}_0\langle \mathbf{q}(\vec{p}'_1), \mathbf{g}(\vec{k}') | \mathbf{q}(\vec{p}_1), \mathbf{g}(\vec{k}) \rangle_0, \\ &= \mathcal{Z} + \alpha_s C_F \int_{\mathbf{k}} \frac{1}{\mathbf{k}^2} \times \int_{k_{\min}^+}^{p_0^+} \frac{dk^+}{k^+} \frac{(k^+)^2}{(p_0^+)^2} \left[\left(1 - \frac{2p_0^+}{k^+}\right)^2 + (D-3) \right] \\ &= \mathcal{Z} + \alpha_s C_F \int_{\mathbf{k}} \frac{1}{\mathbf{k}^2} \times \left[-3 + 4 \ln \frac{p_0^+}{k_{\min}^+} \right] \\ &= \mathcal{Z} + \frac{\alpha_s C_F}{2\pi} \left(\frac{1}{\epsilon_{\text{UV}}} - \frac{1}{\epsilon_{\text{IR}}} \right) \left(-\frac{3}{2} + 2 \ln \frac{p_0^+}{k_{\min}^+} \right) + \mathcal{O}(\epsilon_{\text{UV}}), \end{aligned} \quad (\text{E.7})$$

and finally:

$$\mathcal{Z} = \left[1 - \frac{\alpha_s C_F}{2\pi} \left(\frac{1}{\epsilon_{\text{UV}}} - \frac{1}{\epsilon_{\text{IR}}} \right) \left(-3 + 2 \ln \frac{p_0^+}{k_{\min}^+} + 2 \ln \frac{p_1^+}{k_{\min}^+} \right) \right]. \quad (\text{E.8})$$

Open Access. This article is distributed under the terms of the Creative Commons Attribution License ([CC-BY 4.0](https://creativecommons.org/licenses/by/4.0/)), which permits any use, distribution and reproduction in any medium, provided the original author(s) and source are credited.

References

- [1] V.N. Gribov and L.N. Lipatov, *Deep inelastic e p scattering in perturbation theory*, *Sov. J. Nucl. Phys.* **15** (1972) 438 [[INSPIRE](#)].
- [2] Y.L. Dokshitzer, *Calculation of the Structure Functions for Deep Inelastic Scattering and e⁺e⁻ Annihilation by Perturbation Theory in Quantum Chromodynamics*, *Sov. Phys. JETP* **46** (1977) 641 [[INSPIRE](#)].
- [3] G. Altarelli and G. Parisi, *Asymptotic Freedom in Parton Language*, *Nucl. Phys. B* **126** (1977) 298 [[INSPIRE](#)].
- [4] S. Catani, M. Ciafaloni and F. Hautmann, *Gluon contributions to small x heavy flavor production*, *Phys. Lett. B* **242** (1990) 97 [[INSPIRE](#)].
- [5] S. Catani, M. Ciafaloni and F. Hautmann, *High-energy factorization and small x heavy flavor production*, *Nucl. Phys. B* **366** (1991) 135 [[INSPIRE](#)].

- [6] S. Catani and F. Hautmann, *High-energy factorization and small x deep inelastic scattering beyond leading order*, *Nucl. Phys. B* **427** (1994) 475 [[hep-ph/9405388](#)] [[INSPIRE](#)].
- [7] E.A. Kuraev, L.N. Lipatov and V.S. Fadin, *The Pomeron singularity in Nonabelian Gauge Theories*, *Sov. Phys. JETP* **45** (1977) 199 [[INSPIRE](#)].
- [8] I.I. Balitsky and L.N. Lipatov, *The Pomeron singularity in Quantum Chromodynamics*, *Sov. J. Nucl. Phys.* **28** (1978) 822 [[INSPIRE](#)].
- [9] L.D. McLerran and R. Venugopalan, *Computing quark and gluon distribution functions for very large nuclei*, *Phys. Rev. D* **49** (1994) 2233 [[hep-ph/9309289](#)] [[INSPIRE](#)].
- [10] L.D. McLerran and R. Venugopalan, *Gluon distribution functions for very large nuclei at small transverse momentum*, *Phys. Rev. D* **49** (1994) 3352 [[hep-ph/9311205](#)] [[INSPIRE](#)].
- [11] L.D. McLerran and R. Venugopalan, *Green's functions in the color field of a large nucleus*, *Phys. Rev. D* **50** (1994) 2225 [[hep-ph/9402335](#)] [[INSPIRE](#)].
- [12] J. Jalilian-Marian, A. Kovner, A. Leonidov and H. Weigert, *The BFKL equation from the Wilson renormalization group*, *Nucl. Phys. B* **504** (1997) 415 [[hep-ph/9701284](#)] [[INSPIRE](#)].
- [13] J. Jalilian-Marian, A. Kovner, A. Leonidov and H. Weigert, *The Wilson renormalization group for low x physics: Towards the high density regime*, *Phys. Rev. D* **59** (1998) 014014 [[hep-ph/9706377](#)] [[INSPIRE](#)].
- [14] J. Jalilian-Marian, A. Kovner and H. Weigert, *The Wilson renormalization group for low x physics: Gluon evolution at finite parton density*, *Phys. Rev. D* **59** (1998) 014015 [[hep-ph/9709432](#)] [[INSPIRE](#)].
- [15] A. Kovner, J.G. Milhano and H. Weigert, *Relating different approaches to nonlinear QCD evolution at finite gluon density*, *Phys. Rev. D* **62** (2000) 114005 [[hep-ph/0004014](#)] [[INSPIRE](#)].
- [16] H. Weigert, *Unitarity at small Bjorken x* , *Nucl. Phys. A* **703** (2002) 823 [[hep-ph/0004044](#)] [[INSPIRE](#)].
- [17] E. Iancu, A. Leonidov and L.D. McLerran, *Nonlinear gluon evolution in the color glass condensate. 1*, *Nucl. Phys. A* **692** (2001) 583 [[hep-ph/0011241](#)] [[INSPIRE](#)].
- [18] E. Iancu, A. Leonidov and L.D. McLerran, *The Renormalization group equation for the color glass condensate*, *Phys. Lett. B* **510** (2001) 133 [[hep-ph/0102009](#)] [[INSPIRE](#)].
- [19] E. Ferreiro, E. Iancu, A. Leonidov and L. McLerran, *Nonlinear gluon evolution in the color glass condensate. 2*, *Nucl. Phys. A* **703** (2002) 489 [[hep-ph/0109115](#)] [[INSPIRE](#)].
- [20] L.V. Gribov, E.M. Levin and M.G. Ryskin, *Semihard Processes in QCD*, *Phys. Rept.* **100** (1983) 1 [[INSPIRE](#)].
- [21] I. Balitsky, *Operator expansion for high-energy scattering*, *Nucl. Phys. B* **463** (1996) 99 [[hep-ph/9509348](#)] [[INSPIRE](#)].
- [22] I. Balitsky, *Factorization for high-energy scattering*, *Phys. Rev. Lett.* **81** (1998) 2024 [[hep-ph/9807434](#)] [[INSPIRE](#)].
- [23] I. Balitsky, *Factorization and high-energy effective action*, *Phys. Rev. D* **60** (1999) 014020 [[hep-ph/9812311](#)] [[INSPIRE](#)].
- [24] Y.V. Kovchegov, *Small- x F_2 structure function of a nucleus including multiple pomeron exchanges*, *Phys. Rev. D* **60** (1999) 034008 [[hep-ph/9901281](#)] [[INSPIRE](#)].

- [25] T. Altinoluk, R. Boussarie and P. Kotko, *Interplay of the CGC and TMD frameworks to all orders in kinematic twist*, *JHEP* **05** (2019) 156 [[arXiv:1901.01175](#)] [[INSPIRE](#)].
- [26] T. Altinoluk and R. Boussarie, *Low x physics as an infinite twist (G)TMD framework: unravelling the origins of saturation*, *JHEP* **10** (2019) 208 [[arXiv:1902.07930](#)] [[INSPIRE](#)].
- [27] A. Morreale and F. Salazar, *Mining for Gluon Saturation at Colliders*, *Universe* **7** (2021) 312 [[arXiv:2108.08254](#)] [[INSPIRE](#)].
- [28] G.A. Chirilli, B.-W. Xiao and F. Yuan, *One-loop Factorization for Inclusive Hadron Production in pA Collisions in the Saturation Formalism*, *Phys. Rev. Lett.* **108** (2012) 122301 [[arXiv:1112.1061](#)] [[INSPIRE](#)].
- [29] G.A. Chirilli, B.-W. Xiao and F. Yuan, *Inclusive Hadron Productions in pA Collisions*, *Phys. Rev. D* **86** (2012) 054005 [[arXiv:1203.6139](#)] [[INSPIRE](#)].
- [30] I. Balitsky and G.A. Chirilli, *Photon impact factor in the next-to-leading order*, *Phys. Rev. D* **83** (2011) 031502 [[arXiv:1009.4729](#)] [[INSPIRE](#)].
- [31] I. Balitsky and G.A. Chirilli, *Photon impact factor and k_T -factorization for DIS in the next-to-leading order*, *Phys. Rev. D* **87** (2013) 014013 [[arXiv:1207.3844](#)] [[INSPIRE](#)].
- [32] G. Beuf, *NLO corrections for the dipole factorization of DIS structure functions at low x* , *Phys. Rev. D* **85** (2012) 034039 [[arXiv:1112.4501](#)] [[INSPIRE](#)].
- [33] G. Beuf, *Dipole factorization for DIS at NLO: Loop correction to the $\gamma_{T,L}^* \rightarrow q\bar{q}$ light-front wave functions*, *Phys. Rev. D* **94** (2016) 054016 [[arXiv:1606.00777](#)] [[INSPIRE](#)].
- [34] G. Beuf, *Dipole factorization for DIS at NLO: Combining the $q\bar{q}$ and $q\bar{q}g$ contributions*, *Phys. Rev. D* **96** (2017) 074033 [[arXiv:1708.06557](#)] [[INSPIRE](#)].
- [35] H. Hämmänen, T. Lappi and R. Paatelainen, *One-loop corrections to light cone wave functions: the dipole picture DIS cross section*, *Annals Phys.* **393** (2018) 358 [[arXiv:1711.08207](#)] [[INSPIRE](#)].
- [36] G. Beuf, T. Lappi and R. Paatelainen, *Massive quarks in NLO dipole factorization for DIS: Longitudinal photon*, *Phys. Rev. D* **104** (2021) 056032 [[arXiv:2103.14549](#)] [[INSPIRE](#)].
- [37] G. Beuf, T. Lappi and R. Paatelainen, *Massive Quarks at One Loop in the Dipole Picture of Deep Inelastic Scattering*, *Phys. Rev. Lett.* **129** (2022) 072001 [[arXiv:2112.03158](#)] [[INSPIRE](#)].
- [38] G. Beuf, T. Lappi and R. Paatelainen, *Massive quarks in NLO dipole factorization for DIS: Transverse photon*, *Phys. Rev. D* **106** (2022) 034013 [[arXiv:2204.02486](#)] [[INSPIRE](#)].
- [39] R. Boussarie et al., *Next-to-Leading Order Computation of Exclusive Diffractive Light Vector Meson Production in a Saturation Framework*, *Phys. Rev. Lett.* **119** (2017) 072002 [[arXiv:1612.08026](#)] [[INSPIRE](#)].
- [40] H. Mäntysaari and J. Penttala, *Exclusive production of light vector mesons at next-to-leading order in the dipole picture*, *Phys. Rev. D* **105** (2022) 114038 [[arXiv:2203.16911](#)] [[INSPIRE](#)].
- [41] H. Mäntysaari and J. Penttala, *Exclusive heavy vector meson production at next-to-leading order in the dipole picture*, *Phys. Lett. B* **823** (2021) 136723 [[arXiv:2104.02349](#)] [[INSPIRE](#)].
- [42] H. Mäntysaari and J. Penttala, *Complete calculation of exclusive heavy vector meson production at next-to-leading order in the dipole picture*, *JHEP* **08** (2022) 247 [[arXiv:2204.14031](#)] [[INSPIRE](#)].
- [43] K. Roy and R. Venugopalan, *NLO impact factor for inclusive photon + dijet production in $e + A$ DIS at small x* , *Phys. Rev. D* **101** (2020) 034028 [[arXiv:1911.04530](#)] [[INSPIRE](#)].

- [44] R. Boussarie, A.V. Grabovsky, L. Szymanowski and S. Wallon, *On the one loop $\gamma^{(*)} \rightarrow q\bar{q}$ impact factor and the exclusive diffractive cross sections for the production of two or three jets*, *JHEP* **11** (2016) 149 [[arXiv:1606.00419](#)] [[INSPIRE](#)].
- [45] M. Fucilla et al., *NLO computation of diffractive di-hadron production in a saturation framework*, *JHEP* **03** (2023) 159 [[arXiv:2211.05774](#)] [[INSPIRE](#)].
- [46] P. Caucal, F. Salazar and R. Venugopalan, *Dijet impact factor in DIS at next-to-leading order in the Color Glass Condensate*, *JHEP* **11** (2021) 222 [[arXiv:2108.06347](#)] [[INSPIRE](#)].
- [47] F. Bergabo and J. Jalilian-Marian, *One-loop corrections to dihadron production in DIS at small x* , *Phys. Rev. D* **106** (2022) 054035 [[arXiv:2207.03606](#)] [[INSPIRE](#)].
- [48] F. Bergabo and J. Jalilian-Marian, *Dihadron production in DIS at small x at next-to-leading order: Transverse photons*, *Phys. Rev. D* **107** (2023) 054036 [[arXiv:2301.03117](#)] [[INSPIRE](#)].
- [49] F. Bergabo and J. Jalilian-Marian, *Single inclusive hadron production in DIS at small x : next to leading order corrections*, *JHEP* **01** (2023) 095 [[arXiv:2210.03208](#)] [[INSPIRE](#)].
- [50] P. Taels, T. Altinoluk, G. Beuf and C. Marquet, *Dijet photoproduction at low x at next-to-leading order and its back-to-back limit*, *JHEP* **10** (2022) 184 [[arXiv:2204.11650](#)] [[INSPIRE](#)].
- [51] I. Balitsky and G.A. Chirilli, *Rapidity evolution of Wilson lines at the next-to-leading order*, *Phys. Rev. D* **88** (2013) 111501 [[arXiv:1309.7644](#)] [[INSPIRE](#)].
- [52] A. Kovner, M. Lublinsky and Y. Mulian, *Jalilian-Marian, Iancu, McLerran, Weigert, Leonidov, Kovner evolution at next to leading order*, *Phys. Rev. D* **89** (2014) 061704 [[arXiv:1310.0378](#)] [[INSPIRE](#)].
- [53] A. Kovner, M. Lublinsky and Y. Mulian, *NLO JIMWLK evolution unabridged*, *JHEP* **08** (2014) 114 [[arXiv:1405.0418](#)] [[INSPIRE](#)].
- [54] M. Lublinsky and Y. Mulian, *High Energy QCD at NLO: from light-cone wave function to JIMWLK evolution*, *JHEP* **05** (2017) 097 [[arXiv:1610.03453](#)] [[INSPIRE](#)].
- [55] A. Ayala, M. Hentschinski, J. Jalilian-Marian and M.E. Tejeda-Yeomans, *Polarized 3 parton production in inclusive DIS at small x* , *Phys. Lett. B* **761** (2016) 229 [[arXiv:1604.08526](#)] [[INSPIRE](#)].
- [56] E. Iancu and Y. Mulian, *Forward trijet production in proton-nucleus collisions*, *Nucl. Phys. A* **985** (2019) 66 [[arXiv:1809.05526](#)] [[INSPIRE](#)].
- [57] T. Altinoluk, R. Boussarie, C. Marquet and P. Taels, *TMD factorization for dijets + photon production from the dilute-dense CGC framework*, *JHEP* **07** (2019) 079 [[arXiv:1810.11273](#)] [[INSPIRE](#)].
- [58] T. Altinoluk, R. Boussarie, C. Marquet and P. Taels, *Photoproduction of three jets in the CGC: gluon TMDs and dilute limit*, *JHEP* **07** (2020) 143 [[arXiv:2001.00765](#)] [[INSPIRE](#)].
- [59] E. Iancu and Y. Mulian, *Forward dijets in proton-nucleus collisions at next-to-leading order: the real corrections*, *JHEP* **03** (2021) 005 [[arXiv:2009.11930](#)] [[INSPIRE](#)].
- [60] E. Iancu and Y. Mulian, *Dihadron production in DIS at NLO: the real corrections*, *JHEP* **07** (2023) 121 [[arXiv:2211.04837](#)] [[INSPIRE](#)].
- [61] F.G. Celiberto et al., *The next-to-leading order Higgs impact factor in the infinite top-mass limit*, *JHEP* **08** (2022) 092 [[arXiv:2205.02681](#)] [[INSPIRE](#)].

- [62] S.D. Drell and T.-M. Yan, *Massive Lepton Pair Production in Hadron-Hadron Collisions at High-Energies*, *Phys. Rev. Lett.* **25** (1970) 316 [Erratum *ibid.* **25** (1970) 902] [INSPIRE].
- [63] F. Gelis and J. Jalilian-Marian, *Dilepton production from the color glass condensate*, *Phys. Rev. D* **66** (2002) 094014 [hep-ph/0208141] [INSPIRE].
- [64] A. Stasto, B.-W. Xiao and D. Zaslavsky, *Drell-Yan Lepton-Pair-Jet Correlation in pA collisions*, *Phys. Rev. D* **86** (2012) 014009 [arXiv:1204.4861] [INSPIRE].
- [65] E. Basso et al., *Drell-Yan phenomenology in the color dipole picture revisited*, *Phys. Rev. D* **93** (2016) 034023 [arXiv:1510.00650] [INSPIRE].
- [66] A. van Hameren, P. Kotko and K. Kutak, *Resummation effects in the forward production of $Z_0 + jet$ at the LHC*, *Phys. Rev. D* **92** (2015) 054007 [arXiv:1505.02763] [INSPIRE].
- [67] M. Deak et al., *Calculation of the $Z+jet$ cross section including transverse momenta of initial partons*, *Phys. Rev. D* **99** (2019) 094011 [arXiv:1809.03854] [INSPIRE].
- [68] LHCb collaboration, *Study of forward $Z + jet$ production in pp collisions at $\sqrt{s} = 7$ TeV*, *JHEP* **01** (2014) 033 [arXiv:1310.8197] [INSPIRE].
- [69] A.H. Mueller and H. Navelet, *An Inclusive Minijet Cross-Section and the Bare Pomeron in QCD*, *Nucl. Phys. B* **282** (1987) 727 [INSPIRE].
- [70] E.L. Berger, J.-W. Qiu and X.-F. Zhang, *QCD factorized Drell-Yan cross-section at large transverse momentum*, *Phys. Rev. D* **65** (2002) 034006 [hep-ph/0107309] [INSPIRE].
- [71] A. Dumitru, A. Hayashigaki and J. Jalilian-Marian, *The Color glass condensate and hadron production in the forward region*, *Nucl. Phys. A* **765** (2006) 464 [hep-ph/0506308] [INSPIRE].
- [72] T. Altinoluk and A. Kovner, *Particle Production at High Energy and Large Transverse Momentum — ‘The Hybrid Formalism’ Revisited*, *Phys. Rev. D* **83** (2011) 105004 [arXiv:1102.5327] [INSPIRE].
- [73] T. Altinoluk, N. Armesto, A. Kovner and M. Lublinsky, *Single inclusive particle production at next-to-leading order in proton-nucleus collisions at forward rapidities: Hybrid approach meets TMD factorization*, *Phys. Rev. D* **108** (2023) 074003 [arXiv:2307.14922] [INSPIRE].
- [74] A.H. Mueller, *Small x Behavior and Parton Saturation: A QCD Model*, *Nucl. Phys. B* **335** (1990) 115 [INSPIRE].
- [75] N.N. Nikolaev and B.G. Zakharov, *Color transparency and scaling properties of nuclear shadowing in deep inelastic scattering*, *Z. Phys. C* **49** (1991) 607 [INSPIRE].
- [76] J.B. Kogut and D.E. Soper, *Quantum Electrodynamics in the Infinite Momentum Frame*, *Phys. Rev. D* **1** (1970) 2901 [INSPIRE].
- [77] J.D. Bjorken, J.B. Kogut and D.E. Soper, *Quantum Electrodynamics at Infinite Momentum: Scattering from an External Field*, *Phys. Rev. D* **3** (1971) 1382 [INSPIRE].
- [78] S.J. Brodsky, H.-C. Pauli and S.S. Pinsky, *Quantum chromodynamics and other field theories on the light cone*, *Phys. Rept.* **301** (1998) 299 [hep-ph/9705477] [INSPIRE].
- [79] G. 't Hooft and M.J.G. Veltman, *Regularization and Renormalization of Gauge Fields*, *Nucl. Phys. B* **44** (1972) 189 [INSPIRE].
- [80] A.H. Mueller, *Soft gluons in the infinite momentum wave function and the BFKL pomeron*, *Nucl. Phys. B* **415** (1994) 373 [INSPIRE].

- [81] R.K. Ellis, W.J. Stirling and B.R. Webber, *QCD and collider physics*, Cambridge University Press (2011) [DOI:10.1017/CB09780511628788] [INSPIRE].
- [82] Y.L. Dokshitzer, G.D. Leder, S. Moretti and B.R. Webber, *Better jet clustering algorithms*, *JHEP* **08** (1997) 001 [hep-ph/9707323] [INSPIRE].
- [83] M. Wobisch and T. Wengler, *Hadronization corrections to jet cross-sections in deep inelastic scattering*, in the proceedings of the *Workshop on Monte Carlo Generators for HERA Physics (Plenary Starting Meeting)*, Hamburg Germany, April 27–30 (1998), p. 270–279 [hep-ph/9907280] [INSPIRE].
- [84] G. Beuf, *Improving the kinematics for low- x QCD evolution equations in coordinate space*, *Phys. Rev. D* **89** (2014) 074039 [arXiv:1401.0313] [INSPIRE].
- [85] I.S. Gradshteyn and I.M. Ryzhik, *Table of Integrals, Series, and Products*, Academic Press (1943) [DOI:10.1016/B978-0-12-294757-5.X5000-4] [INSPIRE].
- [86] J. Jalilian-Marian and A.H. Rezaeian, *Prompt photon production and photon-hadron correlations at RHIC and the LHC from the Color Glass Condensate*, *Phys. Rev. D* **86** (2012) 034016 [arXiv:1204.1319] [INSPIRE].
- [87] A.H. Rezaeian, *Semi-inclusive photon-hadron production in pp and pA collisions at RHIC and LHC*, *Phys. Rev. D* **86** (2012) 094016 [arXiv:1209.0478] [INSPIRE].
- [88] S. Benić and A. Dumitru, *Prompt photon-jet angular correlations at central rapidities in $p + A$ collisions*, *Phys. Rev. D* **97** (2018) 014012 [arXiv:1710.01991] [INSPIRE].
- [89] V.P. Goncalves, Y. Lima, R. Pasechnik and M. Šumbera, *Isolated photon production and pion-photon correlations in high-energy pp and pA collisions*, *Phys. Rev. D* **101** (2020) 094019 [arXiv:2003.02555] [INSPIRE].
- [90] S. Benić, O. Garcia-Montero and A. Perkov, *Isolated photon-hadron production in high energy pp and pA collisions at RHIC and LHC*, *Phys. Rev. D* **105** (2022) 114052 [arXiv:2203.01685] [INSPIRE].
- [91] I. Ganguli, A. van Hameren, P. Kotko and K. Kutak, *Forward $\gamma + jet$ production in proton-proton and proton-lead collisions at LHC within the FoCal calorimeter acceptance*, *Eur. Phys. J. C* **83** (2023) 868 [arXiv:2306.04706] [INSPIRE].
- [92] ALICE collaboration, *Letter of Intent: A Forward Calorimeter (FoCal) in the ALICE experiment*, CERN-LHCC-2020-009, CERN, Geneva (2020).
- [93] ALICE collaboration, *Physics of the ALICE Forward Calorimeter upgrade*, ALICE-PUBLIC-2023-001 (2023).
- [94] D. Boer, P.J. Mulders, J. Zhou and Y.-J. Zhou, *Suppression of maximal linear gluon polarization in angular asymmetries*, *JHEP* **10** (2017) 196 [arXiv:1702.08195] [INSPIRE].
- [95] F. Dominguez, B.-W. Xiao and F. Yuan, *k_t -factorization for Hard Processes in Nuclei*, *Phys. Rev. Lett.* **106** (2011) 022301 [arXiv:1009.2141] [INSPIRE].
- [96] P.J. Mulders and J. Rodrigues, *Transverse momentum dependence in gluon distribution and fragmentation functions*, *Phys. Rev. D* **63** (2001) 094021 [hep-ph/0009343] [INSPIRE].
- [97] J. Collins, *Foundations of perturbative QCD*, Cambridge University Press (2013) [DOI:10.1017/9781009401845] [INSPIRE].
- [98] A.H. Mueller, B.-W. Xiao and F. Yuan, *Sudakov Resummation in Small- x Saturation Formalism*, *Phys. Rev. Lett.* **110** (2013) 082301 [arXiv:1210.5792] [INSPIRE].

- [99] A.H. Mueller, B.-W. Xiao and F. Yuan, *Sudakov double logarithms resummation in hard processes in the small- x saturation formalism*, *Phys. Rev. D* **88** (2013) 114010 [[arXiv:1308.2993](#)] [[INSPIRE](#)].
- [100] P. Caucal, F. Salazar, B. Schenke and R. Venugopalan, *Back-to-back inclusive dijets in DIS at small x : Sudakov suppression and gluon saturation at NLO*, *JHEP* **11** (2022) 169 [[arXiv:2208.13872](#)] [[INSPIRE](#)].
- [101] P. Caucal et al., *Back-to-back inclusive dijets in DIS at small x : gluon Weizsäcker-Williams distribution at NLO*, *JHEP* **08** (2023) 062 [[arXiv:2304.03304](#)] [[INSPIRE](#)].
- [102] P. Caucal et al., *Back-to-back inclusive dijets in DIS at small x : Complete NLO results and predictions*, [arXiv:2308.00022](#) [[INSPIRE](#)].
- [103] F. Hautmann and H. Jung, *Angular correlations in multi-jet final states from k -perpendicular-dependent parton showers*, *JHEP* **10** (2008) 113 [[arXiv:0805.1049](#)] [[INSPIRE](#)].
- [104] M. Deak, F. Hautmann, H. Jung and K. Kutak, *Forward Jet Production at the Large Hadron Collider*, *JHEP* **09** (2009) 121 [[arXiv:0908.0538](#)] [[INSPIRE](#)].
- [105] P. Sun, B.-W. Xiao and F. Yuan, *Gluon Distribution Functions and Higgs Boson Production at Moderate Transverse Momentum*, *Phys. Rev. D* **84** (2011) 094005 [[arXiv:1109.1354](#)] [[INSPIRE](#)].
- [106] M. Deak, F. Hautmann, H. Jung and K. Kutak, *Forward Jets and Energy Flow in Hadronic Collisions*, *Eur. Phys. J. C* **72** (2012) 1982 [[arXiv:1112.6354](#)] [[INSPIRE](#)].
- [107] S. Dooling, F. Hautmann and H. Jung, *Hadroproduction of electroweak gauge boson plus jets and TMD parton density functions*, *Phys. Lett. B* **736** (2014) 293 [[arXiv:1406.2994](#)] [[INSPIRE](#)].
- [108] I. Balitsky and A. Tarasov, *Rapidity evolution of gluon TMD from low to moderate x* , *JHEP* **10** (2015) 017 [[arXiv:1505.02151](#)] [[INSPIRE](#)].
- [109] S. Marzani, *Combining Q_T and small- x resummations*, *Phys. Rev. D* **93** (2016) 054047 [[arXiv:1511.06039](#)] [[INSPIRE](#)].
- [110] M. Hentschinski, A. Kusina and K. Kutak, *Transverse momentum dependent splitting functions at work: quark-to-gluon splitting*, *Phys. Rev. D* **94** (2016) 114013 [[arXiv:1607.01507](#)] [[INSPIRE](#)].
- [111] M. Bury et al., *Calculations with off-shell matrix elements, TMD parton densities and TMD parton showers*, *Eur. Phys. J. C* **78** (2018) 137 [[arXiv:1712.05932](#)] [[INSPIRE](#)].
- [112] M. Hentschinski, A. Kusina, K. Kutak and M. Serino, *TMD splitting functions in k_T factorization: the real contribution to the gluon-to-gluon splitting*, *Eur. Phys. J. C* **78** (2018) 174 [[arXiv:1711.04587](#)] [[INSPIRE](#)].
- [113] B.-W. Xiao, F. Yuan and J. Zhou, *Transverse Momentum Dependent Parton Distributions at Small- x* , *Nucl. Phys. B* **921** (2017) 104 [[arXiv:1703.06163](#)] [[INSPIRE](#)].
- [114] J. Zhou, *Scale dependence of the small x transverse momentum dependent gluon distribution*, *Phys. Rev. D* **99** (2019) 054026 [[arXiv:1807.00506](#)] [[INSPIRE](#)].
- [115] A. Stasto, S.-Y. Wei, B.-W. Xiao and F. Yuan, *On the Dihadron Angular Correlations in Forward pA collisions*, *Phys. Lett. B* **784** (2018) 301 [[arXiv:1805.05712](#)] [[INSPIRE](#)].

- [116] C. Marquet, S.-Y. Wei and B.-W. Xiao, *Probing parton saturation with forward Z^0 -boson production at small transverse momentum in $p + p$ and $p + A$ collisions*, *Phys. Lett. B* **802** (2020) 135253 [[arXiv:1909.08572](#)] [[INSPIRE](#)].
- [117] E. Blanco et al., *Z boson production in proton-lead collisions at the LHC accounting for transverse momenta of initial partons*, *Phys. Rev. D* **100** (2019) 054023 [[arXiv:1905.07331](#)] [[INSPIRE](#)].
- [118] A. van Hameren, P. Kotko, K. Kutak and S. Sapeta, *Broadening and saturation effects in dijet azimuthal correlations in p - p and p - Pb collisions at $\sqrt{s} = 5.02$ TeV*, *Phys. Lett. B* **795** (2019) 511 [[arXiv:1903.01361](#)] [[INSPIRE](#)].
- [119] D.-X. Zheng and J. Zhou, *Sudakov suppression of the Balitsky-Kovchegov kernel*, *JHEP* **11** (2019) 177 [[arXiv:1906.06825](#)] [[INSPIRE](#)].
- [120] M. Hentschinski, K. Kutak and A. van Hameren, *Forward Higgs production within high energy factorization in the heavy quark limit at next-to-leading order accuracy*, *Eur. Phys. J. C* **81** (2021) 112 [*Erratum ibid.* **81** (2021) 262] [[arXiv:2011.03193](#)] [[INSPIRE](#)].
- [121] I. Balitsky, *Gauge-invariant TMD factorization for Drell-Yan hadronic tensor at small x* , *JHEP* **05** (2021) 046 [[arXiv:2012.01588](#)] [[INSPIRE](#)].
- [122] M.A. Nefedov and V.A. Saleev, *High-Energy Factorization for Drell-Yan process in pp and $p\bar{p}$ collisions with new Unintegrated PDFs*, *Phys. Rev. D* **102** (2020) 114018 [[arXiv:2009.13188](#)] [[INSPIRE](#)].
- [123] A. van Hameren, P. Kotko, K. Kutak and S. Sapeta, *Sudakov effects in central-forward dijet production in high energy factorization*, *Phys. Lett. B* **814** (2021) 136078 [[arXiv:2010.13066](#)] [[INSPIRE](#)].
- [124] M. Hentschinski, *Transverse momentum dependent gluon distribution within high energy factorization at next-to-leading order*, *Phys. Rev. D* **104** (2021) 054014 [[arXiv:2107.06203](#)] [[INSPIRE](#)].
- [125] M. Nefedov, *Sudakov resummation from the BFKL evolution*, *Phys. Rev. D* **104** (2021) 054039 [[arXiv:2105.13915](#)] [[INSPIRE](#)].
- [126] D. Boer, Y. Hagiwara, J. Zhou and Y.-J. Zhou, *Scale evolution of T -odd gluon TMDs at small x* , *Phys. Rev. D* **105** (2022) 096017 [[arXiv:2203.00267](#)] [[INSPIRE](#)].
- [127] M.A. Al-Mashad et al., *Dijet azimuthal correlations in $p - p$ and $p - Pb$ collisions at forward LHC calorimeters*, *JHEP* **12** (2022) 131 [[arXiv:2210.06613](#)] [[INSPIRE](#)].
- [128] I. Balitsky and G.A. Chirilli, *Rapidity evolution of TMDs with running coupling*, *Phys. Rev. D* **106** (2022) 034007 [[arXiv:2205.03119](#)] [[INSPIRE](#)].
- [129] Y. Shi, S.-Y. Wei and J. Zhou, *Parton shower generator based on the Gribov-Levin-Ryskin equation*, *Phys. Rev. D* **107** (2023) 016017 [[arXiv:2211.07174](#)] [[INSPIRE](#)].
- [130] A. van Hameren et al., *Searching for saturation in forward dijet production at the LHC*, *Eur. Phys. J. C* **83** (2023) 947 [[arXiv:2306.17513](#)] [[INSPIRE](#)].
- [131] I. Balitsky, *Rapidity-only TMD factorization at one loop*, *JHEP* **03** (2023) 029 [[arXiv:2301.01717](#)] [[INSPIRE](#)].
- [132] Y. Shi, S.-Y. Wei and J. Zhou, *Parton shower algorithm with saturation effect*, [[arXiv:2307.04185](#)] [[INSPIRE](#)].
- [133] F. Giuli, private communication.

- [134] M. Winn, private communication.
- [135] L. Motyka, M. Sadzikowski and T. Stebel, *Twist expansion of Drell-Yan structure functions in color dipole approach*, *JHEP* **05** (2015) 087 [[arXiv:1412.4675](#)] [[INSPIRE](#)].
- [136] L. Motyka, M. Sadzikowski and T. Stebel, *Lam-Tung relation breaking in Z^0 hadroproduction as a probe of parton transverse momentum*, *Phys. Rev. D* **95** (2017) 114025 [[arXiv:1609.04300](#)] [[INSPIRE](#)].
- [137] D. Brzeminski, L. Motyka, M. Sadzikowski and T. Stebel, *Twist decomposition of Drell-Yan structure functions: phenomenological implications*, *JHEP* **01** (2017) 005 [[arXiv:1611.04449](#)] [[INSPIRE](#)].
- [138] F.G. Celiberto, D. Gordo Gómez and A. Sabio Vera, *Forward Drell-Yan production at the LHC in the BFKL formalism with collinear corrections*, *Phys. Lett. B* **786** (2018) 201 [[arXiv:1808.09511](#)] [[INSPIRE](#)].
- [139] M.E. Peskin and D.V. Schroeder, *An Introduction to quantum field theory*, Addison-Wesley, Reading, U.S.A. (1995) [[INSPIRE](#)].
- [140] G. Passarino and M.J.G. Veltman, *One Loop Corrections for e^+e^- Annihilation Into $\mu^+\mu^-$ in the Weinberg Model*, *Nucl. Phys. B* **160** (1979) 151 [[INSPIRE](#)].